8-2023

The Influence of Spectral Quality on Primary and Secondary Metabolism of Hydroponically Grown Basil

Hunter Albright Hammock
University of Tennessee, Knoxville, hhammoc1@vols.utk.edu

To the Graduate Council:

I am submitting herewith a dissertation written by Hunter Albright Hammock entitled "The Influence of Spectral Quality on Primary and Secondary Metabolism of Hydroponically Grown Basil." I have examined the final electronic copy of this dissertation for form and content and recommend that it be accepted in partial fulfillment of the requirements for the degree of Doctor of Philosophy, with a major in Plant, Soil and Environmental Sciences.

Carl Sams, Major Professor

We have read this dissertation and recommend its acceptance:

Dennis Deyton, John Munafo, Curtis Luckett

Accepted for the Council:

Dixie L. Thompson

Vice Provost and Dean of the Graduate School

(Original signatures are on file with official student records.)

The Influence of Spectral Quality on Primary and Secondary Metabolism of Hydroponically Grown Basil

A Dissertation Presented for the

Doctor of Philosophy

Degree

The University of Tennessee, Knoxville

Hunter Albright Hammock

August 2023

Dedication

This dissertation is dedicated to my beloved parents, whose love, support, and guidance have been the driving forces behind my academic journey. From the very beginning, you instilled in me a thirst for knowledge and an unwavering belief in my abilities. You made me question how the world works and gave me the desire to find out. Your constant encouragement has not only fueled my academic pursuits but also molded me into the person I am today.

To my mother, whose nurturing spirit and unwavering faith in my capabilities have always been my source of strength. You're a teacher at heart and gifted me with your drive to help others learn. Your tireless efforts to provide me with the best opportunities and your ceaseless prayers for my success have been the backbone of my journey. Your wisdom, resilience, and grace continue to inspire me every day.

To my father, who taught me the value of hard work and perseverance. Your dedication to your own career has always been a model for my own academic endeavors. You taught me that working overtime and burning the midnight oil is required sometimes to be successful. Your insightful advice, patient teaching, and endless encouragement have guided me through every challenge and setback.

You have been my greatest cheerleaders, my strongest supporters, and my most trusted advisors, always holding my best interest to heart. Your consistent belief in my abilities have helped to propel me forward, even when the journey seemed insurmountable. You kept me motivated through the blood, sweat and tears (sometime all three working in the greenhouse). You have both sacrificed so much to give me an opportunity to pursue my dreams, and I will never take that for granted.

The road to earning this PhD was paved with many challenges and trials, but your love and support have made every hurdle surmountable. You have remined me to take small steps up steep slopes. This achievement is not just mine, but ours. For every late-night writing session you stayed up with me, for every word of encouragement during moments of self-doubt, for every sacrifice you've made for my education -- I dedicate this dissertation to you.

In the pages of this document, in every discovery and conclusion, through every word typed into existence, your influence is evident. None of this would have been possible without you. As I stand on the threshold of my future, ready to use the knowledge and skills I've acquired, I carry with me the lessons you've taught me. Your love, guidance, and support continue to inspire me to reach for greater heights.

Thank you, Mom and Dad, for everything. I hope to be one day give my children the same unwavering love and support you've given me. This PhD is a testament to your love, and a tribute to your unwavering faith in me. I hope to make you prouder still in all my future endeavors.

Acknowledgements

I would like to express my deepest gratitude to everyone who has supported and guided me throughout my academic journey at the University of Tennessee. I am humbled by the wealth of knowledge and kindness I have received, and I am sincerely appreciative of each contribution that has shaped my growth and success.

First and foremost, I extend my heartfelt thanks to my primary mentor, Dr. Carl Sams. Your guidance, expertise, and unwavering support throughout this research process have been invaluable. I am profoundly grateful for your mentorship and the wisdom you have imparted.

To my PhD committee members, Drs. Dennis Deyton, John Munafo, and Curtis Luckett, thank you for your valuable feedback, support, and encouragement. Your collective insights and perspectives have greatly enriched my research and academic experience.

I am equally grateful for my peers at UT, who have challenged me, inspired me, and helped me grow as a researcher. A special thanks go to my lab supervisors/assistants/colleagues Jennifer Wheeler, Jonathan Chase, Nick Ballew, Ben Levine, Maddie Spradley, Sara Burns, Skyler Brazel, Katelynn Rector, Tracy Hawk, Brooke Keadle, and Benjamin Prichard. Your dedication, hard work, and camaraderie have made our shared journey both productive and enjoyable.

My sincere appreciation extends to the staff and the resources provided by the University of Tennessee Institute of Agriculture (UTIA). Your support has been instrumental in my success. I would also like to acknowledge the Graduate Student Senate, the National Society of Leadership and Success, the American Society for Horticultural Science, and Leadership Knoxville Scholars for providing opportunities for leadership, service, and professional growth.

Last but certainly not least, I want to express my deepest gratitude to my parents, family, and friends. Your unwavering belief in me, your constant encouragement, and your love have been

my source of strength throughout this journey. You have celebrated my successes, lifted me during challenging times, and stood by me every step of the way.

As I reflect on my time at UT, I am filled with gratitude for the experiences I have had, the lessons I have learned, and the relationships I have built. The knowledge and skills I have acquired here have not only shaped my academic journey but also laid a strong foundation for my professional career. I hope to use these skills to help feed future generations. I am deeply grateful for the opportunity to learn, grow, and contribute to such a vibrant academic community. Thank you, Rocky Top.

Abstract

This dissertation explores the influence of spectral quality from supplemental lighting and seasonal changes on primary and secondary metabolism in hydroponically grown greenhouse basil. It aims to enhance understanding of plant/light interactions and provide practical insights for light emitting diode (LED) manufacturers and commercial growers. The research is premised on the hypothesis that altering spectral quality can significantly impact primary and secondary metabolism, potentially improving flavor and increasing phytonutrients with health benefits. This project involved four phases, each building on the results of the previous ones. In Phase 1, different basil varieties were evaluated to determine aroma volatile profiles and concentrations of key secondary metabolites. In Phase 2, discrete narrow-band blue/red (B/R) wavelengths were used to investigate their impact on aroma volatile concentrations and secondary metabolic resource partitioning in basil, revealing the influence of both seasonal and supplemental lighting effects on plant metabolism. Phase 3 explored the impacts of full spectrum white LEDs and high pressure sodium (HPS) on yield and nutrient accumulation, comparing these to the optimal narrowband B/R identified in Phase 2. The final phase connected all phases, comparing the best narrowband and full spectrum treatments to a traditional HPS treatment and natural light control. These treatments were tested across various parameters, with photosynthesis and primary metabolic data recorded, yields and biometric data taken, aroma compound concentrations, and other secondary metabolic data collected. A sensory panel was conducted, and mRNA sequencing performed to determine differences in metabolic pathway expression based on lighting treatment. Analytical data from the different light treatments, sensory panel, and mRNA data were evaluated to determine which lighting regime had the most positive impact on plant physiology and biochemistry. Variation in spectral quality across seasons influences primary and secondary

metabolism, in addition to the spectral qualities of different types of supplemental lighting treatments. This holistic, interdisciplinary approach revealed a light treatment that balances yield, nutrient content, and flavor preference, providing a superior product highly preferred by consumers. The research presented in this document significantly expands our understanding of the complex interplay between light conditions and plant physiology, with implications for improving crop yield and quality in controlled environment agriculture.

Table of Contents

List of Tables

List of Figures

CHAPTER 1: INTRODUCTION

Controlled Environment Agriculture

Controlled Environment Agriculture (CEA) is a technique that uses a physical structure to control the growing environment of a crop (Massa et al., 2008; Mccartney and Lefsrud, 2018). This can include covered rows, high tunnels, greenhouses, indoor growing chambers, vertical farms, and urban agriculture. Improvements in technology, along with many years of research and collaboration, have transformed basic coverings and structures into modern-day optimized plant factories (Craver et al., 2019; Engler and Krarti, 2021; Mccartney and Lefsrud, 2018; Mitchell, 2022).

Humans have used coverings to protect plants and improve the yields of crops for centuries (Mitchell, 2022). The origins of American CEA research can be traced to the early 1900s, with the work of Liberty Hyde Bailey, a renowned horticulturist. Bailey was one of the first to conduct experiments using glass greenhouses to improve crop growth and advocated for their use in agricultural production. His work (and his creation of the American Society for Horticultural Science) was just one of the many global contributions that have sought to develop new techniques for improving crop production in controlled environments. CEA has progressed significantly since the early days of Bailey's greenhouse experiments (Ramin Shamshiri et al., 2018; Van Delden et al., 2021). Modern CEA systems can produce a wide range of crops, including fruits, vegetables, herbs, and flowers. Some of the most commonly grown crops in CEA systems include tomatoes, cucumbers, lettuce, and peppers (Dou et al., 2017; Engler and Krarti, 2021; Massa et al., 2008; Mccartney and Lefsrud, 2018; Mitchell, 2022; Modarelli et al., 2022).

CEA involves various disciplines, including plant science, engineering, physics, chemistry, and computer science (Engler and Krarti, 2021; Gómez et al., 2019; Mitchell, 2004). Some of the typical environmental parameters that can be controlled include temperature, humidity, light,

moisture, nutrients, airflow, carbon dioxide (CO2) concentrations, and light (intensity, spectral quality, duration) (Craver et al., 2019; Engler and Krarti, 2021; Mccartney and Lefsrud, 2018). The physical structure, system specifications, and goals of the CEA operation (such as research, commercial production, etc.) directly impact the level of control/tolerance for the management of each environmental parameter (Mccartney and Lefsrud, 2018). It is possible to precisely control each parameter and fully optimize the environment to enhance the growth and development of a specific crop. On the other hand, a more practical approach for a commercial CEA operation would be to economically control the growing environment for a specific crop in order to make a profit. It has been well established that changing the environment of an organism will change its genetic expression, and this can be used to enhance specific quality traits (Olle and Viršile, 2013; Paradiso and Proietti, 2021; Samuoliene et al., 2012; Santin et al., 2021; Singh et al., 2015; Stagnari et al., 2018; Tan et al., 2020; Tuan et al., 2013; Turner, 2009).

Practically any crop can be grown using CEA, but some are more economical than others. High-value specialty crops, such as small fruits/vegetables, herbs, etc., are prevalent in a variety of CEA systems (e.g., high tunnels, glass greenhouses, vertical farms, etc.) and are grown in both soil and soilless substrates (El-Ramady et al., 2020; Larsen et al., 2020; Mccartney and Lefsrud, 2018). Supplemental lighting (SL) has become more prevalent in some CEA systems (i.e., greenhouses), which has prompted significant research efforts to determine optimal lighting intensity, quality, duration, and electrical efficiency (Craver et al., 2019; Jiang et al., 2020; Randall and Lopez, 2014; Singh et al., 2015). There can be many variations in the type of systems used to control the environment, deliver nutrients, and provide all the requirements for unhindered and sustainable growth (Benke and Tomkins, 2017; Mccartney and Lefsrud, 2018; Mitchell, 2004).

Designing a CEA system, each parameter's variable control and required tolerances on a particular crop's demands should be considered (Engler and Krarti, 2021).

Vertical farms and plant factories have steadily gained popularity since the early 2000s (Benke and Tomkins, 2017; Engler and Krarti, 2021). This is due to several factors, which involve advancements in technology, economics, and sustainability (Engler and Krarti, 2021; Larsen et al., 2020; Mccartney and Lefsrud, 2018; Ramin Shamshiri et al., 2018; Van Delden et al., 2021). Many of the vertical farms require sole-source lighting, which necessitates the use of energy efficient lighting systems. The cost of LEDs has decreased dramatically with recent advancements in semiconductor technology. LED lighting sources are more energy efficient and produce less heat than traditional lighting technologies in horticulture (Dutta Gupta, 2017). Artificial intelligence and innovations in computer science have also contributed significantly to the boom in popularity and potential for increased efficiency (Graamans et al., 2017; Xu et al., 2016). One of the primary drivers is the sustainability of food production (El-Ramady et al., 2020). The technologies utilized in CEA can significantly reduce water use (Engler and Krarti, 2021; Mccartney and Lefsrud, 2018; Ramin Shamshiri et al., 2018). Some of the other advantages over traditional farming include consistent year-round production, reduction of pollution, protection from inclement weather, space use efficiency, reduction of pest and pathogen pressures, reduction in pesticides, higher quality crops, and more profit for high-value specialty crops (Benke and Tomkins, 2017; Engler and Krarti, 2021; Larsen et al., 2020; Mccartney and Lefsrud, 2018; Rajan et al., 2019; Ramin Shamshiri et al., 2018; Sharathkumar et al., 2020; Van Delden et al., 2021). CEA systems (more specifically, vertical farms) can be strategically placed near food deserts (Benke and Tomkins, 2017; Mccartney and Lefsrud, 2018; Mitchell, 2004). Communities in need can utilize locally grown produce. Growing food closer to the consumer also has numerous benefits, including

reduced costs, fewer carbon emissions, and better shelf life (Engler and Krarti, 2021). CEA can even improve food safety by reducing/removing potential sources of contamination (Rajan et al., 2019; Van Delden et al., 2021).

Some of the highest expenditures across all indoor farming systems include startup costs, energy use, and labor (Engler and Krarti, 2021; Mccartney and Lefsrud, 2018; Mitchell, 2022; Ramin Shamshiri et al., 2018; Sharathkumar et al., 2020; Van Delden et al., 2021; Walters et al., 2020a). Lighting systems will decrease in cost as the technology improves, and energy efficiency will increase, but it will be vital to implement creative solutions to mitigate the electrical dependence of CEA operations on our power grid in the near future. Further integration of CEA operations into our current food production systems will bolster our food security and help ensure the supply chain can keep up with increasing demand.

Supplemental Lighting in Horticulture

Supplemental lighting is often used in horticulture to improve plant productivity in greenhouses and indoor growing environments (Massa et al., 2008; Morrow, 2008). It has been well-established that the intensity, spectral quality, and duration of light influence genetic expression, which, in turn, determines the phytonutrient content of many high-value specialty crops (Dou et al., 2017; Goins et al., 1997; Smith, 1982; Tennessen et al., 1994). Using supplemental lighting has been shown to improve crop quality and yield. A large volume of research on supplemental lighting (SL) focuses on finding the most efficient and effective ways to use light to improve plant growth (Engler and Krarti, 2021; Mitchell, 2022; Morrow, 2008; Paradiso and Proietti, 2021). In order to optimize light for any crop in any CEA operation, it is necessary to have a thorough understanding of how light affects plant growth. Research regarding

the interactions between lighting systems and plants will help growers optimize production, reduce energy costs, and produce high-quality crops (Bugbee, 2016; Hammock et al., 2020; Kelly and Runkle, 2020; Kim et al., 2019; Piovene et al., 2015). Growers may benefit from manipulating the spectral quality of supplementary lighting, since it would allow them to better manage their crops' physiology, morphology, and biochemistry (Kopsell et al., 2007; Li and Kubota, 2009)

Commercial greenhouses often must implement supplemental lighting systems, which can be expensive, in order to create the best possible conditions for growth (Massa et al., 2008; Morrow, 2008). In some cases, these lights are costly to maintain; however, they produce significant results in terms of increased plant development and production (Mitchell et al., 2015; Samuoliene et al., 2013). By examining different wavelengths and intensities produced by various greenhouse lighting systems, we can discover how to upgrade current supplemental lighting systems in a way that is both efficient and practical on a large scale. This would have substantial benefits for improving sensory quality and yield.

Horticultural lighting systems can be divided into two categories: supplemental and sole source. To satisfy growing customer demand year-round, it is necessary to optimize greenhouse lighting systems to improve production quality and lower costs (Groher et al., 2019; Martineau et al., 2012; Morrow, 2008; Nelson and Bugbee, 2014). Since the amount of light varies throughout the year (in the vast majority of locations across the globe), SL systems are sometimes utilized in greenhouse operations with the intention of improving quality and yields. Indoor farms and CEA systems that do not utilize sunlight must provide sole source lighting for crops to survive; this further emphasizes the importance of horticultural lighting systems (i.e., performance, longevity, durability, energy efficiency, heat distribution, intensity, and spectral output). This dissertation will only focus on supplemental lighting (SL) under standard greenhouse conditions and will not

incorporate sole-source lighting. The goal of this document is to improve knowledge of current horticulture SL systems, and their application, to assist growers in terms of improving the yield/quality of high-value specialty crops. That being said, there is significant value in exploring the impacts of sole-source lighting (i.e., to isolate the effects of discrete narrowband wavelengths' impact on physiology), which can then be applied to commercial greenhouse SL systems and applications.

Two primary horticultural lighting systems are pertinent for this discussion, both historically and currently: high-pressure sodium (HPS) and light-emitting diodes (LEDs). HPS lamps have not traditionally been viewed as the best choice for supplemental greenhouse lighting, because they have poor spectral quality (i.e., fewer blues/reds, more orange and yellow, not ideal for photosynthesis) and generate significant amounts of heat (Massa et al., 2008; Morrow, 2008). However, these systems have often been chosen because they are more available and affordable than other options. HPS has been used extensively in horticulture, but LEDs are becoming increasingly popular (Mitchell et al., 2015).

Since the first LED research was conducted with plants, it has developed into a thriving industry (Mitchell, 2004; Mitchell, 2022; Singh et al., 2015). Advances in LED technologies have allowed researchers to study individual narrowband wavelengths and determine how plants react to light at a fundamental level (Massa et al., 2008; Mitchell et al., 2015). Some insight into the influence of spectral quality on plant growth was gained by applying filters to conventional lighting systems, but supplementation of specific narrow wavelengths was not feasible until LED technology became available (Mitchell, 2022). This opens countless possibilities for experimenting with different spectral compositions (Massa et al., 2008; Pimputkar et al., 2009). Currently, LEDs are used for various purposes in the horticultural industry, including controlled

environment research, tissue culture and propagation, photoperiod control, daily light integral extension, and supplemental lighting regimes with specific spectra and intensities (Mitchell, 2022).

A light-emitting diode, or LED, is a source of light that uses semiconductor technology rather than a filament or gas discharge (Hasan et al., 2017). When an electric current is passed through the semiconductor material, electrons can flow across the gap and release energy in the form of photons (Pattison et al., 2018). The wavelength of the light emitted by an LED depends on the chemical composition of the semiconductor material. LEDs are used in many applications outside of horticulture, including electronic displays, automotive lighting, and general lighting (Xu et al., 2016). They require much less electricity to produce the same amount of light as traditional incandescent bulbs or fluorescent tubes (Bantis et al., 2018; Bispo-Jr et al., 2021; Singh et al., 2015). In addition, LEDs are long-lasting and durable and do not contain toxic materials. As a result, LEDs are becoming increasingly popular as a more environmentally friendly alternative to traditional forms of lighting. Their lifetime can reach up to 100,000 h, as compared to HPS lighting, which is rated to perform a maximum of 20,000 h under optimal conditions (Mitchell, 2004). LEDs are the first lighting source to provide the capability of accurate spectral control, something that has not been possible using previous lighting technologies. The higher initial cost of LEDs is quickly offset by the decreased energy consumption of HPS lighting and positive yield impacts, especially as manufacturing costs continue to decrease over time (Katzin et al., 2021; Sipos et al., 2020). Unlike HPS lights, or other high intensity discharge (HID) lamps, LEDs do not require a warm-up time and can be programmed with complex lighting schedules and spectral adjustments without the risk of damage/lifespan reduction, such as photoperiod compensation and targeted intra-canopy lighting. Because they are solid-state devices, they can be easily integrated into

complex digital control systems. LED lighting is an exciting new technology with tremendous potential in the horticultural industry (Weaver et al., 2019).

Fundamentals of Light and Its Interaction with Plants

Plants convert light energy into chemical energy and execute primary/secondary metabolic functions using that chemical energy. The amount of light, its duration, direction, and spectral quality have a direct influence on plant growth and development (Colquhoun et al., 2013; Smith, 1982). Even though we have a fair understanding of the primary and secondary metabolic pathways for various plant species, some information is still either missing or unconfirmed. To date, we have not fully explored how different wavelengths affect secondary metabolism in plants, nor interactions between primary and secondary metabolism in response to changes in light quality (Bugbee, 2016; Kelly and Runkle, 2020; Shumskaya and Wurtzel, 2013; Tarakanov et al., 2022). These interactions between pathways could result in positive or negative effects on various critical products both pre- and post-harvest.

Photosynthetically active radiation (PAR) is known as the portion of the light spectrum that is most active in photosynthesis (Mccree, 1971). It ranges from 400-700 nm and is closely correlated with the visible spectrum of the human eye (Barta et al., 1992). The quantity of light provided throughout the PAR region is adequate for photosynthesis and primary metabolism. A growing body of literature suggests that other wavelengths, primarily far-red, also have photosynthetic effects (Demotes-Mainard et al., 2016; Leiser et al., 1960; Mokvist et al., 2014; Pazuki, 2017; Ritz et al., 2000; Sakshaug et al., 1997; Thapper et al., 2009; Zhang et al., 2020; Zhen and Bugbee, 2020; Zhen et al., 2021). Light quality concerns the spectral distribution of radiation supplied and what wavebands are transmitted by the source (Mccree, 1973).

Plant tissues include several pigments and photoactive chemicals that require specific wavebands of energy to function (Briggs and Huala, 1999; Fraikin et al., 2013). Chlorophyll and carotenoids absorb light energy in the range of 380-400 nanometers, while violet, blue, and green light can be found in the range of 400-520 nm (Buchanan, 2015). These wavelengths are responsible for photosynthesis and other metabolic processes in plants. Red and far-red light are found in the range of 620-750 nm and significantly impact plant physiology (Buchanan, 2015). Changes in intensity/spectral quality of light directly impact plant physiology and biochemistry (Figure 1.5), and responses from environmental stressors (i.e., changes in light intensity and spectra) prompt a diverse range of photomorphogenic responses across many plant species (Davis and Burns, 2016; Fraikin et al., 2013; Kusuma and Bugbee, 2021; Larsen et al., 2020; Metallo et al., 2018; Paradiso and Proietti, 2021; Santin et al., 2021). It has been well documented that plants do not absorb all wavelengths of light at the same rate, and that adding abiotic stressors (such as light) to a plant's environment can impact secondary metabolite production (Hammock et al., 2021; Kopsell et al., 2015; Landi et al., 2020; Lichtenthaler, 1987; Mccree, 1971; Ouzounis et al., 2015; Yeum and Russell, 2002; Young, 1991). Plants absorb light energy at different wavelengths depending on the concentrations photo-receptive pigments present in tissues (Figures 1.1-1.4). Knowing the mechanisms behind various photoreceptors and pigments, what electromagnetic radiation they accept and absorb, and their effects on plant growth are vital to developing efficient LED light protocols.

In addition to affecting the physical growth and metabolism of plants, light also affects their biochemical composition. Plants produce a wide variety of chemicals, including pigments, proteins, enzymes, and secondary metabolites (Buchanan, 2015). These compounds are essential for plant growth, development, and metabolism. Light affects the production of these chemicals in

two ways: directly and indirectly. Direct effects of light on metabolism occur when light energy is converted into chemical energy by pigments or other molecules in the plant (Buchanan, 2015; Wink, 2010). This conversion can result in the synthesis of new molecules or the breakdown of existing molecules. Indirect effects of light on metabolism occur when light affects the activity of enzymes that are involved in biochemical synthesis or degradation (Banthorpe et al., 1971; Frank and Cogdell, 1996; Schmitt and Wulff, 1993; Smith, 1982; Young, 1991).

Light duration is the amount of time (h) a crop receives light within a 24 h cycle. Light duration should not be confused with daily light integral (DLI), which is the cumulative amount of light energy (mol of photons within PAR region) provided over a given period (Faust et al., 2005; Gent, 2014; Korczynski et al., 2002; Poorter et al., 2019). Photoperiod primarily impacts reproductive growth and development, flowering, and some other metabolic processes (Singh et al., 2015). DLI is the cumulative amount of photosynthetically active photons (i.e., PAR) received by the plant's canopy in a 24 h period ($mol \cdot m^{-2} \cdot d^{-1}$) (Fausey et al., 2005). Photosynthesis rapidly and asymptotically increases with intensity, as photons within the PAR region begin to hit leaf tissues, until it reaches a specific saturation limit for the species (Faust et al., 2005). It has been shown that some responses are specific to the plant species and dependent on the spectral quality of light (Carvalho et al., 2016; Faust et al., 2005; Li and Kubota, 2009; Smith, 1982).

DLI requirements vary considerably across species, but it has been generalized that most perennial crops require 10-16 $mol \cdot m^{-2} \cdot d^{-1}$ to satisfy quality standards (Faust et al., 2005). The effect of DLI on biomass accumulation (DM) has previously been investigated in several herbaceous crops and revealed to be linear until around 20 or 30 $mol \cdot m^{-2} \cdot d^{-1}$ (higher DLIs exist for a wide range of other species, such as C4 crops) (Faust et al., 2005; Warner and Erwin, 2003, 2005). Other studies observed linear increases in biomass, plant quality, and inflorescence number on various

herbaceous crops with increasing DLI from around 5-20 $mol \cdot m^{-2} \cdot d^{-1}$ (Fausey et al., 2005; Frąszczak and Knaflewski, 2009; Runkle and Heins, 2006). The southeast region of the United States receives anywhere from 2-15 $mol \cdot m^{-2} \cdot d^{-1}$ throughout the fall and winter (Korczynski et al., 2002). The amount of available light can also be decreased by outside factors such as bad weather, or even something as simple as a dirty greenhouse covering (Currey et al., 2012; Frąszczak and Knaflewski, 2009; Hutchinson et al., 2012; Moccaldi and Runkle, 2007). It is common for growers to provide supplemental lighting during winter months, due to the low light intensity, which then provides a daily light integral (DLI) that satisfies crop requirements (Baumbauer et al., 2019; Chong et al., 2014; Christiaens et al., 2014; Currey et al., 2012; Currey and Lopez, 2015; Fausey et al., 2005; Garland et al., 2010; Hutchinson et al., 2012; Mitchell, 2004; Mitchell et al., 2015; Oh et al., 2009; Warner and Erwin, 2003). Many commercial producers use supplemental light for a total of 12-24 hours each day, with intensities usually ranging from 100-400 $\mu mols \cdot m^{-2} \cdot sec^{-1}$ for high-value specialty crops (Craver et al., 2019; Długosz-Grochowska et al., 2016; Gómez and Mitchell, 2014; Gómez et al., 2013; Li and Kubota, 2009; Randall and Lopez, 2014; Weaver et al., 2019; Zhang et al., 2019), under standard United States greenhouse conditions, which is generally sufficient for acceptable yields and quality for a range of specialty crops.

Brief Overview of Primary Metabolism in Higher Plants

Primary metabolism is defined as the set of chemical reactions that are necessary to maintain the basic structure and function of cells (i.e., survival and reproduction) (Buchanan, 2015). In order to understand the primary metabolism of plants, it is important first to understand the role of photosynthesis at a basic level. Photosynthesis is the process that produces chemical energy from essential elements using the sun's energy (Taiz et al., 2015). Plants use these organic molecules to create new cells, thereby allowing plants to grow and mature. The primary

metabolism of plants can be divided into three main categories: biosynthesis, catabolism, and anabolism (Buchanan, 2015). Biosynthesis refers to the creation of new organic molecules from simple inorganic elemental nutrients. In higher plants, this typically occurs through the process of photosynthesis. The sun's energy is used to convert water and carbon dioxide into oxygen and glucose. Plants then use glucose and other sugars to create new cells and tissues. Catabolism refers to the breakdown of larger organic molecules into smaller ones. In plants, this typically occurs through the process of respiration. Respiration is the process by which sugars are broken down to release energy for plant growth and metabolic functions. Anabolism refers to the synthesis of larger organic molecules from smaller ones. In plants, this typically occurs through the process of growth and development. Growth involves synthesizing new cells and tissues, while development involves differentiating these cells and tissues into specialized structures (Buchanan, 2015; Taiz et al., 2015). This section will provide a basic overview of the known primary metabolism in higher plants to facilitate the analysis of experimental data presented later in this document.

As previously described, light emitted from the sun contains photons in a broad spectrum of wavelengths. For photosynthesis, organisms primarily utilize a portion of the electromagnetic spectrum called photosynthetically active radiation (PAR). It should be noted that other wavelengths outside of 400-700 nm profoundly impact plant physiology and growth, with recent studies indicating wavelengths outside of PAR (i.e., extended PAR or ePAR) influence photosynthesis (Zhang et al., 2020; Zhen and Bugbee, 2020; Zhen et al., 2021). Plants contain pigments that facilitate the capture of wavelengths of light in the visible light range. The color of each pigment comes from the wavelengths of light reflected. Plants appear green because they reflect yellow/green wavelengths of light, while blue/red wavelengths of light are absorbed by these pigments, providing the energy used for photosynthesis. These chemical reactions occur

within plant cells in specialized structures known as chloroplasts (Buchanan, 2015; Taiz et al., 2015).

Photosynthesis in C3 plants consists of two sets of reactions: the light-dependent reactions and the Calvin cycle. Within the chloroplast are small disk-like structures called thylakoids, surrounded by a fluid-filled space called the stroma. The reactions that synthesize glucose from the Calvin cycle occur in the stroma. The light-dependent reactions occur in thylakoids. Thylakoids contain pairs of photosystems called photosystem I and photosystem II that work together to produce energy that will later be used in the stroma to manufacture sugars. The photosystems of the thylakoid consist of a network of accessory pigment molecules and chlorophyll, the molecules that absorb light. The absorbed light energy excites electrons to a higher state, and the photosystems channel the excitation energy gathered by the pigment molecules to a reaction center (Buchanan, 2015; Carson, 2019; Taiz et al., 2015; Wink, 2010).

A chlorophyll molecule will then pass the electrons to a series of proteins located on the thylakoid membrane—photons of light strike photosystems I and II simultaneously. Photons striking photosystem II create energized electrons, which are then passed from the reaction center of photosystem II to an electron transport chain. The electrons lost by photosystem II are replaced by the process of photolysis, which involves the oxidation of a water molecule producing free electrons and oxygen gas. While this oxygen gas is a byproduct of photosynthesis, it is an essential input to the cellular respiration pathways as electrons pass through the electron transport chain. The energy from these electrons is then used to pump hydrogen ions from the stroma to the thylakoid, creating a concentration gradient of H^+ ions. These gradients supply energy to adenosine triphosphate (ATP) synthase proteins, which phosphorylate adenosine diphosphate (ADP) to form ATP. It is energetically favorable for protons to diffuse back down the gradient into the stroma,

and their only route of passage is through the enzyme APT synthase. The low-energy electrons leaving photosystem II are shuttled to photosystem I, where low-energy electrons are reenergized and passed through an electron transport chain, which is then used to reduce the electron carrier nicotinamide adenine dinucleotide phosphate ($NADP^+$) to the reduced form of nicotinamide adenine dinucleotide phosphate (NADPH). When the chloroplast receives a steady supply of photons, NADPH and ATP molecules will be rapidly shuttled to the metabolic pathways in the stroma. The ATP and NADPH formed during light-dependent reactions will then be used in the stroma to fuel the Calvin cycle reactions (Buchanan, 2015; Carson, 2019; Taiz et al., 2015; Wink, 2010).

The Calvin cycle involves reactions that reduce carbon dioxide to produce the carbohydrate glyceraldehyde-3-phosphate (G3P). The cycle consists of three steps. The first is carbon fixation. In this step, carbon dioxide is attached to ribulose 1,5-bisphosphate (RuBP), resulting in a 6-carbon molecule that splits into two, three-carbon molecules. The second step is a sequence of reactions using electrons from NADPH and some of the ATP to reduce carbon dioxide. In the final step, RuBP is regenerated, and for every three turns of the cycle, five molecules of G3P are used to reform three molecules of RuBP. The remaining G3P is then used to make glucose, fatty acids, or glycerol. It takes two molecules of G3P to make one molecule of glucose phosphate. The Calvin cycle must run six times to produce one molecule of glucose. These molecules can remove their phosphate and add fructose to form sucrose, which plants use to transport carbohydrates throughout their system. Glucose phosphate is also the starting molecule for synthesizing starch and cellulose. Plants produce sugars to use as storage molecules and structural components for their benefit. By utilizing the sun's energy and inputs of water and carbon dioxide, plants can fix carbon for the creation of sugars. These simple sugar molecules are then transported throughout

the plant to be used in cellular respiration or as starting materials for more complex carbohydrates such as starch and cellulose. In higher plants, primary metabolism includes the synthesis of these types of small molecules (e.g., sugars, amino acids, nucleotides) that are used to build larger molecules (e.g., proteins, enzymes, DNA) (Buchanan, 2015; Taiz, 2010).

When discussing primary metabolism and photosynthesis in higher plants, it is important to note the differences between C3 and C4 plants. The notation of C3 and C4 plants is used to describe two different photosynthetic pathways with varying efficiencies depending on sun intensity and temperature. These two pathways are thought to have evolved from separate lineages and be advantageous based on the climate (tropical vs. temperate). The enzyme RuBisCO is the determinate factor for carbon fixation efficiency in the Calvin cycle and is the most abundant enzyme on earth. Around 5% of plants are C4, with the vast majority being C3. The primary product from C3 is 3-phosphoglyceric acid, while C4 produces a four-carbon compound (oxaloacetate). Carbon fixation of C3 plants occurs in the mesophyll cells, while carbon fixation of C4 plants occurs in both mesophyll cells and bundle sheath shells. C3 plants can be found in cool, wet areas and make up 95% of green plants. C4 plants can be found in dryer areas and do not have photorespiration. C4 plants have leaves with Kranz anatomy, while 3C3 does not (Kranz anatomy is defined as a plant having vascular bundles that are surrounded by mesophilic photosynthetic tissue in a ring-like fashion) (Buchanan, 2015; Taiz, 2010).

Carbon fixation is faster and more efficient in C4 plants, but they do not do well under low light intensities or temperatures because their efficiency is significantly reduced due to the inherent mechanism of C4 metabolism. In C4, the initial steps are carried out in the mesophyll cells, and the remaining steps are completed in the bundle sheath cells. In contrast, all light-independent

steps occur in the mesophyll cells of C3 plants, and photosynthesis is inhibited when stomata are closed (Buchanan, 2015).

Respiration is the opposite of photosynthesis, as it frees up energy from carbohydrates for cellular use. Reduced cellular carbon generated by photosynthesis is oxidized to carbon dioxide and water. This oxidation is coupled to the synthesis of ATP. Respiration takes place through four main pathways: glycolysis, the oxidative pentose phosphate pathway, the citric acid cycle, and oxidative phosphorylation. In glycolysis, carbohydrates are converted into pyruvate in the cytosol, and a small amount of ATP is synthesized. If oxygen is not available, fermentation generates NAD+ for glycolysis. It is also regulated from the bottom up by its own products. Carbohydrates can be oxidized via the oxidative pentose phosphate pathway and provide biosynthetic building blocks/reducing power (NADPH). In the citric acid cycle, pyruvate is oxidized to carbon dioxide within the mitochondrial matrix. Oxidative phosphorylation occurs in terms of mitochondrial electron transport and ATP synthesis. During aerobic respiration, up to 60 molecules of ATP are produced from a single sucrose molecule. It is estimated that a plant may respire more than 50% of its daily photosynthetic yield, with widely ranging ratios based on species and environmental conditions. Respiration is also involved with lipid metabolism. Lipids are broken down to produce fatty acids and glycerol. These can be used to produce cell membranes, waxes, and energy storage (Buchanan, 2015; Carson, 2019; Taiz et al., 2015; Wink, 2010).

Secondary Metabolism in Higher Plants

In higher plants, secondary metabolism is a term that describes metabolic processes and pathways that are not necessary for life (Wink, 2010). However, these pathways often serve important direct and indirect roles in survival, including the plant's response to environmental stressors such as herbivory, pathogens, and abiotic stressors (Buchanan, 2015). Secondary

metabolites often involve plant defense mechanisms, such as deterring herbivores or pathogenic fungi. In some cases, plants can also use secondary metabolites to attract helpful insects, such as pollinators (Wink, 2010).

The three classes of secondary metabolites in plants are terpenoids, phenolics, and alkaloids (Wink, 2010). Terpenoids are a large and diverse class of compounds that includes essential oils, hormones, and vitamins. Phenolics are a group of aromatic compounds that often function as antioxidants or ultraviolet (UV) absorbance. Alkaloids are a group of nitrogen-containing compounds that can have toxic effects on humans (Buchanan, 2015; Wink, 2010).

While all plants produce secondary metabolites, the type and number of metabolites can vary widely among species. Different plant families tend to specialize in producing specific classes of secondary metabolites. For example, the Solanaceae family (which includes potatoes, tomatoes, and peppers) is known for its high alkaloid content, while the Asteraceae family (which includes sunflowers, daisies, and chrysanthemums) is known for its high phenolic content. The biosynthetic pathways for secondary metabolites are often very complex, involving the coordinated regulation of multiple enzymes. These pathways often utilize unique enzymes that are not found in primary metabolism. Secondary metabolism is often considered to be more flexible and adaptable than primary metabolism. While the exact role of some secondary metabolites in plant biology is still not fully understood, these various compounds play essential roles in plant development and ecology (Wink, 2010).

Favorable hereditary characteristics (such as the capacity to synthesize secondary metabolites that aid in survival and reproduction) have been naturally selected over time via evolution. Examples include fragrant volatiles and colorful pigments that entice pollinators that disperse seeds, metabolic compounds that relieve or negate abiotic or biotic stressors, tastes and

sugars that attract animals, and the ability to produce noxious or toxic chemicals that repel pathogens, physical damage, consumption, and/or growth of neighboring vegetation (Buchanan, 2015; Wink, 2010).

Chemotaxonomy is the branch of knowledge that deals with the arrangement of plants according to their chemical constituents. The discipline has gained popularity due to recent discoveries of varying concentrations and prevalence of compounds within each plant species (Shumskaya and Wurtzel, 2013). Many factors are important to consider when looking at the three main classes of secondary metabolites, but two significant ones are genetic lineage and botanical nomenclature. An excellent example of this is phenolics, being found in all higher plants because they play a role in numerous defense mechanisms and the synthesis of lignin, flavonoids, anthocyanins, tannins, etc. (Bantis et al., 2016; Bourgaud et al., 2001; Castronuovo et al., 2019). On the other hand, alkaloid chemicals are more narrowly distributed in the plant kingdom and are often more species-specific. Terpenoids are a category of hydrocarbon-based natural compounds produced from isoprene units. Not only do these compounds have low boiling points and high volatilities, but they also possess unique physical/chemical properties. Terpenoids play an essential role in plant health, including the synthesis of plant hormones, attracting pollinators, and defense against pathogens and herbivores (Bourgaud et al., 2001; Bouwmeester et al., 2019). Many studies have demonstrated that secondary metabolism is directly linked to primary metabolism (Ashraf and Harris, 2013; Briggs and Huala, 1999; Frank and Cogdell, 1996; Lichtenthaler, 1987; Young, 1991).

Plants produce a wealth of compounds with significant economic value due to their high biological activity and low concentration in plant tissue. Humans have used secondary plant compounds for centuries, such as medicines, psychotropics, flavorings, and poisons. Secondary

compounds are frequently used in modern pharmaceuticals and holistic treatments (Abdel-Aal and Akhtar, 2006; Avneet et al., 2010; Bramley, 2000; Farnsworth, 1990; Rao and Rao, 2007; S Bendre and D Rajput, 2016; Santin et al., 2021). Plants have been prominent in sophisticated traditional medical systems used for thousands of years globally. Many pharmaceuticals are made from natural materials, and many additional synthetic goods are chemical modifications of natural products. Farnsworth stated that 119 characterized drugs were obtained commercially from higher plants, and over 74% were found from ethnobotanical sources (Farnsworth, 1990). Regarding any research conducted, both harmful/helpful biological activity in humans, acute sensitivity, and potential long-term effects must be considered, emphasizing secondary plant metabolites that have been shown to benefit general human health and vitality.

As stated before, light directly impacts primary and secondary metabolism (Taiz, 2010). It is a significant environmental stimulus that controls vital events in the plant life cycle, such as seed germination, blooming, and fruit ripening. Light also stimulates physiological and biochemical responses in the plant, allowing it to adapt to its surroundings and increasing its chances of survival/reproduction (Brody, 2011; Buchanan, 2015). Plant photoreceptors, such as phytochromes, cryptochromes, and phototropins, have been shown to up and down-regulate metabolic pathways that have a direct impact on plant growth, development, secondary metabolism, and physiology through the stimulation of light sensors (Briggs and Christie, 2002; Briggs and Huala, 1999; Christie, 2007). Blue wavelengths are the primary stimulators of cryptochromes and phototropins, while phytochromes respond to red and far-red wavebands (Briggs and Olney, 2001; Chaves et al., 2011; Fraikin et al., 2013; Kang et al., 2009; Santin et al., 2021). Changes in blue wavelengths that target phototropins or cryptochromes can affect primary and secondary metabolism, volatile production, carotenoid, and chlorophyll pigment

bioaccumulation, circadian rhythms, stomatal opening/closing, intermodal length, leaf area, and leaf thickness (Briggs and Christie, 2002; Briggs and Huala, 1999; Cashmore, 2003; Chaves et al., 2011; Chen and Chory, 2011; Christie, 2007; Fraikin et al., 2013; Galvao and Fankhauser, 2015; Kusuma and Bugbee, 2021; Sakai et al., 2001; Schmitt and Wulff, 1993)

Changes in particular red wavelengths that target phytochromes have a negative impact on germination rates, vegetative and reproductive growth/development, leaf size/thickness, and phenolic/antioxidant pathways. Sole source monochromatic light has been shown to inhibit plant growth and development, while full spectrum light, as well as specific mixtures of different blue (B) and red (R) wavelengths, promote it (Lin et al., 2013; Modarelli et al., 2022; Paradiso and Proietti, 2021; Shelford and Both, 2021; Sipos et al., 2021; Spalholz et al., 2020). Members associated with our research group have shown that various intensity ratios of B and R LED supplements significantly impact yield, carotenoid bioaccumulation, and nutrient uptake for a variety of specialty crops (Abney et al., 2013; Barickman et al., 2017; Hammock, 2018; Hammock et al., 2020; Hammock et al., 2021; Hammock and Sams, 2021; Kopsell and Sams, 2013; Kopsell et al., 2014; Kopsell et al., 2007; Kopsell et al., 2015; Kopsell et al., 2017; Lefsrud et al., 2008; Metallo et al., 2018). Our group has also shown that primary and secondary metabolism can be manipulated by applying warm/cool full-spectrum white light (2500-6500K), which will be documented in this dissertation.

Isoprenoids

Isoprenoids represent the largest and most diverse group of primary and secondary metabolites (Wink, 2008). They are primarily found in the plant kingdom, and many have considerable economic value. It has been well documented that metabolic flux within the

isoprenoid pathway is highly regulated and causes significant changes in secondary metabolic resource allocation. This regulation is achieved by the activity of several enzymes that catalyze the formation and degradation of isoprenoids (Wink, 2010). The main aim of this project is to study how different spectral qualities influence the production of metabolic products (such as aroma volatiles, flavonoids, carotenoids, etc.) because of this, comprehending the mechanisms of enzymes and genes that control the isoprenoid metabolic network will be crucial. Figures 1.6 and 1.7 show pertinent terpenoid and isoprenoid pathways, respectively (Wink, 2010).

All isoprenoids are formed from two universal C_5 precursors: Isopentenyl pyrophosphate (IPP) and dimethylallyl pyrophosphate (DMAPP). Isoprenoids are classified into specific groups according to the number of C_5 units they contain. The simplest known isoprenoid, isoprene, only has one C_5 unit and is a hemiterpene. Monoterpenes consist of two C_5 units, sesquiterpenes have three C_5 units, diterpenes have four C_5 units, triterpenes have six C_5 units, and polyterpenes have more than eight C_5 units (Buchanan, 2015; Wink, 2008, 2010).

Two known pathways are utilized to biosynthesize isoprenoid base units in plants, the mevalonate (MVA) pathway and deoxyxylulose 5-phosphate/2-C-methyl-D-erythritol 4-phosphate (DXP/MEP) pathway (also called MEP pathway). The MVA pathway occurs primarily in the cytosol, while the MEP pathway occurs in the plastid and is mevalonate-independent (Bick and Lange, 2003). The equilibrium of IPP and DMAPP is primarily controlled by IPP isomerase (IPPI), which reversibly converts IPP to DMAPP. The synthesis of IPP and DMAPP can be conceptually viewed as the first module of the isoprenoid pathway network. The MVA pathway primarily synthesizes sterols, some sesquiterpenes, ubiquinones, etc., while the MEP pathway predominately synthesizes hemiterpenes, monoterpenes, diterpenes, and some polyterpenes. While both pathways are in different parts of the cell, there is significant communication between the

two. Homologs of all known enzymes for cytoplasmic and plastid IPP synthesis are found in all analyzed plant species, suggesting that both MVA and MEP pathways are highly conserved in plants. In addition, the equilibrium of these two compounds is controlled by a complex network of genes and enzymes, which are vital for secondary metabolism resource allocation (i.e., the amount of downstream metabolic products that are produced from isoprene building blocks) and defense against environmental stressors (Buchanan, 2015; Taiz et al., 2015; Wink, 2010).

The MVA pathway begins with the condensation of three units of acetyl-CoA to 3-hydroxy-3-methylglutaryl-CoA (HMG-CoA) and is then reduced to mevalonate (MVA), followed by successive phosphorylation steps at C-5 of mevalonate, and a decarboxylation/elimination step leading to IPP (Bohlmann and Keeling, 2008). IPP derived from this pathway is then used to create cytosolic and mitochondrial isoprenoids such as sesquiterpenes, sterols, and the side chain of ubiquinone (Buchanan, 2015; Wink, 2010).

Acetyl-CoA: Acetyl-CoA C-acetyltransferase (AACT) catalyzes the first step of the MVA pathway, which is the condensation of two acetyl-CoA molecules to form acetoacetyl-CoA. AACT belongs to the thiolase family and has been cataloged in multiple species, such as Arabidopsis and the mint family. 3-hydroxy-3methylglutaryl-CoA synthase (HMGS) catalyzes the condensation of acetyl-CoA with acetoacetyl-CoA to produce HMG-CoA and CoA. HMGS can be broken by the inhibitor F244, which will break the MVA pathway. Plants with high HMGS expression show rapid cell growth and increased secondary metabolic products, suggesting that this gene is highly regulated at the beginning of the MVA pathway. 3-hydroxy-3-methylglutaryl-CoA reductase (HMGR) is a rate-limiting enzyme necessary for the MVA pathway and synthesizing triterpenoids. Two kinases of this pathway include the mevalonate kinase (MK) and mevalonate 5-diphosphate kinase (PMK). Mevalonate 5-diphosphate decarboxylase (MDC) converts MVPP and IPP

isomerase. IPP isomerase (IPI) converts IPP to DMAPP and is the only gene/enzyme that is not limited to the cytosol, which proves critical for the equilibrium regulation of IPP and DMAPP (Buchanan, 2015; Cunningham and Gantt, 1998; Wink, 2010)

Plastid isoprenoids derive IPP synthesized by the MEP pathway. The initial reaction of the MEP pathway is catalyzed by 1-deoxy-D-xylulose 5-phosphate synthase (DXS) and requires the condensation of hydroxyethyl thiamin derived from pyruvate with the C1 aldehyde group of D-glyceraldehyde 3-phosphate (GA-3P) to produce DXP. A reduction of DXP by the enzyme DXP reductoisomerase (DXR) yields MEP. After the conversion of MEP into 2-C-methyl-D-erythritol 2,4-cyclodiphosphate (ME-2,4cPP) in three enzymatic steps, a reduction catalyzed by 1-hydroxy-2-methyl-2-butenyl 4-diphosphate (HMBPP) synthase (HDS) produces HMBPP, which is finally converted into IPP and dimethylallyl diphosphate (DMAPP) by the enzyme HMBPP reductase (HDR). DMAPP is considered a reactive starter molecule for subsequent condensation reactions with IPP (Lange et al., 2000; Wink, 2010).

Light has a profound impact on the MEP isoprenoid pathway. This is expected because metabolites derived from this pathway include carotenoids, chlorophylls, xanthophylls, etc., which are the pigment-protein complexes used to absorb light energy. While the light intensity and spectral quality regulate MEP pathway activity and many downstream branches of this pathway, MVA pathway activity has been shown to be negatively impacted by light (decrease of HMGR expression) (Buchanan, 2015; Wink, 2010).

1-Deoxy-D-xylulose 5-phosphate synthase (DXPS) is the first enzyme in the MEP pathway and is considered to be rate-limiting. In tomatoes, the DXPS gene shows developmental and organ-specific regulation of mRNA accumulation with a strong correlation to increased carotenoid synthesis during fruit development (Lois et al., 2000). 1-Deoxy-D-xylulose 5-phosphate

reductoisomerase (DXR) catalyzes the subsequent reduction of DXP to form MEP and is a building block for alkaloids. DXR is also a target protein for developing herbicides because of its prominent role in producing isoprenoids. 4-(Cytidine 5'-diphospho)-2-C-methyl-D-erythritol kinase (CMK) has few reported activities in plants but is light dependent and requires Mg^{2+} for its activity. Hydroxymethylbutenyl 4-diphosphate synthase (HDS) is required for the final two steps of the MEP pathway, namely the formation of HMBPP and the conversion to a 5:1 mixture of IPP and DMAPP via IDS. HDS has also exhibited high expression during carotenoid accumulation in ripening tomato fruit (Khachik et al., 2002; Wink, 2010).

By observing the regulation of these genes and enzymes across various spectral qualities and quantifying the metabolites at each step within pertinent pathways, we can determine which of them significantly impacts critical metabolic pathways important for flavor and quality. This project will investigate additional genes to determine which are responsible for specific bioaccumulation of secondary metabolic products (such as carotenoids, VOCs, flavonoids, etc.) (Buchanan, 2015; Wink, 2010).

Carotenoids

Carotenoids are a class of organic compounds produced by plants and algae. They are responsible for the pigmentation of many fruits and vegetables. Carotenoids are created through the process of photosynthesis, and they are composed of a long chain of carbon atoms. There are two main types of carotenoids: carotenes and xanthophylls. Carotenes are responsible for plants' yellow and orange pigmentation, while xanthophylls give plants their red and pink colors. Carotenoids serve several vital functions in plant biology. For example, they help protect plants from damage caused by ultraviolet light and play a role in photosynthesis. Additionally,

carotenoids can be converted into Vitamin A, which is essential for human health. As a result, carotenoids play a vital role in both plant and human biology (Wink, 2010). This project will emphasize carotenoid metabolism, along with other isoprenoids.

Over 600 carotenoids are known to date. They belong to the category of tetraterpenoids, meaning they contain 40 carbon atoms and are built from four individual terpene units. The physical structure of carotenoids is responsible for chemical properties and human health benefits, as well as colorations that range from pale yellow to deep red (Khoo et al., 2011). Carotenoids are most effective in absorbing wavelengths that fall within the 400-550 nm range. The color of these tissues is commonly hidden by chlorophyll in photosynthetic tissues but may become apparent in reproductive tissues such as fruits, flowers, and tubers (Frank and Cogdell, 1996; Lichtenthaler, 1987; Young, 1991).

The carotenoid biosynthetic pathway plays important roles in plant biochemistry, such as photosynthesis, photoprotection, plant development, and stress hormones (Buchanan, 2015; Wink, 2010). There are at least five different roles carotenoids are thought to play in photosynthesis, which include light harvesting, photoprotection via triplet state chlorophyll quenching, singlet oxygen scavenging, excess energy dissipation, and structure stabilization/assembly (Esteban et al., 2015; Frank and Cogdell, 1996).

Metabolic products of the carotenoid pathway are typically vibrant hues and fragrant aromas, which play a role in plant signaling communication, influence food flavor and nutritional characteristics, and mediate plant-animal interactions (Khoo et al., 2011; Shumskaya and Wurtzel, 2013). Carotenoids are primarily localized on membranes of plastids, which are known to be the site of carotenoid biosynthesis (Kopsell et al., 2005; Yeum and Russell, 2002). Plastids are dynamic organelles that undergo constant chemical and structural changes, and carotenoid

synthesis is particularly sensitive to them (Frank and Cogdell, 1996; Young, 1991). The location and composition of a synthesis site determine the fate of its metabolic products. The majority of carotenoids are produced on thylakoid membranes for use in photosynthesis, photoprotection, quenching, etc., whereas carotenoids found on the chloroplast envelope membranes and plastogloubles typically become apocarotenoids that mediate signaling, etc. (Esteban et al., 2015; Felemban et al., 2019; Shumskaya and Wurtzel, 2013; Sun et al., 2018). Biological roles and synthesis sites of the metabolic end products produced by carotenoid pathways need further study to determine how to improve the bioaccumulation of nutritionally important carotenoids in edible tissues. Furthermore, comprehensive knowledge of the various effects each chemical component fulfills in general physiology and its interactions with spectral quality is necessary (Frank and Cogdell, 1996; Kopsell et al., 2005; Ouzounis et al., 2015; Shumskaya and Wurtzel, 2013; Yeum and Russell, 2002; Young, 1991).

The xanthophyll cycle is a process that helps regulate photosynthesis in plants. It does this by controlling the amount of light energy that is available for use (Demmig-Adams and Adams, 1996; Eskling et al., 1997; Latowski et al., 2004). The cycle involves several metabolites, including zeaxanthin, violaxanthin, and antheraxanthin. These molecules play essential roles in the absorption and dissipation of light energy. The xanthophyll cycle helps plants adapt to light intensity and spectrum changes. When a plant is overexposed to light, the carotenoid molecules help prevent damage by quenching radicals and dissipating heat. Violaxanthin is converted into zeaxanthin via antheraxanthin, which can help protect against photooxidative stress and lipid peroxidation as well as quench chlorophyll triplet states (Demmig-Adams and Adams, 1996; Frank and Cogdell, 1996; Wink, 2010).

Based on the current literature, there is strong evidence that greenhouse production with narrowband supplemental lighting is the best method for optimizing carotenoid accumulation in popular basil cultivars. Leafy specialty crops already contain high levels of nutritionally beneficial carotenoids and other phytonutrients, and supplemental lighting can drastically increase concentrations of those compounds. In the field, sweet basil may naturally accumulate high levels of nutritionally beneficial carotenoids, but supplementing high phytonutrient-containing basil cultivars with LED light in optimized greenhouses and/or vertical farms may have significant human health advantages.

The carotenoid pathway provides many metabolites that have beneficial antioxidant capacities for humans. These antioxidants can help protect the body against some types of disease and aspects of aging. These potent compounds have been proven to benefit human health in various ways (Namitha and Negi, 2010; Olson, 1999; Perera and Yen, 2007; Voutilainen et al., 2006) Consuming a wide range of fruit and vegetable crops with various combinations of carotenoid compounds was found to be strongly linked with decreased risks of cancer and ocular disease when compared to monomolecular carotenoid supplements (Rao and Rao, 2007; Voutilainen et al., 2006). For example, lutein and zeaxanthin have been shown to be protective against age-related macular degeneration (AMD), the leading cause of blindness in adults over the age of 55. Lutein and zeaxanthin are found in high concentrations in the central area of the retina called the macula. These carotenoids help to filter blue light and protect the retina from oxidative stress. A diet rich in these carotenoids has been linked with a reduced risk of AMD (Olson, 1999; Perera and Yen, 2007). Other carotenoids, such as beta-carotene, have also been shown to provide health benefits. Beta-carotene is converted into vitamin A in the body and is protective against cancer and other diseases. Vitamin A is essential for healthy vision, skin, and immune function (Rao and Rao,

2007). Enhancing and/or manipulating secondary metabolism (i.e., improving carotenoid bioaccumulation) in high-value specialty crops using supplemental lighting could result in improved nutritional quality and a decreased risk of common maladies and illnesses (Abdel-Aal and Akhtar, 2006; Fraser and Bramley, 2004; Khachik et al., 2002). This study aims to prove that LED light is an efficient and economical method for optimizing carotenoid accumulation in high-value specialty crops such as sweet basil, providing consumers with improved nutritional quality and health.

Sensory Analysis and Food Science Fundamentals

Taste and smell are two of the most important senses when it comes to sensory perception of food. Our sense of taste helps us determine the flavors of what we eat and how sweet, salty, sour, or bitter a particular food is. Sensory analysis is the scientific study of how humans perceive taste, smell, texture, and color in foods (Meligaard et al., 2007). This information can be used to improve the flavor and texture of foods and develop new products that appeal to consumers' senses. By understanding the fundamentals of sensory analysis, food scientists can create products that are nutritious and enjoyable to eat. The human sense of taste is mediated by taste receptors, which are specialized cells located in the tongue and palate. These receptors send information about the food's flavor to the brain, where it is interpreted. The four primary tastes are sweet, salty, sour, and bitter. In addition to these four tastes, there are also umami and fat tastes. Umami is a savory taste that is often described as "meaty" or "brothy." It is produced by amino acids, such as glutamic acid, found in many foods, including meats, cheeses, and soy sauce. The fat taste is mediated by a different type of receptor cell than the other tastes. Fat taste receptors are located in the mouth and send information about the fat content of food to the brain. Depending on the individual, fat tastes can be pleasurable or unpleasant (Lawless, 2010).

The sense of smell is another important sense when it comes to the consumption of food. The human nose can detect thousands of different odors, which helps us identify the foods we eat. Odors are molecules that dissolve in the mucus of the nose and bind to receptors in the olfactory epithelium, a thin layer of tissue in the upper part of the nose. The binding of an odor molecule to a receptor triggers a reaction that sends a signal to the brain, where the odor is interpreted (Lawless, 2010; Meligaard et al., 2007).

By definition, a volatile chemical compound readily vaporizes under standard temperature and atmospheric conditions (Alam, 2012). Highly volatile compounds will evaporate quickly and tend to exist in the vapor state at standard temperature and pressure (STP). Vapor pressure is the measurement of how readily a liquid (or other phase) forms vapor at a given temperature. Compounds with higher vapor pressures tend to evaporate more quickly. A compound's physical and chemical properties determine its vapor pressure. Volatiles tend to have low molecular weights, low polarity, and minimal intermolecular forces (i.e., no bonding interactions between other molecules in the mixture). Volatiles also tend to diffuse rapidly once they have transitioned to the vapor phase (i.e., high diffusion coefficient). The partial pressure of each volatile compound in a mixture contributes proportionally (both concentration and vapor pressure relative to the other compounds) to the overall vapor pressure of the total mixture (Alam, 2012). The terms flavor and aroma tend to denote naturally occurring compounds, while fragrance typically refers to synthetic compounds. Aromatic flavor compounds usually have low molecular weights (<300 Daltons), which directly contributes to their volatility along with chemical structure and high vapor pressures. Aroma affects both taste and smell, whereas fragrances only affect smell (Lawless, 2010; Wink, 2010).

An odorant is known as a chemical compound that gives off a particular smell or odor. Odorants are also known as active aroma compounds. Aroma active compounds have specific chemical structures that allow for the activation of olfactory receptors in humans, which, in turn, triggers a smell response (Meligaard et al., 2007). In nature, the large majority of aroma active compounds are considered to be volatile. Various receptors can detect a wide range of compounds across a wide range of affinities, and this combination (including both antagonistic and synergistic effects) is what we consider "smell." The concepts of volatility and aroma activity are related, but not synonymous. Volatility is the term used in physical chemistry to describe a compound's homeostatic and transitional phase behavior, while aroma active is a term used in sensory/food science to indicate that a compound produces a notable olfactory response in humans. In other words, aroma active compounds indicate that humans have an olfactory response, compared to a substance with high volatility that may or may not stimulate an olfactory response in humans but rapidly disperses in the gaseous phase under STP (Grosch, 2001; Lawless, 2010; Meligaard et al., 2007).

Many odorants are chemically classified as volatile compounds, as high volatility is needed to transport a compound to olfactory receptors (Meligaard et al., 2007). It is important to note that the terms aroma active compound and volatile compound are non-mutually exclusive. Not all volatiles are considered aroma active. Not all aroma active compounds are volatiles, but this is rare; some compounds that contribute heavily to aroma perception are transferred to the olfactory system via other volatile compounds present in the mixture (i.e., the vapor pressure of the total mixture higher than a specific compound in the mixture) (Alam, 2012; Meligaard et al., 2007).

Several analytical chemistry techniques, procedures, and instruments have been developed to identify and quantify important aroma active compounds; those important to sensory perception

and food science will be discussed in this section. Gas chromatography (GC) is an analytical lab instrument that can be used to separate, and quality/quantify unique compounds from a sample mixture. This instrument utilizes differences in physical and chemical properties of compounds to separate them from a sample mixture using an inert, pressurized gas and a long separatory column with specific column chemistry and known dimensions. A detector then analyzes these compounds to gain analytical information regarding each compound as it elutes from the column (Alam, 2012). Two common types of detection methods for gas chromatography include mass spectroscopy (MS), a measure of mass to charge ratio of ions in order to determine identity, and flame ionization detection (FID), a flame ionizes the flammable column effluent and measures the change in voltage, in units of ions per unit time, across the flame, to determine the sample concentration (Alam, 2012).

Static headspace sampling is a volatile technique commonly used with GC-MS. This technique is performed by placing a sample in a glass tube, applying standardized heat/vibration in some cases, and sampling the equalized headspace over the sample (commonly using helium or another inert gas for MS). Dynamic headspace sampling is similar, but the headspace is purged with a sizeable known volume of gas and removes a higher concentration of volatiles from the sample (compounds volatilize into the headspace in an attempt to reach equilibrium as the gas purges the headspace causing disequilibrium, and volatile compounds are directed from the headspace sampler to the GC injection port) (Alam, 2012).

Headspace sampling has a wide range of uses and can be paired with many detector types depending on the analysis goals. Headspace is excellent for biological or “dirty” samples that contain many undesirable compounds. It works well for a wide range of sample types, especially samples that cannot be easily extracted or have stability concerns. Headspace analysis requires

very little sample prep (compared to labor-intensive extractions), which provides the opportunity for high throughput and sample volume. Headspace shows a wide range of volatile compounds and metabolites. This is particularly useful for metabolomics and biochemistry research to determine the manipulation of pathways or resource allocation in response to environmental stimuli. In addition, some separation/extraction methods have shown bias and have varying extraction efficiencies toward certain compounds, which could cause issues with the analysis (Alam, 2012; Loughrin and Kasperbauer, 2003; Ochiai et al., 2014).

One of the critical drawbacks is that headspace sampling may not pick up all aroma active odorants in a particular matrix. For this reason, various techniques should be employed before analyzing compounds because of their physical/chemical properties. Most volatiles are unstable and will transform/degrade when exposed to high temperatures. This includes when headspace samples enter the GC inlet. Some volatile compounds are not stable, even at room temperature. Stabilization of key volatiles with other extraction methods has the potential for more reproducible results in this respect (Alam, 2012; Loughrin and Kasperbauer, 2003; Ochiai et al., 2014; Pourmortazavi and Hajimirsadeghi, 2007).

Headspace sampling is also not indicative of sensory perception unless paired with olfactometry or other sensory evaluation procedures. To get the most accurate understanding of aroma (and flavor), it is best to use multiple analytical and sensory techniques. Compounds with lower volatility will not be released at the same rate as high-volatility compounds, which may cause bias (Lawless, 2010; Meligaard et al., 2007). If headspace is saturated over a sample, some other volatiles with lower vapor pressures may not have the ability to volatilize. This may cause a bias towards samples with high concentrations and high vapor pressures, even though these compounds may not produce a significant flavor response (one benefit of dynamic headspace over

static). Metabolism of plants does not end after harvest, and poor sampling techniques could introduce variation into datasets (Buchanan, 2015). Immediate freezing is recommended to halt metabolism for plants and other biological samples, but extreme temperatures or rapid changes in temperatures may cause chemical degradation or alteration to the key compounds in the sample. Unequal treatment of each sample in terms of time in/out freezer, handling samples, etc., can also introduce unwanted variation (Lawless, 2010; Taylor, 1996).

Headspace can be used with either MS/FID but is better employed on MS so that it can be used to detect a wide range of compounds that have not been quantified with standards (i.e., exploratory research as compared to quantification study). MS can also be used with internal and/or external standards for quantification. FIDs are highly sensitive, and compounds typically must be quantified with external standards to determine the retention times of targeted compounds as well as the relationship among compounds (Alam, 2012). FID would not be ideal for an exploratory study but is great for high throughput and identifying known compounds. Samples with large quantities of unknown volatiles or unextracted biological samples (dirty) will not produce high-quality results using FID; therefore, extractions/separations are commonly employed. Extraction techniques can be used with headspace and are ideal for investigating a few specific compounds. Optimizing an extraction technique/column chemistry to obtain higher recovery/fewer variable results when analyzing key compounds is commonplace. It is always best to use multiple extraction protocols, instruments, and sampling methods to compare all aroma active compounds (Alam, 2012; Bayramoglu et al., 2008; Selli et al., 2014; Taylor, 1996).

Solid phase microextraction (SPME) is a headspace technique that uses a thin fiber with special coatings to absorb volatiles over a sample's enclosed headspace. This fiber is then placed directly into the GC for analysis. This technique is highly sensitive when compared to static

headspace and much less laborious than dynamic headspace. Compared to other protocols, this SPME is of relatively low cost. It is straightforward to automate the extraction and insertion process. It eliminates the need for solvent extraction, further reducing cost and consumables. This technique has a relatively short processing time. It has the ability for quick turnaround and high throughput. It can be used with solvent extractions or with non-extracted biological samples; cleaning up biological samples using SPME fibers will increase the longevity of the column/consumables as compared to standard headspace sampling of biological samples (Cheong et al., 2010; Martendal et al., 2011).

One drawback is that it is easy to over-saturate the fiber, which will skew results. Once the fiber is saturated, no other volatiles can be absorbed, which introduces sampling time as a factor (i.e., absorbance rates). Not all volatiles will bond to the sorbent at the same rate, and bias will lean towards compounds with high absorbance potential to the fiber coating (based on the chemistry of fiber coating and each compound). Compounds with higher volatility (i.e., more interactions per second with the SPME bonding sites) will also have a slight bias towards higher sorption rates. This method also requires an extra step between headspace absorption and release to the GC column and will tend to favor certain compounds. This has the potential to either clean up a sample and/or eliminate important components. It can be ideal for flavor volatiles, but compounds with lower volatility will not be suitable with this method (i.e., lipid oxidation, etc.). Similar to headspace, compounds with less vapor pressures may be inhibited from transforming to the gaseous phase (either by temperature or complete saturation of headspace) (Alam, 2012; Junior et al., 2011; Pourmortazavi and Hajimirsadeghi, 2007).

Solvent-assisted flavor evaporation (SAFE) is a direct distillation technique used to efficiently extract and isolate aroma volatiles from a wide variety of complex mixtures. This

method is used for sensory analysis to obtain high-quality volatile extracts that are free from non-volatile compounds, in addition to the interactions they can cause in chromatographic separation. Removal of non-volatile compounds is necessary for the accurate identification and quantification of key food odorants; non-volatile compounds have the potential to cause odorant discrimination (Engel, 1999).

Many prior distillation and separation methods did not perform efficiently (i.e., too much non-volatile matrix and not enough volatile compounds), and/or key compounds were degraded/chemically altered during the distillation process. SAFE has been shown to effectively separate many different types of food/aqueous matrices to obtain high-quality aqueous distillates that can be used for sensory analysis/odorant studies. To utilize this method effectively, a detailed knowledge of the chemical and physical properties of all compounds and solvents involved is required. SAFE uses temperature differences, pressure, and solvents (takes advantage of chemical/physical properties between volatile and non-volatile compounds) to obtain a high-quality extraction, solving many of the issues that were caused by previous distillation and solvent extraction methods. The temperature, pressure, and solvent chemistry parameters can be manipulated to improve extraction efficiency (Engel, 1999).

SAFE is considered the gold standard method for flavor extractions used in determining food odorants and other types of sensory studies. That being said, this method has a few drawbacks. If other compounds are removed from a food sample, it could also eliminate the potential positive and negative effects of those chemicals interacting with each other. While it has exceptional efficiency at isolating flavor volatiles, such as aromatic compounds, ethers, and esters, it has less efficiency extracting compounds like ketones, acids, pyrazines, etc., that may contribute to flavor (in which SPME does much better). As mentioned previously, combining extraction/analysis

methods allows for a better understanding of flavor chemistry and which compounds are the most important in sensory perception (Engel, 1999; Lucchesi et al., 2004; Murray et al., 2020; Pourmortazavi and Hajimirsadeghi, 2007; Reverchon and De Marco, 2006).

Aroma extract dilution analysis (AEDA) is a technique in which specific volatile extracts are serially diluted and then analyzed by gas chromatography-olfactometry (GC-O) to determine the maximum dilution value for a wide range of volatile odorants. The result is expressed as the flavor dilution (FD) factor, which is the concentration ratio of odorant in the primary extract to the most dilute in which the odorant is detected by GC-O (Murray et al., 2020). In other words, the FD of an odorant corresponds to the maximum dilution in which the odorant can still be detected. Compounds with higher FD are more potent. The FD is proportional to the odor activity value (OAV) in air. This analysis technique is primarily used to evaluate the relative potency and importance of odorants for further investigation in aroma analysis experiments. The downside to AEDA is that it does not take into account the unstable nature of volatiles, and there is potential for the degradation of notable odorants or transformation into other odorants that impact the overall profile (Lawless, 2010; Meligaard et al., 2007; Murray et al., 2020).

Stable isotope dilution analysis (SIDA) is an internal standard method that uses a stable isotope to quantify odorants of interest in a volatile extract. It can also help determine the recovery efficiency of extraction or distillation methods. Using this method helps improve the accuracy and precision of odorant quantification over conventional methods. Depending on your experimental objectives and procedures, it is possible to get inaccurate results with other calibration methods due to losses during extraction processes, volatile reactivity, and degradation (Lawless, 2010; Meligaard et al., 2007).

The SIDA method is considered the gold standard for quantifying odorants in the discipline of food science. It is ideal for liquid matrices but can be problematic for solid foods (i.e., solvent extraction/distillation vs. observing raw food matrices). Preparation of aroma models is much more difficult for solid foods, as it is impossible to reproduce the odorant compounds' distribution and chemical composition with stable isotopes throughout biological tissues (in this case, basil leaf tissue). This is not an issue if the odorants are free of interaction and are identical in the headspace (air) above the solid sample. Freshly synthesized stable isotopes for all compounds being analyzed must be on-hand during sample processing, which may be considered labor-intensive and cost-prohibitive depending on the lab conditions. Introducing internal standards to a liquid or solid matrix also has the potential to interfere with the matrix chemistry if the concentrations added are significant. For example, consider a compound found naturally at extremely low concentrations and close to the MS detection lower limit. The fraction of detectable isotope must be 90% of the natural volatile being observed (<5% suggested by literature), or it will not be detected by the MS. Adding a high concentration of isotope relative to the natural volatile will cause interference in the matrix with other compounds being separated during the extraction and MS analysis. Metabolomics and targeted volatile quantification for unprocessed solid biological samples typically use external calibration curves in the discipline of plant science, but using both types of methods can bridge the gap between sensory analysis and plant physiology. Lastly, the SIDA method works very well with MS but will not work with FID detectors because of the inability to differentiate masses (only the rate of change of ions concentration passing the flame). External calibration curves work well for both MS and FID, depending on the application and project objectives. It is advantageous to compare various calibration methods and detector types to get the most accurate results (Lawless, 2010; Murray et al., 2020; Van Eck et al., 2021).

Odor activity value (OAV) is a calculation used to determine the relative importance of each odorant's contribution to the aroma. Odor detection threshold values are calculated for each compound of importance. To determine the OAV, the concentration of a specific substance in a matrix is divided by the odor detection threshold concentration for that specific compound. It is typically assumed that odorants with higher OAVs contribute more strongly to the aroma.

It is essential to confirm the results of aroma analysis to ensure an aroma model is accurate. Therefore, it is necessary to construct synthetic blends of odorants using quantified analytical data and compare them against the original aroma model using a sensory panel. Disagreement indicates that the aroma model is incorrect and should be revised. This process is used for both solid and liquid matrices (Grosch, 2001; Lawless, 2010; Meligaard et al., 2007).

Omission studies are conducted to determine which of the more potent odorants significantly contribute to the aroma. Despite having a well-matched aroma model using dilution experiments, it is not possible to understand potential interactions such as inhibition and suppression of significant odorants. In these studies, each component is omitted to determine how it impacts the overall aroma model and whether it induces a significant change. This method helps bridge the gap between physical chemistry and human aroma perception, as the analytical data and OAVs cannot predict how the various odorant compounds will interact with one another to influence human sensory perception. A high OAV and/or high concentration compound does not necessarily indicate a high level of contribution to the overall aroma (Grosch, 2001).

Odorants, by definition, incite a sensory response. Many odorants are present in food and liquid samples, but a significant amount is in minute concentrations and cannot be decerned by the human nose. Those odorants may or may not contribute to the overall aroma of a sample depending on many factors. Key odorants are essential for the overall aroma of a sample (Lawless, 2010;

Meligaard et al., 2007). They are the compounds indicative of that sample, and an aroma model cannot be accurately reconstructed without all key odorants. Key odorants will have an OAV greater than 1. Altering the proportions of any of the key odorants will significantly change the overall aroma profile (Grosch, 2001; Lawless, 2010).

Optimizing the concentrations of key odorants has the potential to improve aroma perception and increase consumer preference of certain culinary herbs. Increasing all odorants and/or changing the ratios of those odorants would not necessarily lead to improved flavor or increased liking. It is necessary to determine what the consumers prefer rather than assuming that more volatiles lead to better flavor. Increasing all key odorants (proportional) may increase the intensity of perceived aroma, but this could lead to palate overwhelm and customer dissatisfaction. Knowing consumer preference can inform the choice of adding environmental stressors (i.e., light, temperature, water, etc.) to optimize ratios/concentrations of key odorants (Grosch, 2001; Lawless, 2010). Collaborating with sensory and food science when evaluating potential aroma changes in CEA research with high-value specialty crops is vital for successful applied research. This is especially true for experiments involving plant/light interactions (i.e., spectral quality, intensity, and duration).

In terms of volatile organic compounds (VOCs) in basil, oxygenated VOC substances are highly aromatic and account for the bulk of the flavor. According to dozens of different studies, it is believed that terpenes are the most aroma active compounds in basil. Many abiotic and biotic conditions, such as temperature, sunlight, turgor pressure, stomatal opening, humidity, and pest and pathogen pressures affect the insect-controlled release of these compounds. Emission is mainly confined to the surface of leaves with open stomata, but if structural damage occurs, specific defensive molecules may be released (Klimánková et al., 2008; Yousif et al., 1999).

At least two hundred distinct volatile compounds have been detected in basil varieties across many scientific studies employing a variety of analytical methods and extraction processes (GC-FID, GC-MS, LC-MS, HPLC, etc., combined with expeller press extraction, solvent extraction, hydrodistillation, steam distillation, low-pressure microwave extraction, simultaneous distillation-extraction, etc.); many of them have biological activities and pleasant aromas (Banthorpe et al., 1971; Bantis et al., 2016; Deschamps and Simon, 2006; Hasan et al., 2017; Lawless, 2010; Lee et al., 2005; Soran et al., 2009; Tarchoune et al., 2013). Although many of the essential aroma compounds have been identified, limited knowledge exists on relative basil VOC concentrations in relation to human bioactivity (i.e., taste and aroma perception) in conjunction with LED supplementary lighting. The relationships between the sensory, chemical, and physical properties of key aroma/flavor compounds with high and low biological activities should be explored (i.e., compounds sensed at very low concentrations vs. compounds sensed and higher concentrations). Specific types of basil (and other high-value specialty crops) in high demand should be further evaluated to determine their chemical composition and why people like them. It would also be beneficial to compare the human sensory perception of key aroma volatiles of basil (both positive and negative) in conjunction with changes to tissue concentration levels of those each respective compound; this provides more details about complex relationship of aroma volatile profiles and perception, which are the result of environmental manipulation or other stressors, and have significant potential to impact consumer perception and liking (Lawless, 2010; Meligaard et al., 2007; Seeburger et al., 2023; Tan et al., 2020; Walters et al., 2020b).

Molecular Techniques

Biotechnology and molecular techniques have revolutionized many aspects of biology and allowed for the examination of cellular processes on a much more detailed level. The development of these techniques has allowed for the examination of gene expression, protein synthesis, and metabolic pathways. They have also allowed for the identification of genes that are involved in specific pathways. This information can then be used to modify or engineer these genes to improve plant growth and productivity. Deoxyribonucleic acid (DNA) and ribonucleic acid (RNA) both play a vital role in the cell, as they are responsible for encoding the genetic information of the organism (Buchanan, 2015; Carson, 2019).

DNA is a long polymer chain of molecules of nucleotides. DNA holds the genetic code for biological organisms (and viruses) and forms the basic building blocks/instructions for life. It provides instructions for the production of proteins. Most proteins are enzymes that are necessary for many biological processes and metabolism. Each nucleotide comprises a phosphate group, a sugar group, and a nitrogen base. There are four nucleotides: guanine (G), cytosine (C), adenine (A), and thymine (T). The order of these four bases encodes genetic information. These nucleotides connect to form a double helix structure. The phosphate group and sugar group are on the sides, and the bases connect in the center. These base pairs are complementary, A-T and G-C. Combinations of these pairs (three) code for specific proteins. Organisms have both coding and non-coding DNA, meaning that some of the sequences are used while others are not. Some non-coding DNA is not used to make proteins, while others are transcribed into non-coding RNAs, regulatory RNAs, etc.; the ratio of coding vs. non-coding varies widely among species. It is thought, though still debated, that non-coding DNA was evolutionarily advantageous and provided redundancy/regulatory functions to help stabilize the genome across generations and reduce the

frequency of random mutations from becoming detrimental to survival/reproduction (Buchanan, 2015; Carson, 2019).

Messenger RNA (mRNA) is a single-stranded molecule (as compared to double-stranded DNA) and corresponds to a specific genetic sequence from DNA. The primary purpose of mRNA is to carry genetic information from the DNA in the nucleus to ribosomes in the cytoplasm, where proteins are made. mRNA is in the sequence of nucleotides, which are arranged in codons consisting of three base pairs. These are UCAG (uracil instead of thymine). DNA cannot leave the nucleus because of its length and bonding sites with histone proteins; mRNA can move out of the nucleus and react with the cellular machinery outside of the nucleus. Each codon represents a specific amino acid. The sequence of base pairs is transcribed from DNA by the enzyme RNA polymerase. mRNA processing significantly differs among eukaryotic (requires several processing steps before transport) and prokaryotic (rarely requires processing before transport and commonly matures directly after translation) cells (Buchanan, 2015; Carson, 2019; Taiz et al., 2015).

Transport also varies among eukaryotic and prokaryotic cells. Eukaryotic transcription and translation are spatially separated in the cell and require export to the cytoplasm (Buchanan, 2015; Carson, 2019; Taiz et al., 2015). Translation is the next step, in which mRNA translates the sequence of base pairs into a series of amino acids which form proteins. These proteins (primarily enzymes) are used for various metabolic processes. Translation can occur as free-floating ribosomes in the cytoplasm or directed to the endoplasmic reticulum. mRNA is very unstable. Prokaryotic mRNA commonly lasts a few seconds to a day, while eukaryotic mRNA lasts several minutes to days. Short mRNA lifetimes allow the cell to rapidly adapt to environmental stimuli and alter its biochemistry (i.e., protein synthesis) as needed. The higher the mRNA stability, the more protein could be produced (Carson, 2019).

Transfer RNA (tRNA) is a relatively short molecule (approximately 80 nucleotides) that transports specific amino acid components to the polypeptide chain at the ribosome. tRNA serves as a link between the mRNA and the sequence of proteins. They are necessary for the translation and synthesis of new proteins. The two classes of tRNA are cytoplasmic and mitochondrial. There are different tRNAs for each amino acid, and each has a specific site for the amino acid to attach. The primary role of tRNA is to specify which part from the genetic sequence relates to which amino acid during the process of protein synthesis (i.e., tRNA recognizes each of the codons within the mRNA sequence). An anticodon is a unit of three nucleotides that correspond with the three bases of an mRNA codon. The anticodon is on one end of the tRNA, while the complementary amino acid is on the other. Each tRNA has a specific anticodon sequence that can form the three complementary base pairs. Some codons code for the same amino acid, and there are several tRNA molecules with various codons that carry the same amino acid. During protein biosynthesis, tRNA molecules “deliver” amino acids to the new polypeptide chain in sequence. In reality, they are rapidly moving, and many tRNA molecules interact with one another in the matrix. When the proper tRNA anticodon strikes the next mRNA codon, the polymerization reaction (energetically favorable) occurs, which will either start/add to the polypeptide chain. When comparing the different types of RNA, mRNA brings the encoded message to the ribosome, and tRNA brings the building blocks. mRNA and tRNA (along with the catalytic ability/metabolic machinery of the ribosomes) allow for the synthesis of proteins based on the organism's genetic code (Buchanan, 2015; Carson, 2019; Taiz et al., 2015).

These three components (along with many other types of RNA and very complex mechanisms) are what encode and create all biological life. The encoding and translation of biological information are essential for the survival and adaptation of all organisms. The genetic

code is the sequence of codons, which are the building blocks of DNA. These codons are translated into proteins, which carry out metabolic processes necessary for life. The sequence of codons is determined by the order of base pairs in DNA, dictated by genes. Genes are distinct sequences of nucleotides that code for specific traits, commonly known as the basic physical functional unit of heredity. Gene expression is the process by which the information in a gene is used to synthesize a protein. This can be regulated by a variety of factors, including environmental stimuli. The transcription of DNA into mRNA is a highly regulated process that occurs in the nucleus of cells. This process is initiated by specific transcription factors that bind to promoter regions upstream of the gene. The promoter region is a sequence of DNA that signals the start of transcription. This region contains sequences that interact with proteins called transcription factors, which are responsible for activating gene transcription. There are many different transcription factors, and each one can activate or repress transcription from different genes. The translation of mRNA into proteins occurs in the cytoplasm and can be directed to different locations within the cell. The ribosomes are the site of protein synthesis, and they are composed of two subunits: a large subunit and a small subunit. The small subunit binds to mRNA and recognizes the codons, while the large subunit catalyzes the peptide bond formation between adjacent amino acids. tRNA molecules serve as intermediates between mRNA and protein synthesis, and they specifically recognize each codon and deliver its corresponding amino acid to the ribosome (Arif et al., 2010; Buchanan, 2015; Carson, 2019; Somssich, 2022; Taiz et al., 2015).

Environmental stimuli can alter protein synthesis, which can, in turn, affect gene expression. For example, exposure to stress hormones can activate specific genes that encode proteins involved in stress responses. This can allow the cell to adapt to changes in its environment rapidly. Gene expression can also be regulated by epigenetic mechanisms, which are chemical

modifications to DNA that can control gene function without changing the underlying sequence. These modifications can be passed down from one generation to the next, allowing organisms to respond quickly to changes in their environment (Buchanan, 2015; Carson, 2019; Taiz et al., 2015).

One of the most prevalent molecular techniques is RNA sequencing (RNA-Seq). This technique allows for the examination of the transcriptome, or the RNA expressed from a given gene. RNA-Seq can be used to examine gene expression at different stages of development, in different tissues, or in response to different environmental conditions (Arif et al., 2010; Carson, 2019; Gonda et al., 2020; Sams et al., 2011; Somssich, 2022). The results of such studies can be used to determine how different light spectra affect specific primary and secondary metabolic pathways. This data can be used to optimize light conditions to grow high-quality crops in greenhouses or vertical farms. Additional details regarding specific techniques and methods related to the project can be found later in this document.

Basil Background

The herb commonly known as "sweet basil" belongs to the Plantae Kingdom, Magnoliophyta Phylum, Magnoliopsida Class, Lamiales Order, Lamiacaea Family, *Ocimum* Genus, and *Basilicum* Species (Tucker and Debaggio, 2009). The *Ocimum* genus has more than 65 known species and can survive in both tropic/subtropic regions (Klimánková et al., 2008; Tucker and Debaggio, 2009). Basil is an annual flowering plant that originated in India. Depending on the variety, it can grow anywhere from 20-150 cm in height. It is highly nutritious, produces distinctive flavor compounds, and can be used in a wide range of applications (Kopsell et al., 2005; Naznin et al., 2019; Shanmugam et al., 2018).

Significant morphological and biochemical differences naturally exist among different basil varieties (Tucker and Debaggio, 2009). Sweet basil has been broadly classified into seven different morphotypes, which include: 1) tall, slender types; 2) 'Italian' large-leafed types; 3) dwarf types ('Bush' or 'Spicy Globe' basils); 4) compact types ('Thai' basils); 5.) purple types ('Purple Petra'); 6) *purpurascens* types ('Dark Opal' and other sweet purple basils); and 7) *citriodorum* types (flavored types) (Hussain et al., 2008; Tucker and Debaggio, 2009). Flavor profiles, culinary/medicinal uses, customer preference, and demand/popularity vary significantly among these different morphotypes (Deschamps and Simon, 2006; Klimánková et al., 2008). Genome sequencing has shown that sweet basil is a tetraploid organism with a genome size of approximately 2.13 Gbp (Gonda et al., 2020).

Basil has been used in many ways throughout human history. Some of these applications include direct/indirect consumption, culinary use, medicinal use, and even the manufacture of secondary products like essential oils, soaps, perfumes, tinctures, etc. (Raimondi et al., 2006; Tucker and Debaggio, 2009). The primary use of both fresh and dried basil is cooking. It has been cultivated and used as a flavoring agent for centuries across the globe. The essential oil extracted from fresh basil tissue contributes many flavors, aromas, and other phytonutrients to products in the food and cosmetic industries (Barbieri et al., 2004).

In general, the basil market has seen a shift in taste preference from Italian large leaf varieties to flavored varieties. This trend has been compounded by the popularity of breeding trials, specific LED supplemental lighting treatments, and other types of deliberate manipulations of environmental parameters to change flavor profiles. Basil consumption in the U.S. increased about 8-fold from 1960 to 1996 (Klimánková et al., 2008). It currently has one of the highest market values out of common culinary herbs. In addition, the global basil market (including food,

beverage, pharmaceutical, and cosmetic industries) was estimated at 58 million USD in 2021 and is expected to reach 64 million USD by 2028 (Marketwatch, 2022).

Basil has traditionally been cultivated in open fields; a large part of the global supply is still produced outdoors. Outdoor crops may be subject to unfavorable environmental conditions in addition to disease and pest pressures. Extreme weather, such as harsh temperatures and water stress, negatively impacts yield and quality parameters. Greenhouse hydroponic basil production provides optimal environmental control and fertility conditions, which can directly improve yields and quality. In addition to controlling temperature, humidity, and irrigation, many commercial greenhouse basil producers implement some type of supplemental lighting system to overcome adverse lighting conditions (i.e., lack of quality or intensity during winter months).

Basil was chosen for this experiment for several reasons. It makes an excellent model crop to use for light experiments and can be used to predict the impacts of light spectral quality/intensity on other high-value specialty crops (both at the primary and secondary metabolic level), specifically those in the Lamiaceae family (i.e., economically relevant). It contains a large portion of the secondary pathways that are required to produce important flavor, aroma, and medicinal compounds (isoprenoids, phenols, flavonoids, antioxidants) that are of great interest to both industry and research. The genome for basil has been fully sequenced, which will provide a solid baseline for our proposed mRNA sequencing experiments. Finally, sweet basil is among the most popular medicinal/culinary herbs across many cultures and cuisines.

Determining how spectral quality affects the aroma perception of basil and other high-value specialty crops will be vital as indoor production and vertical farms become more popular. If we can manipulate spectral quality to increase phytonutrient concentrations in basil (and other popular crops), we can provide healthier food and indirectly improve consumers' health.

Research Objectives

The primary objective of this project is to explore how alterations in spectral quality (from supplementary lighting and seasonal changes) affect primary and secondary metabolism in hydroponically grown greenhouse basil. We aim to push the bounds of current knowledge regarding plant/light interaction and provide practical advice to LED manufacturers and commercial growers. Based on previous and current studies, we believe altering spectral quality will significantly impact primary and secondary metabolism and can be used as a tool to improve flavor and/or increase phytonutrients with human health benefits.

During the transition semester between my MS and PhD, I conducted research to obtain the optimal ratio of B/R narrowband LED lighting across a variety of yield and quality parameters for greenhouse basil production. In addition to my MS research (Hammock, 2018), the results of those experiments established the ratio of B20/R80 to be ideal in terms of edible tissue biomass, nutrient uptake, carotenoid bioaccumulation, and aroma volatile products. We showed that the ideal B/R ratio and DLI provided with supplemental light varies according to the season (i.e., spectral quality and DLI requirements will change depending on the time of year and location) (Hammock, 2018). Variety trials were also performed to determine ideal basil varieties for experimentation. With this optimized lighting regime in mind, we sought to further explore the interaction between spectral quality and plant primary and secondary metabolism by designing a number of concurrent experiments that would build on our previous studies.

Phase 1 -- B/R Narrowband Light

During the first year of this project, we took various wavelengths of narrowband light and further explored the optimal ratio of B20/R80 from my master's research (Hammock, 2018; Hammock et al., 2020; Hammock et al., 2021).

The first objective was to determine the impact of discrete narrow-band blue/red (B/R) wavelengths on key aroma volatile concentrations in hydroponically grown basil. The second objective was to investigate secondary metabolic resource partitioning in response to specific blue/red supplemental wavelengths and variation in natural light (NL) intensity/spectral quality across growing seasons. By adding the same intensity of light across all treatments at the same ratio, but changing the specific narrowband blue wavelengths provided (i.e., 400 nm, 420 nm, 450 nm, 470 nm), we were able to show the influence of spectral quality (both seasonal and supplemental lighting effects) on primary and secondary metabolism. HPS, narrowband physiospec (blue/red), and full spectrum neutral white LED were added as a baseline. After exploring how combinations of different narrowband wavelengths influenced basil metabolism, we obtained a specific combination of B/R wavelengths (at the 20/80 ratio) that was ideal for yield (i.e., edible fresh and dry mass), aroma, and other quality parameters.

Phase 2 -- Warm/Cool Full Spectrum White Light

There has been significant discussion about the advantages and disadvantages between full spectrum supplements and narrowband B/R LEDs. A growing body of literature has shown the impacts of various broad and narrowband spectral distributions across many high-value crops. In the second year of this project, we explored the impact of two types of full spectrum white LEDs ("cool" LEDs with a higher B/R ratio and "warm" LEDs with a lower B/R ratio) on the same yield

and quality parameters that were looked at in the first experiment. We compared the best B/R ratio (from my MS) (Hammock, 2018; Hammock et al., 2020; Hammock et al., 2021), along with the optimal blend of wavelengths (from phase 1 of PhD), to warm and cool full spectrum LEDs. This experiment aimed to determine the metabolic impacts of our optimal wavelength/ratio narrowband B/R compared to broad-spectrum LEDs. We observed a wide range of impacts to yield and quality parameters imparted by our lighting treatments.

Phase 3 -- Sensory Panel, mRNA, and Analytical Data Analysis

Finally, our third and final set of experiments were designed to connect all the research from my projects. After determining the best narrowband and full spectrum treatment, we compared those to a traditional HPS treatment at natural light (NL) control. These treatments were tested across various parameters, both summer and winter.

Photosynthesis and primary metabolic data were recorded. Yields and biometric data were taken. VOC concentrations, carotenoids, and other secondary metabolic data were collected. A sensory panel was conducted to identify specific aroma notes, determine overall liking, and establish primary drivers for liking. mRNA sequencing was performed to determine differences in metabolic pathway expression based on lighting treatment. Finally, we evaluated analytical data (GCMS, HPLC, etc.) from the different light treatments along with the sensory panel and mRNA data to determine which lighting regime had the most positive impact on plant physiology and biochemistry. By combing and analyzing these datasets together, we were able to obtain a comprehensive picture of what is occurring at the molecular, metabolic, and whole plant level.

This holistic, interdisciplinary approach determined an "ideal" treatment across all parameters evaluated in this final experiment, which is defined as best compromise between yields,

nutrient content, and flavor preference. Every treatment influenced different aspects of plant morphology, biochemistry, physiology, and aroma profile. Therefore, it is crucial to consider two factors when choosing a lighting treatment for any given crop and growing operation: the individual metabolic effects as well as the overall metabolic effects a lighting regime will incur. Depending on the situation, a specific lighting treatment may be ideal for pushing a particular pathway, focusing on the maximum yield, or balancing many quality parameters for better flavor. Each strategy is ideal for different circumstances. Pushing specific pathways is great for essential oil extractions, food/beverage industries, and pharmaceuticals. Pushing for maximum yield may be ideal if quality or flavor is not a central selling point. Most commercial growing operations (involving high-value specialty crops) will typically strive to balance yield and flavor (i.e., primary and secondary metabolism) for a superior product highly preferred by consumers.

This dissertation, and the results provided within, will add to the growing body of literature regarding the complex interaction between light and plants. It will also further advise light manufacturers and commercial growers on which supplemental lighting regimes work best for their unique circumstances.

References

Abdel-Aal, E.S. and M. Akhtar. 2006. Recent Advances in the Analyses of Carotenoids and Their Role in Human Health. *Current Pharmaceutical Analysis* 2:195-204. doi:10.2174/157341206776819319

Abney, K.R., D.A. Kopsell, C.E. Sams, S. Zivanovic, and D.E. Kopsell. 2013. Uv-B Radiation Impacts Shoot Tissue Pigment Composition in *Allium Fistulosum* L. Cultigens. *ScientificWorldJournal* 2013:513867. doi:10.1155/2013/513867

Alam, M.A., M; Asif, H. 2012. Textbook of Practical Analytical Chemistry. Elsevier Health Sciences APAC, London.

Arif, I.A., M.A. Bakir, H.A. Khan, A.H. Al Farhan, A.A. Al Homaidan, A.H. Bahkali, M.A. Sadoon, and M. Shobrak. 2010. A Brief Review of Molecular Techniques to Assess Plant Diversity. *Int J Mol Sci* 11:2079-2096. doi:10.3390/ijms11052079

Ashraf, M. and P.J.C. Harris. 2013. Photosynthesis under Stressful Environments: An Overview. *Photosynthetica* 51:163-190. doi:10.1007/s11099-013-0021-6

Avneet, R., K. Jitendra, A.K. Chauhan, A. Rajoria, and J. Kumar. 2010. Anti-Oxidative and Anti-Carcinogenic Role of Lycopene in Human Health - a Review. *Journal of Dairying, Foods and Home Sciences* 29:157-165.

Banthorpe, D., B. Charlwood, and M. Francis. 1971. The Biosynthesis of Monoterpenes. *Chemical Reviews* 72:115-155.

Bantis, F., T. Ouzounis, and K. Radoglou. 2016. Artificial LED Lighting Enhances Growth Characteristics and Total Phenolic Content of *Ocimum Basilicum*, but Variably Affects Transplant Success. *Scientia Horticulturae* 198:277-283. doi:10.1016/j.scienta.2015.11.014

Bantis, F., S. Smirnakou, T. Ouzounis, A. Koukounaras, N. Ntagkas, and K. Radoglou. 2018. Current Status and Recent Achievements in the Field of Horticulture with the Use of Light-Emitting Diodes (LEDs). *Scientia Horticulturae* 235:437-451. doi:10.1016/j.scienta.2018.02.058

Barbieri, S., M. Elustondo, and M. Urbicain. 2004. Retention of Aroma Compounds in Basil Dried with Low Pressure Superheated Steam. *Journal of Food Engineering* 65:109-115. doi:10.1016/j.foodeng.2004.01.003

Barickman, T.C., D.A. Kopsell, and C.E. Sams. 2017. Abscisic Acid Improves Tomato Fruit Quality by Increasing Soluble Sugar Concentrations. *Journal of Plant Nutrition* 40:964-973. doi:10.1080/01904167.2016.1231812

Barta, D.J., T.W. Tibbitts, R.J. Bula, and R.C. Morrow. 1992. Evaluation of Light Emitting Diode Characteristics for a Space-Based Plant Irradiation Source. *Adv Space Res* 12:141-149. doi:10.1016/0273-1177(92)90020-x

Baumbauer, D.A., C.B. Schmidt, and M.H. Burgess. 2019. Leaf Lettuce Yield Is More Sensitive to Low Daily Light Integral Than Kale and Spinach. *HortScience* 54:2159-2162. doi:10.21273/hortsci14288-19

Bayramoglu, B., S. Sahin, and G. Sumnu. 2008. Solvent-Free Microwave Extraction of Essential Oil from Oregano. *Journal of Food Engineering* 88:535-540. doi:10.1016/j.jfoodeng.2008.03.015

Benke, K. and B. Tomkins. 2017. Future Food-Production Systems: Vertical Farming and Controlled-Environment Agriculture. *Sustainability: Science, Practice and Policy* 13:13-26. doi:10.1080/15487733.2017.1394054

Bick, J.A. and B.M. Lange. 2003. Metabolic Cross Talk between Cytosolic and Plastidial Pathways of Isoprenoid Biosynthesis: Unidirectional Transport of Intermediates across the Chloroplast Envelope Membrane. *Archives of Biochemistry and Biophysics* 415:146-154. doi:10.1016/s0003-9861(03)00233-9

Bispo-Jr, A.G., L.F. Saraiva, S.a.M. Lima, A.M. Pires, and M.R. Davolos. 2021. Recent Prospects on Phosphor-Converted LEDs for Lighting, Displays, Phototherapy, and Indoor Farming. *Journal of Luminescence* 237. doi:10.1016/j.jlumin.2021.118167

Bohlmann, J. and C.I. Keeling. 2008. Terpenoid Biomaterials. *Plant J* 54:656-669. doi:10.1111/j.1365-313X.2008.03449.x

Bourgaud, F., A. Gravot, S. Milesi, and E. Gontier. 2001. Production of Plant Secondary Metabolites: A Historical Perspective. *Plant Science* 161:839-851. doi:10.1016/s0168-9452(01)00490-3

Bouwmeester, H., R.C. Schuurink, P.M. Bleeker, and F. Schiestl. 2019. The Role of Volatiles in Plant Communication. *Plant J* 100:892-907. doi:10.1111/tpj.14496

Bramley, P.M. 2000. Is Lycopene Beneficial to Human Health? *Phytochemistry* 54:233-236. doi:10.1016/s0031-9422(00)00103-5

Briggs, W.R. and J.M. Christie. 2002. Phototropins 1 and 2: Versatile Plant Blue-Light Receptors. *Trends Plant Sci* 7:204-210. doi:10.1016/s1360-1385(02)02245-8

Briggs, W.R. and E. Huala. 1999. Blue-Light Photoreceptors in Higher Plants. *Annu Rev Cell Dev Biol* 15:33-62. doi:10.1146/annurev.cellbio.15.1.33

Briggs, W.R. and M.A. Olney. 2001. Photoreceptors in Plant Photomorphogenesis to Date. Five Phytochromes, Two Cryptochromes, One Phototropin, and One Superchrome. *Plant Physiol* 125:85-88. doi:10.1104/pp.125.1.85

Brody, S. 2011. The Genetics of Circadian Rhythms. 1st ed. Academic Press, San Diego, CA, USA.

Buchanan, B.G., W.; Jones, R. 2015. Biochemistry and Molecular Biology of Plants, Second Edition. Wiley Blackwell.

Bugbee, B. 2016. Toward an Optimal Spectral Quality for Plant Growth and Development: The Importance of Radiation Capture. *Acta Horticulturae*:1-12. doi:10.17660/ActaHortic.2016.1134.1

Carson, S.M., H.; Witherow, D.; Srougi, M. 2019. Molecular Biology Techniques.

Carvalho, S.D., M.L. Schwieterman, C.E. Abrahan, T.A. Colquhoun, and K.M. Folta. 2016. Light Quality Dependent Changes in Morphology, Antioxidant Capacity, and Volatile Production in Sweet Basil (*Ocimum Basilicum*). *Front Plant Sci* 7:1328. doi:10.3389/fpls.2016.01328

Cashmore, A.R. 2003. Cryptochromes. *Cell* 114:537-543. doi:10.1016/j.cell.2003.08.004

Castronuovo, D., D. Russo, R. Libonati, I. Faraone, V. Candido, P. Picuno, P. Andrade, P. Valentao, and L. Milella. 2019. Influence of Shading Treatment on Yield, Morphological Traits and Phenolic Profile of Sweet Basil (*Ocimum Basilicum* L.). *Scientia Horticulturae* 254:91-98. doi:10.1016/j.scienta.2019.04.077

Chaves, I., R. Pokorny, M. Byrdin, N. Hoang, T. Ritz, K. Brettel, L.O. Essen, G.T. Van Der Horst, A. Batschauer, and M. Ahmad. 2011. The Cryptochromes: Blue Light Photoreceptors in Plants and Animals. *Annu Rev Plant Biol* 62:335-364. doi:10.1146/annurev-arplant-042110-103759

Chen, M. and J. Chory. 2011. Phytochrome Signaling Mechanisms and the Control of Plant Development. *Trends Cell Biol* 21:664-671. doi:10.1016/j.tcb.2011.07.002

Cheong, K.W., C.P. Tan, H. Mirhosseini, N.S.A. Hamid, A. Osman, and M. Basri. 2010. Equilibrium Headspace Analysis of Volatile Flavor Compounds Extracted from Soursop (*Annona Muricata*) Using Solid-Phase Microextraction. *Food Research International* 43:1267-1276. doi:10.1016/j.foodres.2010.03.001

Chong, J.A., U.C. Samarakoon, and J.E. Faust. 2014. Effects of Daily Light Integral and Canopy Density on Shoot Growth and Development in a Poinsettia (*Euphorbia Pulcherrima* Willd. Ex. Klotsch) Stock Plant Canopy. *HortScience* 49:51-54. doi:10.21273/hortsci.49.1.51

Christiaens, A., P. Lootens, I. Roldán-Ruiz, E. Pauwels, B. Gobin, and M.C. Van Labeke. 2014. Determining the Minimum Daily Light Integral for Forcing of Azalea (*Rhododendron Simsii*). *Scientia Horticulturae* 177:1-9. doi:10.1016/j.scienta.2014.07.028

Christie, J.M. 2007. Phototropin Blue-Light Receptors. *Annu Rev Plant Biol* 58:21-45. doi:10.1146/annurev.arplant.58.032806.103951

Colquhoun, T.A., M.L. Schwieterman, J.L. Gilbert, E.A. Jaworski, K.M. Langer, C.R. Jones, G.V. Rushing, T.M. Hunter, J. Olmstead, D.G. Clark, and K.M. Folta. 2013. Light Modulation of Volatile Organic Compounds from Petunia Flowers and Select Fruits. *Postharvest Biology and Technology* 86:37-44. doi:10.1016/j.postharvbio.2013.06.013

Craver, J.K., J.K. Boldt, and R.G. Lopez. 2019. Comparison of Supplemental Lighting Provided by High-Pressure Sodium Lamps or Light-Emitting Diodes for the Propagation and Finishing of Bedding Plants in a Commercial Greenhouse. *HortScience* 54:52-59. doi:10.21273/hortsci13471-18

Cunningham, F.X. and E. Gantt. 1998. Genes and Enzymes of Carotenoid Biosynthesis in Plants. *Annu Rev Plant Physiol Plant Mol Biol* 49:557-583. doi:10.1146/annurev.arplant.49.1.557

Currey, C.J., V.A. Hutchinson, and R.G. Lopez. 2012. Growth, Morphology, and Quality of Rooted Cuttings of Several Herbaceous Annual Bedding Plants Are Influenced by Photosynthetic Daily Light Integral During Root Development. *HortScience* 47:25-30. doi:10.21273/hortsci.47.1.25

Currey, C.J. and R.G. Lopez. 2015. Biomass Accumulation and Allocation, Photosynthesis, and Carbohydrate Status of New Guinea Impatiens, Geranium, and Petunia Cuttings Are Affected by Photosynthetic Daily Light Integral During Root Development. *Journal of the American Society for Horticultural Science* 140:542-549. doi:10.21273/jashs.140.6.542

Davis, P.A. and C. Burns. 2016. Photobiology in Protected Horticulture. *Food and Energy Security* 5:223-238. doi:10.1002/fes3.97

Demmig-Adams, B. and W.W. Adams. 1996. The Role of Xanthophyll Cycle Carotenoids in the Protection of Photosynthesis. *Trends in Plant Science* 1:21-26. doi:10.1016/s1360-1385(96)80019-7

Demotes-Mainard, S., T. Péron, A. Corot, J. Bertheloot, J. Le Gourrierec, S. Pelleschi-Travier, L. Crespel, P. Morel, L. Huché-Thélier, R. Boumaza, A. Vian, V. Guérin, N. Leduc, and S. Sakr. 2016. Plant Responses to Red and Far-Red Lights, Applications in Horticulture. *Environmental and Experimental Botany* 121:4-21. doi:10.1016/j.envexpbot.2015.05.010

Deschamps, C. and J.E. Simon. 2006. Terpenoid Essential Oil Metabolism in Basil (*Ocimum Basilicum* L.) Following Elicitation. *Journal of Essential Oil Research* 18:618-621. doi:10.1080/10412905.2006.9699183

Długosz-Grochowska, O., A. Kołton, and R. Wojciechowska. 2016. Modifying Folate and Polyphenol Concentrations in Lamb's Lettuce by the Use of LED Supplemental Lighting

During Cultivation in Greenhouses. *Journal of Functional Foods* 26:228-237. doi:10.1016/j.jff.2016.07.020

Dou, H., G. Niu, M. Gu, and J. Masabni. 2017. Effects of Light Quality on Growth and Phytonutrient Accumulation of Herbs under Controlled Environments. *Horticulturae* 3. doi:10.3390/horticulturae3020036

Dutta Gupta, S. 2017. Light Emitting Diodes for Agriculture.

El-Ramady, H., M. Olle, B. Eichler-Lobermann, and E. Schnug. 2020. Towards a New Concept of Sustainable Plant Nutrition. *Environment, Biodiversity and Soil Security* 4:1-5. doi:10.21608/jenvbs.2020.21970.1080

Engel, W.B., W.; Schieberle, P. 1999. Solvent Assisted Flavour Evaporation - a New and Versatile Technique for the Careful and Direct Isolation of New Aroma Compounds from Complex Food Matrices. *Eur Food Res Technol* 209:237-241.

Engler, N. and M. Krarti. 2021. Review of Energy Efficiency in Controlled Environment Agriculture. *Renewable and Sustainable Energy Reviews* 141:110786. doi:10.1016/j.rser.2021.110786

Eskling, M., P.-O. Arvidsson, and H.-E. Akerlund. 1997. The Xanthophyll Cycle, Its Regulation and Components. *Physiologia Plantarum* 100:806-816. doi:10.1111/j.1399-3054.1997.tb00007.x

Esteban, R., J.F. Moran, J.M. Becerril, and J.I. García-Plazaola. 2015. Versatility of Carotenoids: An Integrated View on Diversity, Evolution, Functional Roles and Environmental Interactions. *Environmental and Experimental Botany* 119:63-75. doi:10.1016/j.envexpbot.2015.04.009

Farnsworth, N.R. 1990. The Role of Ethnopharmacology in Drug Development. *Ciba Found Symp* 154:2-11; discussion 11-21. doi:10.1002/9780470514009.ch2

Fausey, B.A., R.D. Heins, and A.C. Cameron. 2005. Daily Light Integral Affects Flowering and Quality of Greenhouse-Grown Achillea, Gaura, and Lavandula. *HortScience* 40:114-118. doi:10.21273/hortsci.40.1.114

Faust, J.E., V. Holcombe, N.C. Rajapakse, and D.R. Layne. 2005. The Effect of Daily Light Integral on Bedding Plant Growth and Flowering. *HortScience* 40:645-649. doi:10.21273/hortsci.40.3.645

Felemban, A., J. Braguy, M.D. Zurbriggen, and S. Al-Babili. 2019. Apocarotenoids Involved in Plant Development and Stress Response. *Frontiers in Plant Science* 10. doi:10.3389/fpls.2019.01168

Fraikin, G.Y., M.G. Strakhovskaya, and A.B. Rubin. 2013. Biological Photoreceptors of Light-Dependent Regulatory Processes. *Biochemistry (Mosc)* 78:1238-1253. doi:10.1134/S0006297913110047

Frank, H.A. and R.J. Cogdell. 1996. Carotenoids in Photosynthesis. *Photochem Photobiol* 63:257-264. doi:10.1111/j.1751-1097.1996.tb03022.x

Fraser, P.D. and P.M. Bramley. 2004. The Biosynthesis and Nutritional Uses of Carotenoids. *Prog Lipid Res* 43:228-265. doi:10.1016/j.plipres.2003.10.002

Frąszczak, B. and M. Knaflewski. 2009. Effect of Light Conditions and Temperature on Fresh Yield of Some Spice Plants Grown in Containers. *Journal of Fruit and Ornamental Plant Research* 71:59-67. doi:10.2478/v10032-009-0027-6

Galvao, V.C. and C. Fankhauser. 2015. Sensing the Light Environment in Plants: Photoreceptors and Early Signaling Steps. *Curr Opin Neurobiol* 34:46-53. doi:10.1016/j.conb.2015.01.013

Garland, K.F., S.E. Burnett, L.B. Stack, and D. Zhang. 2010. Minimum Daily Light Integral for Growing High-Quality Coleus. *HortTechnology* 20:929-933. doi:10.21273/horttech.20.5.929

Gent, M. 2014. Effect of Daily Light Integral on Composition of Hydroponic Lettuce. *HortScience* 49:173-179.

Goins, G.D., N.C. Yorio, M.M. Sanwo, and C.S. Brown. 1997. Photomorphogenesis, Photosynthesis, and Seed Yield of Wheat Plants Grown under Red Light-Emitting Diodes (LEDs) with and without Supplemental Blue Lighting. *J Exp Bot* 48:1407-1413. doi:10.1093/jxb/48.7.1407

Gómez, C., C.J. Currey, R.W. Dickson, H.-J. Kim, R. Hernández, N.C. Sabeh, R.E. Raudales, R.G. Brumfield, A. Laury-Shaw, A.K. Wilke, R.G. Lopez, and S.E. Burnett. 2019. Controlled Environment Food Production for Urban Agriculture. *HortScience* 54:1448-1458. doi:10.21273/hortsci14073-19

Gómez, C. and C.A. Mitchell. 2014. Supplemental Lighting for Greenhouse-Grown Tomatoes: Intracanopy LED Towers Vs. Overhead Hps Lamps. *Acta Horticulturae*:855-862. doi:10.17660/ActaHortic.2014.1037.114

Gómez, C., R.C. Morrow, C.M. Bourget, G.D. Massa, and C.A. Mitchell. 2013. Comparison of Intracanopy Light-Emitting Diode Towers and Overhead High-Pressure Sodium Lamps for Supplemental Lighting of Greenhouse-Grown Tomatoes. *HortTechnology* 23:93-98. doi:10.21273/horttech.23.1.93

Gonda, I., A. Faigenboim, C. Adler, R. Milavski, M.J. Karp, A. Shachter, G. Ronen, K. Baruch, D. Chaimovitsh, and N. Dudai. 2020. The Genome Sequence of Tetraploid Sweet Basil, *Ocimum Basilicum* L., Provides Tools for Advanced Genome Editing and Molecular Breeding. *DNA Res* 27. doi:10.1093/dnares/dsaa027

Graamans, L., A. Van Den Dobbelsteen, E. Meinen, and C. Stanghellini. 2017. Plant Factories: Crop Transpiration and Energy Balance. *Agricultural Systems* 153:138-147. doi:10.1016/j.agsy.2017.01.003

Groher, T., S. Rohlen-Schmittgen, A. Fiebig, G. Noga, and M. Hunsche. 2019. Influence of Supplementary LED Lighting on Physiological and Biochemical Parameters of Tomato (*Solanum Lycopersicum* L.) Leaves. *Scientia Horticulturae* 250:154-158. doi:10.1016/j.scienta.2019.02.046

Grosch, W. 2001. Evaluation of the Key Odorants of Foods by Dilution Experiments, Aroma Models and Omission. *Chem Senses* 26:533-545.

Hammock, H.A. 2018. The Impact of Blue and Red LED Lighting on Biomass Accumulation, Flavor Volatile Production, and Nutrient Uptake in Hydroponically Grown Genovese Basil. University of Tennessee, Knoxville, MS Horticulture.

Hammock, H.A., D.A. Kopsell, and C.E. Sams. 2020. Supplementary Blue and Red LED Narrowband Wavelengths Improve Biomass Yield and Nutrient Uptake in Hydroponically Grown Basil. *HortScience* 55:1888-1897. doi:10.21273/hortsci15267-20

Hammock, H.A., D.A. Kopsell, and C.E. Sams. 2021. Narrowband Blue and Red LED Supplements Impact Key Flavor Volatiles in Hydroponically Grown Basil across Growing Seasons. *Front Plant Sci* 12:623314. doi:10.3389/fpls.2021.623314

Hammock, H.A. and C.E. Sams. 2021. Quantification of Medicinally Important Volatile Organic Compounds in Common Basil Cultivars. *Acta Horticulturae*:113-122. doi:10.17660/ActaHortic.2021.1329.14

Hasan, M.M., T. Bashir, R. Ghosh, S.K. Lee, and H. Bae. 2017. An Overview of LEDs' Effects on the Production of Bioactive Compounds and Crop Quality. *Molecules* 22. doi:10.3390/molecules22091420

Hussain, A.I., F. Anwar, S.T. Hussain Sherazi, and R. Przybylski. 2008. Chemical Composition, Antioxidant and Antimicrobial Activities of Basil (Ocimum Basilicum) Essential Oils Depends on Seasonal Variations. *Food Chem* 108:986-995. doi:10.1016/j.foodchem.2007.12.010

Hutchinson, V.A., C.J. Currey, and R.G. Lopez. 2012. Photosynthetic Daily Light Integral During Root Development Influences Subsequent Growth and Development of Several Herbaceous Annual Bedding Plants. *HortScience* 47:856-860. doi:10.21273/hortsci.47.7.856

Jiang, J., A. Mohagheghi, and M. Moallem. 2020. Energy-Efficient Supplemental LED Lighting Control for a Proof-of-Concept Greenhouse System. *IEEE Transactions on Industrial Electronics* 67:3033-3042. doi:10.1109/tie.2019.2912762

Junior, S.B., A. De Marchi Tavares De Melo, C.A. Zini, and H.T. Godoy. 2011. Optimization of the Extraction Conditions of the Volatile Compounds from Chili Peppers by Headspace Solid Phase Micro-Extraction. *J Chromatogr A* 1218:3345-3350. doi:10.1016/j.chroma.2010.12.060

Kang, C.Y., H.L. Lian, F.F. Wang, J.R. Huang, and H.Q. Yang. 2009. Cryptochromes, Phytochromes, and Cop1 Regulate Light-Controlled Stomatal Development in Arabidopsis. *Plant Cell* 21:2624-2641. doi:10.1105/tpc.109.069765

Katzin, D., L.F.M. Marcelis, and S. Van Mourik. 2021. Energy Savings in Greenhouses by Transition from High-Pressure Sodium to LED Lighting. *Applied Energy* 281. doi:10.1016/j.apenergy.2020.116019

Kelly, N. and E.S. Runkle. 2020. Spectral Manipulations to Elicit Desired Quality Attributes of Herbaceous Specialty Crops. *European Journal of Horticultural Science* 85:339-343. doi:10.17660/eJHS.2020/85.5.5

Khachik, F., L. Carvalho, P.S. Bernstein, G.J. Muir, D.Y. Zhao, and N.B. Katz. 2002. Chemistry, Distribution, and Metabolism of Tomato Carotenoids and Their Impact on Human Health. *Exp Biol Med (Maywood)* 227:845-851. doi:10.1177/153537020222701002

Khoo, H.E., K.N. Prasad, K.W. Kong, Y. Jiang, and A. Ismail. 2011. Carotenoids and Their Isomers: Color Pigments in Fruits and Vegetables. *Molecules* 16:1710-1738. doi:10.3390/molecules16021710

Kim, H.J., M.Y. Lin, and C.A. Mitchell. 2019. Light Spectral and Thermal Properties Govern Biomass Allocation in Tomato through Morphological and Physiological Changes. *Environmental and Experimental Botany* 157:228-240. doi:10.1016/j.envexpbot.2018.10.019

Klimánková, E., K. Holadová, J. Hajšlová, T. Čajka, J. Poustka, and M. Koudela. 2008. Aroma Profiles of Five Basil (*Ocimum Basilicum* L.) Cultivars Grown under Conventional and Organic Conditions. *Food Chemistry* 107:464-472. doi:10.1016/j.foodchem.2007.07.062

Kopsell, D.A., D.E. Kopsell, and J. Curran-Celentano. 2005. Carotenoid and Chlorophyll Pigments in Sweet Basil Grown in the Field and Greenhouse. *HortScience* 40:1230-1233. doi:10.21273/hortsci.40.5.1230

Kopsell, D.A. and C.E. Sams. 2013. Increases in Shoot Tissue Pigments, Glucosinolates, and Mineral Elements in Sprouting Broccoli after Exposure to Short-Duration Blue Light from Light Emitting Diodes. *Journal of the American Society for Horticultural Science* 138:31-37. doi:10.21273/jashs.138.1.31

Kopsell, D.A., C.E. Sams, T.C. Barickman, and R.C. Morrow. 2014. Sprouting Broccoli Accumulate Higher Concentrations of Nutritionally Important Metabolites under Narrow-Band Light-Emitting Diode Lighting. *Journal of the American Society for Horticultural Science* 139:469-477. doi:10.21273/jashs.139.4.469

Kopsell, D.A., C.E. Sams, C.S. Charron, W.M. Randle, and D.E. Kopsell. 2007. Kale Carotenoids Remain Stable While Glucosinolates and Flavor Compounds Respond to Changes in Selenium and Sulfur Fertility. *Acta Horticulturae* 744:303-310. doi:10.17660/ActaHortic.2007.744.31

Kopsell, D.A., C.E. Sams, and R.C. Morrow. 2015. Blue Wavelengths from LED Lighting Increase Nutritionally Important Metabolites in Specialty Crops. *HortScience* 50:1285-1288. doi:10.21273/hortsci.50.9.1285

Kopsell, D.A., C.E. Sams, and R.C. Morrow. 2017. Interaction of Light Quality and Fertility on Biomass, Shoot Pigmentation and Xanthophyll Cycle Flux in Chinese Kale. *J Sci Food Agric* 97:911-917. doi:10.1002/jsfa.7814

Korczynski, P.C., J. Logan, and J.E. Faust. 2002. Mapping Monthly Distribution of Daily Light Integrals across the Contiguous United States. *HortTechnology* 12:12-16. doi:10.21273/horttech.12.1.12

Kusuma, P. and B. Bugbee. 2021. Far-Red Fraction: An Improved Metric for Characterizing Phytochrome Effects on Morphology. *Journal of the American Society for Horticultural Science* 146:3-13. doi:10.21273/jashs05002-20

Landi, M., M. Zivcak, O. Sytar, M. Brestic, and S.I. Allakhverdiev. 2020. Plasticity of Photosynthetic Processes and the Accumulation of Secondary Metabolites in Plants in Response to Monochromatic Light Environments: A Review. *Biochim Biophys Acta Bioenerg* 1861:148131. doi:10.1016/j.bbabio.2019.148131

Lange, B.M., T. Rujan, W. Martin, and R. Croteau. 2000. Isoprenoid Biosynthesis: The Evolution of Two Ancient and Distinct Pathways across Genomes. *Proc Natl Acad Sci U S A* 97:13172-13177. doi:10.1073/pnas.240454797

Larsen, D.H., E.J. Woltering, C.C.S. Nicole, and L.F.M. Marcelis. 2020. Response of Basil Growth and Morphology to Light Intensity and Spectrum in a Vertical Farm. *Front Plant Sci* 11:597906. doi:10.3389/fpls.2020.597906

Latowski, D., J. Grzyb, and K. Strzalka. 2004. The Xanthophyll Cycle—Molecular Mechanism and Physiological Significance. *Acta Physiol Plant* 26:197-212.

Lawless, H.H., H. . 2010. Sensory Evaluation of Food. SpringerLink.

Lee, S.J., K. Umano, T. Shibamoto, and K.G. Lee. 2005. Identification of Volatile Components in Basil (*Ocimum Basilicum* L.) and Thyme Leaves (*Thymus Vulgaris* L.) and Their Antioxidant Properties. *Food Chemistry* 91:131-137. doi:10.1016/j.foodchem.2004.05.056

Lefsrud, M.G., D.A. Kopsell, and C.E. Sams. 2008. Irradiance from Distinct Wavelength Light-Emitting Diodes Affect Secondary Metabolites in Kale. *HortScience* 43:2243-2244. doi:10.21273/hortsci.43.7.2243

Leiser, A.T., A.C. Leopold, and A.L. Shelley. 1960. Evaluation of Light Sources for Plant Growth. *Plant Physiol* 35:392-395. doi:10.1104/pp.35.3.392

Li, Q. and C. Kubota. 2009. Effects of Supplemental Light Quality on Growth and Phytochemicals of Baby Leaf Lettuce. *Environmental and Experimental Botany* 67:59-64. doi:10.1016/j.envexpbot.2009.06.011

Lichtenthaler, H.K. 1987. Chlorophylls and Carotenoids: Pigments of Photosynthetic Biomembranes. *PLOS ONE* 148:350-382. doi:10.1016/0076-6879(87)48036-1

Lin, K.-H., M.-Y. Huang, W.-D. Huang, M.-H. Hsu, Z.-W. Yang, and C.-M. Yang. 2013. The Effects of Red, Blue, and White Light-Emitting Diodes on the Growth, Development, and Edible Quality of Hydroponically Grown Lettuce (Lactuca Sativa L. Var. Capitata). *Scientia Horticulturae* 150:86-91. doi:10.1016/j.scienta.2012.10.002

Lois, L.M., M. Rodriguez-Concepcion, F. Gallego, N. Campos, and A. Boronat. 2000. Carotenoid Biosynthesis During Tomato Fruit Development: Regulatory Role of 1-Deoxy-D-Xylulose 5-Phosphate Synthase. *Plant J* 22:503-513. doi:10.1046/j.1365-313x.2000.00764.x

Loughrin, J.H. and M.J. Kasperbauer. 2003. Aroma Content of Fresh Basil (*Ocimum Basilicum* L.) Leaves Is Affected by Light Reflected from Colored Mulches. *J Agric Food Chem* 51:2272-2276. doi:10.1021/jf021076c

Lucchesi, M.E., F. Chemat, and J. Smadja. 2004. Solvent-Free Microwave Extraction of Essential Oil from Aromatic Herbs: Comparison with Conventional Hydro-Distillation. *J Chromatogr A* 1043:323-327. doi:10.1016/j.chroma.2004.05.083

Marketwatch. 2022. Basil Leaves Market Size Growth Expected at 1.36% Cagr by Forecast 2028. https://www.marketwatch.com/press-release/basil-leaves-market-size-growth-expected-at-136-cagr-by-forecast-2028-118-pages-report-2022-08-11

Martendal, E., C.D. De Souza Silveira, G.S. Nardini, and E. Carasek. 2011. Use of Different Sample Temperatures in a Single Extraction Procedure for the Screening of the Aroma Profile of Plant Matrices by Headspace Solid-Phase Microextraction. *J Chromatogr A* 1218:3731-3736. doi:10.1016/j.chroma.2011.04.032

Martineau, V., M. Lefsrud, M.T. Naznin, and D.A. Kopsell. 2012. Comparison of Light-Emitting Diode and High-Pressure Sodium Light Treatments for Hydroponics Growth of Boston Lettuce. *HortScience* 47:477-482. doi:10.21273/hortsci.47.4.477

Massa, G.D., H.H. Kim, R.M. Wheeler, and C.A. Mitchell. 2008. Plant Productivity in Response to LED Lighting. *HortScience* 43:1951-1956.

Mccartney, L. and M. Lefsrud. 2018. Protected Agriculture in Extreme Environments: A Review of Controlled Environment Agriculture in Tropical, Arid, Polar, and Urban Locations. *Applied Engineering in Agriculture* 34:455-473. doi:10.13031/aea.12590

Mccree, K.J. 1971. The Action Spectrum, Absorptance and Quantum Yield of Photosynthesis in Crop Plants. *Agricultural Meteorology* 9:191-216. doi:10.1016/0002-1571(71)90022-7

Mccree, K.J. 1973. The Measurement of Photosynthetically Active Radiation. *Solar Energy* 15:83-87. doi:10.1016/0038-092x(73)90010-8

Meligaard, M., G.V. Civile, and B.T. Carr. 2007. Sensory Evaluation Techniques, Fourth Edition CRC Press.

Metallo, R.M., D.A. Kopsell, C.E. Sams, and N.R. Bumgarner. 2018. Influence of Blue/Red Vs. White LED Light Treatments on Biomass, Shoot Morphology, and Quality Parameters of

Hydroponically Grown Kale. *Scientia Horticulturae* 235:189-197. doi:10.1016/j.scienta.2018.02.061

Mitchell, C.A. 2004. Controlled Environments in Plant-Science Research and Commercial Agriculture. *Int J Biom* 33:1-12.

Mitchell, C.A. 2022. History of Controlled Environment Horticulture: Indoor Farming and Its Key Technologies. *HortScience* 57:247-256. doi:10.21273/hortsci16159-21

Mitchell, C.A., J.F. Burr, M.J. Dzakovich, C. Gómez, R. Lopez, R. Hernández, C. Kubota, C.J. Currey, Q. Meng, E.S. Runkle, C.M. Bourget, R.C. Morrow, and A.J. Both. 2015. Light-Emitting Diodes in Horticulture. *Horticultural Reviews* 43:1-87.

Moccaldi, L.A. and E.S. Runkle. 2007. Modeling the Effects of Temperature and Photosynthetic Daily Light Integral on Growth and Flowering of Salvia Splendens and Tagetes Patula. *Journal of the American Society for Horticultural Science* 132:283-288. doi:10.21273/jashs.132.3.283

Modarelli, G.C., R. Paradiso, C. Arena, S. De Pascale, and M.-C. Van Labeke. 2022. High Light Intensity from Blue-Red LEDs Enhance Photosynthetic Performance, Plant Growth, and Optical Properties of Red Lettuce in Controlled Environment. *Horticulturae* 8. doi:10.3390/horticulturae8020114

Mokvist, F., F. Mamedov, and S. Styring. 2014. Defining the Far-Red Limit of Photosystem I: The Primary Charge Separation Is Functional to 840 Nm. *J Biol Chem* 289:24630-24639. doi:10.1074/jbc.M114.555649

Morrow, R.C. 2008. LED Lighting in Horticulture. *HortScience* 43:1947-1950. doi:10.21273/hortsci.43.7.1947

Murray, A.F., P.C.K. Wickramasinghe, and J.P. Munafo, Jr. 2020. Key Odorants from the Fragrant Bolete, *Suillus Punctipes*. *J Agric Food Chem* 68:8621-8628. doi:10.1021/acs.jafc.0c03389

Namitha, K.K. and P.S. Negi. 2010. Chemistry and Biotechnology of Carotenoids. *Crit Rev Food Sci Nutr* 50:728-760. doi:10.1080/10408398.2010.499811

Naznin, M.T., M. Lefsrud, V. Gravel, and M.O.K. Azad. 2019. Blue Light Added with Red LEDs Enhance Growth Characteristics, Pigments Content, and Antioxidant Capacity in Lettuce, Spinach, Kale, Basil, and Sweet Pepper in a Controlled Environment. *Plants (Basel)* 8. doi:10.3390/plants8040093

Nelson, J.A. and B. Bugbee. 2014. Economic Analysis of Greenhouse Lighting: Light Emitting Diodes Vs. High Intensity Discharge Fixtures. *PLOS ONE* 9:e99010. doi:10.1371/journal.pone.0099010

Ochiai, N., J. Tsunokawa, K. Sasamoto, and A. Hoffmann. 2014. Multi-Volatile Method for Aroma Analysis Using Sequential Dynamic Headspace Sampling with an Application to Brewed Coffee. *J Chromatogr A* 1371:65-73. doi:10.1016/j.chroma.2014.10.074

Oh, W., I.H. Cheon, K.S. Kim, and E.S. Runkle. 2009. Photosynthetic Daily Light Integral Influences Flowering Time and Crop Characteristics of Cyclamen Persicum. *HortScience* 44:341-344. doi:10.21273/hortsci.44.2.341

Olle, M. and A. Viršile. 2013. The Effects of Light-Emitting Diode Lighting on Greenhouse Plant Growth and Quality. *Agricultural and Food Science* 22:223-234. doi:10.23986/afsci.7897

Olson, J.A. 1999. Carotenoids and Human Health. *Arch Latinoam Nutr* 49:7S-11S.

Ouzounis, T., E. Rosenqvist, and C.O. Ottosen. 2015. Spectral Effects of Artificial Light on Plant Physiology and Secondary Metabolism: A Review. *HortScience* 50:1128-1135.

Paradiso, R. and S. Proietti. 2021. Light-Quality Manipulation to Control Plant Growth and Photomorphogenesis in Greenhouse Horticulture: The State of the Art and the Opportunities of Modern LED Systems. *Journal of Plant Growth Regulation* 41:742-780. doi:10.1007/s00344-021-10337-y

Pattison, P.M., J.Y. Tsao, G.C. Brainard, and B. Bugbee. 2018. LEDs for Photons, Physiology and Food. *Nature* 563:493-500. doi:10.1038/s41586-018-0706-x

Pazuki, A.A., F.; Pessarakli, Mohammad; Gurel, E.; Gurel, S. 2017. Plant Responses to Extended Photosynthetically Active Radiation (Epar). *Advances in Plants & Agriculture Research* 7. doi:10.15406/apar.2017.07.00260

Perera, C.O. and G.M. Yen. 2007. Functional Properties of Carotenoids in Human Health. *International Journal of Food Properties* 10:201-230. doi:10.1080/10942910601045271

Pimputkar, S., J.S. Speck, S.P. Denbaars, and S. Nakamura. 2009. Prospects for LED Lighting. *Nature Photonics* 3:180-182. doi:10.1038/nphoton.2009.32

Piovene, C., F. Orsini, S. Bosi, R. Sanoubar, V. Bregola, G. Dinelli, and G. Gianquinto. 2015. Optimal Red:Blue Ratio in Led Lighting for Nutraceutical Indoor Horticulture. *Scientia Horticulturae* 193:202-208. doi:10.1016/j.scienta.2015.07.015

Poorter, H., U. Niinemets, N. Ntagkas, A. Siebenkas, M. Maenpaa, S. Matsubara, and T. Pons. 2019. A Meta-Analysis of Plant Responses to Light Intensity for 70 Traits Ranging from Molecules to Whole Plant Performance. *New Phytol* 223:1073-1105. doi:10.1111/nph.15754

Pourmortazavi, S.M. and S.S. Hajimirsadeghi. 2007. Supercritical Fluid Extraction in Plant Essential and Volatile Oil Analysis. *J Chromatogr A* 1163:2-24. doi:10.1016/j.chroma.2007.06.021

Raimondi, G., F. Orsini, A. Maggio, S. De Pascale, and G. Barbieri. 2006. Yield and Quality of Hydroponically Grown Sweet Basil Cultivars. *Acta Horticulturae*:357-360. doi:10.17660/ActaHortic.2006.723.48

Rajan, P., R.R. Lada, and M.T. Macdonald. 2019. Advancement in Indoor Vertical Farming for Microgreen Production. *American Journal of Plant Sciences* 10:12. doi:10.4236/ajps.2019.108100

Ramin Shamshiri, R., F. Kalantari, K. C. Ting, K. R. Thorp, I. A. Hameed, C. Weltzien, D. Ahmad, and Z. Mojgan Shad. 2018. Advances in Greenhouse Automation and Controlled Environment Agriculture: A Transition to Plant Factories and Urban Agriculture. *International Journal of Agricultural and Biological Engineering* 11:1-22. doi:10.25165/j.ijabe.20181101.3210

Randall, W.C. and R.G. Lopez. 2014. Comparison of Supplemental Lighting from High-Pressure Sodium Lamps and Light-Emitting Diodes During Bedding Plant Seedling Production. *HortScience* 49:589-595. doi:10.21273/hortsci.49.5.589

Rao, A.V. and L.G. Rao. 2007. Carotenoids and Human Health. *Pharmacol Res* 55:207-216. doi:10.1016/j.phrs.2007.01.012

Reverchon, E. and I. De Marco. 2006. Supercritical Fluid Extraction and Fractionation of Natural Matter. *The Journal of Supercritical Fluids* 38:146-166. doi:10.1016/j.supflu.2006.03.020

Ritz, T., A. Damjanovic, K. Schulten, J.P. Zhang, and Y. Koyama. 2000. Efficient Light Harvesting through Carotenoids. *Photosynth Res* 66:125-144. doi:10.1023/A:1010750332320

Runkle, E.S. and R.D. Heins. 2006. Manipulating the Light Environment to Control Flowering and Morphogenesis of Herbaceous Plants. *Acta Horticulturae*:51-60. doi:10.17660/ActaHortic.2006.711.4

S Bendre, R. and J. D Rajput. 2016. Outlooks on Medicinal Properties of Eugenol and Its Synthetic Derivatives. *Natural Products Chemistry & Research* 04. doi:10.4172/2329-6836.1000212

Sakai, T., T. Kagawa, M. Kasahara, T.E. Swartz, J.M. Christie, W.R. Briggs, M. Wada, and K. Okada. 2001. Arabidopsis Nph1 and Npl1: Blue Light Receptors That Mediate Both Phototropism and Chloroplast Relocation. *Proc Natl Acad Sci U S A* 98:6969-6974. doi:10.1073/pnas.101137598

Sakshaug, E., A. Bricaud, Y. Dandonneau, P.G. Falkowski, D.A. Kiefer, L. Legendre, A. Morel, J. Parslow, and M. Takahashi. 1997. Parameters of Photosynthesis: Definitions, Theory and Interpretation of Results. *Journal of Plankton Research* 19:1637-1670. doi:10.1093/plankt/19.11.1637

Sams, C.E., D.R. Panthee, C.S. Charron, D.A. Kopsell, and J.S. Yuan. 2011. Selenium Regulates Gene Expression for Glucosinolate and Carotenoid Biosynthesis in Arabidopsis. *Journal of the American Society for Horticultural Science* 136:23-34. doi:10.21273/jashs.136.1.23

Samuoliene, G., A. Brazaityte, R. Sirtautas, A. Virsile, J. Sakalauskaite, S. Sakalauskiene, and P. Duchovskis. 2013. LED Illumination Affects Bioactive Compounds in Romaine Baby Leaf Lettuce. *J Sci Food Agric* 93:3286-3291. doi:10.1002/jsfa.6173

Samuoliene, G., R. Sirtautas, A. Brazaityte, and P. Duchovskis. 2012. LED Lighting and Seasonality Effects Antioxidant Properties of Baby Leaf Lettuce. *Food Chem* 134:1494-1499. doi:10.1016/j.foodchem.2012.03.061

Santin, M., A. Ranieri, and A. Castagna. 2021. Anything New under the Sun? An Update on Modulation of Bioactive Compounds by Different Wavelengths in Agricultural Plants. *Plants (Basel)* 10. doi:10.3390/plants10071485

Schmitt, J. and R.D. Wulff. 1993. Light Spectral Quality, Phytochrome and Plant Competition. *Trends Ecol Evol* 8:47-51. doi:10.1016/0169-5347(93)90157-K

Seeburger, P., A. Herdenstam, P. Kurtser, A. Arunachalam, V.C. Castro-Alves, T. Hyotylainen, and H. Andreasson. 2023. Controlled Mechanical Stimuli Reveal Novel Associations between Basil Metabolism and Sensory Quality. *Food Chem* 404:134545. doi:10.1016/j.foodchem.2022.134545

Selli, S., H. Kelebek, M.T. Ayseli, and H. Tokbas. 2014. Characterization of the Most Aroma-Active Compounds in Cherry Tomato by Application of the Aroma Extract Dilution Analysis. *Food Chem* 165:540-546. doi:10.1016/j.foodchem.2014.05.147

Shanmugam, K., J. Gimbun, B. Ranganathan, P. Suganthi, R.P. Srinivasan, and B. Purushothaman. 2018. A Comprehensive Review on Ocimum Basilicum. *Journal of Natural Remedies* 18:71-85. doi:10.18311/jnr/2018/21324

Sharathkumar, M., E. Heuvelink, and L.F.M. Marcelis. 2020. Vertical Farming: Moving from Genetic to Environmental Modification. *Trends Plant Sci* 25:724-727. doi:10.1016/j.tplants.2020.05.012

Shelford, T.J. and A.-J. Both. 2021. On the Technical Performance Characteristics of Horticultural Lamps. *Agriengineering* 3:716-727. doi:10.3390/agrieengineering3040046

Shumskaya, M. and E.T. Wurtzel. 2013. The Carotenoid Biosynthetic Pathway: Thinking in All Dimensions. *Plant Science* 208:58-63. doi:10.1016/j.plantsci.2013.03.012

Singh, D., C. Basu, M. Meinhardt-Wollweber, and B. Roth. 2015. LEDs for Energy Efficient Greenhouse Lighting. *Renewable and Sustainable Energy Reviews* 49:139-147. doi:10.1016/j.rser.2015.04.117

Sipos, L., L. Balázs, G. Székely, A. Jung, S. Sárosi, P. Radácsi, and L. Csambalik. 2021. Optimization of Basil (*Ocimum Basilicum* L.) Production in LED Light Environments – a Review. *Scientia Horticulturae* 289. doi:10.1016/j.scienta.2021.110486

Sipos, L., I.F. Boros, L. Csambalik, G. Székely, A. Jung, and L. Balázs. 2020. Horticultural Lighting System Optimalization: A Review. *Scientia Horticulturae* 273. doi:10.1016/j.scienta.2020.109631

Smith, H. 1982. Light Quality, Photoperception, and Plant Strategy. *Annual Review of Plant Physiology* 33:481-518. doi:10.1146/annurev.pp.33.060182.002405

Somssich, M. 2022. The Dawn of Plant Molecular Biology: How Three Key Methodologies Paved the Way. *Curr Protoc* 2:e417. doi:10.1002/cpz1.417

Soran, M.L., S.C. Cobzac, C. Varodi, I. Lung, E. Surducan, and V. Surducan. 2009. The Extraction and Chromatographic Determination of the Essentials Oils from *Ocimum Basilicum* L. By Different Techniques. *Journal of Physics: Conference Series* 182:012016. doi:10.1088/1742-6596/182/1/012016

Spalholz, H., P. Perkins-Veazie, and R. Hernández. 2020. Impact of Sun-Simulated White Light and Varied Blue:Red Spectrums on the Growth, Morphology, Development, and Phytochemical Content of Green- and Red-Leaf Lettuce at Different Growth Stages. *Scientia Horticulturae* 264. doi:10.1016/j.scienta.2020.109195

Stagnari, F., C. Di Mattia, A. Galieni, V. Santarelli, S. D'egidio, G. Pagnani, and M. Pisante. 2018. Light Quantity and Quality Supplies Sharply Affect Growth, Morphological, Physiological

and Quality Traits of Basil. *Industrial Crops and Products* 122:277-289. doi:10.1016/j.indcrop.2018.05.073

Sun, T., H. Yuan, H. Cao, M. Yazdani, Y. Tadmor, and L. Li. 2018. Carotenoid Metabolism in Plants: The Role of Plastids. *Mol Plant* 11:58-74. doi:10.1016/j.molp.2017.09.010

Taiz, L., E. Zeiger, I.M. Møller, and A. Murphy. 2015. Plant Physiology and Development. Sixth ed. Sinauer Associates, Inc.

Taiz, L.Z., E. 2010. Plant Physiology, Fifth Edition.

Tan, L., H. Nuffer, J. Feng, S.H. Kwan, H. Chen, X. Tong, and L. Kong. 2020. Antioxidant Properties and Sensory Evaluation of Microgreens from Commercial and Local Farms. *Food Science and Human Wellness* 9:45-51. doi:10.1016/j.fshw.2019.12.002

Tarakanov, I.G., D.A. Tovstyko, M.P. Lomakin, A.S. Shmakov, N.N. Sleptsov, A.N. Shmarev, V.A. Litvinskiy, and A.A. Ivlev. 2022. Effects of Light Spectral Quality on Photosynthetic Activity, Biomass Production, and Carbon Isotope Fractionation in Lettuce, Lactuca Sativa L., Plants. *Plants (Basel)* 11. doi:10.3390/plants11030441

Tarchoune, I., O. Baâtour, J. Harrathi, P.L. Cioni, M. Lachaâl, G. Flamini, and Z. Ouerghi. 2013. Essential Oil and Volatile Emissions of Basil (*Ocimum Basilicum*) Leaves Exposed to Nacl or Na2so4 Salinity. *Journal of Plant Nutrition and Soil Science* 176:748-755. doi:10.1002/jpln.201200278

Taylor, A.J. 1996. Volatile Flavor Release from Foods During Eating. *Crit Rev Food Sci Nutr* 36:765-784. doi:10.1080/10408399609527749

Tennessen, D.J., E.L. Singsaas, and T.D. Sharkey. 1994. Light-Emitting Diodes as a Light Source for Photosynthesis Research. *Photosynth Res* 39:85-92. doi:10.1007/BF00027146

Thapper, A., F. Mamedov, F. Mokvist, L. Hammarstrom, and S. Styring. 2009. Defining the Far-Red Limit of Photosystem Ii in Spinach. *Plant Cell* 21:2391-2401. doi:10.1105/tpc.108.064154

Tuan, P.A., A.A. Thwe, Y.B. Kim, J.K. Kim, S.J. Kim, S. Lee, S.O. Chung, and S.U. Park. 2013. Effects of White, Blue, and Red Light-Emitting Diodes on Carotenoid Biosynthetic Gene Expression Levels and Carotenoid Accumulation in Sprouts of Tartary Buckwheat (Fagopyrum Tataricum Gaertn.). *J Agric Food Chem* 61:12356-12361. doi:10.1021/jf4039937

Tucker, A.O. and T. Debaggio. 2009. The Encylopedia of Herbs: A Comprehensive Reference to Herbs of Flavor and Fragrance. Timber Press, Portland, OR.

Turner, B.M. 2009. Epigenetic Responses to Environmental Change and Their Evolutionary Implications. *Philos Trans R Soc Lond B Biol Sci* 364:3403-3418. doi:10.1098/rstb.2009.0125

Van Delden, S.H., M. Sharathkumar, M. Butturini, L.J.A. Graamans, E. Heuvelink, M. Kacira, E. Kaiser, R.S. Klamer, L. Klerkx, G. Kootstra, A. Loeber, R.E. Schouten, C. Stanghellini, W. Van Ieperen, J.C. Verdonk, S. Vialet-Chabrand, E.J. Woltering, R. Van De Zedde, Y. Zhang, and L.F.M. Marcelis. 2021. Current Status and Future Challenges in Implementing and Upscaling Vertical Farming Systems. *Nature Food* 2:944-956. doi:10.1038/s43016-021-00402-w

Van Eck, A., M. Pedrotti, R. Brouwer, A. Supapong, V. Fogliano, E. Scholten, F. Biasioli, and M. Stieger. 2021. In Vivo Aroma Release and Dynamic Sensory Perception of Composite Foods. *Journal of Agricultural and Food Chemistry* 69:10260-10271. doi:10.1021/acs.jafc.1c02649

Voutilainen, S., T. Nurmi, J. Mursu, and T.H. Rissanen. 2006. Carotenoids and Cardiovascular Health. *Am J Clin Nutr* 83:1265-1271. doi:10.1093/ajcn/83.6.1265

Walters, K.J., B.K. Behe, C.J. Currey, and R.G. Lopez. 2020a. Historical, Current, and Future Perspectives for Controlled Environment Hydroponic Food Crop Production in the United States. *HortScience* 55:758-767. doi:10.21273/hortsci14901-20

Walters, K.J., R.G. Lopez, and B.K. Behe. 2020b. Leveraging Controlled-Environment Agriculture to Increase Key Basil Terpenoid and Phenylpropanoid Concentrations: The Effects of Radiation Intensity and Co(2) Concentration on Consumer Preference. *Front Plant Sci* 11:598519. doi:10.3389/fpls.2020.598519

Warner, R.M. and J.E. Erwin. 2003. Effect of Photoperiod and Daily Light Integral on Flowering of Five *Hibiscus* Sp. *Scientia Horticulturae* 97:341-351. doi:10.1016/s0304-4238(02)00157-7

Warner, R.M. and J.E. Erwin. 2005. Prolonged High Temperature Exposure and Daily Light Integral Impact Growth and Flowering of Five Herbaceous Ornamental Species. *Journal of the American Society for Horticultural Science* 130:319-325. doi:10.21273/jashs.130.3.319

Weaver, G.M., M.W. Van Iersel, and J.M. Velni. 2019. A Photochemistry-Based Method for Optimising Greenhouse Supplemental Light Intensity. *Biosystems Engineering* 182:123-137. doi:10.1016/j.biosystemseng.2019.03.008

Wink, M. 2008. Plant Secondary Metabolism: Diversity, Function and Its Evolution. *Natural Product Communications* 3. doi:10.1177/1934578x0800300801

Wink, M. 2010. Biochemistry of Plant Secondary Metabolism. Wiley.

Xu, Y.C., Y.X. Chang, G.Y. Chen, and H.Y. Lin. 2016. The Research on LED Supplementary Lighting System for Plants. *Optik* 127:7193-7201. doi:10.1016/j.ijleo.2016.05.056

Yeum, K.J. and R.M. Russell. 2002. Carotenoid Bioavailability and Bioconversion. *Annu Rev Nutr* 22:483-504. doi:10.1146/annurev.nutr.22.010402.102834

Young, A.J. 1991. The Photoprotective Role of Carotenoids in Higher-Plants. *Physiologia Plantarum* 83:702-708. doi:10.1111/j.1399-3054.1991.tb02490.x

Yousif, A.N., C.H. Scaman, T.D. Durance, and B. Girard. 1999. Flavor Volatiles and Physical Properties of Vacuum-Microwave- and Air-Dried Sweet Basil (*Ocimum Basilicum* L.). *J Agric Food Chem* 47:4777-4781. doi:10.1021/jf990484m

Zhang, M., C.M. Whitman, and E.S. Runkle. 2019. Manipulating Growth, Color, and Taste Attributes of Fresh Cut Lettuce by Greenhouse Supplemental Lighting. *Scientia Horticulturae* 252:274-282. doi:10.1016/j.scienta.2019.03.051

Zhang, N., A. Van Westreenen, N.P.R. Anten, J.B. Evers, and L.F.M. Marcelis. 2020. Disentangling the Effects of Photosynthetically Active Radiation and Red to Far-Red Ratio on Plant Photosynthesis under Canopy Shading: A Simulation Study Using a Functional-Structural Plant Model. *Ann Bot* 126:635-646. doi:10.1093/aob/mcz197

Zhen, S. and B. Bugbee. 2020. Far-Red Photons Have Equivalent Efficiency to Traditional Photosynthetic Photons: Implications for Redefining Photosynthetically Active Radiation. *Plant Cell Environ* 43:1259-1272. doi:10.1111/pce.13730

Zhen, S., M. Van Iersel, and B. Bugbee. 2021. Why Far-Red Photons Should Be Included in the Definition of Photosynthetic Photons and the Measurement of Horticultural Fixture Efficacy. *Front Plant Sci* 12:693445. doi:10.3389/fpls.2021.693445

Appendix A

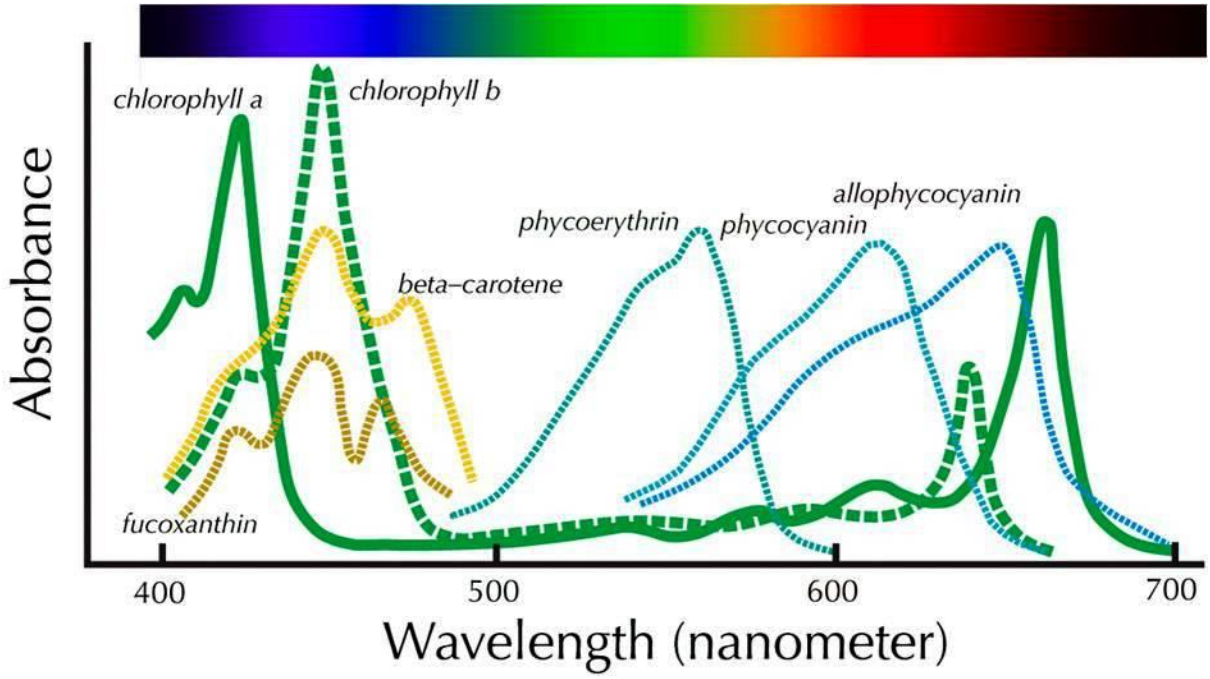

Figure 1.1. Absorption spectra of common carotenoids and chlorophyll pigments.

Source: (Taiz et al., 2015)

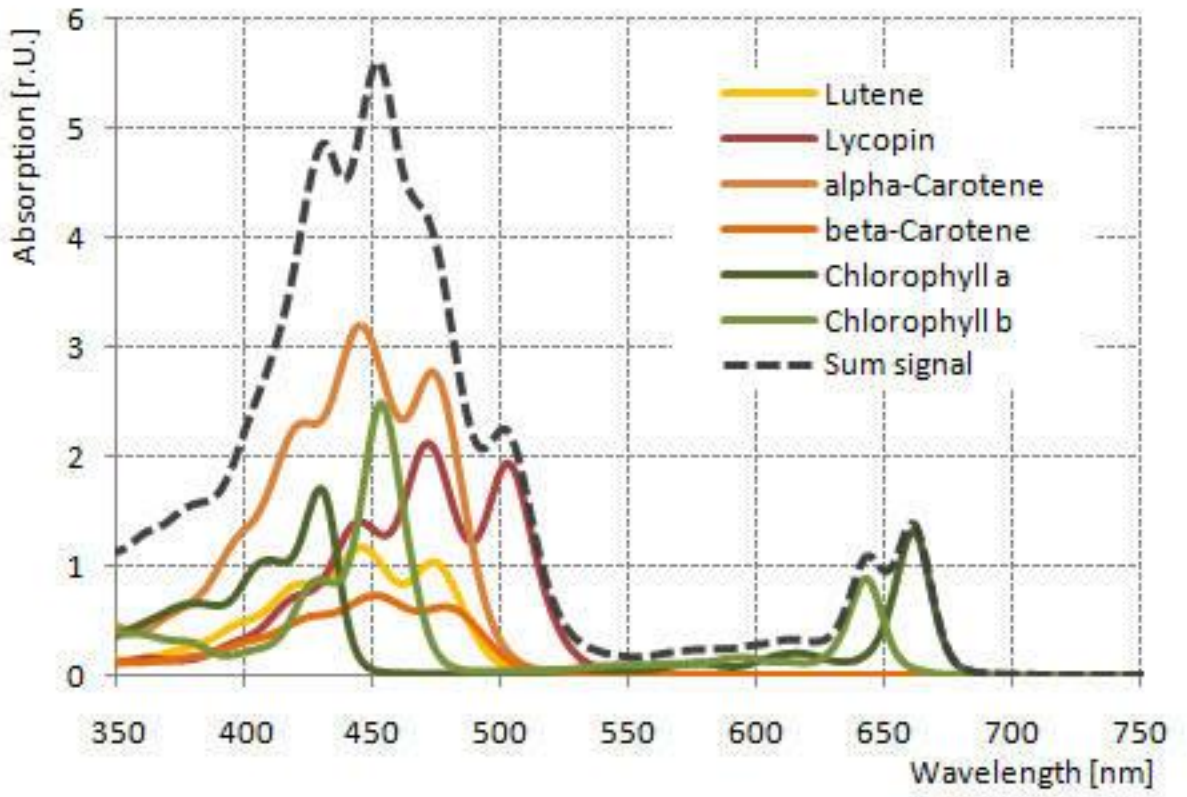

Figure 1.2. Absorption spectra of common carotenoids and chlorophyll pigments.

Source: (HYDRALED, 2022)

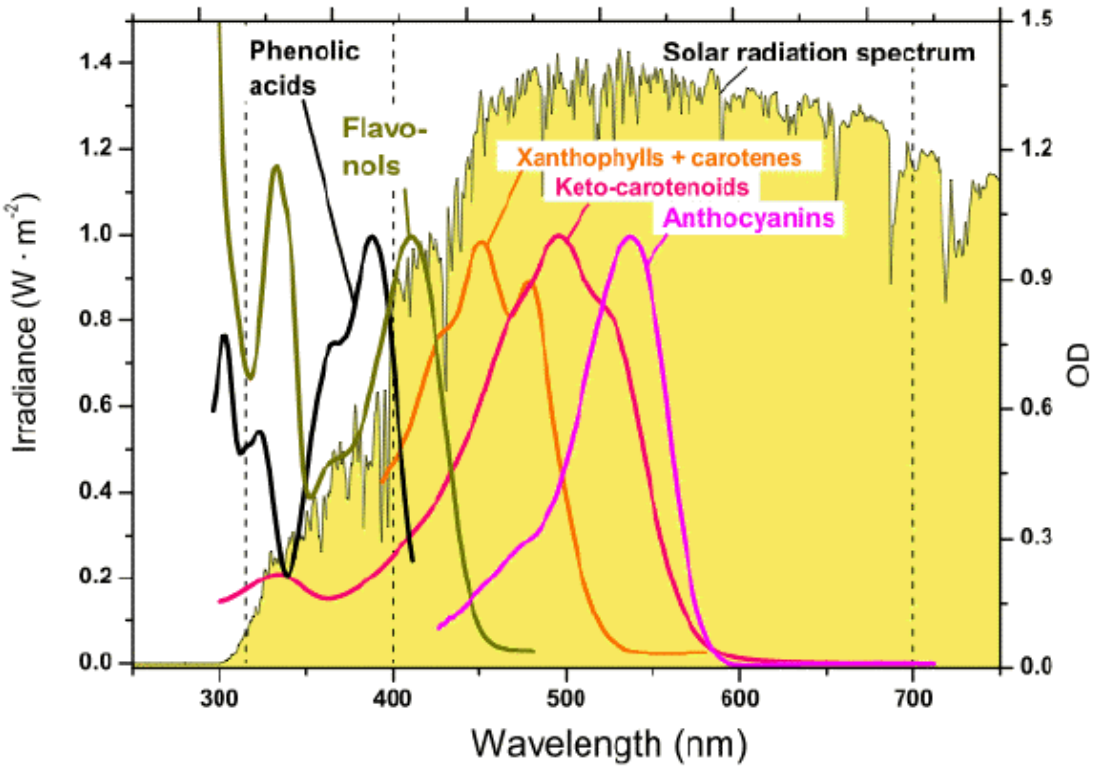

Figure 1.3. Absorption spectra of common isoprenoids.

Source: (Solovchenko, 2010)

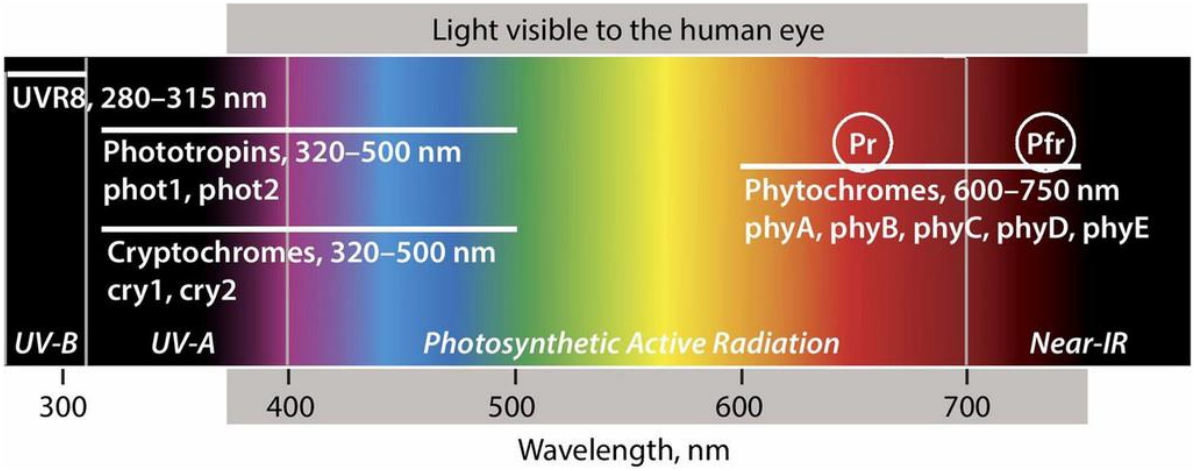

Figure 1.4. The range of wavelengths that are sensed by the primary plant photoreceptors (phytochromes, cryptochromes, phototropins, and UVR8), allowing light-driven developmental adaptations.

Source: (Ouzounis et al., 2015)

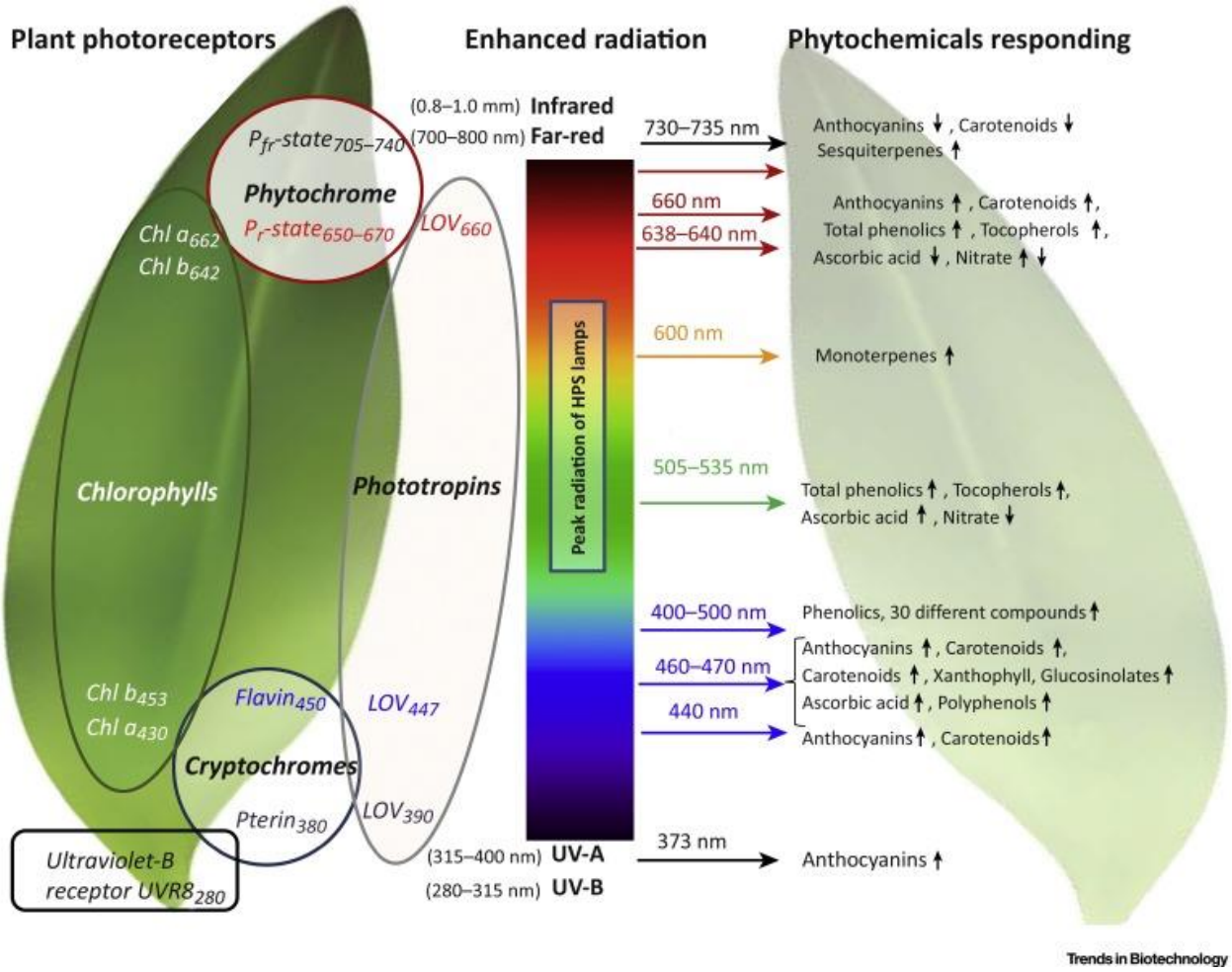

Figure 1.5. The impact of various narrowband wavelength enhancements on secondary metabolism.

Source: (Holopainen et al., 2018)

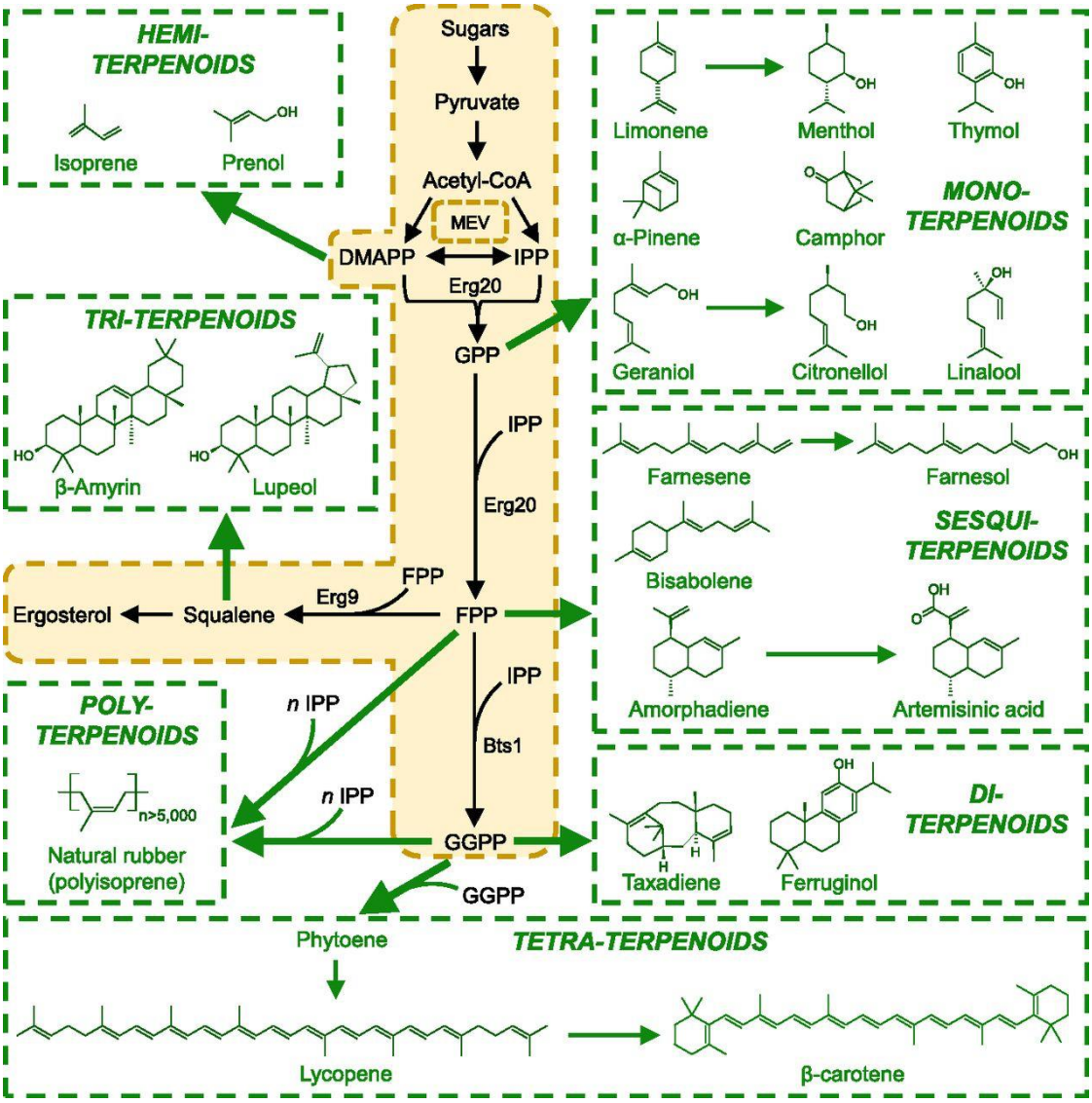

Figure 1.6. Plant terpenoid secondary metabolic reactions and pathways.

Source: (Wink, 2010)

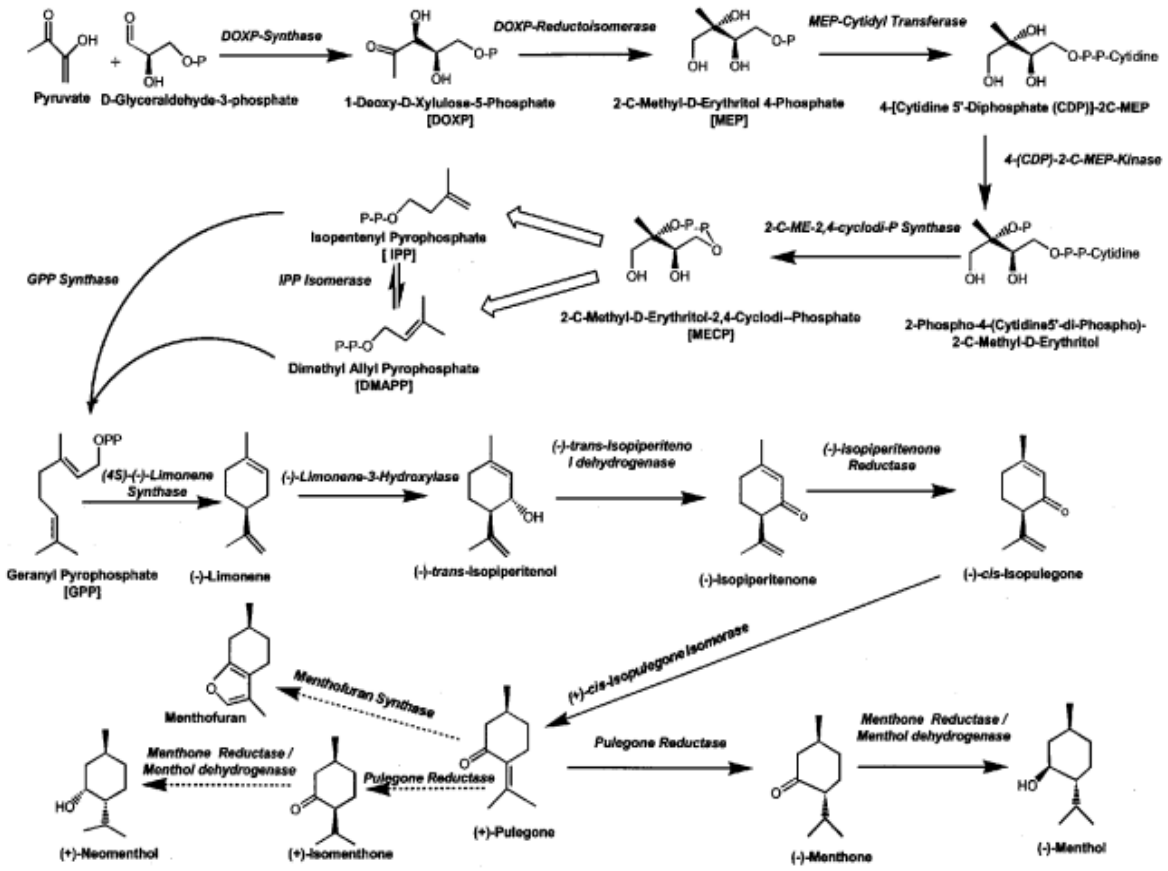

Figure 1.7. Isoprenogenic pathway for key volatile secondary metabolites in the mint family.

Source: (Wink, 2010)

CHAPTER 2: QUANTIFICATION OF MEDICINALLY IMPORTANT VOLATILE ORGANIC COMPOUNDS IN COMMON BASIL VARIETIES

Hunter A. Hammock and Carl E. Sams
Department of Plant Sciences, The University of Tennessee, Knoxville, TN 37996

Correspondence: Carl E. Sams, carlsams@utk.edu

Keywords: Bioactive Compounds, Controlled Environment, Flavor Volatiles, Ocimum Basilicum, Secondary Metabolism, Terpenoids, and VOCs

Author Contributions:
Conceptualization – HAH, CES
Methodology – HAH, CES
Software – HAH, CES
Validation – HAH
Formal analysis – HAH
Investigation – HAH
Resources – CES
Data curation – HAH
Writing (original draft preparation) - HAH
Writing (review and editing) – HAH, CES
Visualization – HAH
Supervision and project administration – CES
Funding acquisition – CES

Author Statement:
All authors have reviewed the manuscript and agree with the reported findings. There are no reported conflicts between the authors and the present study.

Funding:
This research was supported by The AgResearch Dean's Office within the University of Tennessee Institute of Agriculture. No external funds were used for the present study.

Disclosure:
This manuscript and its contents were published in Acta Horticulturae in November, 2021.

Citation:
Hammock, H.A. and Sams, C.E. (2021). Quantification of medicinally important volatile organic compounds in common basil cultivars. *Acta Hortic*. 1329, 113-122
DOI: 10.17660/ActaHortic.2021.1329.14

Abstract

Basil is a globally cultivated herb with considerable demand because of its wide range of culinary and medicinal uses. Basil has high levels of aromatic terpenoids, also known as volatile organic compounds (VOCs). Many of these volatiles are known for their positive health benefits in addition to being primary drivers of flavor and aroma. Inhalation and dietary consumption of terpenes have been shown to induce several medically significant effects such as reducing inflammation, preventing heart disease/cancer, managing pain, curing fungal/bacterial infections, and decreasing anxiety/depression symptoms. To date, there are very few studies that evaluate the VOC profiles of basil varieties in relation to key flavor volatiles and human health benefits. The objective of this study was to quantify VOCs with known medicinal benefits in common varieties of basil. Seven basil varieties were used: 'Genovese,' 'Siam Queen,' 'Spicy Globe,' 'Dark Opal,' (*Ocimum basilicum*); Thai Basil (*Ocimum basilicum* var. thyrsiflora); Lemon Basil (*Ocimum basilicum* x *citriodora*); and Holy Basil (*Ocimum tenuiflorum*). Plants were grown under standard greenhouse conditions and harvested 45 d after seeding. Volatile profiles were analyzed using an Agilent headspace sampler and GC-MS. Terpinene was 2x higher in Lemon and 'Spicy Globe' basil, while terpinolene was 2-5x higher in Thai basil than other varieties. (R+/S-)-Limonene concentrations were 3-25x greater in 'Genovese,' 'Thai,' and Holy basil. 'Dark Opal' had significantly more methyl eugenol than other varieties. Linalool concentrations were 3-10x higher in 'Genovese,' 'Siam Queen,' and Holy basil. Total concentrations of α/β-pinene were highly variable across varieties, but α/β ratio was consistent (4:1). Knowing relative concentrations of these key volatiles will allow growers and processers to optimize essential oil extractions based on crop, with the potential to produce high potential natural supplements as an alternative to synthetic pharmaceuticals. It also establishes a reference point for consumers and medical professionals

wishing to improve overall general health, prevent disease, and even treat specific conditions using slight dietary modifications.

Introduction

Basil is an annual culinary and medicinal herb with a complex aroma profile used extensively by restaurants and professional chefs. (Deschamps and Simon, 2006; Klimánková et al., 2008).(Deschamps and Simon, 2006; Tucker and DeBaggio, 2009). Sweet basil has been broadly classified into seven different morphotypes, which include: 1) tall, slender types; 2) 'Italian' large-leafed types; 3) dwarf types ('bush' or "spicy globe basils); 4) compact types ('thai' basils); 5) purple types ('purple petra'); 6) *purpurascens* types ('dark opal,' sweet purple basils); and 7) *citriodorum* types (flavored types) (Hussain et al., 2008). Significant morphological and biochemical differences exist among various basil varieties due to genetic variation. Customer preference, medicinal use and demand/popularity vary greatly among these different morphotypes (Deschamps and Simon, 2006; Klimánková et al., 2008; Tarchoune et al., 2013). In addition, various basil types possess distinctive flavor volatile profiles that are used both fresh/dried in a variety of culinary dishes (Klimánková et al., 2008; Lee et al., 2005).

Basil is largely used as a flavoring agent and is cultivated globally (Claudia, 2013). This herb has variety of purposes throughout human history, including direct consumption, cooking, and even in the manufacture of products such as essential oils, soaps, perfumes, medicines, etc. (Raimondi et al., 2006; Succop and Newman, 2004). Essential oils are the most valuable commercial forms of basil and contribute to the flavor/aroma of many products in the food and cosmetic industries (Barbieri et al., 2004; Kopsell et al., 2005). Basil produced for dried leaf markets and fresh markets rank second and third, respectively (Putievsky and Galambosi, 1999). Volatile organic compounds (VOCs) are defined as organic molecules that have high vapor

pressure at ordinary room temperatures. Low boiling points, chemical structure, and other physical properties determine the high vapor pressures of volatile compounds (Taylor, 1996). These compounds include both naturally occurring and man-made compounds. Most scents, flavors, odors, and aromas are VOCs and are contained in essential oils (Charles and Simon, 1990).

Many common herbs and other high-value specialty crops are processed to obtain valuable essential oil products. These essential oils have various medicinal purposes, which include aroma therapy, direct application, and sometimes ingestion (after dilution). These herbs have also been associated with high antioxidant activity and a variety of human health benefits (Raimondi et al., 2006). Basil contains a variety of compounds that are nutritionally significant to humans, including flavonoids, carotenoids, phenolics, VOCs, etc. (Bourgaud et al., 2001; Hussain et al., 2008). In previous surveys, basil has been reported as having one of the highest antioxidant concentrations in comparison to other popular herbs and spices (Kopsell et al., 2005; Lee et al., 2005; Politeo et al., 2007). Antioxidants consumed from natural sources have been linked with major health benefits such as reducing the effects of aging, risk of cancer, and effects of heart disease. In addition, antioxidants from artificial sources have been shown to have some negative effects on human health (Pourmortazavi and Hajimirsadeghi, 2007).

Various research groups using various analytical methods and extraction techniques (i.e., GC-FID, GC-MS, LC-MS, and HPLC) have identified at least two hundred separate volatile compounds across many basil varieties, many of which have high biological activities (Bantis et al., 2016; Deschamps and Simon, 2006; Lee et al., 2005; Soran et al., 2009; Tarchoune et al., 2013). While many of the pertinent flavor and aroma compounds have been identified through GC-MS analysis, little information is known about relative VOC concentrations of common basil varieties in relation to potential human health benefits. Further research should be conducted on

specific basil cultivars that have high market value to determine their overall chemical composition and flavor profiles in relation to each other. Concentration changes in key flavor volatiles (both positive and negative) should also be evaluated in comparison to human sensory experience, customer perception, and benefits to human health via dietary consumption and/or inhalation of essential oils.

The primary objective of this study was to evaluate key flavor volatile concentrations with proven human health benefits across popular basil cultivars. Knowing relative concentrations of these key volatiles will allow growers and processers to optimize essential oil extractions based on crop, with the potential to produce high-potency aroma therapy products and natural supplements as an alternative to synthetic pharmaceuticals. It also establishes a reference point for consumers and medical professionals wishing to improve overall general health, prevent disease, and even treat specific conditions using slight dietary modifications.

Materials and Methods

Cultural Techniques and Environmental Growing Conditions

This project was conducted at The University of Tennessee Institute of Agriculture (UTIA) in Knoxville, TN, USA (35°56'44.5"N, 83°56'17.3"W). Growing dates for two separate experimental growing cycles occurred from August 2015 to December 2016. Seven basil varieties were used in this experiment: 'Genovese,' 'Siam Queen,' 'Spicy Globe,' 'Dark Opal,' (*Ocimum basilicum*); Thai Basil (*Ocimum basilicum* var. thyrsiflora); Lemon Basil (*Ocimum basilicum* x citriodora); and Holy Basil (*Ocimum tenuiflorum*). All seeds came from Johnny's Select Seeds (Johnny's Select Seeds, Winslow, ME). Seeds were germinated in peat moss-based cubes (Park's Bio Dome Sponges, Hodges, SC) at 83 ºC and 95% RH. After 2 weeks, seedlings were transplanted

into 5x5 cm plastic pots using 1-part peat moss (Black Gold Canadian Sphagnum Peat Moss, Agawam, MA) to 3 parts perlite (Krum Horticultural Perlite, Hodgkins, IL) potting mix. Relative humidity during the growth period averaged 55%. Across two growing seasons, day temperatures averaged 28.6 ºC, while night temperatures averaged 22.7 ºC. The daily light integral (DLI) of the NL control averaged 10.5 $mol \cdot m^{-2} \cdot d^{-1}$ across all growing cycles (ranging from 4 to 20 $mol \cdot m^{-2} \cdot d^{-1}$).

Basil plants were grown in ebb and flow hydroponic systems and sub irrigated for 5 min each day with a full strength, modified Hoagland's solution. Nutrient solution elemental concentrations were (ppm): N (207.54), P (50.87), K (298.23), Ca (180.15), Mg (77.10), S (136.45), Fe (3.95), Mn (0.90), Zn (0.40), Mo (0.09), Cu (0.90), and B (0.90). The fertility regime was kept constant across the duration of all seasons. Total growth time lasted approximately 45 d across two experimental growing cycles. Like many commercial basil growing operations, harvest occurred as the first signs of change from vegetative to reproductive growth were observed (i.e., 8-10 nodes).

GC-MS Headspace Volatile Analysis

Three g of fresh plant material (two basil plants per sample, 1.5 g of representative material from each plant) were placed in 20-mL borosilicate glass vials then immediately sealed and placed onto a Network Headspace Sampler (Agilent G1888, Santa Clara, CA, USA). Samples were heated to 80 ºC for 10 min and pressurized with Helium (Air Gas, analytical purity) to 95.21 kPa for 1 min. The tube was then vented for 1 min into the headspace transfer line (110 ºC) and injected (port at 250 ºC) into the GC (Agilent Technologies 6890N Network GC System). The volatiles were separated by an HP-5MS capillary column (5%-Phenyl)-methylpolysiloxane, length: 30m, ID: 0.250 mm, film thickness: 1µm, Agilent Technologies) using analytical purity Helium carrier gas at 95.21 kPa with constant column pressure. At the start of data acquisition, temperature was

held at 40 ºC for 5 min, ramped-up from 40 ºC to 250 ºC (5 ºC per min), then held constant for the duration of the run. Total run time was 70 min, including post-run and cool-down phases. After sample separation and column elution, the analytes were passed through a mass selective detector (Agilent Technologies 5973 Network Mass Selective Detector) at 250 ºC and collected over the course of the sample run. The transfer line, ion source, and quadrupole temperatures were 250 ºC, 230 ºC, and 170 ºC, respectively. The full scan mass range was set to 40-550 m/z (threshold: 150).

Agilent ChemStation was used for data collection and processing. Calibration curves were previously established using analytical standards found in basil and shown in the literature to be important for human sensory perception. Over 200 separate compounds were identified throughout this experiment, but emphasis was placed on key flavor compounds that have been calibrated to our GC-MS and HP-5MS column using analytical standards (Sigma-Aldrich, St. Louis, MO) to determine leaf tissue concentrations of key VOCs on a fresh plant weight basis. The MS spectra from analytical standards and fresh samples were compared to NIST, ADMIS, and a basil reference library created from calibrated analytical standards to confirm peak identity and retention times. MassHunter Workstation Software Version B.06.00 (Agilent Technologies, Inc., 2012) was used to automatically integrate peaks. Relative peak areas were automatically adjusted based on analytical standards and multiple library references.

Statistical Analyses

A Randomized Complete Block Design (RCBD) was used for this experiment. All data sets were analyzed by GLM and Mixed Model Analysis of Variance procedures using the statistical software SAS (version 9.4, SAS Institute, Cary, NC). Design and Analysis macro (DandA.sas), created by Dr. Arnold Saxton, was utilized in addition to Tukey's adjustment, regression analysis, and univariate/normalization procedures to provide additional statistical

insights on the complete data set. Treatments were separated by least significant difference (LSD) at α=0.05. All volatile concentrations units are reported in micromolarity of analyte concentration per g of fresh mass (FM) leaf tissue ($\mu M \cdot g^{-1}$ FM) to represent VOC emissions most accurately from the collected headspace sample above fresh plant tissues under specific reproducible analytical conditions.

Results and Discussion

As expected, many of the compounds that were evaluated in this study showed significant tissue concentration differences across basil variety. Terpinene is an important and frequently used flavor compound found in a variety of herbs and spices. It has a pleasant turpentine-like odor and is a primary constituent of tea tree oil, cardamom oil, and marjoram oil (Banthorpe et al., 1972; Kesselmeier and Staudt, 1999). Terpinene tissue concentrations showed significant separation across basil variety ($P \leq 0.0001$; $F = 1.87$). Tissue concentrations ranged from 0 to 7.9 $\mu M \cdot g^{-1}$ FM headspace emission (Fig. 2.1). Lemon basil had the highest concentration and separated from most of the varieties with the exception of 'Spicy Globe.' Terpinene was detected in all varieties except for 'Dark Opal.' It is well known that genetics play direct roles in secondary metabolism, and variation in genetic profiles across basil varieties is the basis for different VOC profiles (Wink, 2010). Terpinene has been shown to possess antioxidant, antimicrobial, and stress properties (Petrovic et al., 2019; Rudback et al., 2012; Sartorelli et al., 2007).

Terpinolene is an isomer of terpinene and has a sweet pine odor with terpene taste. It is another important flavor compound in basil and many other herbs (Bohlmann and Keeling, 2008; Deschamps and Simon, 2006; Kesselmeier and Staudt, 1999). Terpinolene tissue concentrations showed significant separation across basil variety ($P \leq 0.0001$; $F = 2.07$). Terpinolene was detected in all varieties, and tissue concentrations ranged from 0.5 to 12.5 $\mu M \cdot g^{-1}$ FM headspace emission

(Fig. 2.1). Thai basil had the highest concentration (at least 2x than any other variety) and separated from all of the other varieties with the exception holy basil. Terpinolene has been shown to reduce the risk of heart disease and inhibit the growth of cancerous cells (Grassmann et al., 2005; Okumura et al., 2012).

(S)-(-)-Limonene and (R)-(+)-Limonene are two critical flavor components of basil and have been shown to possess significant human health benefits (Fahlbusch et al., 2003; Hussain et al., 2008). Limonene is a non-nutrient dietary component and flavor volatile found in basil. It is considered an aliphatic hydrocarbon and is classified as a monoterpene (Banthorpe et al., 1972; Deschamps and Simon, 2006). (R+/S-)-Limonene was detected in all basil varieties. Tissue concentrations showed significant separation ($P \leq 0.0001$; $F = 23.21$), and ranged from 43 to 2928 $\mu M \cdot g^{-1}$ FM headspace emission (Fig. 2.2).

Many studies have shown that limonene can reduce the growth of cancerous cells without toxicity to normal cells (Sobral et al., 2014). In one experiment investigating prostate cancer treatment via induction of apoptosis, the use of d-limonene increased the antitumor effect of docetaxel against cancer cells without being toxic to normal prostate epithelial cells (Rabi and Bishayee, 2009). It has been shown to inhibit the growth of lung cancer cells in mice (Yu et al., 2018). Aroma therapy with limonene has the potential to promote relaxation and mental focus, while reducing the severity and incidence of stress, depression, and anxiety (Joung; et al., 2014). Both the dietary consumption and inhalation of limonene essential oil has great potential for specific medical treatments as well as improving mental health. Studies have also shown that limonene has strong antimicrobial properties (Dorman and Deans, 2000; Vuuren and Viljoen, 2007). Pine oil was was shown to be highly active against a range of food borne pathogens (Ozogul

et al., 2015) and has the potential to be used as a food preservative in addition to a natural flavoring agent.

Methyl eugenol is a phenolic compound that has a strong, spicy, herbaceous aroma and greatly contributes to the flavor of many basil varieties. Eugenol compounds are the primary constituents of clove oil and possesses a clove-like flavor (Petersen et al., 2010; Tarchoune et al., 2013). It is also known to have a wide range of medicinal benefits both through aromatherapy and direct consumption (Lee et al., 2005). Methyl eugenol tissue concentrations showed significant separation across basil variety ($P = 0.0080$; $F = 4.21$). Methyl eugenol was detected in all varieties, and tissue concentrations ranged from 18 to 3150 $\mu M \cdot g^{-1}$ FM headspace emission (Fig. 2.3).

'Dark Opal' had the highest concentration by far. It had 6x greater tissue concentration than the next highest variety (Thai Basil). All of the other varieties averaged 140 $\mu M \cdot g^{-1}$ FM, while 'Dark Opal' leaf tissue had 3150 $\mu M \cdot g^{-1}$ FM. Methyl eugenol has been labeled as an antioxidant, antimutagen, antigenotoxic, and anti-inflammatory (Bendre et al., 2016). Eugenol tissue concentrations showed significant separation across basil variety (P *P* $= 0.0017$; $F = 5.77$). Eugenol was detected in all varieties but did not follow the same pattern as methyl eugenol. Tissue concentrations ranged from 5 to 310 $\mu M \cdot g^{-1}$ FM headspace emission (Fig. 2.4). Holy basil had the highest concentration but did not separate from Thai basil or 'Genovese.' The lowest concentrations were found in 'Spicy Globe,' 'Siam Queen,' and Lemon Basil, ranging 5-21 $\mu M \cdot g^{-1}$ FM. Eugenol has shown similar medicinal properties as methyl eugenol, including significant anticancer activity (Carvalho et al., 2016; S Bendre and D Rajput, 2016). Total eugenol (i.e., methyl eugenol and eugenol) tissue concentrations showed significant separation across basil variety ($P \leq 0.0001$; $F = 10.18$). 'Dark Opal' had the highest concentrations of total eugenol primarily because its high methyl eugenol concentration, approximately 4x higher than the second

highest (Thai Basil) (Fig. 2.3). ‘Dark Opal’ separated from all other varieties, and the other varieties did not separate among themselves.

The aroma of linalool is described as sweet and floral. This compound is used extensively in the food processing and fragrance industries. It has strong antioxidant and anti-inflammatory properties as well as calming, mental clarity, and numerous other health benefits (Guzman-Gutierrez et al., 2015). Mice exposed to linalool vapors have shown reduced levels of anxiety and lower depression-like behaviors (Carvalho-Freitas and Costa, 2002; Guzman-Gutierrez et al., 2012). Linalool has also been shown to reverse neuropathological and biological impairments in mice caused by Alzheimer’s (Sabogal-Guaqueta et al., 2016). Linalool tissue concentrations showed significant separation across basil variety ($P \leq 0.0001$; $F = 12.76$). Linalool was detected in all varieties and was split into two groups (Fig. 2.4). Tissue concentrations for ‘Genovese,’ ‘Siam Queen,’ and Holy Basil averaged 2000 $\mu M \cdot g^{-1}$ FM. Tissue concentrations for Lemon Basil, ‘Spicy Globe,’ ‘Dark Opal,’ and Thai Basil averaged 120 $\mu M \cdot g^{-1}$ FM. Both of these groups statistically separated from each other, but the varieties within each group did not separate from one another.

Camphene has a damp, pungent, herbal aroma with pine notes. It is considered a monoterpene and is a component of many essential oils (Banthorpe et al., 1972; Fahlbusch et al., 2003). Camphene tissue concentrations showed significant separation across basil varieties ($P = 0.0080$; $F = 4.21$). Camphene was detected in all varieties and split into two groups (Fig. 2.4). Tissue concentrations for ‘Dark Opal’ were significantly higher than any other variety, 6x higher than the second-best variety. ‘Dark Opal’ had 3100 $\mu M \cdot g^{-1}$ FM, as compared to the other varieties which averaged 140 $\mu M \cdot g^{-1}$ FM. None of the other varieties statistically separated from one another. Camphene has a high antioxidant activity (Quintans-Junior et al., 2013) and has the ability

reduce stress via inhalation (Seo et al., 2016). It has been shown to reduce inflammation in mice (Lima et al., 2012).

Methyl salicylate is a benzoate ester and is derived from salicylic acid. It is the primary constituent of wintergreen oil and is used extensively in food, beverages, fragrances, and medicines (Bourgaud et al., 2001). Methyl salicylate tissue concentrations showed significant separation across basil variety ($P = 0.0006$; $F = 6.91$). Methyl salicylate was detected in all varieties except 'Dark Opal' and showed mixed separation (Fig. 2.4). Tissue concentrations for 'Genovese' and Thai Basil statistically separated from 'Lemon', 'Spicy Globe,' and 'Dark Opal.' Holy Basil and 'Siam Queen' did not separate from the other basil varieties. Tissue concentrations ranged from 0-2500 $\mu M \cdot g^{-1}$ FM. Methyl salicylate is commonly used as a rubefacient/analgesic and is commonly used to relieve minor aches and pains (Hebert et al., 2014). It is also added to mouthwashes and disinfectants because of its antiseptic properties.

α-Pinene and β-pinene are two monoterpenes that greatly influence the flavor and aroma of basil. They are both primarily found in pine resin and are one of the most abundant terpenes found in nature (Banthorpe et al., 1972). α-Pinene tissue concentrations showed significant separation across basil variety ($P \leq 0.0001$; $F = 12.22$). α-Pinene was detected in all varieties. and tissue concentrations ranged from 18 to 3150 $\mu M \cdot g^{-1}$ FM headspace emission (Fig. 2.5).

α-Pinene ranged from 9.8 $\mu M \cdot g^{-1}$ FM ('Dark Opal') to 2350 $\mu M \cdot g^{-1}$ FM (Holy Basil). 'Genovese,' 'Siam Queen,' and Holy Basil had the highest concentrations and statistically separated from Lemon Basil, 'Spicy Globe,' 'Dark Opal,' and Thai Basil. β-pinene tissue concentrations showed significant separation across basil variety ($P = 0.0017$; $F = 5.77$). β-Pinene was detected in all varieties and showed a similar pattern as its enantiomer (Fig. 2.5). α-Pinene made up approximately 80% total pinene concentration, while β-pinene made up the remaining

20%. It ranged from 2.4 $\mu M \cdot g^{-1}$ FM ('Dark Opal') to 575 $\mu M \cdot g^{-1}$ FM (Holy Basil). 'Genovese,' 'Siam Queen,' and Holy Basil had the highest concentrations and statistically separated from Lemon Basil, 'Spicy Globe,' 'Dark Opal,' and Thai Basil. Total pinene tissue concentrations (α-pinene and β-pinene) showed significant separation across basil variety ($P \leq 0.0001$; $F = 24.71$). 'Genovese,' 'Siam Queen,' and Holy Basil had the highest concentrations and statistically separated from Lemon Basil, 'Spicy Globe,' 'Dark Opal,' and Thai Basil (Fig. 2.5). Across all basil varieties, the ratio of α/β-pinene tissue concentrations was approximately 4:1, and concentration ratio variance was less than 4% across all varieties. Both α/β-pinene have been shown to possess a wide range of pharmacological activity and have many therapeutic applications for both direct consumption and inhalation. These include anticoagulant, antitumor, antiseptic, antimicrobial, antioxidant, and anti-inflammatory (Rivas Da Silva et al., 2012; Salehi et al., 2019).

Conclusion

The purpose of this study was to quantify VOCs with known medicinal benefits in common varieties of basil. Seven basil varieties were analyzed using GC-MS to determine flavor profiles and pertinent compounds with human health benefits. Each variety had a specific flavor profile with varying concentrations of each flavor compound. The most abundant VOCs detected for 'Genovese' included (R+/S-)-limonene, linalool, methyl salicylate, and α/β-pinene. 'Siam Queen' had high concentrations of linalool, methyl salicylate, and α/β-pinene. Lemon Basil and 'Spicy Globe' primarily had terpinene. The most abundant VOCs for 'Dark Opal' included methyl eugenol and camphene. Thai Basil exhibited terpinolene, (R+/S-)-limonene, eugenol, and methyl salicylate. Holy Basil had high concentrations (R+/S-)-limonene, eugenol, linalool, methyl salicylate, α/β-pinene. Quantifying key flavor volatile concentrations in common basil varieties

will assist growers and processers in their quest to optimize essential oil extractions. Other secondary metabolites with significant human health benefits should be further evaluated. Specific varieties can be chosen based on their flavor profile as well as health benefits, with the potential to produce quality fresh/dried basil for dietary consumption, essential oils, and high-potency natural supplements.

References

Banthorpe, D.V., B.V. Charlwood, and M.J. Francis. 1972. The Biosynthesis of Monoterpenes. *Chem Rev* 72:115-155. doi:10.1021/cr60276a002

Bantis, F., T. Ouzounis, and K. Radoglou. 2016. Artificial LED Lighting Enhances Growth Characteristics and Total Phenolic Content of *Ocimum Basilicum*, but Variably Affects Transplant Success. *Scientia Horticulturae* 198:277-283. doi:10.1016/j.scienta.2015.11.014

Barbieri, S., M. Elustondo, and M. Urbicain. 2004. Retention of Aroma Compounds in Basil Dried with Low Pressure Superheated Steam. *Journal of Food Engineering* 65:109-115. doi:10.1016/j.foodeng.2004.01.003

Bohlmann, J. and C.I. Keeling. 2008. Terpenoid Biomaterials. *Plant J* 54:656-669. doi:10.1111/j.1365-313X.2008.03449.x

Bourgaud, F., A. Gravot, S. Milesi, and E. Gontier. 2001. Production of Plant Secondary Metabolites: A Historical Perspective. *Plant Science* 161:839-851. doi:10.1016/s0168-9452(01)00490-3

Carvalho, S.D., M.L. Schwieterman, C.E. Abrahan, T.A. Colquhoun, and K.M. Folta. 2016. Light Quality Dependent Changes in Morphology, Antioxidant Capacity, and Volatile

Production in Sweet Basil (*Ocimum Basilicum*). *Front Plant Sci* 7:1328. doi:10.3389/fpls.2016.01328

Carvalho-Freitas, M.I. and M. Costa. 2002. Anxiolytic and Sedative Effects of Extracts and Essential Oil from *Citrus Aurantium* L. *Biol Pharm Bull* 25:1629-1633. doi:10.1248/bpb.25.1629

Charles, D.J. and J.E. Simon. 1990. Comparison of Extraction Methods for the Rapid-Determination of Essential Oil Content and Composition of Basil. *Journal of the American Society for Horticultural Science* 115:458-462.

Claudia, M.R., And P. Alberto. 2013. Influence of Nitrogen Nutrition on Growth and Accumulation of Rosmarinic Acid in Sweet Basil (Ocimum Basilicum L.) Grown in Hydroponic Culture. *Australian Journal of Crop Science* 7:321-327.

Deschamps, C. and J.E. Simon. 2006. Terpenoid Essential Oil Metabolism in Basil (*Ocimum Basilicum* L.) Following Elicitation. *Journal of Essential Oil Research* 18:618-621. doi:10.1080/10412905.2006.9699183

Dorman, H.J. and S.G. Deans. 2000. Antimicrobial Agents from Plants: Antibacterial Activity of Plant Volatile Oils. *J Appl Microbiol* 88:308-316. doi:10.1046/j.1365-2672.2000.00969.x

Fahlbusch, K.-G., F.-J. Hammerschmidt, J. Panten, W. Pickenhagen, D. Schatkowski, K. Bauer, D. Garbe, and H. Surburg. 2003. Flavors and Fragrances. doi:10.1002/14356007.a11_141

Grassmann, J., S. Hippeli, R. Spitzenberger, and E.F. Elstner. 2005. The Monoterpene Terpinolene from the Oil of Pinus Mugo L. In Concert with Alpha-Tocopherol and Beta-Carotene Effectively Prevents Oxidation of Ldl. *Phytomedicine* 12:416-423. doi:10.1016/j.phymed.2003.10.005

Guzman-Gutierrez, S.L., H. Bonilla-Jaime, R. Gomez-Cansino, and R. Reyes-Chilpa. 2015. Linalool and Beta-Pinene Exert Their Antidepressant-Like Activity through the Monoaminergic Pathway. *Life Sci* 128:24-29. doi:10.1016/j.lfs.2015.02.021

Guzman-Gutierrez, S.L., R. Gomez-Cansino, J.C. Garcia-Zebadua, N.C. Jimenez-Perez, and R. Reyes-Chilpa. 2012. Antidepressant Activity of Litsea Glaucescens Essential Oil: Identification of Beta-Pinene and Linalool as Active Principles. *J Ethnopharmacol* 143:673-679. doi:10.1016/j.jep.2012.07.026

Hebert, P.R., E.J. Barice, and C.H. Hennekens. 2014. Treatment of Low Back Pain: The Potential Clinical and Public Health Benefits of Topical Herbal Remedies. *J Altern Complement Med* 20:219-220. doi:10.1089/acm.2013.0313

Hussain, A.I., F. Anwar, S.T. Hussain Sherazi, and R. Przybylski. 2008. Chemical Composition, Antioxidant and Antimicrobial Activities of Basil (Ocimum Basilicum) Essential Oils Depends on Seasonal Variations. *Food Chem* 108:986-995. doi:10.1016/j.foodchem.2007.12.010

Joung;, D., C. Song;, H. Ikei;, T. Okuda;, M. Igarashi;, H. Koizumi;, B.J. Park;, T. Yamaguchi;, M. Takagaki;, and Y. Miyazaki. 2014. Physiological and Psychological Effects of Olfactory Stimulation with D-Limonene. *Advances in Horticultural Science* 28(2), 90-94. doi:10.13128/ahs-22808

Kesselmeier, J. and M. Staudt. 1999. Biogenic Volatile Organic Compounds (Voc): An Overview on Emission, Physiology and Ecology. *Journal of Atmospheric Chemistry* 33:23-88. doi:10.1023/a:1006127516791

Klimánková, E., K. Holadová, J. Hajšlová, T. Čajka, J. Poustka, and M. Koudela. 2008. Aroma Profiles of Five Basil (*Ocimum Basilicum* L.) Cultivars Grown under Conventional and Organic Conditions. *Food Chemistry* 107:464-472. doi:10.1016/j.foodchem.2007.07.062

Kopsell, D.A., D.E. Kopsell, and J. Curran-Celentano. 2005. Carotenoid and Chlorophyll Pigments in Sweet Basil Grown in the Field and Greenhouse. *HortScience* 40:1230-1233. doi:10.21273/hortsci.40.5.1230

Lee, S.J., K. Umano, T. Shibamoto, and K.G. Lee. 2005. Identification of Volatile Components in Basil (*Ocimum Basilicum* L.) and Thyme Leaves (*Thymus Vulgaris* L.) and Their Antioxidant Properties. *Food Chemistry* 91:131-137. doi:10.1016/j.foodchem.2004.05.056

Lima, D.K., L.J. Ballico, F. Rocha Lapa, H.P. Goncalves, L.M. De Souza, M. Iacomini, M.F. Werner, C.H. Baggio, I.T. Pereira, L.M. Da Silva, V.A. Facundo, and A.R. Santos. 2012. Evaluation of the Antinociceptive, Anti-Inflammatory and Gastric Antiulcer Activities of the Essential Oil from *Piper Aleyreanum* C.Dc in Rodents. *J Ethnopharmacol* 142:274-282. doi:10.1016/j.jep.2012.05.016

Okumura, N., H. Yoshida, Y. Nishimura, Y. Kitagishi, and S. Matsuda. 2012. Terpinolene, a Component of Herbal Sage, Downregulates Akt1 Expression in K562 Cells. *Oncol Lett* 3:321-324. doi:10.3892/ol.2011.491

Ozogul, Y., E. Kuley, Y. Ucar, and F. Ozogul. 2015. Antimicrobial Impacts of Essential Oils on Food Borne-Pathogens. *Recent Pat Food Nutr Agric* 7:53-61. doi:10.2174/2212798407666150615112153

Petersen, M., J. Hans, and U. Matern. 2010. Biosynthesis of Phenylpropanoids and Related Compounds. *Biochemistry of Plant Secondary Metabolism, 2nd Edition* 40:182-257. doi:10.1002/9781444320503.ch4

Petrovic, J., D. Stojkovic, and M. Sokovic. 2019. Terpene Core in Selected Aromatic and Edible Plants: Natural Health Improving Agents. *Adv Food Nutr Res* 90:423-451. doi:10.1016/bs.afnr.2019.02.009

Politeo, O., M. Jukic, and M. Milos. 2007. Chemical Composition and Antioxidant Capacity of Free Volatile Aglycones from Basil (Ocimum Basilicum L.) Compared with Its Essential Oil. *Food Chemistry* 101:379-385. doi:10.1016/j.foodchem.2006.01.045

Pourmortazavi, S.M. and S.S. Hajimirsadeghi. 2007. Supercritical Fluid Extraction in Plant Essential and Volatile Oil Analysis. *J Chromatogr A* 1163:2-24. doi:10.1016/j.chroma.2007.06.021

Quintans-Junior, L., J.C. Moreira, M.A. Pasquali, S.M. Rabie, A.S. Pires, R. Schroder, T.K. Rabelo, J.P. Santos, P.S. Lima, S.C. Cavalcanti, A.A. Araujo, J.S. Quintans, and D.P. Gelain. 2013. Antinociceptive Activity and Redox Profile of the Monoterpenes (+)-Camphene, P-Cymene, and Geranyl Acetate in Experimental Models. *ISRN Toxicol* 2013:459530. doi:10.1155/2013/459530

Rabi, T. and A. Bishayee. 2009. D -Limonene Sensitizes Docetaxel-Induced Cytotoxicity in Human Prostate Cancer Cells: Generation of Reactive Oxygen Species and Induction of Apoptosis. *J Carcinog* 8:9. doi:10.4103/1477-3163.51368

Raimondi, G., F. Orsini, A. Maggio, S. De Pascale, and G. Barbieri. 2006. Yield and Quality of Hydroponically Grown Sweet Basil Cultivars. *Proceedings of the 1st International Symposium on the Labiatae: Advances in Production, Biotechnology and Utilisation*:353-+. doi:10.17660/ActaHortic.2006.723.48

Rivas Da Silva, A.C., P.M. Lopes, M.M. Barros De Azevedo, D.C. Costa, C.S. Alviano, and D.S. Alviano. 2012. Biological Activities of Alpha-Pinene and Beta-Pinene Enantiomers. *Molecules* 17:6305-6316. doi:10.3390/molecules17066305

Rudback, J., M.A. Bergstrom, A. Borje, U. Nilsson, and A.T. Karlberg. 2012. Alpha-Terpinene, an Antioxidant in Tea Tree Oil, Autoxidizes Rapidly to Skin Allergens on Air Exposure. *Chem Res Toxicol* 25:713-721. doi:10.1021/tx200486f

S Bendre, R. and J. D Rajput. 2016. Outlooks on Medicinal Properties of Eugenol and Its Synthetic Derivatives. *Natural Products Chemistry & Research* 04. doi:10.4172/2329-6836.1000212

Sabogal-Guaqueta, A.M., E. Osorio, and G.P. Cardona-Gomez. 2016. Linalool Reverses Neuropathological and Behavioral Impairments in Old Triple Transgenic Alzheimer's Mice. *Neuropharmacology* 102:111-120. doi:10.1016/j.neuropharm.2015.11.002

Salehi, B., S. Upadhyay, I. Erdogan Orhan, A. Kumar Jugran, L.D.J. S, A.D. D, F. Sharopov, Y. Taheri, N. Martins, N. Baghalpour, W.C. Cho, and J. Sharifi-Rad. 2019. Therapeutic Potential of Alpha- and Beta-Pinene: A Miracle Gift of Nature. *Biomolecules* 9. doi:10.3390/biom9110738

Sartorelli, P., A.D. Marquioreto, A. Amaral-Baroli, M.E. Lima, and P.R. Moreno. 2007. Chemical Composition and Antimicrobial Activity of the Essential Oils from Two Species of Eucalyptus. *Phytother Res* 21:231-233. doi:10.1002/ptr.2051

Seo, M., K. Sowndhararajan, and S. Kim. 2016. Influence of Binasal and Uninasal Inhalations of Essential Oil of Abies Koreana Twigs on Electroencephalographic Activity of Human. *Behav Neurol* 2016:9250935. doi:10.1155/2016/9250935

Sobral, M.V., A.L. Xavier, T.C. Lima, and D.P. De Sousa. 2014. Antitumor Activity of Monoterpenes Found in Essential Oils. *ScientificWorldJournal* 2014:953451. doi:10.1155/2014/953451

Soran, M.L., S.C. Cobzac, C. Varodi, I. Lung, E. Surducan, and V. Surducan. 2009. The Extraction and Chromatographic Determination of the Essentials Oils from *Ocimum Basilicum* L. By Different Techniques. *Journal of Physics: Conference Series* 182:012016. doi:10.1088/1742-6596/182/1/012016

Succop, C.E. and S.E. Newman. 2004. Organic Fertilization of Fresh Market Sweet Basil in a Greenhouse. *HortTechnology* 14:235-239. doi:10.21273/horttech.14.2.0235

Tarchoune, I., O. Baâtour, J. Harrathi, P.L. Cioni, M. Lachaâl, G. Flamini, and Z. Ouerghi. 2013. Essential Oil and Volatile Emissions of Basil (*Ocimum Basilicum*) Leaves Exposed to Nacl or Na2so4 Salinity. *Journal of Plant Nutrition and Soil Science* 176:748-755. doi:10.1002/jpln.201200278

Taylor, A.J. 1996. Volatile Flavor Release from Foods During Eating. *Crit Rev Food Sci Nutr* 36:765-784. doi:10.1080/10408399609527749

Vuuren, S.F.V. and A.M. Viljoen. 2007. Antimicrobial Activity of Limonene Enantiomers and 1,8-Cineole Alone and in Combination. *Flavour and Fragrance Journal* 22:540-544. doi:10.1002/ffj.1843

Wink, M. 2010. Biochemistry of Plant Secondary Metabolism. Wiley.

Yu, X., H. Lin, Y. Wang, W. Lv, S. Zhang, Y. Qian, X. Deng, N. Feng, H. Yu, and B. Qian. 2018. D-Limonene Exhibits Antitumor Activity by Inducing Autophagy and Apoptosis in Lung Cancer. *Onco Targets Ther* 11:1833-1847. doi:10.2147/OTT.S155716

Appendix B

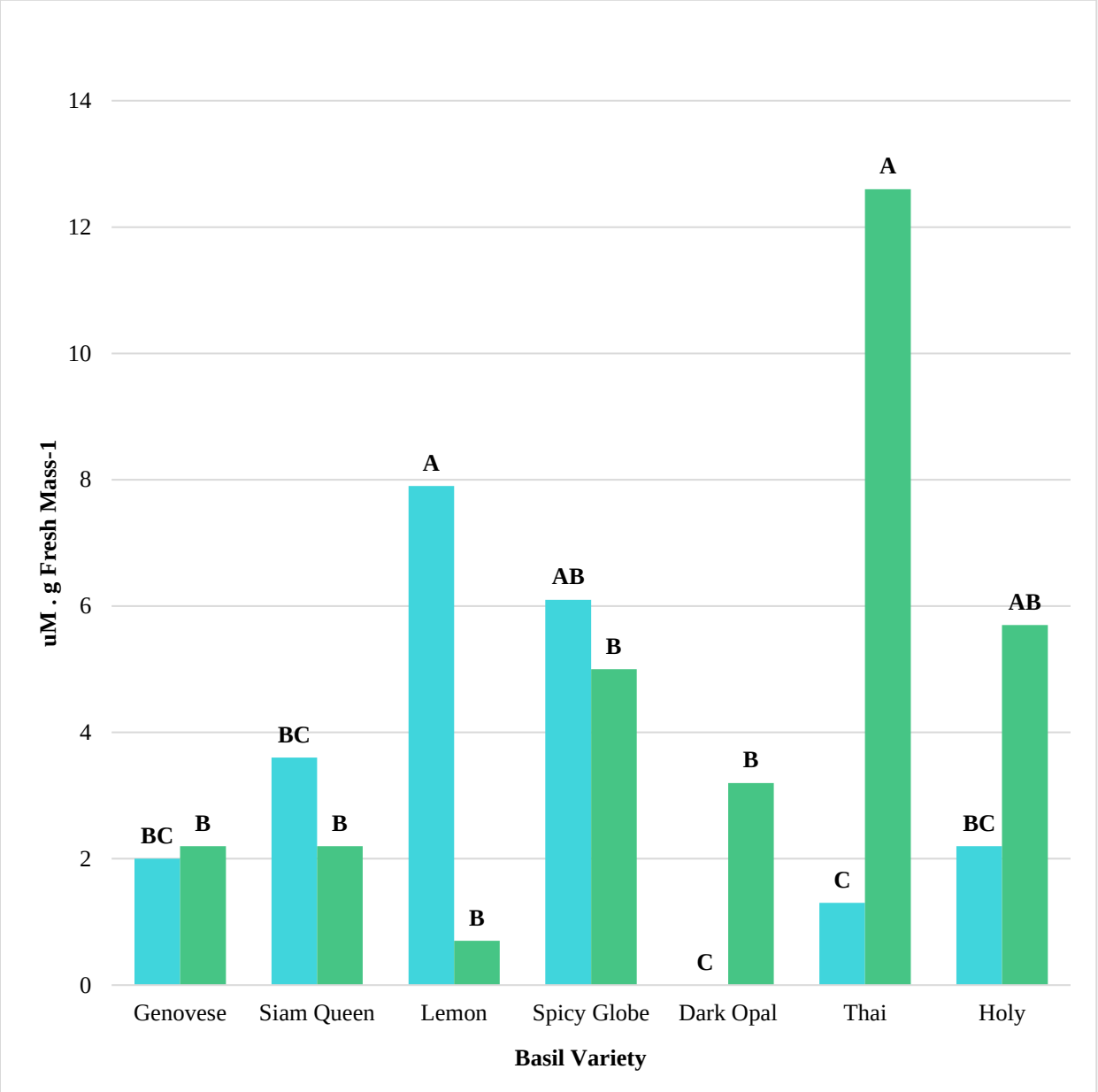

Figure 2.1. Terpinene (blue) and terpinolene (green) tissue concentrations ($\mu M \cdot g^{-1}$ FM) across seven common basil varieties. Values were analyzed using Tukey's protected LSD, and those followed by the same letter are not significantly different (α=0.05).

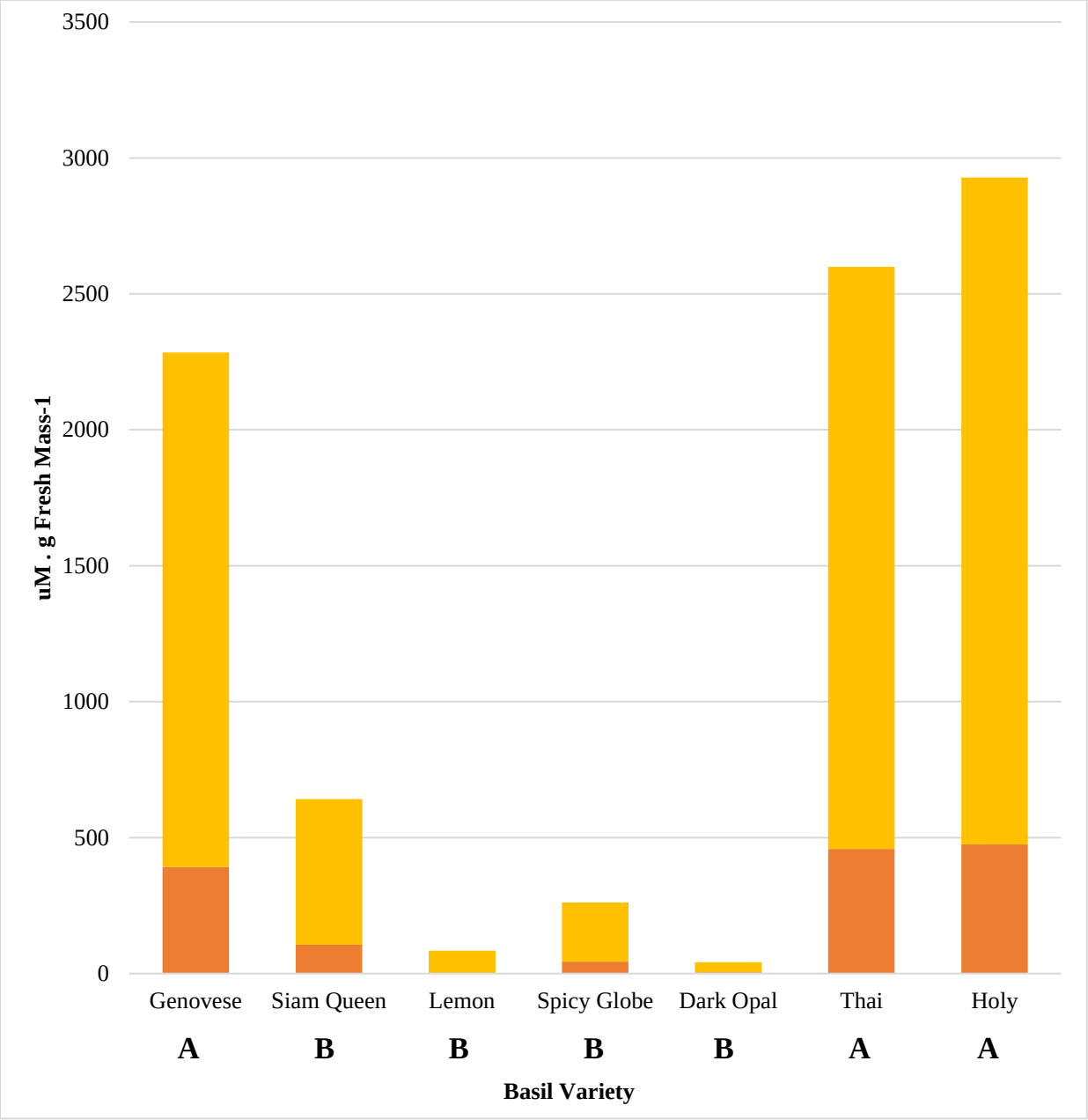

Figure 2.2. (R+/S-)-Limonene tissue concentrations (µM·g^{-1} FM) across seven common basil varieties. R+ enantiomer is displayed in orange, and the S- enantiomer in yellow. Values were analyzed using Tukey's protected LSD, and data followed by the same letter across varieties are not significantly different for each of the two compounds (α=0.05). Total limonene concentration mean separations are presented below each column, and varieties followed by the same letter are not significantly different (α=0.05).

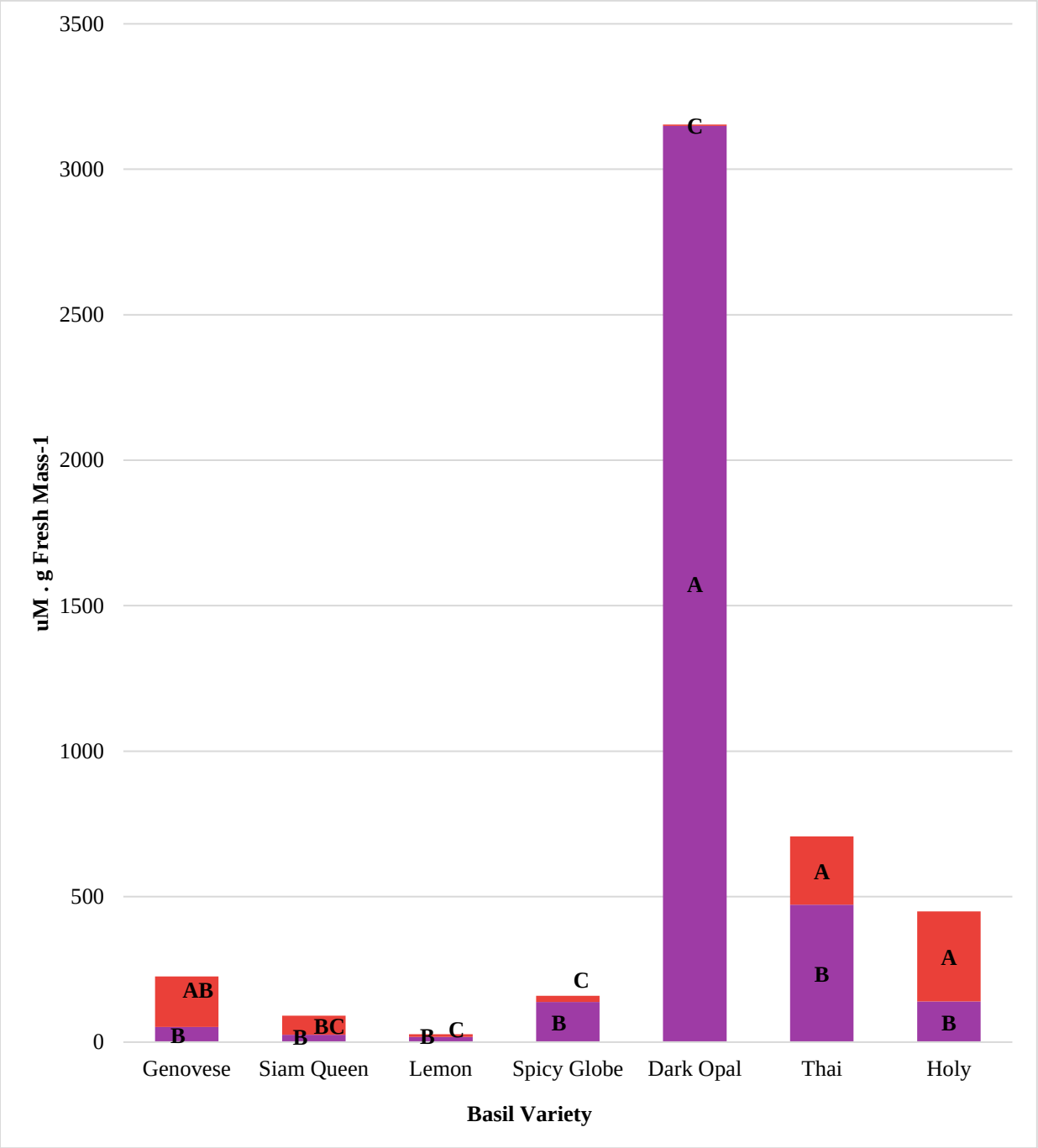

Figure 2.3. Methyl eugenol (purple) and eugenol (red) tissue concentrations ($\mu M \cdot g^{-1}$ FM) across seven common basil varieties. Values were analyzed using Tukey's protected LSD, and data followed by the same letter across varieties are not significantly different for each of the two compounds (α=0.05).

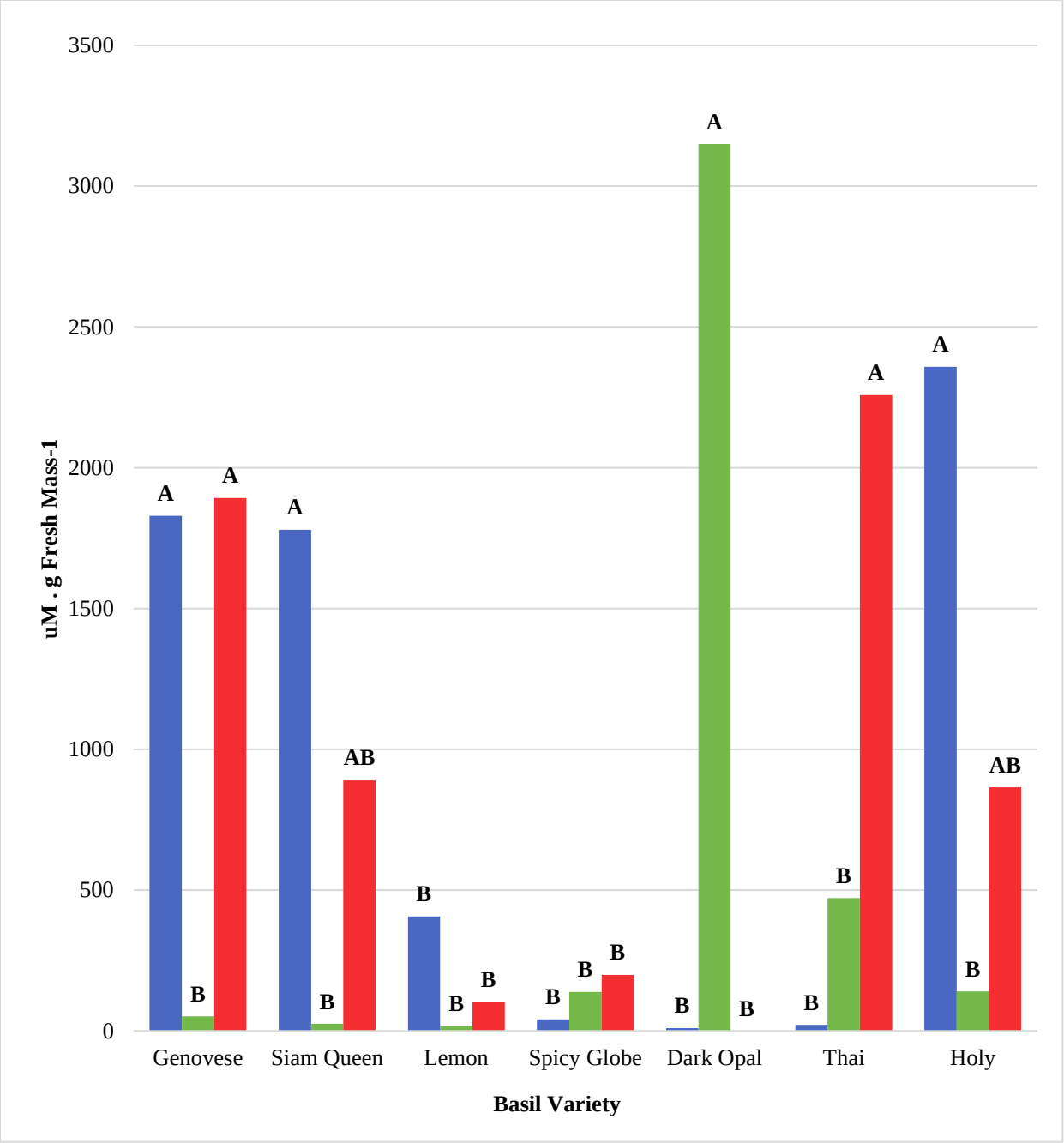

Figure 2.4. Linalool (blue), camphene (green), and methyl salicylate (red) tissue concentrations (μM·g^{-1} FM) across seven common basil varieties. Values were analyzed using Tukey's protected LSD, and those followed by the same letter are not significantly different (α=0.05).

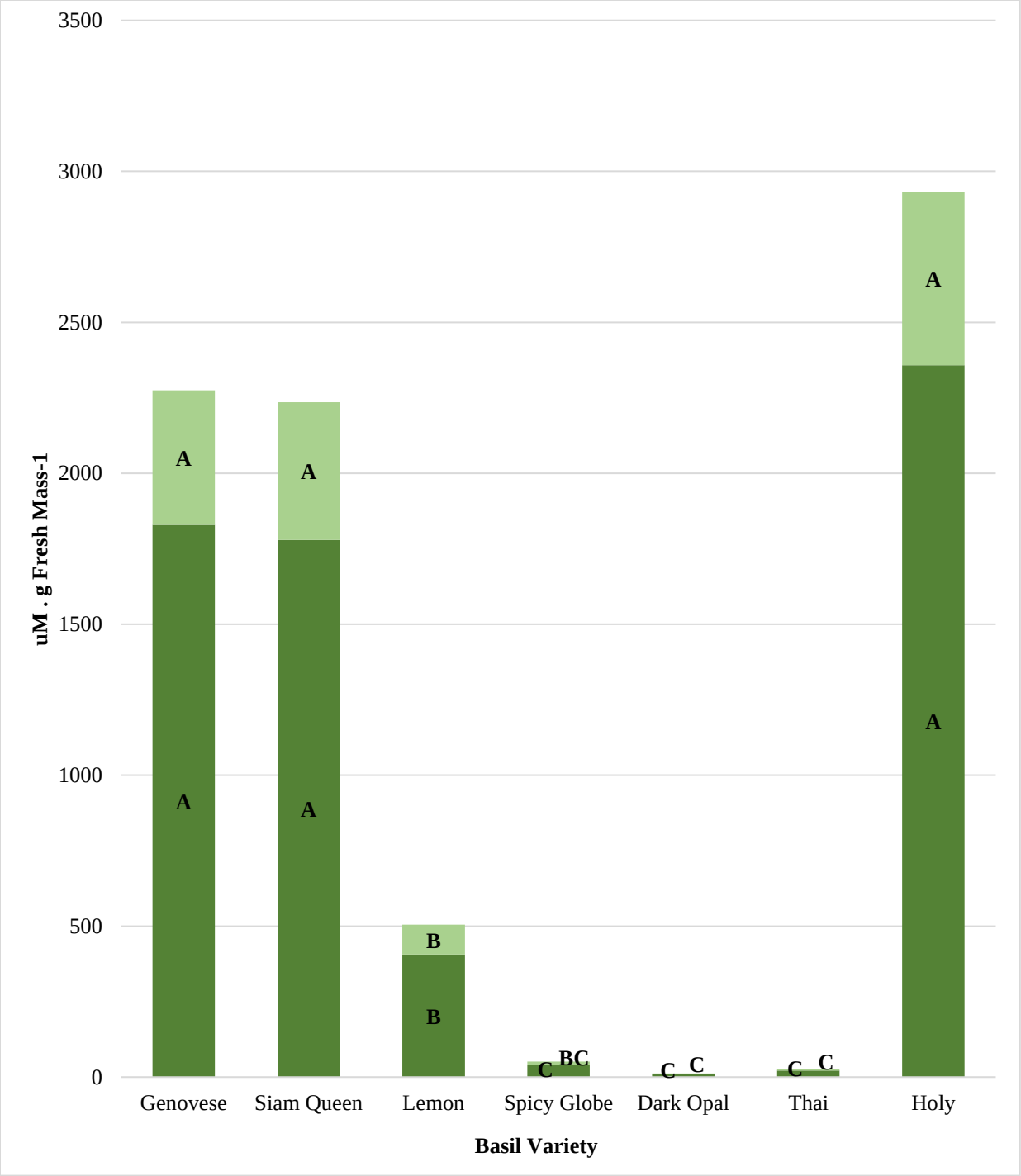

Figure 2.5. α-Pinene (dark green) and β-pinene (light green) tissue concentrations (μM·g^{-1} FM) across seven common basil varieties. Values were analyzed using Tukey's protected LSD, and data followed by the same letter across varieties are not significantly different for each of the two compounds (α=0.05).

CHAPTER 3: VARIATION IN SUPPLEMENTAL LIGHTING QUALITY INFLUENCES KEY AROMA VOLATILES IN HYDROPONICALLY GROWN 'ITALIAN LARGE LEAF' BASIL

Hunter A. Hammock and Carl E. Sams
Department of Plant Sciences, The University of Tennessee, Knoxville, TN 37996

Correspondence: Carl E. Sams, carlsams@utk.edu

Keywords: Controlled Environment Agriculture, Light Emitting Diodes, Narrowband LEDs, Spectral Quality, *Ocimum basilicum*, High Pressure Sodium, Supplemental Lighting, Secondary Metabolism, Terpenes

Author Contributions:
Conceptualization – HAH, CES
Methodology – HAH, CES
Software – HAH, CES
Validation – HAH
Formal analysis – HAH
Investigation – HAH
Resources – CES
Data curation – HAH
Writing (original draft preparation) - HAH
Writing (review and editing) – HAH, CES
Visualization – HAH
Supervision and project administration – CES
Funding acquisition – CES

Author Statement:
All authors have reviewed the manuscript and agree with the reported findings. There are no reported conflicts between the authors and the present study.

Funding:
This research was supported by The AgResearch Dean's Office within the University of Tennessee Institute of Agriculture. No external funds were used for the present study.

Disclosure:
This manuscript and its contents were published in Frontiers in Plant Sciences June 20th, 2023.

Citation:
Hammock HA and Sams CE (2023). Variation in supplemental lighting quality influences key aroma volatiles in hydroponically grown 'Italian Large Leaf' basil. Front. Plant Sci. 14:1184664. doi: 10.3389/fpls.2023.1184664

Abstract

The spectral quality of supplemental greenhouse lighting can directly influence aroma volatiles and secondary metabolic resource allocation (i.e., specific compounds and classes of compounds). Research is needed to determine species-specific secondary metabolic responses to supplemental lighting (SL) sources with an emphasis on variations in spectral quality. The primary objective of this experiment was to determine the impact of supplemental narrowband blue (B) and red (R) LED lighting ratios and discrete wavelengths on flavor volatiles in hydroponic basil (*Ocimum basilicum* var. Italian Large Leaf). A natural light (NL) control and different broadband lighting sources were also evaluated to establish the impact of adding discrete and broadband supplements to the ambient solar spectrum. Each SL treatment provided 8.64 $mol \cdot m^{-2} \cdot d^{-1}$ (100 $\mu mol \cdot m^{-2} \cdot s^{-1}$, 24 $h \cdot d^{-1}$) photon flux. The daily light integral (DLI) of the NL control averaged 11.75 $mol \cdot m^{-2} \cdot d^{-1}$ during the growth period (ranging from 4 to 20 $mol \cdot m^{-2} \cdot d^{-1}$). Basil plants were harvested 45 d after seeding. Using GC-MS, we explored, identified, and quantified several important volatile organic compounds (VOCs) with known influence on sensory perception and/or plant physiological processes of sweet basil. We found that the spectral quality from SL sources, in addition to changes in the spectra and DLI of ambient sunlight across growing seasons, directly influence basil aroma volatile concentrations. Further, we found that specific ratios of narrowband B/R wavelengths, combinations of discrete narrowband wavelengths, and broadband wavelengths directly and differentially influence the overall aroma profile as well as specific compounds. Based on the results of this study, we recommend supplemental 450 and 660 nm (± 20 nm) wavelengths at a ratio of approximately 10B/90R at 100-200 $\mu mol \cdot m^{-2} \cdot s^{-1}$, 12-24 $h \cdot d^{-1}$ for sweet basil grown under standard greenhouse conditions, with direct consideration of the natural solar spectrum and DLI provided for any given location and growing season. This experiment demonstrates the ability

to use discrete narrowband wavelengths to augment the natural solar spectrum to provide an optimal light environment across variable growing seasons. Future experiments should investigate SL spectral quality for the optimization of sensory compounds in other high-value specialty crops.

Introduction

Light plays a crucial role in the growth, yield, and metabolic processes of plants (Schmitt and Wulff, 1993; Massa et al., 2008; Olle and Viršile, 2013). It is one of the most important abiotic factors that regulate various physiological signals as well as primary (Darko et al., 2014; Thoma et al., 2020) and secondary (Ouzounis et al., 2015; Landi et al., 2020) metabolic responses in plants. The quality, intensity, and photoperiod of light directly impact plant growth and development (Smith, 1982; Fausey et al., 2005; Jiao et al., 2007). Photosynthetically active radiation (PAR) is composed of different wavelengths within the visible spectrum (400-700 nm) (McCree, 1973), but ultraviolet (Behn et al., 2010; Sakalauskaite et al., 2013; Santin et al., 2021) and far-red (Halaban, 1969; Mokvist et al., 2014; Kalaitzoglou et al., 2019; Zhen and Bugbee, 2020) wavelengths can be perceived and utilized by many species of higher plants.

The roles of light in activating pathways that shape plant growth and development are multifaceted and complex (Fankhauser and Chory, 1997; Chen et al., 2004). Plants possess a unique array of photoreceptors that sense various wavebands across the spectrum (Fankhauser and Chory, 1997; Folta and Carvalho, 2015; Galvao and Fankhauser, 2015). These include phytochromes which detect red and far-red light, cryptochromes which detect ultraviolet, blue, and green light; and phototropins, which respond primarily to blue light (Casal, 2000; Briggs and Olney, 2001). These sensors initiate downstream physiological and metabolic changes (Chen et al., 2004; Casal and Yanovsky, 2005; Rockwell et al., 2006). For example, isoprenoid and

phenylpropanoid synthesis are differentially affected by the spectral quality of light received (Bourgaud et al., 2001; Vranova et al., 2012; Lu et al., 2017). Overlapping interactions between narrowband wavelengths have been shown to cause synergistic or antagonistic effects on primary and secondary metabolic pathways (Colquhoun et al., 2013; Carvalho et al., 2016; Pennisi et al., 2019a).

Discrete narrowband wavelengths within the natural solar spectrum are known to play an important role in the quality of plants, affecting flavor, aroma, color, texture, and other human sensory aspects (Kelly and Runkle, 2020; Hammock et al., 2021; Paradiso and Proietti, 2021). Altering the spectral quality of light provided to greenhouse crops, whether that be using filters or supplemental lighting (SL), can directly influence secondary metabolic pathways (Ouzounis et al., 2015; Pennisi et al., 2019a). Different wavelengths of light have been shown to produce other effects in high-value specialty crops such as herbs (Dou et al., 2017; Pennisi et al., 2019b; Larsen et al., 2020), spices (Dou et al., 2017), flowers (Colquhoun et al., 2010; Currey et al., 2012; Colquhoun et al., 2013), strawberries (Kasperbauer et al., 2001), tomatoes (Gómez and Mitchell, 2014; Kaiser et al., 2018; Dannehl et al., 2021), and tea leaves (Fu et al., 2015); all of these crops could utilize variable light exposure to modify volatile metabolites responsible for their sensory qualities (Carvalho et al., 2016). For example, narrowband red and blue wavelengths are known to improve the sensory quality of certain crops. Manipulating the spectral quality of greenhouse crops using SL has been shown to enhance the production of secondary metabolites, which can be used for culinary, medicinal, and commercial purposes (Holopainen et al., 2018).

Horticultural lighting systems are sometimes employed in greenhouse operations when natural light intensity and/or spectral quality are insufficient for sustained plant growth and development (Faust et al., 2005; Sipos et al., 2020). It is well known that solar spectral quality,

irradiance, daily light integral (DLI), and photoperiod are variable depending on the time of day, the year, location, and local weather patterns (Korczynski et al., 2002; Thorne et al., 2009; Faust and Logan, 2018). Numerous studies have proven that such SL can noticeably improve both the yield and quality of various high-value specialty crops (Morrow, 2008; Singh et al., 2015). However, it is important to use the correct spectral qualities for each application to maximize plant performance, as many light responses are species-specific (Taulavuori et al., 2016a; Kyriacou et al., 2019; Santin et al., 2021). Despite being costly to purchase, maintain, and operate, commercial greenhouses lighting systems can be used to create the best possible conditions for growth. They can also be used to enhance the natural solar spectrum and impart desirable metabolic effects, such as the accumulation of aroma compounds and phytonutrients with known human health benefits (Rao and Rao, 2007; Poiroux-Gonord et al., 2010; Petrovic et al., 2019). By analyzing the impact of specific wavelengths created by existing greenhouse lighting systems on plant metabolism, we can develop energy-efficient SL strategies to enhance yields and the overall sensory quality of many high-value specialty crops.

One of the most popular and highly valued annual culinary herbs is sweet basil. It has a complex and unique aroma profile desired by professional chefs and restaurants worldwide (Putievsky and Galambosi, 1999; Hiltunen and Holm, 2003). It has a high harvest index and profit margin, is relatively easy to grow, and is well adapted for commercial greenhouse hydroponics and other controlled environment agriculture (CEA) systems (Sipos et al., 2021). The use of greenhouse hydroponics to cultivate basil can provide ideal climate and nutrient conditions that could help diminish any changes in plant growth or development caused by seasonal variations in environmental conditions (Kopsell et al., 2005; Kiferle et al., 2013). Basil is rich in phenolic and terpenoid compounds, many of which are important for human sensory perception and possess

human health benefits (Pattison et al., 2018). The 'Italian Large Leaf' variety is known for its strong and intense flavor, vigorous growth, and large leaves, with extensive use in Western and Mediterranean cuisines (Shanmugam et al., 2018). Because of its popularity, demand, and intense VOC profile, sweet basil makes for an excellent model crop to explore the interactions of SL, the natural solar spectrum, and secondary metabolic resource allocation.

The intricacy of sweet basil's taxonomy is due to its hybridization, mislabeling, and abundance of cultivars (Sipos et al., 2021). Recent studies have highlighted that even though these cultivars may look alike and often share the same name, they are genetically distinct from one another. Variations in the genetic background will profoundly impact light-mediated responses associated with secondary metabolism and aroma volatiles (De Masi et al., 2006; Bernhardt et al., 2015). The optimization of basil production in controlled environments depends on many factors, specifically the intensity and spectral quality of light provided.

Light-emitting diodes (LEDs) allow growers to precisely provide discrete narrowband wavelengths to their crops compared to traditional broadband lighting systems (i.e., high-pressure sodium). Spectral manipulation using LEDs can be used to alter the traits of basil, including its biomass and morphology, as well as its biochemical composition during growth and post-harvest (Hasan et al., 2017; Sipos et al., 2020). The potential for this physiological manipulation has been demonstrated with increases in total phenolic and isoprenoid concentrations when using narrowband blue and red light supplements. Research has shown that the addition of yellow and/or green wavelengths to blue and red wavelengths increased several monoterpenes, sesquiterpenes, and phenylpropanoids in basil compared with blue and red wavelength spectra (Stagnari et al., 2018; Sipos et al., 2020; Kivimaenpa et al., 2022). Further, many studies have demonstrated the species-specific (in some cases, even variety-specific) nature of secondary metabolic responses to

narrowband wavelengths, warranting further investigation of both phenolics and terpenoids in basil and other high-value specialty crops (Kyriacou et al., 2019; Toscano et al., 2021). Because of their importance in human sensory perception, the phenolic and terpenoid pathways should be thoroughly evaluated using various analytical and molecular techniques, since light-mediated secondary metabolic resource allocation will impact the expression/bioaccumulation of certain compounds as well as entire secondary metabolic pathways. To date, no published scientific investigations have explored the impact of discrete supplemental narrowband wavelengths and broadband lighting sources on the aroma volatile profile of 'Italian Large Leaf' basil across the changing natural solar spectrum under glass greenhouses across growing seasons.

With this in mind, we designed a set of experiments to determine the overall impact of spectral quality variation of SL on a common variety of greenhouse-produced hydroponically grown basil. The goals of this project were to (1) explore, identify, and quantify plant volatile organic compounds with known impacts on sensory perception or plant physiological processes of basil using headspace gas chromatography-mass spectrometry (HS GC-MS); (2) determine the impact of spectral quality from ambient sunlight and SL sources on aroma volatile concentrations, including specific ratios of narrowband blue/red wavelengths, combinations of discrete narrowband wavelengths, and broadband wavelength; and (3) provide physiology-based recommendations for lighting regimes (spectral quality of supplemental horticultural lighting systems) for commercial greenhouse basil production.

We hypothesize that discrete waveband supplements will differentially influence specific aroma volatiles and secondary metabolic resource allocation (i.e., particular compounds and classes of compounds). We predict this experiment will confirm that manipulating the spectral

quality of SL has a considerable impact on basil volatiles and can potentially enhance the human olfactory experience.

Materials and Methods

Cultural Techniques and Environmental Growing Conditions

This project was conducted at The University of Tennessee Institute of Agriculture (UTIA) in Knoxville, TN, USA (35°56'44.5"N, 83°56'17.3"W). Growing dates for these four experimental runs occurred from January 2019 to October 2019 and have been labeled as growing seasons. *Ocimum Basilicum* var. Italian Large Leaf basil seeds (Johnny's Select Seeds, Winslow, ME, United States) were germinated in peat moss-based cubes (2 × 2 × 6 cm) (Park's Bio Dome Sponges, Hodges, SC, United States) at 28.3°C and 95% RH. The 'Italian Large Leaf' variety of sweet basil was specifically chosen because of its unique flavor profile, high market demand, high yields, and preference among professional chefs. After two weeks, seedlings were transferred to nutrient film technique (NFT) hydroponic systems with full-strength general mix nutrient solution; the fertility regime was kept constant across the duration of all seasons. The nutrient solution was kept consistent at 5.9 pH and changed weekly. Elemental nutrient concentrations were as follows (ppm): Nitrogen (207.54), Phosphorous (50.87), Potassium (298.23), Calcium (180.15), Magnesium (77.10), Sulfur (136.45), Iron (3.95), Manganese (0.90), Zinc (0.40), Molybdenum (0.09), Copper (0.90), and Boron (0.90). Water samples were analyzed using Inductively Coupled Plasma Mass Spectrometry (Agilent Technologies, Santa Clara, CA, United States) throughout each experiment to ensure consistent nutrient composition. Total growth time lasted approximately 45 d across all four experimental runs (growing seasons). Relative humidity during the growth period averaged 52.5%. Day temperatures averaged 28.5 °C, and night temperatures averaged 21.2 °C. The DLI of the natural light control averaged 11.75 $mol \cdot m^{-2} \cdot d^{-1}$ during the growth period

(ranging from 4 to 20 $mol \cdot m^{-2} \cdot d^{-1}$). Specific growing parameters for each of the seasons may be found in Table 3.1.

This experiment evaluated the impact of discrete narrowband wavelength combinations from SL systems on tissue concentrations of plant volatile organic compounds (PVOCs) pertinent to flavor/aroma profile and human sensory perception. A total of 12 lighting treatments were used in this experiment, which included one non-supplemented natural light (NL) control (Fig. 3.1) and eleven supplemental lighting (SL) treatments of equal intensity with varying spectral distributions (Figs. 3.2 A-K). LEDs (Fluence Bioengineering, Austin, TX) and HPS lamps (Hortilux DE, Mentor OH) provided 8.64 $mol \cdot m^{-2} \cdot d^{-1}$ (equal intensity of 100 $\mu mol \cdot m^{-2} \cdot s^{-1}$ for 24 $h \cdot d^{-1}$) for each SL treatment, in addition to natural sunlight (Fig. 3.1). Lighting treatments are denoted by their wavelengths applied, and each wavelength in series was applied at equal intensities (i.e., a ratio of 1:1:1, with target intensities of 33.3/33.3/33.3 $\mu mol \cdot m^{-2} \cdot s^{-1}$). The intensity and duration of the lighting treatments in this experiment were selected based on current literature with the intention of maximizing the production of key secondary metabolites known to influence flavor perception in basil.

Four treatments applied narrowband red wavelengths across varying narrowband blue wavelengths (ratio of 1B:2R as 660/400/660, 660/420/660, 660/450/660, and 660/470/660) (Fluence Bioengineering, Austin, TX). One treatment applied a high dose of only narrowband blue wavelengths (470/450/420) (Fluence Bioengineering, Austin, TX), while another applied a moderated amount of narrowband blue wavelengths with some narrowband red wavelengths (ratio of 2B:1R as 450/660/470) (Fluence Bioengineering, Austin, TX). Two PhysioSpec lighting systems (Fluence Bioengineering, Austin, TX) were used to evaluate the ratio of narrowband blue and red wavelengths (ratios of 3B:47R and 3B:22R, as 6B/94R and 12B/88R, respectively).

Finally, three broadband supplemental treatments of various color temperatures were used, which included a high blue (450/W/470) (Fluence Bioengineering, Austin, TX), a neutral white (W/W/W) (Fluence Bioengineering, Austin, TX), and a high orange/red (HPS) (Hortilux DE, Mentor OH). As previously stated, all SL treatments were provided at equal intensity and duration. Treatments were measured with an Apogee PS-200 spectroradiometer (Apogee Instruments, Logan UT) multiple times per week (after dark) and regularly adjusted to ensure consistent SL intensities and spectral distributions across growing seasons.

Each SL treatment was physically separated to ensure no bleed-over effects between treatments (average of 1.1 ± 0.6 $\mu mol \cdot m^{-2} \cdot s^{-1}$ SL bleed-over at the treatment edges). 1.2 m x 1.2 m sections of basil were grown, with 1.2 m separation between treatments (i.e., measurement edge-to-edge of hydroponic systems within the greenhouse). Tissue samples were only harvested from within the middle 0.6 m of each treatment to ensure further reduction of SL contamination between treatments (0.3 m around the edge of each treatment was considered the buffer zone and was not used for sampling). SL bleed-over was <0.1 $\mu mol \cdot m^{-2} \cdot s^{-1}$ within the harvest zone of each treatment (i.e., below the instrumentation detection limit). Harvests occurred directly after sunrise, and samples were immediately sealed and frozen in liquid nitrogen, then transferred to a -80 °C freezer until the time of analysis to preserve all volatile compounds and inhibit post-harvest changes to metabolism.

Gas Chromatography and Mass Spectrometry Method

Three g of fresh leaf tissue (two basil plants per sample rep, 1.5 g of representative material from each plant, nodes four and eight) were placed in 20 mL borosilicate glass vials, then immediately frozen in liquid nitrogen, and stored in a -80 ºC freezer until time of analysis. Samples

were run within 72 hours of collection. Frozen samples were placed onto a Network Headspace Sampler (Agilent G1888, Santa Clara, CA, United States). Ten sample reps were used per treatment. Samples were heated to 80 ºC for 10 min and pressurized with Helium (Air Gas, analytical purity) to 95.21 kPa for 1 min. The tube was then vented for 1 min into the headspace transfer line (110 ºC) and injected (port at 250 ºC) into the GC (Agilent Technologies 6890N Network GC System). The volatiles were separated by an HP-5MS capillary column ((5%-Phenyl)-methylpolysiloxane, length: 30 m, ID: 0.250 mm, film thickness: 1 µm, Agilent Technologies) using analytical purity Helium carrier gas at 95.21 kPa with constant column pressure. At the start of data acquisition, the temperature was held at 40 ºC for 5 min, ramped up from 40 ºC to 250 ºC (5 ºC per min), then held constant for the duration of the run. The total run time was 70 min, including post-run and cool-down phases. After sample separation and column elution, the analytes were passed through a mass selective detector (Agilent Technologies 5973 Network Mass Selective Detector) at 250 ºC and collected over the course of the sample run. The transfer line, ion source, and quadrupole temperatures were 250 ºC, 230 ºC, and 170 ºC, respectively. The full scan mass range was set to 40-550 m/z (threshold: 150).

Agilent ChemStation was used for data collection and processing. Over 200 separate compounds were identified throughout this experiment, but emphasis was placed on key aroma compounds (i.e., shown in the literature to be essential for human sensory perception and/or plant metabolic processes) that have been calibrated to our GC-MS and HP-5MS column using pure analytical standards (Sigma-Aldrich, St. Louis, MO) to determine leaf tissue emissions of key VOCs on a fresh plant weight basis. The MS spectra from pure analytical standards and fresh samples were compared to NIST, ADMIS, and our custom basil reference library created from calibrated analytical standards to confirm peak identity and retention times. MassHunter

Workstation Software Version B.06.00 (Agilent Technologies, Inc., 2012) was used to integrate peaks automatically. Relative peak areas and retention times were automatically adjusted based on authentic analytical standards and multiple library references. Over 200 compounds were identified in this experiment, with approximately 50 of those being quantified using pure analytical standards.

All volatile concentration units are reported in micro molarity of analyte concentration (suspended in a known volume of gaseous headspace matrix) per g of fresh leaf tissue ($\mu M \cdot g^{-1}$ FM) to represent VOC emissions most accurately from the collected headspace sample above fresh plant tissues under specific reproducible analytical conditions (Tables 2-4; Figs 3, 4). This unit (compared to $\mu mol \cdot g^{-1}$ FM) was utilized because of its commonality in biological headspace GC-MS sampling and incorporates the concentration of each analyte per unit volume of headspace gas above the plant tissue (i.e., samples the dynamic and complex gaseous matrix which contains numerous pertinent VOCs), which is important for sensory-based studies. This provides the foundation for future sensory panel experiments aimed at determining the influence of light on consumer acceptance and preference of basil aroma profiles.

Statistical Analyses

A Randomized Complete Block Design was used for this experiment. All data sets were analyzed by Generalized Linear Model (GLM) and Mixed Model Analysis of Variance ($p = 0.05$) procedures using the statistical software SAS (version 9.4, SAS Institute, Cary, NC). Design and Analysis macro (DandA.sas), created by Dr. Arnold Saxton, was utilized in addition to Tukey's adjustment, regression analysis, and univariate/normalization procedures to provide additional statistical insights on the complete data set. Treatments were separated by least significant

difference (LSD) at α=0.05. Principal component analysis was performed using JMP Pro 17 (SAS Institute, Cary, NC). Due to the overwhelming number of compounds analyzed, only statically significant separations of compounds with known plant physiological function and/or human sensory impact were reported in this study. Key volatiles were analyzed and presented on a fresh mass (FM) basis as compared to calibration curves created from pure analytical standards.

Results

Plant volatile organic compound (PVOC) leaf tissue concentrations were evaluated in this experiment, many of which were influenced by growing season, lighting treatment, and season treatment interactions. Total VOC concentrations of basil leaf tissues were found to be statistically significant across both lighting treatment (F=103.01; $P \leq 0.0001$) (Fig. 3.3) and season (F=391.62; $P \leq 0.0001$) (Fig. 3.4). Statistical summary for individual compounds evaluated in this study are included (Table 3.1) and separated by category based on chemical class and metabolic origin. Categories include alcohols, aldehydes, benzyl aldehydes, amides and furans, hydrocarbons, acyclic monoterpenes, bicyclic monoterpenes, cyclic monoterpenes, sesquiterpenes, organosulfur, and phenylpropanoids.

Alcohols

(E)-3-Hexen-1-ol concentrations were significantly impacted by season (F=18.44; $P \leq 0.0001$), but not by lighting treatment (F=0.81; P=0.6264) or season*treatment interactions (F=0.67; P=0.8682) (Table 3.2). When averaged across all treatments, June and September had higher average concentrations, as compared to the January and April seasons. Season concentrations ranged from 2.27 $\mu M \cdot g^{-1}$ FM to 6.24 $\mu M \cdot g^{-1}$ FM (Table 3.3).

1-Octen-3-ol concentrations were significantly influenced by season (F=23.16; $P \leq 0.0001$), lighting treatment (F=3.47; $P \leq 0.0001$), and season*treatment interactions (F=2.32; $P \leq 0.0001$) (Table 3.2). The June growing season had the highest concentration averages as compared to any other season. September had the lowest but did not separate from January. Season concentrations ranged from 13.03 $\mu M \cdot g^{-1}$ FM to 39.72 $\mu M \cdot g^{-1}$ FM (Table 3.3). When averaged across all seasons, treatments 450/W/470 and 660/470/660 statistically separated from the 660/420/660 treatment, but the others did not show clear separation. Treatment concentration averages ranged from 15.15 $\mu M \cdot g^{-1}$ FM to 35.65 $\mu M \cdot g^{-1}$ FM (Table 3.4).

2-Octyn-1-ol concentrations were significantly impacted by season (F=36.42; $P \leq 0.0001$), lighting treatment (F=10.78; $P \leq 0.0001$), and season*treatment interactions (F=3.58; $P \leq 0.0001$) (Table 3.2). June again had the highest concentration as compared to any other season. September again had the lowest concentration. Season concentrations ranged from 395.22 $\mu M \cdot g^{-1}$ FM to 653.76 $\mu M \cdot g^{-1}$ FM (Table 3.3). While there was statistical separation for the two compounds across lighting treatments, no clear patterns were evident (Table 3.4).

2-Phenylethanol concentrations were significantly influenced by season (F=44.24; $P \leq 0.0001$), lighting treatment, (F=11.18; $P \leq 0.0001$) and season*treatment interactions (F=3.9; $P \leq 0.0001$) (Table 3.2). June again had the highest concentration as compared to any other season. September again had the lowest concentration but did not statistically separate from January. Season concentrations ranged from 19.56 $\mu M \cdot g^{-1}$ FM to 58.43 $\mu M \cdot g^{-1}$ FM (Table 3.3). The 6B/94R treatment had the highest concentration and statistically separated from all other treatments. The lowest concentration was found in the 660/420/660 and HPS treatments, but they were not statistically separate from many other treatments. Treatment concentrations ranged from 19.62 $\mu M \cdot g^{-1}$ FM to 74.13 $\mu M \cdot g^{-1}$ FM (Table 3.4).

Benzyl Aldehydes

3-Ethylbenzaldehyde concentrations were significantly influenced by season (F=140.11; $P \leq 0.0001$), lighting treatment (F=9.66; $P \leq 0.0001$), and season*treatment interactions (F=3.95; $P \leq 0.0001$) (Table 3.2). The June growing season had the highest concentration and was statistically separated from the lowest seasons, which were January and September. The season concentrations ranged from 4.28 $\mu M \cdot g^{-1}$ FM to 17.15 $\mu M \cdot g^{-1}$ FM (Table 3.3). The 6B/94R treatment had the highest concentration and was statistically separated from many other treatments; this includes 660/420/660, 660/450/660, and the NL control, which had three of the lowest concentrations and did not statistically separate. The treatment concentrations ranged from 5.35 $\mu M \cdot g^{-1}$ FM to 15.18 $\mu M \cdot g^{-1}$ FM (Table 3.4).

Benzeneacetaldehyde concentrations were significantly influenced by season (F=196.22; $P \leq 0.0001$), lighting treatment (F=19.32; $P \leq 0.0001$), and season*treatment interactions (F=7.76; $P \leq 0.0001$) (Table 3.2). The June growing season had the highest concentration and was statistically separated from the lowest season, which was September. The season concentrations had a considerable range, from 9.92 $\mu M \cdot g^{-1}$ FM to 250.85 $\mu M \cdot g^{-1}$ FM (Table 3.3). The 6B/94R again had the highest concentration and statistically separated from all other treatments. In general, the narrowband treatments had higher concentrations than the broadband treatments. NL control had the lowest concentration, but did not separate from the 660/420/660, HPS, and W/W/W treatments. The treatment concentrations ranged from 69.70 $\mu M \cdot g^{-1}$ FM to 276.22 $\mu M \cdot g^{-1}$ FM (Table 3.4).

Hydrocarbons

1,4-Cyclohexadiene concentrations were significantly influenced by growing season (F=80.31; $P \leq 0.0001$), lighting treatment (F=8.46; $P \leq 0.0001$), and season*treatment interactions (F=2.74; $P \leq 0.0001$) (Table 3.2). June and September growing seasons had statistically higher tissue concentrations than those in January and April. The January growing season had the lowest concentrations. The growing season concentrations ranged from 6.00 $\mu M \cdot g^{-1}$ FM to 17.34 $\mu M \cdot g^{-1}$ FM (Table 3.3). The treatment 6B/94R again had the highest tissue concentration, statistically greater than many of the narrowband and broadband SL treatments. The 660/420/660 again had the lowest tissue concentration of any treatment, and did not statistically separate from the NL control. The treatment tissue concentrations ranged from 6.38 $\mu M \cdot g^{-1}$ FM to 18.66 $\mu M \cdot g^{-1}$ FM (Table 3.4).

2-Cyclopropyl-2-pentene concentrations were significantly influenced by season (F=58.3; $P \leq 0.0001$), treatment (F=9.00; $P \leq 0.0001$), and season*treatment interactions (F=1.98; $P = 0.0013$) (Table 3.2). This compound showed similar seasonal patterns to previous hydrocarbons. June and September growing seasons had statistically higher tissue concentrations than those in January and April. The January growing season again had the lowest concentrations. The season concentrations ranged from 12.09 $\mu M \cdot g^{-1}$ FM to 25.58 $\mu M \cdot g^{-1}$ FM (Table 3.3). The 6B/94R treatment again had the highest tissue concentration, separating from some of the other treatments. The 660/420/660 had the lowest tissue concentration of any treatment, and did not statistically separate from the NL control and some of the SL treatments. The treatment concentrations ranged from 14.51 $\mu M \cdot g^{-1}$ FM to 27.61 $\mu M \cdot g^{-1}$ FM (Table 3.4).

Decane concentrations were significantly influenced by season (F=158.69; $P \leq 0.0001$), treatment (F=5.79; $P \leq 0.0001$), and season*treatment interactions (F=2.66; $P \leq 0.0001$) (Table 3.2).

June growing season had the highest tissue concentration, which statistically separated from all other seasons. The two seasons with the lowest concentrations were January and September. The season concentrations ranged from 9.99 $\mu M \cdot g^{-1}$ FM to 37.07 $\mu M \cdot g^{-1}$ FM (Table 3.3). The 660/470/660 and 6B/94R treatments had the two highest tissue concentrations, and did not separate from each other. The broadband treatments generally did not have as high concentrations as the narrowband treatments; the HPS and W/W/W treatments did not separate from the NL control, which had the lowest concentration. The treatment concentrations ranged from 13.10 $\mu M \cdot g^{-1}$ FM to 25.92 $\mu M \cdot g^{-1}$ FM (Table 3.4).

(E)-3-Methyl-1,3,5-hexatriene concentrations were significantly influenced by season (F=6.53; P=0.0003), but not by lighting treatment (F=1.78; P=0.0558) or season*treatment interactions (F=1.04; P=0.4103) (Table 3.2). The September growing season had the highest tissue concentration, but did not statistically separate from the June season. The January growing season had the lowest tissue concentration but did not separate from the April or June seasons. The season concentrations ranged from 2.00 $\mu M \cdot g^{-1}$ FM to 3.19 $\mu M \cdot g^{-1}$ FM (Table 3.3).

1,3-cis,5-cis-Octatriene concentrations were significantly influenced by season (F=42.07; $P \leq 0.0001$), lighting treatment (F=8.62; $P \leq 0.0001$), and season*treatment interactions (F=1.71; P=0.01) (Table 3.2). The June growing season had the highest tissue concentration, but did not statistically separate from the September season. The January growing season had the lowest tissue concentration but did not separate from the April season. The season concentrations ranged from 5.41 $\mu M \cdot g^{-1}$ FM to 8.84 $\mu M \cdot g^{-1}$ FM (Table 3.3). The 6B/94R treatment had the highest tissue concentration, but did not separate from the 450/W/470 or 12B/88R treatments. The 660/420/660 again had the lowest tissue concentration of any other treatment, and did not statistically separate

from the NL control and some of the LED treatments. The treatment concentrations ranged from 5.08 μM·g^{-1} FM to 9.77 μM·g^{-1} FM (Table 3.4).

1,4-Octadiene concentrations were significantly influenced by season (F=27.54; $P \leq 0.0001$), lighting treatment (F=3.60; $P \leq 0.0001$), and season*treatment interactions (F=2.18; $P=0.0003$) (Table 3.2). The June growing season had the highest tissue concentration. The September growing season had the lowest tissue concentration but did not separate from the January season. The season concentrations ranged from 7.28 μM·g^{-1} FM to 40.63 μM·g^{-1} FM (Table 3.3). The treatments 660/470/660 and 450/W/470 had the highest two tissue concentrations and did not statistically from each other, as well many of the other treatments and control. The lowest tissue concentrations were found in the 660/420/660 treatment, which only statistically separated from the highest two treatments in addition to the 6B/94R treatment. The treatment concentrations ranged from 8.98 μM·g^{-1} FM to 35.66 μM·g^{-1} FM (Table 3.4).

2-Methyl-2-hepten-4-yne concentrations were significantly influenced by season (F=31.70; $P \leq 0.0001$), lighting treatment (F=9.23; $P \leq 0.0001$), and season*treatment interactions (F=2.07; $P=0.0006$) (Table 3.2). The September growing season had the highest tissue concentration, but did not statistically separate from the June season. The January growing season had the lowest tissue concentration but did not separate from the April season. The season concentrations ranged from 6.56 μM·g^{-1} FM to 9.08 μM·g^{-1} FM (Table 3.3). The treatment 6B/94R had the highest tissue concentration, but did not separate from the 450/W/470 and 12B/88R treatments. The lowest tissue concentrations were again found in the 660/420/660 treatment, which did not separate from the NL control and some of the LED treatments. The treatment concentrations ranged from 5.52 μM·g^{-1} FM to 10.20 μM·g^{-1} FM (Table 3.4).

1-Methylcyclohexene concentrations were significantly influenced by season (F=135.93; $P \leq 0.0001$) and lighting treatment (F=1.92; $P=0.0356$), but not by season*treatment interactions (F=1.04; $P=0.4174$) (Table 3.2). The September growing season had the highest tissue concentrations, which separated from all other seasons. The lowest tissue concentrations were found during the January growing season, but did not separate from the April and June seasons. The season concentrations ranged from 23.40 $\mu M \cdot g^{-1}$ FM to 89.07 $\mu M \cdot g^{-1}$ FM (Table 3.3). The treatment concentrations ranged from 179.01 $\mu M \cdot g^{-1}$ FM to 235.55 $\mu M \cdot g^{-1}$ FM; while the p-value from ANOVA did pass the 0.05 threshold, Tukey's protected LSD test did not indicate separation of means across treatments (Tables 2 and 4).

Cycloheptene concentrations were significantly influenced by season (F=3.18; $P=0.0258$), but not by lighting treatment (F=0.67; $P=0.7661$) or season*treatment interactions (F=1.05; $P=0.411$) (Table 3.2). This compound was found in very low concentrations. The June and September growing seasons had the two highest concentrations and did not statistically separate. The January and April growing seasons had the two lowest concentrations and did not statistically separate. The season concentrations ranged from 0.73 $\mu M \cdot g^{-1}$ FM to 1.09 $\mu M \cdot g^{-1}$ FM (Table 3.3). Treatment concentrations ranged from 0.70 $\mu M \cdot g^{-1}$ FM to 1.01 $\mu M \cdot g^{-1}$ FM (Table 3.4).

Acyclic Monoterpenes

2,6-Dimethyl-2,4,6-octatriene concentrations were significantly influenced by season (F=65.54; $P \leq 0.0001$), lighting treatment (F=12.59; $P \leq 0.0001$), and season*treatment interactions (F=3.43; $P \leq 0.0001$) (Table 3.2). The June growing season had the highest tissue concentration, while the lowest concentration was found in January. Each of the growing seasons statistically separated. The season concentrations ranged from 1.77 $\mu M \cdot g^{-1}$ FM to 6.30 $\mu M \cdot g^{-1}$ FM (Table 3.3).

The 6B/94R treatment had the highest tissue concentration, which statistically separated from all other treatments. The NL control had the lowest concentration of any treatment, and did not statistically separate from many of the LED treatments as well as the HPS and W/W/W treatments. The treatment tissue concentrations ranged from 2.55 $\mu M \cdot g^{-1}$ FM to 7.65 $\mu M \cdot g^{-1}$ FM (Table 3.4).

cis-β-Ocimene concentrations were significantly influenced by season (F=48.61; $P \leq 0.0001$), lighting treatment (F=3.18; $P=0.0004$), and season*treatment interactions (F=1.81; $P=0.0048$) (Table 3.2). The June growing season had the highest tissue concentration, while the lowest concentration was found in September. Each of the growing seasons statistically separated. The season concentrations ranged from 145.81 $\mu M \cdot g^{-1}$ FM to 754.18 $\mu M \cdot g^{-1}$ FM (Table 3.3). The 6B/94R treatment again had the highest tissue concentrations, and statistically separated from some of the LED treatments as well as the HPS and W/W/W treatments. The NL control had the lowest concentration, but did not separate from the broadband treatments and many of the LED treatments. The treatment tissue concentrations ranged from 343.47 $\mu M \cdot g^{-1}$ FM to 756.25 $\mu M \cdot g^{-1}$ FM (Table 3.4).

Citronellyl Acetate concentrations were significantly influenced by season (F=13.31; $P \leq 0.0001$), lighting treatment (F=2.7; $P=0.0024$), and season*treatment interactions (F=1.75; $P=0.0085$) (Table 3.2). The June growing season had the highest tissue concentration, while the lowest concentration was found in January. September statistically separated from June and January, but not from the April growing season. The season concentrations ranged from 188.27 $\mu M \cdot g^{-1}$ FM to 193.66 $\mu M \cdot g^{-1}$ FM (Table 3.3). The 6B/94R treatment had the highest tissue concentrations, and statistically separated from some of the LED treatments, but not the NL control or broadband treatments. The high blue 470/450/420 treatment had the lowest concentration, but

only separated from the 6B/94R treatment. The treatment tissue concentrations ranged from 189.24 $\mu M \cdot g^{-1}$ FM to 194.78 $\mu M \cdot g^{-1}$ FM (Table 3.4).

Linalool concentrations were significantly influenced by season (F=47.53; $P \leq 0.0001$), lighting treatment (F=2.17; $P=0.0152$), and season*treatment interactions (F=1.57; $P=0.0262$) (Table 3.2). The January growing season had the highest tissue concentration, while the lowest concentration was found in September. January, April, and June all statistically separated from September, but not from each other. The season concentrations ranged from 239.32 $\mu M \cdot g^{-1}$ FM to 925.12 $\mu M \cdot g^{-1}$ FM (Table 3). The 660/470/660 treatment had the highest tissue concentrations, but only statistically separated from the 660/420/660 treatment; none of the other treatments showed statistical separation. The treatment tissue concentrations ranged from 602.95 $\mu M \cdot g^{-1}$ FM to 924.86 $\mu M \cdot g^{-1}$ FM (Table 3.4).

trans-β-Ocimene concentrations were significantly influenced by season (F=80.44; $P \leq 0.0001$), lighting treatment (F=6.97; $P \leq 0.0001$), and season*treatment interactions (F=3.19; $P \leq 0.0001$) (Table 3.2). The June growing season had the highest tissue concentration, while the lowest concentration was found in September. September statistically separated from June and April, but not from the January growing season. The season concentrations ranged from 57.16 $\mu M \cdot g^{-1}$ FM to 351.14 $\mu M \cdot g^{-1}$ FM (Table 3.3). The 6B/94R treatment had the highest tissue concentrations, and statistically separated from all the other treatments except for 450/W/470. Many of the LED treatments do not show separation among themselves. The lowest concentration was found in the 660/420/660 treatment, but it did not separate from the NL control, many narrowband treatments, and the HPS and W/W/W treatments. The treatment tissue concentrations ranged from 111.37 $\mu M \cdot g^{-1}$ FM to 357.86 $\mu M \cdot g^{-1}$ FM (Table 3.4).

α-Ocimene concentrations were significantly influenced by season (F=195.03; $P \leq 0.0001$) and season*treatment interactions (F=2.00; $P=0.0011$), but not by treatment (F=1.29; $P=0.2295$) (Table 3.2). The September growing season had the highest tissue concentration, while the lowest concentration was found in April. September separated from the other seasons, but the January, April, and June seasons did not separate amongst themselves. September had approximately 5-20x tissue concentrations compared to other seasons. The season concentrations ranged from 75.23 $\mu M \cdot g^{-1}$ FM to 493.99 $\mu M \cdot g^{-1}$ FM (Table 3.3). Treatments did not statistically separate, and tissue concentrations ranged from 98.66 $\mu M \cdot g^{-1}$ FM to 212.20 $\mu M \cdot g^{-1}$ FM (Table 3.4).

β-Myrcene concentrations were significantly influenced by season (F=268.9; $P \leq 0.0001$), lighting treatment (F=5.15; $P \leq 0.0001$), and season*treatment interactions (F=2.83; $P \leq 0.0001$) (Table 3.2). The June growing season had the highest tissue concentration, while the lowest concentration was found in September. June did not statistically separate from April; September statistically separated from all other treatments and had drastically lower concentrations when compared to other seasons. The season concentrations ranged from 9.36 $\mu M \cdot g^{-1}$ FM to 407.65 $\mu M \cdot g^{-1}$ FM (Table 3.3). The 6B/94R treatment had the highest tissue concentrations, and statistically separated from the NL control, HPS, and W/W/W treatments. The 660/420/660 treatment had the lowest concentration, which separated from the 660/470/660, 450/W/470, and PhysioSpec treatments. The treatment tissue concentrations ranged from 203.27 $\mu M \cdot g^{-1}$ FM to 345.31 $\mu M \cdot g^{-1}$ FM (Table 3.4).

Bicyclic Monoterpenes

3-Caren-10-al concentrations were significantly influenced by season (F=17.21; $P \leq 0.0001$) and treatment (F=2.24; $P=0.0123$), but not by season*treatment interactions (F=1.06;

P=0.3871) (Table 3.2). The September growing season had the highest concentration and was statistically separated from the lowest season, which was April. Season concentrations ranged from 1.21 μM·g^{-1} FM to 2.51 μM·g^{-1} FM (Table 3). The treatments 450/W/470 and 6B/94R were both significantly higher than the NL control, but the other treatments did not separate statistically. The treatment concentrations ranged from 1.32 μM·g^{-1} FM to 2.40 μM·g^{-1} FM (Table 3.4).

(+)-4-Carene concentrations were significantly influenced by season (F=27.75; *P*≤0.0001), lighting treatment (F=7.00; *P*≤0.0001), and season*treatment interactions (F=1.57; *P*=0.0254) (Table 3.2). The June growing season had the highest tissue concentration, while the lowest concentration was found in January. All of the season concentration averages statistically separated from each other. The season concentrations ranged from 16.93 μM·g^{-1} FM to 61.46 μM·g^{-1} FM (Table 3). The 6B/94R treatment had the highest tissue concentrations, and statistically separated from the NL control, HPS, and W/W/W treatments. The 660/420/660 treatment had the lowest concentration, which separated from the 660/470/660, 450/W/470, and 6B/94R treatments. The treatment tissue concentrations ranged from 18.67 μM·g^{-1} FM to 45.46 μM·g^{-1} FM (Table 3.4).

3-Carene concentrations were significantly influenced by season (F=24.28; *P*≤0.0001) and season*treatment interactions (F=2.35; *P*=0.0005), but not by lighting treatment (F=4.53; *P*=0.0521) (Table 3.2). The June growing season had the highest tissue concentration, but did not statistically separate from April or September. January growing season had the lowest concentration, separating from the other seasons. The season concentrations ranged from 379.21 μM·g^{-1} FM to 559.24 μM·g^{-1} FM (Table 3.3).

Camphene concentrations were significantly influenced by season (F=70.69; *P*≤0.0001), lighting treatment (F=9.41; *P*≤0.0001), and season*treatment interactions (F=1.52; *P*=0.0356) (Table 3.2). The September growing season had the highest tissue concentration, while the lowest

concentration was found in January. The September season statistically separated from the other seasons, but January, April, and June did not separate amongst themselves. The season concentrations ranged from 23.41 $\mu M \cdot g^{-1}$ FM to 55.77 $\mu M \cdot g^{-1}$ FM (Table 3.3). The 450/W/470 treatment had the highest tissue concentrations, but did not statistically separate from the PhysioSpec and 660/470/660 treatments; the 450/W/470 did separate from the HPS, W/W/W, and NL control. The 660/420/660 treatment had the lowest concentration, which separated from the 660/470/660, 450/W/470, and PhysioSpec treatments. The treatment tissue concentrations ranged from 22.72 $\mu M \cdot g^{-1}$ FM to 51.23 $\mu M \cdot g^{-1}$ FM (Table 3.4).

Isoborneol concentrations were significantly influenced by season (F=22.21; $P \leq 0.0001$), lighting treatment (F=3.85; $P \leq 0.0001$), and season*treatment interactions (F=1.51; $P=0.0367$) (Table 3.2). The September growing season had the highest tissue concentration, while the lowest concentration was found in April. September, June, and April all statistically separated, but January did not separate from June and April. The season concentrations ranged from 23.53 $\mu M \cdot g^{-1}$ FM to 49.74 $\mu M \cdot g^{-1}$ FM (Table 3.3). The 6B/94R treatment had the highest tissue concentrations, and statistically separated from the NL control and HPS treatments, as well as some of the LED treatments. The 660/420/660 treatment had the lowest concentration, which did not separate from the NL control and the majority of LED treatments. The treatment tissue concentrations ranged from 22.05 $\mu M \cdot g^{-1}$ FM to 51.35 $\mu M \cdot g^{-1}$ FM (Table 3.4).

trans-Pinocarveol concentrations were significantly influenced by season (F=7.36; $P \leq 0.0001$), lighting treatment (F=3.32; $P=0.0002$), and season*treatment interactions (F=1.89; $P=0.00027$) (Table 3.2). The September growing season had the highest tissue concentration, while the lowest concentration was found in January. The season concentrations ranged from 3.60 $\mu M \cdot g^{-1}$ FM to 6.13 $\mu M \cdot g^{-1}$ FM (Table 3.3). The 6B/94R treatment again had the highest tissue

concentrations, which separated from the 660/420/660, 660/450/660, and W/W/W treatments. The 660/420/660 treatment had the lowest concentration, but the only treatment that was statistically significantly different was the 6B/94R treatment. The treatment tissue concentrations ranged from 3.12 $\mu M \cdot g^{-1}$ FM to 7.30 $\mu M \cdot g^{-1}$ FM (Table 3.4).

trans-Sabinene hydrate concentrations were significantly influenced by season (F=158.38; $P \leq 0.0001$), lighting treatment (F=5.80; $P \leq 0.0001$), and season*treatment interactions (F=2.66; $P \leq 0.0001$) (Table 3.2). The June growing season had the highest tissue concentration, while the lowest concentration was found in January. September and January did not statistically separate. The season concentrations ranged from 10.04 $\mu M \cdot g^{-1}$ FM to 37.07 $\mu M \cdot g^{-1}$ FM (Table 3.3). The 660/470/660 treatment had the highest tissue concentrations, and statistically separated from the NL control, HPS, and W/W/W treatments. The 660/470/660 treatment did not separate from the 6B/94R treatment and some of the other LED treatments. The lowest concentration was found in the NL control, which did not separate from the HPS and W/W/W treatments. The treatment tissue concentrations ranged from 13.09 $\mu M \cdot g^{-1}$ FM to 25.92 $\mu M \cdot g^{-1}$ FM (Table 3.4).

α-Pinene concentrations were significantly influenced by season (F=73.74; $P \leq 0.0001$), lighting treatment (F=9.4; $P \leq 0.0001$), and season*treatment interactions (F=1.65; $P = 0.0152$) (Table 3.2). The September growing season had the highest tissue concentration, while the lowest concentration was found in January. All of the season concentration averages statistically separated, except for April and June. The season concentrations ranged from 17.27 $\mu M \cdot g^{-1}$ FM to 46.27 $\mu M \cdot g^{-1}$ FM (Table 3.3). The 450/W/470 and 6B/94R treatments had the highest tissue concentrations and were not statistically separate. The 660/420/660 treatment again had the lowest concentration, which separated from the 660/470/660, 470/450/420, 450/W/470, and PhysioSpec treatments. The 660/420/660 treatment did not separate from the HPS, W/W/W, or the NL control.

The treatment tissue concentrations ranged from 16.60 μM·g^{-1} FM to 41.75 μM·g^{-1} FM (Table 3.4).

β-Pinene concentrations were significantly influenced by season (F=49.46; $P \leq 0.0001$), lighting treatment (F=5.93; $P \leq 0.0001$), and season*treatment interactions (F=1.86; $P=0.0032$) (Table 3.2). β-Pinene followed a similar pattern to α-Pinene for both season and lighting treatment concentration. In addition, the ratio of α-Pinene to β-Pinene varied less than 8% across all treatments and seasons, and did not show any discernable pattern. The September growing season had the highest tissue concentration, while the lowest concentration was found in January. All of the season concentration averages statistically separated, except for April and June. The season concentrations ranged from 99.30 μM·g^{-1} FM to 208.12 μM·g^{-1} FM (Table 3.3). The 450/W/470 and 6B/94R treatments again had the highest tissue concentrations and were not statistically separate. The 660/420/660 treatment again had the lowest concentration, which separated from the 660/470/660, 470/450/420, 450/W/470, and 6B/94R treatments. The 660/420/660 treatment did not separate from the HPS, W/W/W, or the NL control. The treatment tissue concentrations ranged from 111.86 μM·g^{-1} FM to 190.27 μM·g^{-1} FM (Table 3.4).

Cyclic Monoterpenes

3-Menthene concentrations were significantly influenced by season (F=10.23; $P \leq 0.0001$), lighting treatment (F=4.23; $P \leq 0.0001$), and season*treatment interactions (F=2.34; $P \leq 0.0001$) (Table 3.2). The June growing season had the highest tissue concentration, while the lowest concentration was found in January. The January growing season separated from the other seasons, but April, June, and September did not separate amongst themselves. The season concentrations ranged from 24.22 μM·g^{-1} FM to 46.11 μM·g^{-1} FM (Table 3.3). The 12B/88R treatment had the

highest tissue concentrations and separated from the HPS, and W/W/W, but not the NL control. The 660/420/660 treatment again had the lowest concentration, which separated from the 450/W/470 PhysioSpec treatments. The 660/420/660 treatment did not separate from the HPS, W/W/W, or the NL control. The treatment tissue concentrations ranged from 20.38 $\mu M \cdot g^{-1}$ FM to 53.10 $\mu M \cdot g^{-1}$ FM (Table 3.4).

d-Limonene concentrations were significantly influenced by season (F=29.8; $P \leq 0.0001$), lighting treatment (F=7.17; $P \leq 0.0001$), and season*treatment interactions (F=1.74; $P=0.0076$) (Table 3.2). The June growing season had the highest tissue concentration, while the lowest concentration was found in January. All of the season concentration averages statistically separated, except for April and September. The season concentrations ranged from 234.61 $\mu M \cdot g^{-1}$ FM to 387.51 $\mu M \cdot g^{-1}$ FM (Table 3.3). The 6B/94R treatment had the highest tissue concentration and was separated from the HPS, W/W/W, and NL control. The 660/420/660 treatment had the lowest concentration, which separated from the 660/470/660, 470/450/420, 450/W/470, and PhysioSpec treatments. The 660/420/660 treatment did not separate from the HPS, W/W/W, or the NL control. The treatment tissue concentrations ranged from 224.30 $\mu M \cdot g^{-1}$ FM to 401.22 $\mu M \cdot g^{-1}$ FM (Table 3.4).

Fenchyl acetate concentrations were significantly influenced by season (F=14.98; $P \leq 0.0001$), but not by lighting treatment (F=1.58; $P=0.1019$) or season*treatment interactions (F=0.62; $P=0.9467$) (Table 3.2). The April growing season had the highest tissue concentration, but it did not statistically separate from the January or June seasons. The lowest concentrations were found in the September season. The season concentrations ranged from 81.12 $\mu M \cdot g^{-1}$ FM to 149.80 $\mu M \cdot g^{-1}$ FM (Table 3.3). The treatment tissue concentrations did not statistically separate and ranged from 81.22 $\mu M \cdot g^{-1}$ FM to 115.00 $\mu M \cdot g^{-1}$ FM (Tables 2 and 4).

p-Menth-1-en-8-ol concentrations were significantly influenced by season (F=173.75; $P \leq 0.0001$), lighting treatment (F=10.61; $P \leq 0.0001$) and season*treatment interactions (F=2.56; $P \leq 0.0001$) (Table 3.2). The June growing season had the highest tissue concentration, while the lowest concentration was found in January. All of the season concentration averages statistically separated. The season concentrations ranged from 5.44 $\mu M \cdot g^{-1}$ FM to 19.69 $\mu M \cdot g^{-1}$ FM (Table 3.3). The 6B/94R treatment had the highest tissue concentration and was separated from the HPS, W/W/W, and NL control. The 660/420/660 treatment had the lowest concentration, which separated from the 660/470/660, 470/450/420, 450/W/470, and PhysioSpec treatments. The 660/420/660 treatment did not separate from the HPS or the NL control, as well as a few LED treatments. The treatment tissue concentrations ranged from 7.78 $\mu M \cdot g^{-1}$ FM to 17.03 $\mu M \cdot g^{-1}$ FM (Table 3.4).

Sesquiterpenes

α-Humulene concentrations were significantly influenced by season (F=19.58; $P \leq 0.0001$) and lighting treatment (F=1.87; $P=0.0420$), but not by season*treatment interactions (F=1.12; $P=0.3001$) (Table 3.2). The September growing season had the highest tissue concentration, but did not separate from the June season. While the lowest concentration was found in January, it did not statistically separate from April. The season concentrations ranged from 53.69 $\mu M \cdot g^{-1}$ FM to 59.58 $\mu M \cdot g^{-1}$ FM (Table 3.3). The treatment tissue concentrations did not show statistical separation and ranged from 54.51 $\mu M \cdot g^{-1}$ FM to 59.41 $\mu M \cdot g^{-1}$ FM (Tables 2 and 4).

Organosulfur

Isothiocyanatocyclopropane concentrations were significantly influenced by season (F=9.92; $P \leq 0.0001$), but not by lighting treatment (F=1.69; $P=0.0752$) or season*treatment interactions (F=0.85; $P=0.7103$) (Table 3.2). The September growing season had the highest tissue concentration, while the lowest concentration was found in April. The season concentrations ranged from 1.20 $\mu M \cdot g^{-1}$ FM to 2.28 $\mu M \cdot g^{-1}$ FM (Table 3.3). The treatment tissue concentrations did not show statistical separation, and ranged from 0.99 $\mu M \cdot g^{-1}$ FM to 2.32 $\mu M \cdot g^{-1}$ FM (Table 3.4).

2-Isobutylthiazole concentrations were significantly influenced by season (F=10.79; $P \leq 0.0001$), but not by lighting treatment (F=1.90; $P=0.0591$) or season*treatment interactions (F=1.23; $P=0.2101$) (Table 3.2). The September growing season had the highest tissue concentration, but did not statistically separate from the June season. The lowest concentration was found in January, but it did not separate from the April season. The season concentrations ranged from 5.57 $\mu M \cdot g^{-1}$ FM to 8.94 $\mu M \cdot g^{-1}$ FM (Table 3.3).

Dimethyl Sulfide concentrations were significantly influenced by season (F=25.15; $P \leq 0.0001$), lighting treatment (F=4.30; $P \leq 0.0001$), and season*treatment interactions (F=2.09; $P=0.0005$) (Table 3.2). The April growing season had the highest tissue concentration and statistically separated from all other seasons. The lowest season concentration was found in January, which also separated from all other seasons. The season concentrations ranged from 43.42 $\mu M \cdot g^{-1}$ FM to 121.98 $\mu M \cdot g^{-1}$ FM (Table 3.3). The 660/470/660 treatment had the highest tissue concentration and was separated from the W/W/W and NL control. The NL control had the lowest concentration, which separated from some of the narrowband treatments. The treatment tissue concentrations ranged from 32.68 $\mu M \cdot g^{-1}$ FM to 112.47 $\mu M \cdot g^{-1}$ FM (Table 3.4).

Phenylpropanoids

Eugenol concentrations were significantly influenced by season (F=130.1; $P \leq 0.0001$), lighting treatment (F=9.94; $P \leq 0.0001$), and season*treatment interactions (F=4.43; $P \leq 0.0001$) (Table 3.2). The June growing season had the highest tissue concentration, while the lowest concentration was found in January. All of the season tissue concentration averages statistically separated. The season concentrations ranged from 43.16 $\mu M \cdot g^{-1}$ FM to 280.02 $\mu M \cdot g^{-1}$ FM (Table 3.3). The 6B/94R treatment had the highest tissue concentration and separated from all other treatments. The NL control had the lowest concentration, which separated from the 660/420/660, 660/450/660, 660/470/660, 470/450/420, 450/W/470, W/W/W, and PhysioSpec treatments. The treatment tissue concentrations ranged from 90.09 $\mu M \cdot g^{-1}$ FM to 283.16 $\mu M \cdot g^{-1}$ FM (Table 3.4).

Methyl Eugenol concentrations were significantly influenced by season (F=7.95; $P \leq 0.0001$), but not by lighting treatment (F=1.7; $P = 0.0997$) or season*treatment interactions (F=1.5; $P = 0.1545$) (Table 3.2). The September growing season had the highest tissue concentration, but did not statistically separate from the June season. The lowest concentration was found in January, but did not separate from April. The season concentrations ranged from 131.23 $\mu M \cdot g^{-1}$ FM to 172.11$\mu M \cdot g^{-1}$ FM (Table 3.3). The treatment tissue concentrations ranged from 158.11 $\mu M \cdot g^{-1}$ FM to 165.77 $\mu M \cdot g^{-1}$ FM (Table 3.4).

Principal Component Analysis

A principal component analysis (PCA) comparison of key PVOCs and lighting treatments, represented using a biplot, revealed that two components with eigenvalues > 1 accounted for 60.0% of the total data variability (Fig. 3.5). Component 1 accounted for 42.1% of the variability, while component 2 accounted for 17.9% of the data variability. Many key volatile compounds were positive discriminating factors for component 1 of varying magnitudes, while component 2

evenly separated compounds into positive and negative discriminating factors of various magnitudes. Quadrant I contained positive discriminating factors for both component 1 and component 2, which were the aroma compounds: (E)-2-Hexenal, α-Humulene, 3-Caren-10-al, Camphene, Linalool, α-Pinene, β-Pinene, d-Limonene, p-Menth-1-en-8-ol, 3-Carene, and Eugenol. Concentration increases of these compounds were generally associated with the narrowband LED treatments 470/450/420, 660/470/660, and 660/400/660. Quadrant II and Quadrant III do not contain any of the key aroma compounds and reveal that 450/660/470, 660/420/660, HPS, W/W/W, NL Control, and 660/450/660 are negatively associated with concentration increases of many key aroma volatiles, at various weights. Quadrant IV contained positive discriminating factors for component 1 and negative discriminating factors for component 2, which included the aroma compounds: 2-Phenyl Ethanol, 1-Octen-3-ol, 2-Octyn-1-ol, Benzeneacetaldehyde, trans-Sabinene hydrate, Nonanal, β-Myrcene, and Linalool. Concentration increases of these compounds were generally associated with the PhysioSpec (6B/94R, 12B/88R) and 450/W/470 treatments (Fig. 3.5).

Discussion

Light plays a critical role in the growth and development of many crops, including sweet basil. Spectral quality has a significant impact on secondary metabolism, which can directly influence the concentration of flavor and aroma compounds in plant tissues. Leveraging environmental controls and applying abiotic stressors has the ability to influence the secondary metabolism of high-value specialty crops. The results of this study demonstrate that spectral quality manipulations of supplemental greenhouse lighting can directly influence tissue concentrations of key aroma volatiles and other secondary metabolites in sweet basil. Total basil

tissue VOC concentrations, in addition to many of the concentrations of specific volatile compounds, were significantly impacted by the growing season and lighting treatment.

In Figure 3.3, total VOC concentrations are displayed based on lighting treatment and have been broken down into their respective compound classes. All of the SL treatments provide the same intensity (100 $\mu mol \cdot m^{-2} \cdot s^{-1}$) for the same duration (24 h); this isolates SL spectral quality as a primary independent variable, while the non-supplemented NL control provides a baseline to compare treatments. Statistical analysis reveals that total VOC concentrations separated across lighting treatments, and a few general patterns emerge.

First, the 6B/94R treatment had the highest total VOC concentration, but did not statistically separate from the 12B/88R treatment. The total VOC concentration of the 450/660/470 (i.e., 2B:1R or 66.6B/33.3R) was significantly lower than the 6B/94R treatment, but did not separate from the 12B/88R treatment. In one recent study with green basil (*Ocimum basilicum* L.), the chemical composition of essential oil and total phenolic content was improved by growing plants under 30B/70R light when compared to monochromatic, dichromatic, and broadband sources (Hosseini et al., 2018). Pennisi et. al also found that a ratio of 3 R:B (i.e., 1B:3R) was ideal for resource use efficiency and flavor volatile production in basil (*Ocimum basilicum* L.) (Pennisi et al., 2019a). Our group determined that for 'Genovese' sweet basil (*Ocimum basilicum* L.), maximum concentrations for key compounds varied among narrowband lighting treatment, but most monoterpenes and diterpenes evaluated were highest under a SL treatment of 20B/80R to 50B/50R (Hammock et al., 2021). When comparing previous studies, it is clear that light-mediated responses (i.e., isoprenoid and phenylpropanoid metabolism changes based on B:R ratio) are species and even variety-specific (Taulavuori et al., 2016b; Toscano et al., 2021). Based on the results of this experiment and current literature, we recommend supplemental narrowband B:R

ratios between 20B/80R and 5B/95R (i.e., 1B:4R to 1B:20R) with the intensity of 100-200 $\mu mol \cdot m^{-2} \cdot s^{-1}$ for 12-24 h daily for high-value specialty crops under standard greenhouse conditions, with direct consideration of the unique ambient spectra and DLI provided for any given location and growing season. Further studies should also be conducted on different varieties of basil and other high-value specialty crop species to determine ideal supplemental B:R ratios.

Second, the high blue treatment (470/450/420) performed as well as the 2B:1R narrowband treatment (450/660/470). It has generally been shown that high intensities of blue wavelengths promote the synthesis of many phenols and terpenoids (Colquhoun et al., 2013; Carvalho et al., 2016; Taulavuori et al., 2016b; Toscano et al., 2021; Kivimaenpa et al., 2022). That being said, it is likely that the ambient solar spectrum during the natural daylight hours was sufficient to provide additional wavelengths necessary for normal physiological function and secondary metabolite concentrations as observed in this experiment. Some studies have shown that monochromatic or dichromatic sole-source lighting can be detrimental to primary and secondary metabolic function (Carvalho et al., 2016; Jishi et al., 2016; Kong et al., 2019). Adding small amounts of discrete wavelengths relative to the total intensity of the ambient spectrum has potential to impart desirable secondary metabolic effects while minimizing electrical energy use.

Third, the total VOC concentrations of the four 1B:2R treatments (660/400/660, 660/420/660, 660/450/660, and 660/470/660) each statistically separated from each other. The 660/470/660 had the highest total concentrations, while the 660/420/660 had the lowest. This demonstrates the impact of discrete narrowband blue wavelengths (with the same spectra/intensity of red wavelengths) on total VOC concentration. The 660/470/660 treatment was the only 1B:2R treatment to statistically separate from the NL control. A sole-source lighting study found that several quality parameters and secondary metabolite concentrations in basil (*Ocimum basilicum*

L.) and strawberry (*Fragaria x ananassa)* were improved by using a 0.7 R:B ratio (i.e., 1.4B:1R) (Piovene et al., 2015). A study comparing natural light under standard greenhouse conditions to indoor sole-source lighting treatments determined significant increases to monoterpene concentrations when using blue/red/yellow and blue/red/green in growth chambers (Carvalho et al., 2016). A similar indoor lighting study found that using broadband sources with higher intensities of blue wavelengths (i.e., 1B:2.5R vs. 1B:4R) influenced terpenoid and phenylpropanoid concentrations in relation to phenolic acids (Kivimaenpa et al., 2022). This further demonstrates the wide range of effects from sole source, and SL can be species and variety-specific.

This study differs from many previous studies evaluating basil aroma volatiles in that sole-source lighting is utilized as compared to supplementing the natural solar spectrum with specific wavebands. The ambient solar spectra, as well as differing species-specific light mediated responses it imparts, adds an additional layer of complexity. Determining the influence of varying light spectra with and without ambient solar spectra, as well as comparing both, will improve our understanding of plant/light interaction as well as help commercial growers in both indoor farm and greenhouse operations.

Based on this comparison of discrete blue wavelengths, if using supplemental narrowband B/R lighting for sweet basil production, we also recommend 450 nm blue additions to 660 nm red (± 20 nm) for ideal total VOC bioaccumulation in basil, using the aforementioned B:R ratio range (i.e., 1B:4R to 1B:20R). Further evaluation is warranted on 420 nm in relation to VOC profiles. The wavelengths around 420 nm have been shown to promote VOCs and other secondary metabolites (Singh et al., 2015; Hasan et al., 2017; Ueda et al., 2021). The 660/420/660 actually produced the lowest total VOC concentration, and was statistically lower than many of the

narrowband treatments. Further, it did not statistically separate from the NL control. It is likely that the 420 nm wavelengths promoted the production of other non-volatile secondary metabolites which are not detectable using HS GC-MS, such as carotenoids and flavonoids. Additional experiments evaluating the entire secondary metabolome with various analytical techniques in addition to metabolomics and/or transcriptomics would further elucidate the specific regulation of key pathways. It is also pertinent for future studies to incorporate both primary and secondary metabolic data to determine further resource allocation based on light responses.

Fourth, the broadband spectrum lighting treatments had mixed performance in terms of total VOC concentration. The HPS and W/W/W treatments did not statistically separate from the NL control. The high-blue broad-spectrum treatment (450/W/470) actually had the second-highest total VOC concentration, and did not statistically separate from the 6B/94R and 12B/88R treatments. Further exploration into specific intensities of discrete narrowband wavelengths within broad-spectrum supplement lighting, specifically blue wavelengths, is needed. Additionally, the color temperature (i.e., Kelvin) of broadband white light, should be evaluated in terms of secondary metabolic resource allocation.

Figure 3.4 shows total VOC concentrations based on the growing season and have been broken down into their respective compound classes. All of the total VOC concentrations statistically separated across the growing season. In the order of highest to lowest total VOC concentrations, June had the highest total VOC concentration (6140 $\mu M \cdot g^{-1}$ FM), April had the second highest total VOC concentration (5015 $\mu M \cdot g^{-1}$ FM), January had the third highest total VOC concentration (3840 $\mu M \cdot g^{-1}$ FM), and finally, September had the lowest concentration (2760 $\mu M \cdot g^{-1}$ FM). Greenhouse growing conditions and environmental parameters were similar for all four growing seasons in this experiment (Table 3.1). The non-supplemented NL control provides

a baseline to compare across all seasons. Greenhouse day and night temperatures were held constant within 2 ºC across all growing seasons, which isolates two of the primary independent variables utilized in this experiment: change in spectral quality from ambient sunlight across growing seasons and change in total DLI from ambient sunlight across growing seasons. It would generally be expected that increasing the DLI from ambient sunlight would indirectly increase total volatile concentration, due to the increased primary metabolic capacity and ability to allocate additional resources to secondary pathways (Faust et al., 2005; Garland et al., 2010; Currey and Lopez, 2015). That being said, it was interesting to see that September had the second-highest DLI, but the lowest total VOC concentration. Additionally, January had the lowest DLI, but had the third-highest total VOC concentration. June had the highest DLI, as well as the highest total VOC concentration (Table 3.4). This indicates that the change in both total DLI and spectral quality of the ambient sunlight across growing seasons directly influences total VOC concentrations.

The June growing seasons generally had the highest tissue concentrations of specific volatile compounds, while January generally had the lowest concentrations. Many of the compounds followed the trend of higher tissue concentrations as the average total growing season DLI increased. That being said, some notable exceptions do not trend with seasonal DLI, demonstrating the complex interaction between seasonal spectral quality and secondary metabolism. These exceptions can be separated into three groups. First, the compounds 2-Octyn-1-ol, Nonanal, cis-β-Ocimene, Linalool, and β-Myrcene had the lowest concentrations in the September growing season rather than the January growing season. Second, the compounds 3-Caren-10-al, Camphene, Isoborneol, α-Pinene, and β-Pinene all had the highest concentrations in the September growing season rather than June growing season. Third, Dimethyl Sulfide was the only compound in this experiment to have the highest tissue concentration in the April growing

season, rather than the June growing season. It was interesting to observe the various effects on compounds across different classes and metabolic pathways, which warrants further exploration using analytical techniques as well as metabolomics.

For many of the statistically significant compounds evaluated in this study, the 6B/94R treatment produced the highest concentrations, while the lowest was generally observed in the 660/420/660 treatment. 16 VOCs were determined to be responsible for approximately 90% of the total response area as well as variations in the aromatic profile, which is in agreement with a similar experiment (Pennisi et al., 2019a). Four compounds deviated from this pattern, all of which have proven significant in sensory perception for sweet basil.

Nonanal has a strong and unmistakable scent. Its aroma is described as fatty, citrusy orange peel with notes of sweet floral and rose petals. It adds warmth to fragrances, boosts freshness in floral compositions, and offers a distinctive aldehydic odor. Nonanal rounds off the smell of perfumes and helps make them more palatable to the nose. It also has the ability to lend its waxy character to other flavors, giving it a unique sensorial appeal (Sell, 2019). The highest tissue concentration of Nonanal was found under the 660/470/660 treatment, which was more than double the concentration found in the NL control.

Linalool is a naturally occurring terpene found in many flowers, spices, and other higher plants. The aroma of linalool is described as sweet, fruity, floral, and herbaceous. It has citrus and spice notes, with a light woodsy character reminiscent of lavender and bergamot oil. Linalool is commonly found in herbs such as oregano, thyme, marjoram, rosemary, and basil (Meligaard et al., 2007; Sell, 2019). Linalool tissue concentrations were highest in the 660/470/660, while the lowest was under the 660/420/660 treatment; these were the only two treatments that statistically separated for Linalool.

Dimethyl Sulfide has a strong, pungent aroma that can be described as earthy, fishy, or sulfuric. It is often compared to the smell of cooked cabbage and is used as an ingredient in certain types of food flavorings. It has high bioactivity and can be detected in extremely small concentrations, even at concentrations below 0.1 ppm; relatively low concentrations can lead to negative sensory perception in humans (Meligaard et al., 2007; Sell, 2019). Interestingly, the highest concentration was found in the 660/470/660, but was only statistically separate from the W/W/W and the NL control. It should be noted that the addition of narrowband LED treatments directly increased the concentration of this negatively perceived compound, while the same intensity of broad-spectrum white light (W/W/W) was statistically lower. The broad spectrum white and the NL control, despite different DLIs, did not statistically separate, suggesting that spectral quality has a greater influence on Dimethyl Sulfide tissue concentrations than DLI. Other sulfur compounds in this experiment did not show statistically significant differences in concentration across lighting treatments.

Eugenol is a phenylpropanoid with a sweet, spicy, nutty, and woody aroma, with notes of clove, cinnamon, and allspice. Its scent is reminiscent of bay leaf and is often used as a food flavoring. Eugenol is known for its antimicrobial properties and therapeutic properties. It has been used to create unique perfumes, adding depth and complexity to scents, especially those with a floral or citrus character. It is commonly used to flavor commercially produced food products (Lawless, 2010; Sell, 2019). The highest tissue concentrations were found under the 6B/94R treatment, while the lowest concentrations were found under the NL control, an almost 3.5x difference. The 660/420/660 treatment did not statistically separate from any of the other LED treatments or the NL controls. Additionally, Methyl Eugenol, the synthesis of which is directly related to Eugenol, was not statistically significant across lighting treatments.

Four terpenoid compounds of key aroma volatiles, consisting of different chemical classes at various points within the isoprenoid pathway, followed the same general pattern across lighting treatments. These include α-Pinene, β-Pinene, Camphene, and d-Limonene.

α-Pinene and β-Pinene are two isomers found ubiquitously in nature, most notably in the essential oils of coniferous trees. α-pinene has a sharp, piney aroma. β-pinene, on the other hand, has an earthy and herbaceous scent reminiscent of rosemary and sage. The main difference between these two terpenes is their perceived intensity, as α-Pinene's sharp and intense aroma stands out from β-pinene's more subtle earthy notes. Both terpenes have significant culinary and therapeutic potential (Sell, 2019).

Camphene has a strong, piney, camphoraceous aroma with hints of fir and spices. It is often described as having citrus notes with an underlying musky sweetness. Camphene is used in perfume creation to add a woody and earthy edge to fragrances, particularly those with fresh and herbal elements. Camphene accentuates other flavors like citrus, mint, and earthy notes in food flavorings (Lawless, 2010; Sell, 2019).

d-Limonene has a strong and distinct citrus scent reminiscent of oranges and lemons. It is often described as having a distinctive sweet orange aroma, with notes of lemon and lime. d-Limonene is used in the production of perfumes, cosmetics, food flavorings, and cleaning products due to its pleasant smell. Despite being an undernote of basil aroma, it still plays a significant role in the overall aroma perception of some sweet basil varieties (Lawless, 2010; Sell, 2019).

These four terpenoid compounds all have various physical and chemical properties and reside at different locations within the isoprenoid pathway, but generally maintain the same pattern across lighting treatments. This suggests that these pathways are receiving more upstream products to the biosynthesis of some terpenoid compounds (i.e., resource allocation is being shifted to

terpenoid pathways due to light stress induced from discrete combinations of narrowband wavelengths), while other specific compounds within the isoprenoid and phenylpropanoid pathway are being differentially regulated based on varying spectral quality and/or DLIs.

Although basil is one of the most popular herbs globally, it can be challenging to characterize in terms of light-mediated sensory properties at the genomic and phenotypic levels. One limitation to evaluating the interaction of light and sensory quality is that there are over sixty varieties of Ocimum basilicum, each with specific light-mediated secondary metabolic responses; this complicates the comparison of studies found in current literature (Blank et al., 2004). These light-mediated responses cannot be easily generalized to other high-value specialty crops, which provides numerous unique research opportunities.

Headspace GC-MS is a commonly used analytical technique used to qualify and quantify VOCs from many types of biological samples. It is particularly useful for metabolomics and characterizing aroma profiles for plant tissues and food products. In this experiment, all volatile concentration units are reported in $\mu M \cdot g^{-1}$ FM. This unit (compared to $\mu mol \cdot g^{-1}$ FM) was utilized because it incorporates the concentration of each analyte per unit volume of headspace gas above the plant tissue (i.e., samples the dynamic and complex gaseous matrix which contains numerous pertinent VOCs), which is important for sensory-based studies. Further, VOCs are highly localized and typically require other GC-MS techniques (i.e., liquid solvent extraction/injection) to accurately quantify in terms of $\mu mol \cdot g^{-1}$ of homogenized plant tissue. HS analysis is an ideal GC-MS sampling technique involving sensory studies with plant flavor/aroma, because it accounts for the dynamic release of volatiles from plant tissues under repeatable conditions and can be incorporated with olfactometry (GC-O). Humans primarily detect aroma volatiles that have been volatilized (i.e., released from trichomes and other specialized structures), which then induces an

olfactory response. By accurately calibrating analytical standards to known headspace concentrations, we can determine the micro molarity of each analyte, within a known volume of dynamic gaseous headspace matrix, under repeatable conditions (i.e., temperature and pressure using inert analytical grade He) to which a consumer would be exposed to during consumption. Future studies should use a variety of analytical as well as molecular techniques to determine the primary and secondary metabolic impacts of spectral quality. A multidisciplinary approach would allow for greater insight into the complex interactions between light and plant physiology. This could result in the development of light recipe guidelines based on location and weather conditions, to dynamically attenuate SL spectra to the natural solar spectra as it changes across seasons; season-specific lighting regimes have the potential to maintain consistent flavor and aroma quality throughout the year.

This experiment utilized continuous low-intensity light supplements, which have the potential to manipulate secondary metabolite bioaccumulation while efficiently increasing crop DLI (i.e., utilizing cheaper off-peak electrical rates during night hours). Because basil is grown to vegetative maturity and does not require a photoperiodic response, it tolerates 24 h SL very well; other crops will experience deleterious effects when using this type of lighting regime. Increasing the intensity and/or manipulating the duration of SL also has the potential to differentially influence secondary metabolic profiles and should be further evaluated under greenhouse and growth chamber conditions.

While narrowband B/R wavelengths have been shown to increase total and specific VOC concentrations, varying levels of impact have been observed among different species and specific SL spectral qualities; further exploration into discrete narrowband wavelengths at varying ratios is warranted (i.e., +/- 2 nm within the ambient spectrum). This could be used to push certain

secondary metabolic pathways that could be used to improve flavor, the concentration of phytonutrients, human health benefits, and marketability. Many studies have demonstrated the species-specific nature of secondary metabolic light-mediated responses, which provides a vast range of research opportunities. Factors such as yield, nutrition content, phytonutrient concentrations, texture, and visual characteristics should also be considered when selecting SL regimes. Certain niche markets may utilize the findings of this study to improve flavor quality or push certain metabolic pathways (i.e., terpenoid and phenylpropanoid).

This study utilizes free sunlight and is intended to inform greenhouse basil production with SL requirements. It would be valuable from a scientific perspective to further explore similar methodologies, analytical techniques, and narrowband wavelengths in growth chambers with sole source lighting to determine the influence of ambient solar spectra and if similar results occur without the ambient solar being present. The results of this study show the merit of supplementing broad-spectrum ambient sunlight with targeted discrete narrowband wavelengths to manipulate secondary metabolism. Utilizing growth chambers to manipulate photoperiods and DLI of distinct spectral quality supplements would also prove beneficial for growers, as it would eliminate potential confounding factors from variation in ambient sunlight (i.e., weather, growing location, etc.), as well as provide comparative data for operations that rely on sole-source lighting, such as indoor farms and other types of controlled environment agriculture operations.

The results of this experiment will provide useful information on how SL can be used to optimize the sensory characteristics of sweet basil and provide a baseline to explore other high-value specialty crops. It is possible to significantly alter secondary metabolism by using sole source narrowband lighting, as well as narrowband supplements to ambient sunlight. Further research is

required to determine patterns within different specialty crops and how wavelengths can be optimized for daily and seasonal changes in the solar spectrum.

Conclusions

In this study, we explored, identified, and quantified several important volatile organic compounds with known influence on sensory perception and/or plant physiological processes of greenhouse-grown sweet basil. We determined that the spectral quality from SL sources, in addition to changes in the spectral quality and DLI of ambient sunlight across growing seasons, directly influence aroma volatile concentrations. Further, we found that specific ratios of narrowband blue/red wavelengths, combinations of discrete narrowband wavelengths, and broadband wavelengths directly influence the basil aroma profile as well as specific compounds. The results also show that variation in spectral quality and DLI across seasons can dramatically influence aroma concentrations. Narrowband treatments generally produced higher VOC compound concentrations; based on the results of this experiment and current literature, we suggest supplemental narrowband wavelengths blue (450-470 nm) and red (660-700 nm) at a ratio of approximately 10B/90R at 100-200 $\mu mol \cdot m^{-2} \cdot s^{-1}$ for 12-24 h for maximum total VOC concentration and key individual aroma volatile concentrations in greenhouse-grown 'Italian Large Leaf' sweet basil; future experiments should determine the influence of lighting regimes on VOC profiles in relation to consumer perception and preference. This experiment demonstrates the ability to use discrete narrowband wavelengths to augment the natural solar spectrum in order to provide an optimal light environment across growing seasons. Further, narrowband SL can be used to manipulate key flavor and aroma compound concentrations, which can directly impact human sensory perception. Future work should incorporate different analytical and metabolic techniques to determine the impact on important aroma volatiles as well as other primary and secondary

metabolites; this includes any potential species-specific effects that spectral quality may have on plant physiology with the potential to indirectly impact sensory quality through light-mediated metabolic resource allocation.

References

Behn, H., Albert, A., Marx, F., Noga, G., and Ulbrich, A. (2010). Ultraviolet-B and photosynthetically active radiation interactively affect yield and pattern of monoterpenes in leaves of peppermint (Mentha x piperita L.). *J Agric Food Chem* 58(12)**,** 7361-7367. doi: 10.1021/jf9046072.

Bernhardt, B., Sipos, L., Kokai, Z., Gere, A., Szabo, K., Bernath, J., et al. (2015). Comparison of different Ocimum basilicum L. gene bank accessions analyzed by GC–MS and sensory profile. *Ind. Crops Prod* 67**,** 498-508.

Blank, A.F., Carvalho Filho, J.L.S.d., Santos Neto, A.L.d., Alves, P.B., Arrigoni-Blank, M.d.F., Silva-Mann, R., et al. (2004). Caracterização morfológica e agronômica de acessos de manjericão e alfavaca. *Horticultura Brasileira* 22(1)**,** 113-116. doi: 10.1590/s0102-05362004000100024.

Bourgaud, F., Gravot, A., Milesi, S., and Gontier, E. (2001). Production of plant secondary metabolites: a historical perspective. *Plant Science* 161(5)**,** 839-851. doi: 10.1016/s0168-9452(01)00490-3.

Briggs, W.R., and Olney, M.A. (2001). Photoreceptors in plant photomorphogenesis to date. Five phytochromes, two cryptochromes, one phototropin, and one superchrome. *Plant Physiol* 125(1)**,** 85-88. doi: 10.1104/pp.125.1.85.

Carvalho, S.D., Schwieterman, M.L., Abrahan, C.E., Colquhoun, T.A., and Folta, K.M. (2016). Light Quality Dependent Changes in Morphology, Antioxidant Capacity, and Volatile

Production in Sweet Basil (*Ocimum basilicum*). *Front Plant Sci* 7**,** 1328. doi: 10.3389/fpls.2016.01328.

Casal, J.J. (2000). Phytochromes, cryptochromes, phototropin: photoreceptor interactions in plants. *Photochem Photobiol* 71(1)**,** 1-11. doi: 10.1562/0031-8655(2000)071<0001:pcppii>2.0.co;2.

Casal, J.J., and Yanovsky, M.J. (2005). Regulation of gene expression by light. *Int J Dev Biol* 49(5-6)**,** 501-511. doi: 10.1387/ijdb.051973jc.

Chen, M., Chory, J., and Fankhauser, C. (2004). Light signal transduction in higher plants. *Annu Rev Genet* 38**,** 87-117. doi: 10.1146/annurev.genet.38.072902.092259.

Colquhoun, T.A., Schwieterman, M.L., Gilbert, J.L., Jaworski, E.A., Langer, K.M., Jones, C.R., et al. (2013). Light modulation of volatile organic compounds from petunia flowers and select fruits. *Postharvest Biology and Technology* 86**,** 37-44. doi: 10.1016/j.postharvbio.2013.06.013.

Colquhoun, T.A., Verdonk, J.C., Schimmel, B.C., Tieman, D.M., Underwood, B.A., and Clark, D.G. (2010). Petunia floral volatile benzenoid/phenylpropanoid genes are regulated in a similar manner. *Phytochemistry* 71(2-3)**,** 158-167. doi: 10.1016/j.phytochem.2009.09.036.

Currey, C.J., Hutchinson, V.A., and Lopez, R.G. (2012). Growth, Morphology, and Quality of Rooted Cuttings of Several Herbaceous Annual Bedding Plants Are Influenced by Photosynthetic Daily Light Integral During Root Development. *HortScience* 47(1)**,** 25-30. doi: 10.21273/hortsci.47.1.25.

Currey, C.J., and Lopez, R.G. (2015). Biomass Accumulation and Allocation, Photosynthesis, and Carbohydrate Status of New Guinea Impatiens, Geranium, and Petunia Cuttings Are Affected by Photosynthetic Daily Light Integral during Root Development. *Journal of the*

American Society for Horticultural Science 140(6)**,** 542-549. doi: 10.21273/jashs.140.6.542.

Dannehl, D., Schwend, T., Veit, D., and Schmidt, U. (2021). Increase of Yield, Lycopene, and Lutein Content in Tomatoes Grown Under Continuous PAR Spectrum LED Lighting. *Front Plant Sci* 12**,** 611236. doi: 10.3389/fpls.2021.611236.

Darko, E., Heydarizadeh, P., Schoefs, B., and Sabzalian, M.R. (2014). Photosynthesis under artificial light: the shift in primary and secondary metabolism. *Philos Trans R Soc Lond B Biol Sci* 369(1640)**,** 20130243. doi: 10.1098/rstb.2013.0243.

De Masi, L., Siviero, P., Esposito, C., Castaldo, D., Siano, F., and Laratta, B. (2006). Assessment of agronomic, chemical and genetic variability in common basil (Ocimum basilicum L.). *European Food Research and Technology* 223(2)**,** 273-281. doi: 10.1007/s00217-005-0201-0.

Dou, H., Niu, G., Gu, M., and Masabni, J. (2017). Effects of Light Quality on Growth and Phytonutrient Accumulation of Herbs under Controlled Environments. *Horticulturae* 3(2). doi: 10.3390/horticulturae3020036.

Fankhauser, C., and Chory, J. (1997). Light control of plant development. *Annu Rev Cell Dev Biol* 13**,** 203-229. doi: 10.1146/annurev.cellbio.13.1.203.

Fausey, B.A., Heins, R.D., and Cameron, A.C. (2005). Daily Light Integral Affects Flowering and Quality of Greenhouse-grown Achillea, Gaura, and Lavandula. *HortScience* 40(1)**,** 114-118. doi: 10.21273/hortsci.40.1.114.

Faust, J.E., Holcombe, V., Rajapakse, N.C., and Layne, D.R. (2005). The Effect of Daily Light Integral on Bedding Plant Growth and Flowering. *HortScience* 40(3)**,** 645-649. doi: 10.21273/hortsci.40.3.645.

Faust, J.E., and Logan, J. (2018). Daily light integral: A research review and high-resolution maps of the United States. *HortScience* 53(9)**,** 1250-1257.

Folta, K.M., and Carvalho, S.D. (2015). Photoreceptors and Control of Horticultural Plant Traits. *HortScience* 50(9)**,** 1274-1280. doi: 10.21273/hortsci.50.9.1274.

Fu, X., Chen, Y., Mei, X., Katsuno, T., Kobayashi, E., Dong, F., et al. (2015). Regulation of formation of volatile compounds of tea (Camellia sinensis) leaves by single light wavelength. *Sci Rep* 5**,** 16858. doi: 10.1038/srep16858.

Galvao, V.C., and Fankhauser, C. (2015). Sensing the light environment in plants: photoreceptors and early signaling steps. *Curr Opin Neurobiol* 34**,** 46-53. doi: 10.1016/j.conb.2015.01.013.

Garland, K.F., Burnett, S.E., Stack, L.B., and Zhang, D. (2010). Minimum Daily Light Integral for Growing High-quality Coleus. *HortTechnology* 20(5)**,** 929-933. doi: 10.21273/horttech.20.5.929.

Gómez, C., and Mitchell, C.A. (2014). Supplemental Lighting for Greenhouse-Grown Tomatoes: Intracanopy LED Towers Vs. Overhead HPS Lamps. *Acta Horticulturae* (1037)**,** 855-862. doi: 10.17660/ActaHortic.2014.1037.114.

Halaban, R. (1969). Effects of light quality on the circadian rhythm of leaf movement of a short-day-plant. *Plant Physiol* 44(7)**,** 973-977. doi: 10.1104/pp.44.7.973.

Hammock, H.A., Kopsell, D.A., and Sams, C.E. (2021). Narrowband Blue and Red LED Supplements Impact Key Flavor Volatiles in Hydroponically Grown Basil Across Growing Seasons. *Front Plant Sci* 12**,** 623314. doi: 10.3389/fpls.2021.623314.

Hasan, M.M., Bashir, T., Ghosh, R., Lee, S.K., and Bae, H. (2017). An Overview of LEDs' Effects on the Production of Bioactive Compounds and Crop Quality. *Molecules* 22(9). doi: 10.3390/molecules22091420.

Hiltunen, R., and Holm, Y. (2003). *Basil: The Genus Ocimum.* Amsterdam: CRC Press.

Holopainen, J.K., Kivimaenpaa, M., and Julkunen-Tiitto, R. (2018). New Light for Phytochemicals. *Trends Biotechnol* 36(1)**,** 7-10. doi: 10.1016/j.tibtech.2017.08.009.

Hosseini, A., Zare Mehrjerdi, M., and Aliniaeifard, S. (2018). Alteration of Bioactive Compounds in Two Varieties of Basil (Ocimum basilicum) Grown Under Different Light Spectra. *Journal of Essential Oil Bearing Plants* 21(4)**,** 913-923. doi: 10.1080/0972060x.2018.1526126.

Jiao, Y., Lau, O.S., and Deng, X.W. (2007). Light-regulated transcriptional networks in higher plants. *Nat Rev Genet* 8(3)**,** 217-230. doi: 10.1038/nrg2049.

Jishi, T., Kimura, K., Matsuda, R., and Fujiwara, K. (2016). Effects of temporally shifted irradiation of blue and red LED light on cos lettuce growth and morphology. *Scientia Horticulturae* 198**,** 227-232. doi: 10.1016/j.scienta.2015.12.005.

Kaiser, E., Ouzounis, T., Giday, H., Schipper, R., Heuvelink, E., and Marcelis, L.F.M. (2018). Adding Blue to Red Supplemental Light Increases Biomass and Yield of Greenhouse-Grown Tomatoes, but Only to an Optimum. *Front Plant Sci* 9**,** 2002. doi: 10.3389/fpls.2018.02002.

Kalaitzoglou, P., van Ieperen, W., Harbinson, J., van der Meer, M., Martinakos, S., Weerheim, K., et al. (2019). Effects of Continuous or End-of-Day Far-Red Light on Tomato Plant Growth, Morphology, Light Absorption, and Fruit Production. *Front Plant Sci* 10**,** 322. doi: 10.3389/fpls.2019.00322.

Kasperbauer, M.J., Loughrin, J.H., and Wang, S.Y. (2001). Light reflected from red mulch to ripening strawberries affects aroma, sugar and organic acid concentrations. *Photochem Photobiol* 74(1)**,** 103-107. doi: 10.1562/00318655(2001)074.

Kelly, N., and Runkle, E.S. (2020). Spectral manipulations to elicit desired quality attributes of herbaceous specialty crops. *European Journal of Horticultural Science* 85(5)**,** 339-343. doi: 10.17660/eJHS.2020/85.5.5.

Kiferle, K., Maggini, R., and Pardossi, P. (2013). Influence of nitrogen nutrition on growth and accumulation of rosmarinic acid in sweet basil (Ocimum basilicum L.) grown in hydroponic culture. *Aust. J. Crop Sci* 7(3)**,** 321-327.

Kivimaenpa, M., Mofikoya, A., Abd El-Raheem, A.M., Riikonen, J., Julkunen-Tiitto, R., and Holopainen, J.K. (2022). Alteration in Light Spectra Causes Opposite Responses in Volatile Phenylpropanoids and Terpenoids Compared with Phenolic Acids in Sweet Basil (Ocimum basilicum) Leaves. *J Agric Food Chem* 70(39)**,** 12287-12296. doi: 10.1021/acs.jafc.2c03309.

Kong, Y., Schiestel, K., and Zheng, Y.B. (2019). Pure blue light effects on growth and morphology are slightly changed by adding low-level UVA or far-red light: A comparison with red light in four microgreen species. *Environmental and Experimental Botany* 157**,** 58-68. doi: 10.1016/j.envexpbot.2018.09.024.

Kopsell, D.A., Kopsell, D.E., and Curran-Celentano, J. (2005). Carotenoid and Chlorophyll Pigments in Sweet Basil Grown in the Field and Greenhouse. *HortScience* 40(5)**,** 1230-1233. doi: 10.21273/hortsci.40.5.1230.

Korczynski, P.C., Logan, J., and Faust, J.E. (2002). Mapping Monthly Distribution of Daily Light Integrals across the Contiguous United States. *HortTechnology* 12(1)**,** 12-16. doi: 10.21273/horttech.12.1.12.

Kyriacou, M.C., El-Nakhel, C., Pannico, A., Graziani, G., Soteriou, G.A., Giordano, M., et al. (2019). Genotype-Specific Modulatory Effects of Select Spectral Bandwidths on the Nutritive and Phytochemical Composition of Microgreens. *Front Plant Sci* 10**,** 1501. doi: 10.3389/fpls.2019.01501.

Landi, M., Zivcak, M., Sytar, O., Brestic, M., and Allakhverdiev, S.I. (2020). Plasticity of photosynthetic processes and the accumulation of secondary metabolites in plants in response to monochromatic light environments: A review. *Biochim Biophys Acta Bioenerg* 1861(2)**,** 148131. doi: 10.1016/j.bbabio.2019.148131.

Larsen, D.H., Woltering, E.J., Nicole, C.C.S., and Marcelis, L.F.M. (2020). Response of Basil Growth and Morphology to Light Intensity and Spectrum in a Vertical Farm. *Front Plant Sci* 11**,** 597906. doi: 10.3389/fpls.2020.597906.

Lawless, H.H., H. (2010). *Sensory Evaluation of Food.* SpringerLink.

Lu, N., Bernardo, E.L., Tippayadarapanich, C., Takagaki, M., Kagawa, N., and Yamori, W. (2017). Growth and Accumulation of Secondary Metabolites in Perilla as Affected by Photosynthetic Photon Flux Density and Electrical Conductivity of the Nutrient Solution. *Front Plant Sci* 8**,** 708. doi: 10.3389/fpls.2017.00708.

Massa, G.D., Kim, H.H., Wheeler, R.M., and Mitchell, C.A. (2008). Plant Productivity in Response to LED Lighting. *Hortscience* 43(7)**,** 1951-1956.

McCree, K.J. (1973). The measurement of photosynthetically active radiation. *Solar Energy* 15(1)**,** 83-87. doi: 10.1016/0038-092x(73)90010-8.

Meligaard, M., Civile, G.V., and Carr, B.T. (2007). *Sensory Evaluation Techniques, Fourth Edition* CRC Press.

Mokvist, F., Mamedov, F., and Styring, S. (2014). Defining the far-red limit of photosystem I: the primary charge separation is functional to 840 nm. *J Biol Chem* 289(35)**,** 24630-24639. doi: 10.1074/jbc.M114.555649.

Morrow, R.C. (2008). LED Lighting in Horticulture. *HortScience* 43(7)**,** 1947-1950. doi: 10.21273/hortsci.43.7.1947.

Olle, M., and Viršile, A. (2013). The effects of light-emitting diode lighting on greenhouse plant growth and quality. *Agric. Food Sci* 22**,** 223-234.

Ouzounis, T., Rosenqvist, E., and Ottosen, C.O. (2015). Spectral Effects of Artificial Light on Plant Physiology and Secondary Metabolism: A Review. *Hortscience* 50(8)**,** 1128-1135.

Paradiso, R., and Proietti, S. (2021). Light-Quality Manipulation to Control Plant Growth and Photomorphogenesis in Greenhouse Horticulture: The State of the Art and the Opportunities of Modern LED Systems. *Journal of Plant Growth Regulation* 41(2)**,** 742-780. doi: 10.1007/s00344-021-10337-y.

Pattison, P.M., Tsao, J.Y., Brainard, G.C., and Bugbee, B. (2018). LEDs for photons, physiology and food. *Nature* 563(7732)**,** 493-500. doi: 10.1038/s41586-018-0706-x.

Pennisi, G., Blasioli, S., Cellini, A., Maia, L., Crepaldi, A., Braschi, I., et al. (2019a). Unraveling the Role of Red:Blue LED Lights on Resource Use Efficiency and Nutritional Properties of Indoor Grown Sweet Basil. *Front Plant Sci* 10**,** 305. doi: 10.3389/fpls.2019.00305.

Pennisi, G., Sanyé-Mengual, E., Orsini, F., Crepaldi, A., Nicola, S., Ochoa, J., et al. (2019b). Modelling Environmental Burdens of Indoor-Grown Vegetables and Herbs as Affected by Red and Blue LED Lighting. *Sustainability* 11(15). doi: 10.3390/su11154063.

Petrovic, J., Stojkovic, D., and Sokovic, M. (2019). Terpene core in selected aromatic and edible plants: Natural health improving agents. *Adv Food Nutr Res* 90**,** 423-451. doi: 10.1016/bs.afnr.2019.02.009.

Piovene, C., Orsini, F., Bosi, S., Sanoubar, R., Bregola, V., Dinelli, G., et al. (2015). Optimal red:blue ratio in led lighting for nutraceutical indoor horticulture. *Scientia Horticulturae* 193**,** 202-208. doi: 10.1016/j.scienta.2015.07.015.

Poiroux-Gonord, F., Bidel, L.P., Fanciullino, A.L., Gautier, H., Lauri-Lopez, F., and Urban, L. (2010). Health benefits of vitamins and secondary metabolites of fruits and vegetables and prospects to increase their concentrations by agronomic approaches. *J Agric Food Chem* 58(23)**,** 12065-12082. doi: 10.1021/jf1037745.

Putievsky, E., and Galambosi, B. (1999). *Production systems of basils.* Basil: The Genus Ocimum. Harwood Academic Publishers.

Rao, A.V., and Rao, L.G. (2007). Carotenoids and human health. *Pharmacol Res* 55(3)**,** 207-216. doi: 10.1016/j.phrs.2007.01.012.

Rockwell, N.C., Su, Y.S., and Lagarias, J.C. (2006). Phytochrome structure and signaling mechanisms. *Annu Rev Plant Biol* 57**,** 837-858. doi: 10.1146/annurev.arplant.56.032604.144208.

Sakalauskaite, J., Viskelis, P., Dambrauskiene, E., Sakalauskiene, S., Samuoliene, G., Brazaityte, A., et al. (2013). The effects of different UV-B radiation intensities on morphological and biochemical characteristics in Ocimum basilicum L. *J Sci Food Agric* 93(6)**,** 1266-1271. doi: 10.1002/jsfa.5879.

Santin, M., Ranieri, A., and Castagna, A. (2021). Anything New under the Sun? An Update on Modulation of Bioactive Compounds by Different Wavelengths in Agricultural Plants. *Plants (Basel)* 10(7). doi: 10.3390/plants10071485.

Schmitt, J., and Wulff, R.D. (1993). Light spectral quality, phytochrome and plant competition. *Trends Ecol Evol* 8(2)**,** 47-51. doi: 10.1016/0169-5347(93)90157-K.

Sell, C.S. (2019). *Fundamentals of Fragrance Chemistry.* Wiley.

Shanmugam, K., Gimbun, J., Ranganathan, B., Suganthi, P., Srinivasan, R.P., and Purushothaman, B. (2018). A Comprehensive Review on Ocimum basilicum. *Journal of Natural Remedies* 18(3)**,** 71-85. doi: 10.18311/jnr/2018/21324.

Singh, D., Basu, C., Meinhardt-Wollweber, M., and Roth, B. (2015). LEDs for energy efficient greenhouse lighting. *Renewable and Sustainable Energy Reviews* 49**,** 139-147. doi: 10.1016/j.rser.2015.04.117.

Sipos, L., Balázs, L., Székely, G., Jung, A., Sárosi, S., Radácsi, P., et al. (2021). Optimization of basil (*Ocimum basilicum* L.) production in LED light environments – a review. *Scientia Horticulturae* 289. doi: 10.1016/j.scienta.2021.110486.

Sipos, L., Boros, I.F., Csambalik, L., Székely, G., Jung, A., and Balázs, L. (2020). Horticultural lighting system optimalization: A review. *Scientia Horticulturae* 273. doi: 10.1016/j.scienta.2020.109631.

Smith, H. (1982). Light Quality, Photoperception, and Plant Strategy. *Annual Review of Plant Physiology* 33(1)**,** 481-518. doi: 10.1146/annurev.pp.33.060182.002405.

Stagnari, F., Di Mattia, C., Galieni, A., Santarelli, V., D'Egidio, S., Pagnani, G., et al. (2018). Light quantity and quality supplies sharply affect growth, morphological, physiological and

quality traits of basil. *Industrial Crops and Products* 122**,** 277-289. doi: 10.1016/j.indcrop.2018.05.073.

Taulavuori, E., Taulavuori, K., Hyoky, V., Oksanen, J., and Julkunen-Tiitto, R. (2016a). Speciesspecific differences in synthesis of flavonoids and phenolic acids under increasing periods of enhanced blue light. *Environ. Exp. Bot* 121**,** 145-150.

Taulavuori, K., Hyöky, V., Oksanen, J., Taulavuori, E., and Julkunen-Tiitto, R. (2016b). Species-specific differences in synthesis of flavonoids and phenolic acids under increased periods of enhanced blue light. *Environ. Exp. Bot* 121**,** 145 150.

Thoma, F., Somborn-Schulz, A., Schlehuber, D., Keuter, V., and Deerberg, G. (2020). Effects of Light on Secondary Metabolites in Selected Leafy Greens: A Review. *Front Plant Sci* 11**,** 497. doi: 10.3389/fpls.2020.00497.

Thorne, H.C., Jones, K.H., Peters, S.P., Archer, S.N., and Dijk, D.J. (2009). Daily and seasonal variation in the spectral composition of light exposure in humans. *Chronobiol Int* 26(5)**,** 854-866. doi: 10.1080/07420520903044315.

Toscano, S., Cavallaro, V., Ferrante, A., Romano, D., and Patane, C. (2021). Effects of Different Light Spectra on Final Biomass Production and Nutritional Quality of Two Microgreens. *Plants (Basel)* 10(8). doi: 10.3390/plants10081584.

Ueda, T., Murata, M., and Yokawa, K. (2021). Single Wavelengths of LED Light Supplement Promote the Biosynthesis of Major Cyclic Monoterpenes in Japanese Mint. *Plants (Basel)* 10(7). doi: 10.3390/plants10071420.

Vranova, E., Coman, D., and Gruissem, W. (2012). Structure and dynamics of the isoprenoid pathway network. *Mol Plant* 5(2)**,** 318-333. doi: 10.1093/mp/sss015.

Zhen, S., and Bugbee, B. (2020). Far-red photons have equivalent efficiency to traditional photosynthetic photons: Implications for redefining photosynthetically active radiation. *Plant Cell Environ* 43(5)**,** 1259-1272. doi: 10.1111/pce.13730.

Appendix C

Table 3.1. Important environmental parameters across growing cycles. All crops grown under greenhouse conditions at The University of Tennessee Institute of Agriculture (UTIA) in Knoxville, TN, USA (35°56'44.5"N, 83°56'17.3"W).

	"January"	**"April"**	**"June"**	**"September"**
Growing Period	1/7/19-2/18/19	3/25/19-5/08/19	5/15/19-7/02/19	9/3/19-10/14/19
Average Day Temp (°C)	27.8	28.1	29.4	28.9
Average Night Temp (°C)	20.2	21.7	22.2	21.3
Average Relative Humidity	55%	50%	50%	55%
Average Daily Light Integral (DLI) ($mol \cdot m^{-2} \cdot d^{-1}$)	7.81	10.29	15.65	13.87
Average Day Length (hours)	10:02	13:08	14:29	12:11

Table 3.2. Summary of statistical results for pertinent aroma volatile compounds detected using headspace gas chromatography-mass spectrometry.

Compound Name	CAS Number	F Value			Pr > F		
		Experiment	Treatment	Experiment*Treatment	Experiment	Treatment	Experiment*Treatment
Alcohols							
(E)-3-Hexen-1-ol	928-96-1	18.44	0.81	0.67	<0.0001	0.6264	0.8682
1-Octen-3-ol	3391-86-4	23.16	3.47	2.32	<0.0001	0.0001	<0.0001
2-Octyn-1-ol	20739-58-6	36.42	10.78	3.58	<0.0001	<0.0001	<0.0001
2-Phenylethanol	60-12-8	44.24	11.18	3.90	<0.0001	<0.0001	<0.0001
Aldehydes							
2-Ethyl-2-butenal	19780-25-7	44.87	1.60	2.26	<0.0001	0.0977	0.0002
2-Hexenal	6728-26-3	47.52	2.94	2.11	<0.0001	0.0009	0.0005
Nonanal	124-19-6	199.07	5.41	2.83	<0.0001	<0.0001	<0.0001
Hexanal	66-25-1	7.82	0.98	0.91	<0.0001	0.4703	0.6094
Benzyl Aldehydes							
3-Ethylbenzaldehyde	34246-54-3	140.11	9.66	3.95	<0.0001	<0.0001	<0.0001
Benzeneacetaldehyde	122-78-1	196.22	19.32	7.76	<0.0001	<0.0001	<0.0001
Amides and Furans							
Benzamide	55-21-0	345.39	2.49	2.14	<0.0001	0.0049	0.0003
N-phenyl-Formamide	103-70-8	143.66	1.95	2.31	<0.0001	0.0323	<0.0001
2-Ethyl-furan	3208-16-0	16.32	1.48	1.83	<0.0001	0.1380	0.0045
2-Pentyl-furan	3777-69-3	4.82	2.63	0.90	0.0026	0.0029	0.6374
Hydrocarbons							
1,4-Cyclohexadiene	628-41-1	80.31	8.46	2.74	<0.0001	<0.0001	<0.0001
2-Cyclopropyl-2-pentene	5457-40-9	58.30	9.00	1.98	<0.0001	<0.0001	0.0013
Decane	124-18-5	158.69	5.79	2.66	<0.0001	<0.0001	<0.0001
(E)-3-Methyl-1,3,5-hexatriene	24587-26-6	6.53	1.78	1.04	0.0003	0.0558	0.4103
1,3-cis,5-cis-Octatriene	40087-62-5	42.07	8.62	1.71	<0.0001	<0.0001	0.0100
1,4-Octadiene	5675-25-2	27.54	3.60	2.18	<0.0001	<0.0001	0.0003
2-Methyl-2-hepten-4-yne	58275-91-5	31.70	9.23	2.07	<0.0001	<0.0001	0.0006
1-Methylcyclohexene	591-49-1	135.93	1.92	1.04	<0.0001	0.0356	0.4174
Cycloheptene	628-92-2	3.18	0.67	1.05	0.0258	0.7661	0.4110
Acyclic Monoterpenes							
2,6-Dimethyl-2,4,6-octatriene	673-84-7	65.54	12.59	3.43	<0.0001	<0.0001	<0.0001
cis-β-Ocimene	3338-55-4	48.61	3.18	1.81	<0.0001	0.0004	0.0048
Citronellyl Acetate	150-84-5	13.31	2.70	1.75	<0.0001	0.0024	0.0085
Linalool	78-70-6	47.53	2.17	1.57	<0.0001	0.0152	0.0262
trans-β-Ocimene	3779-61-1	80.44	6.97	3.19	<0.0001	<0.0001	<0.0001
α-Ocimene	6874-44-8	195.03	1.29	2.00	<0.0001	0.2295	0.0011
β-Myrcene	123-35-3	268.90	5.15	2.83	<0.0001	<0.0001	<0.0001
Bicyclic Monoterpenes							
3-Caren-10-al	14595-13-2	17.21	2.24	1.06	<0.0001	0.0123	0.3871
(+)-4-Carene	29050-33-7	27.75	7.00	1.57	<0.0001	<0.0001	0.0254
3-Carene	498-15-7	24.28	4.53	2.35	<0.0001	0.0521	0.0005
Camphene	79-92-5	70.69	9.41	1.52	<0.0001	<0.0001	0.0356
Isoborneol	507-70-0	22.21	3.85	1.51	<0.0001	<0.0001	0.0367
trans-Pinocarveol	5947-36-4	7.36	3.32	1.89	<0.0001	0.0002	0.00027
trans-Sabinene hydrate	17699-16-0	158.38	5.80	2.66	<0.0001	<0.0001	<0.0001
α-Pinene	80-56-8	73.74	9.40	1.65	<0.0001	<0.0001	0.0152
β-Pinene	127-91-3	49.46	5.93	1.86	<0.0001	<0.0001	0.0032
Cyclic Monoterpenes							
3-Menthene	500-00-5	10.23	4.23	2.34	<0.0001	<0.0001	<0.0001
d-Limonene	5989-27-5	29.80	7.17	1.74	<0.0001	<0.0001	0.0076
Fenchyl acetate	13851-11-1	14.98	1.58	0.62	<0.0001	0.1019	0.9467
p-Menth-1-en-8-ol	98-55-5	173.75	10.61	2.56	<0.0001	<0.0001	<0.0001
Sesquiterpenes							
a-Humulene	6753-98-6	19.58	1.87	1.12	<0.0001	0.0420	0.3001
Organosulfur							
Isothiocyanatocyclopropane	56601-42-4	9.92	1.69	0.85	<0.0001	0.0752	0.7103
2-Isobutylthiazole	18640-74-9	10.79	1.90	1.23	<0.0001	0.0391	0.2101
Diallyl Disulfide	2179-57-9	1.69	0.40	0.67	0.1684	0.9559	0.9145
Dimethyl Sulfide	75-18-3	25.15	4.30	2.09	<0.0001	<0.0001	0.0005
Phenylpropanoids							
Eugenol	97-53-0	130.10	9.94	4.43	<0.0001	<0.0001	<0.0001
Methyl Eugenol	93-15-2	7.95	1.70	1.50	0.0010	0.0997	0.1545

Table 3.3. Influence of growing season on aroma volatile tissue concentrations in hydroponically grown greenhouse sweet basil (*Ocimum basilicum* var. Italian Large Leaf).

Compound Name	Growing Season			
	January	April	June	September
Alcohols				
(E)-3-Hexen-1-ol	2.27 b	2.07 b	6.24 a	5.99 a
1-Octen-3-ol	16.43 bc	23.23 b	39.72 a	13.03 c
2-Octyn-1-ol	408.20 c	547.80 b	653.76 a	395.22 d
2-Phenylethanol	19.56 c	35.55 b	58.43 a	26.41 bc
Aldehydes				
2-Ethyl-2-butenal	0.87 c	1.11 bc	1.37 bc	2.32 a
2-Hexenal	3.39 c	4.43 bc	5.39 b	9.69 a
Nonanal	10.05 c	20.82 b	37.32 a	5.26 d
Hexanal	128.96 c	130.21 bc	131.06 ab	132.15 a
Benzyl Aldehydes				
3-Ethylbenzaldehyde	5.82 c	10.14 b	17.15 a	4.28 c
Benzeneacetaldehyde	76.12 c	181.19 b	250.85 a	9.92 d
Amides and Furans				
Benzamide	2.92 b	3.30 b	3.49 b	36.32 a
N-phenyl-Formamide	6.92 b	6.32 b	9.05 b	39.48 a
2-Ethyl-furan	27.51 c	29.83 b	29.59 b	32.22 a
2-Pentyl-furan	4.83 b	5.97 ab	6.33 a	5.27 ab
Hydrocarbons				
1,4-Cyclohexadiene	6.00 c	10.31 b	17.34 a	16.76 a
2-Cyclopropyl-2-pentene	12.09 c	20.43 b	24.59 a	25.58 a
Decane	9.99 c	20.71 b	37.07 a	10.61 c
(E)-3-Methyl-1,3,5-hexatriene	2.00 b	2.15 b	2.67 ab	3.19 a
1,3-cis,5-cis-Octatriene	5.41 b	6.27 b	8.84 a	8.20 a
1,4-Octadiene	16.63 bc	23.04 b	40.63 a	7.28 c
2-Methyl-2-hepten-4-yne	6.56 b	6.80 b	8.85 a	9.08 a
1-Methylcyclohexene	23.40 b	29.14 b	32.83 b	89.07 a
Cycloheptene	0.73 b	0.81 b	1.02 a	1.09 a
Acyclic monoterpenes				
2,6-Dimethyl-2,4,6-octatriene	1.77 d	4.16 c	6.30 a	5.15 b
cis-β-Ocimene	370.45 c	538.33 b	754.18 a	145.81 d
Citronellyl Acetate	188.27 c	190.24 bc	193.66 a	191.75 b
Linalool	925.12 a	876.30 a	870.25 a	239.32 b
trans-β-Ocimene	106.90 c	279.90 b	351.14 a	57.16 c
α-Ocimene	45.66 b	27.88 b	75.23 b	493.99 a
β-Myrcene	281.89 b	371.46 a	407.65 a	9.36 c
Bicyclic monoterpenes				
3-Caren-10-al	1.79 b	1.21 c	1.52 bc	2.51 a
(+)-4-Carene	16.93 d	26.22 c	61.46 a	40.74 b
3-Carene	379.21 b	507.44 a	559.24 a	535.31 a
Camphene	23.41 c	29.25 bc	32.83 bc	55.77 a
Isoborneol	28.97 bc	23.53 c	32.50 b	49.74 a
trans-Pinocarveol	3.60 b	4.89 ab	5.87 a	6.13 a
trans-Sabinene hydrate	10.04 c	20.71 b	37.07 a	10.60 c
α-Pinene	17.27 c	22.81 b	25.94 b	46.27 a
β-Pinene	99.30 c	137.69 b	152.76 b	208.12 a
Cyclic monoterpenes				
3-Menthene	24.22 b	36.08 a	46.11 a	39.59 a
d-Limonene	234.61 c	311.32 b	378.51 a	315.24 b
Fenchyl acetate	132.80 a	149.80 a	127.37 a	81.12 b
p-Menth-1-en-8-ol	5.44 d	9.75 c	19.69 a	13.33 b
Sesquiterpenes				
α-Humulene	53.69 b	54.88 b	58.92 a	59.58 a
Organosulfur				
Isothiocyanatocyclopropane	1.28 b	1.20 b	1.78 ab	2.28 ab
2-Isobutylthiazole	5.57 b	6.74 b	8.86 a	8.94 a
Diallyl Disulfide	0.65 a	0.87 a	1.05 a	1.60 a
Dimethyl Sulfide	43.42 c	121.98 a	68.87 b	69.76 b
Phenylpropanoids				
Eugenol	43.16 d	139.70 c	280.02 a	212.33 b
Methyl Eugenol	131.23 b	138.51 b	160.17 a	172.11 a

All concentrations are presented in micro molarity of analyte per gram of fresh mass ($\mu M \cdot g^{-1}$ FM). Mean values represent two plants per replication and ten replications per treatment. Values for each season are averaged across all treatments within that season. Values were analyzed using Tukey's protected least significant difference. Data in the same row followed by the same letter are not significantly different ($\alpha = 0.05$).

Table 3.4. Influence of light treatment on aroma volatile tissue concentrations in hydroponically grown greenhouse sweet basil (*Ocimum basilicum* var. Italian Large Leaf).

	Lighting Treatments											
Compound Name	**660/400/660**	**660/420/660**	**660/450/660**	**660/470/660**	**470/450/420**	**450/660/470**	**450/W/470**	**6B/94R**	**12B/88R**	**HPS**	**W/W/W**	**NL Control**
Alcohols												
(E)-3-Hexen-1-ol	4.45 a	2.90 a	5.78 a	3.32 a	28.15 a	4.57 a	4.06 a	3.66 a	1.97 a	4.33 a	2.88 a	2.54 a
1-Octen-3-ol	20.48 abc	10.40 c	15.17 bc	36.11 a	16.03 bc	24.75 abc	35.65 a	31.25 ab	24.65 abc	18.57 abc	20.41 abc	24.70 abc
2-Phenylethanol	29.64 bcd	20.70 d	28.35 bcd	42.26 bc	36.71 bcd	33.43 bcd	37.98 bcd	74.13 a	44.78 b	19.62 d	26.80 bcd	24.47 cd
Aldehydes												
2-Ethyl-2-butenal	1.51 a	1.12 a	1.14 a	1.36 a	1.70 a	1.26 a	1.42 a	1.43 a	1.26 a	1.39 a	1.47 a	2.15 a
2-Hexenal	5.84 ab	4.35 b	4.72 b	5.98 ab	4.85 b	5.26 b	6.15 ab	5.82 ab	5.03 b	5.55 b	5.84 ab	9.00 a
Nonanal	20.31 abcd	15.37 cde	16.10 bcde	24.48 a	18.40 abcde	18.82 abcde	23.03 abc	24.14 ab	18.75 bcde	14.58 de	14.18 de	12.02 e
Hexanal	131.48 a	131.12 a	130.58 a	130.03 a	131.23 a	132.24 a	131.00 a	129.98 a	130.56 a	131.11 a	128.63 a	130.84 a
Benzyl Aldehydes												
3-Ethylbenzaldehyde	8.94 bcd	5.35 d	7.71 cd	11.48 abc	8.96 bcd	8.44 bcd	10.98 bc	15.18 a	11.80 abc	7.98 bcd	8.36 bcd	6.91 d
Benzeneacetaldehyde	112.53 bcde	72.21 e	97.43 cde	126.75 bcde	161.13 b	136.60 bcd	158.82 bc	276.22 a	172.59 b	83.91 de	86.51 de	69.70 e
Amides and Furans												
Benzamide	9.97 ab	8.40 b	9.94 ab	10.23 ab	14.69 ab	12.25 ab	16.33 a	14.29 ab	11.89 ab	9.73 ab	11.13 ab	9.49 ab
N-phenyl-Formamide	12.85 ab	16.24 ab	15.69 ab	16.85 ab	9.87 b	22.42 a	11.66 ab	15.04 ab	15.37 ab	15.91 ab	14.69 ab	18.73 ab
2-Ethyl-furan	29.05 a	29.77 a	28.40 a	28.63 a	31.32 a	31.16 a	30.66 a	29.05 a	28.99 a	29.68 a	30.07 a	30.75 a
2-Pentyl-furan	5.74 ab	4.80 ab	5.02 ab	6.52 ab	5.38 ab	5.02 ab	6.79 ab	7.04 a	6.19 ab	5.51 ab	4.81 ab	4.54 b
Hydrocarbons												
1,4-Cyclohexadiene	12.21 bcd	6.38 d	10.39 cd	14.17 abc	12.84 bcd	11.24 bcd	16.01 ab	18.66 a	15.92 ab	10.67 cd	11.74 bcd	9.16 d
2-Cyclopropyl-2-pentene	19.42 cdef	14.51 f	17.05 def	24.41 abc	23.26 abcd	20.81 bcdef	26.17 ab	27.61 a	22.97 abcde	17.43 def	17.71 def	16.74 ef
Decane	21.66 abc	17.05 bcd	16.91 bcd	25.92 a	19.65 abcd	19.96 abcd	24.46 ab	25.57 a	19.90 abcd	15.52 cd	15.58 cd	13.10 d
(E)-3-Methyl-1,3,5-hexatriene	2.33 a	1.78 a	2.25 a	2.28 a	2.50 a	2.81 a	2.59 a	3.37 a	3.38 a	2.30 a	1.95 a	2.56 a
1,3-cis,5-cis-Octatriene	6.81 cd	5.08 d	5.97 cd	7.67 bc	7.42 bc	6.61 cd	8.82 ab	9.77 a	7.86 abc	6.49 cd	7.55 bc	6.19 cd
1,4-Octadiene	19.76 abc	8.98 c	14.86 bc	35.66 a	16.99 abc	24.25 abc	35.60 a	31.24 ab	22.96 abc	17.61 abc	20.19 abc	14.70 abc
2-Methyl-2-hepten-4-yne	7.40 cde	5.52 e	6.74 de	8.27 bcd	7.92 bcd	7.34 cde	9.44 ab	10.20 a	8.72 abc	7.30 cde	7.96 bcd	7.17 cde
1-Methylcyclohexene	198.20 a	153.05 a	190.83 a	191.56 a	200.03 a	181.60 a	235.55 a	234.54 a	207.13 a	179.01 a	163.04 a	188.81 a
Acyclic Monoterpenes												
2,6-Dimethyl-2,4,6-octatriene	3.89 bcde	2.62 e	3.41 cde	4.15 bcde	5.39 b	4.76 bcd	5.27 bc	7.65 a	5.56 b	3.20 de	3.78 bcde	2.55 e
cis-β-Ocimene	454.45 b	345.75 b	474.37 ab	435.78 b	442.53 b	526.31 ab	446.03 b	756.25 a	489.82 ab	380.42 b	331.10 b	343.47 b
Citronellyl Acetate	191.03 ab	189.75 b	190.81 ab	189.65 b	189.24 b	191.93 ab	191.62 ab	194.78 a	190.54 b	191.23 ab	191.00 ab	190.14 ab
Linalool	753.22 ab	602.95 b	628.48 ab	924.86 a	696.32 ab	714.47 ab	767.72 ab	848.92 ab	779.51 ab	650.81 ab	778.87 ab	586.82 ab
trans-β-Ocimene	195.86 bcd	111.37 d	168.39 bcd	239.57 abc	216.57 bcd	232.42 bcd	262.02 ab	357.86 a	205.60 bcd	119.00 cd	158.82 bcd	117.86 cd
α-Ocimene	152.20 a	144.29 a	122.17 a	140.02 a	186.90 a	212.20 a	186.24 a	183.96 a	173.81 a	164.77 a	163.11 a	98.66 a
β-Myrcene	268.91 abcd	203.27 d	225.35 bcd	308.12 ab	287.72 abcd	271.36 abcd	301.56 abc	345.31 a	301.92 abc	245.65 bcd	235.39 bcd	216.54 cd
Bicyclic Monoterpenes												
3-Caren-10-al	1.70 ab	1.54 ab	1.54 ab	1.77 ab	1.61 ab	1.66 ab	2.31 a	2.40 a	1.58 ab	1.75 ab	1.95 ab	1.32 b
(+)-4-Carene	24.34 bc	18.67 c	22.85 bc	35.92 ab	32.04 abc	31.81 abc	40.76 a	45.46 a	30.60 abc	21.72 bc	21.06 bc	20.90 bc
Camphene	35.12 bcd	22.72 d	30.86 bcd	41.10 ab	35.81 bcd	30.27 bcd	51.23 a	51.21 a	38.04 abc	28.27 bcd	32.50 bcd	26.70 cd
Isoborneol	32.04 abc	22.05 c	29.66 bc	37.27 abc	28.57 bc	33.55 abc	44.80 ab	51.35 a	32.38 abc	30.87 bc	37.14 abc	24.62 c
trans-Pinocarveol	4.77 ab	3.12 b	3.67 b	4.68 ab	5.39 ab	5.68 ab	6.46 ab	6.36 ab	7.30 a	4.19 ab	3.66 b	6.27 ab
trans-Sabinene hydrate	21.66 abc	17.05 bcd	16.98 bcd	25.92 a	19.65 abcd	19.91 abcd	24.47 ab	25.63 a	19.90 abcd	15.51 cd	15.57 cd	13.09 d
α-Pinene	28.39 bcd	16.60 d	23.75 bcd	32.82 ab	29.58 bc	24.52 bcd	41.75 a	41.74 a	30.10 abc	22.02 bcd	25.19 bcd	20.42 cd
β-Pinene	155.77 abcd	111.86 d	117.45 cd	167.90 abc	170.62 ab	153.17 abcd	190.27 a	187.17 a	158.70 abcd	134.33 bcd	125.50 bcd	120.90 bcd
Cyclic Monoterpenes												
3-Menthene	35.99 abcd	20.38 d	25.47 bcd	31.81 abcd	41.70 abcd	39.30 abcd	45.50 abc	48.01 ab	53.10 a	29.57 bcd	24.96 cd	42.28 abcd
d-Limonene	308.17 bcd	224.30 d	271.77 cd	343.69 abc	331.01 abc	301.89 bcd	371.93 ab	401.22 a	341.25 abc	281.49 cd	278.99 cd	263.32 cd
Fenchyl acetate	92.03 a	81.94 a	97.62 a	111.13 a	95.53 a	115.00 a	109.94 a	111.16 a	112.12 a	86.90 a	105.84 a	81.22 a
p-Menth-1-en-8-ol	10.99 cdef	7.78 f	9.53 ef	13.32 bcd	12.78 bcde	11.46 bcdef	15.01 ab	17.03 a	14.39 abc	10.77 cdef	11.64 bcde	10.02 def
Sesquiterpene												
a-Humulene	55.29 a	55.99 a	55.79 a	56.25 a	59.41 a	59.01 a	57.52 a	58.82 a	56.25 a	56.05 a	54.51 a	56.36 a
Organosulfur												
Isothiocyanatocyclopropane	1.22 a	1.51 a	2.03 a	1.71 a	1.88 a	1.67 a	1.88 a	2.32 a	1.66 a	1.40 a	1.40 a	0.99 a
Diallyl Disulfide	0.87 a	0.70 a	0.88 a	0.95 a	0.99 a	1.02 a	1.21 a	1.36 a	0.97 a	0.80 a	2.05 a	0.76 a
Dimethyl Sulfide	64.89 abc	104.39 a	88.73 ab	112.47 a	93.37 ab	59.82 abc	88.37 ab	86.28 ab	70.26 abc	65.26 abc	45.70 bc	32.68 c
Phenylpropanoids												
Eugenol	146.53 bcd	178.05 bc	166.69 bc	164.96 bc	151.49 bcd	116.37 cd	208.47 b	283.16 a	202.84 b	151.32 bcd	165.70 bc	90.09 d
Methyl Eugenol	158.96 a	159.54 a	158.58 a	165.77 a	159.72 a	159.72 a	160.49 a	160.12 a	160.38 a	162.91 a	158.11 a	162.05 a

All concentrations are presented in micro molarity of analyte per gram of fresh mass ($\mu M \cdot g^{-1}$ FM). Mean values represent two plants per replication and ten replications per treatment. Values for each treatment are averaged across all four growing seasons. Values were analyzed using Tukey's protected least significant difference. Data in the same row followed by the same letter are not significantly different ($\alpha = 0.05$).

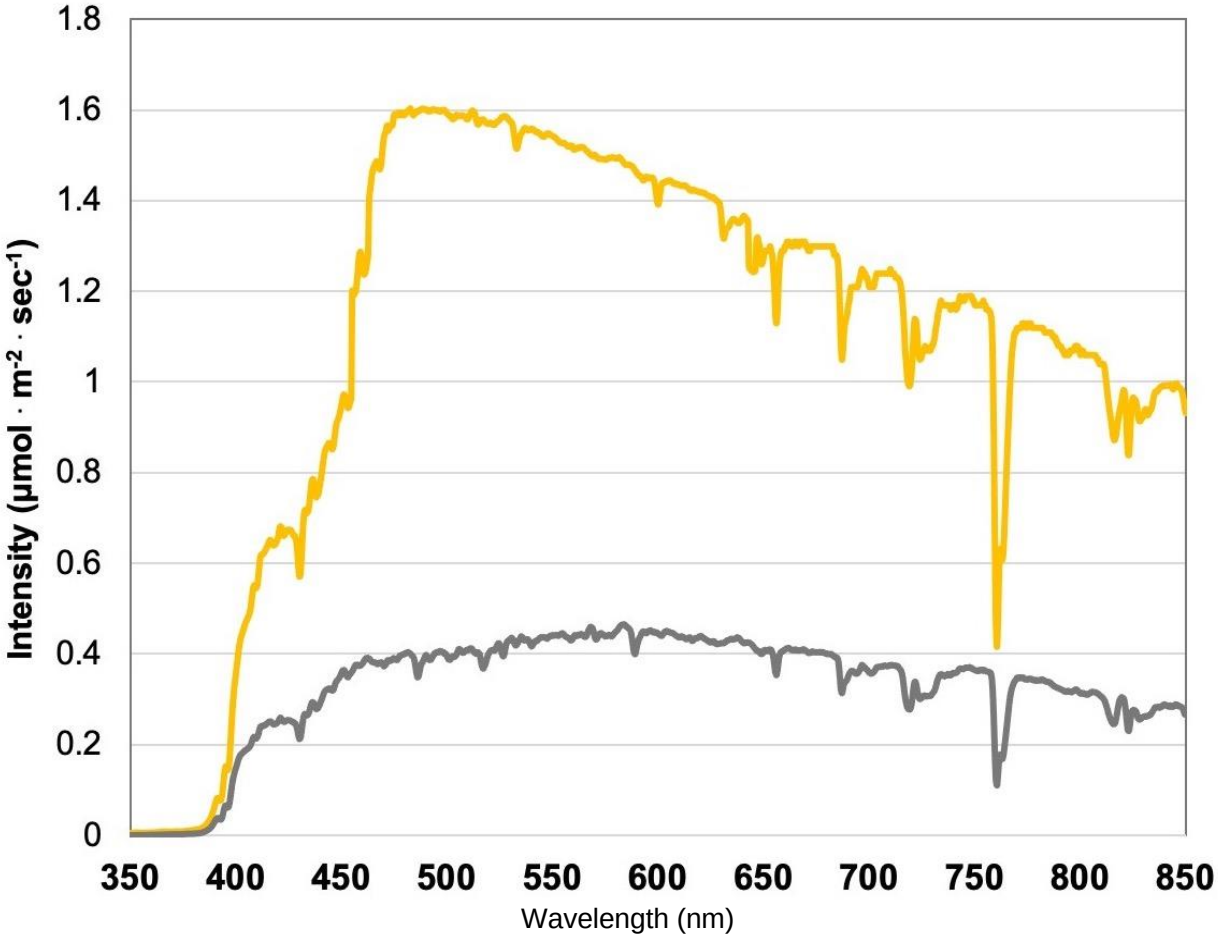

Figure 3.1. Natural light (NL) spectra under greenhouse glass, averaged across all four growing seasons, ranging from 350 nm to 850 nm. Values were taken at solar noon with three replicates for full sun (yellow) and overcast (gray) for each experimental run. The daily light integral (DLI) of the NL control averaged 11.75 mol·m^{-2}·d^{-1} across all growing cycles (ranging from 4 to 20 mol·m^{-2}·d^{-1}).

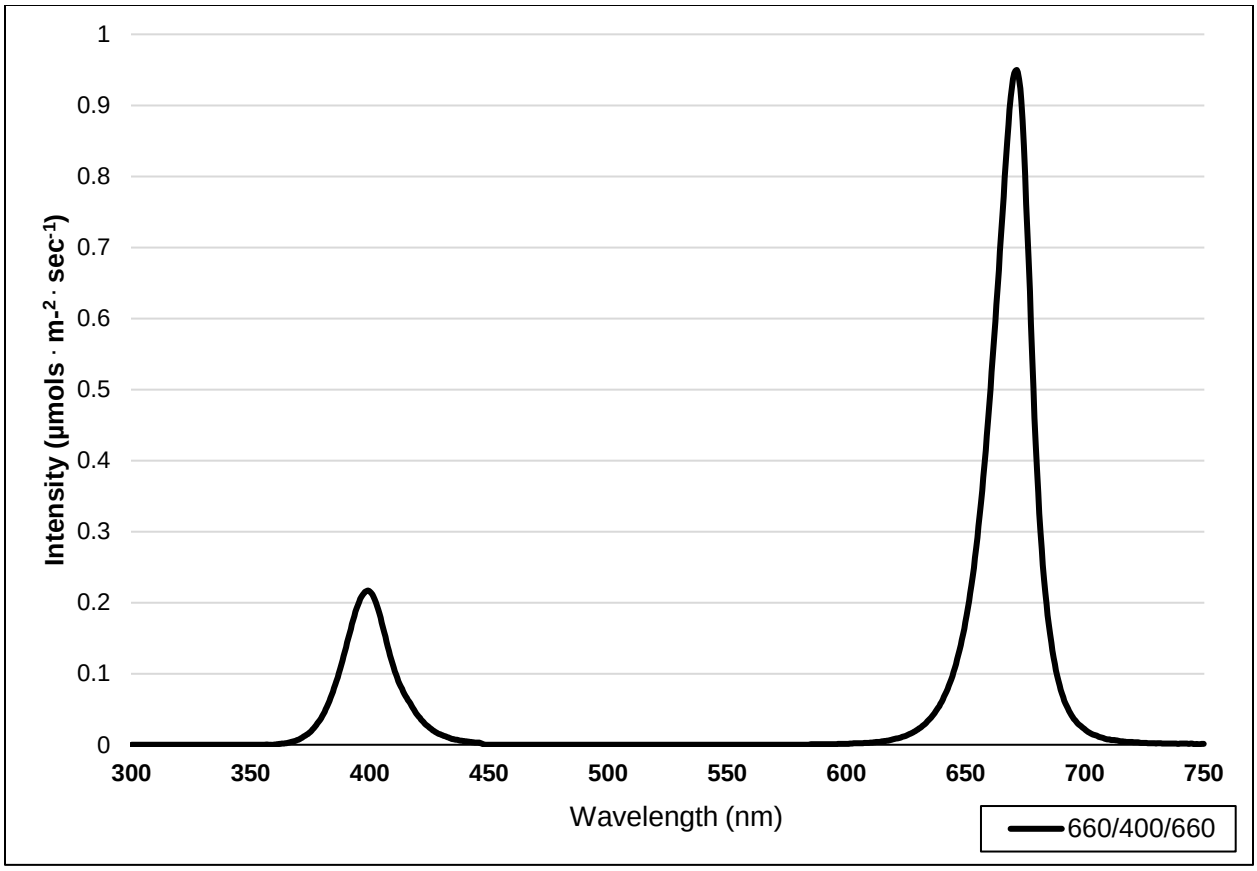

Figure 3.2 (A). Emission spectra of supplemental lighting (SL) treatment 660/400/660 from 300 nm to 750 nm. All SL treatments provided 8.64 mol·m^{-2}·d^{-1} (continuous 100 µmol·m^{-2}·s^{-1}; 24 h·d^{-1}). All lighting treatments were measured with a PS-200 Apogee Spectroradiometer to confirm intensity of specific treatment wavelengths throughout each growing season. Readings were taken at midnight in order to exclude underlying natural solar spectra.

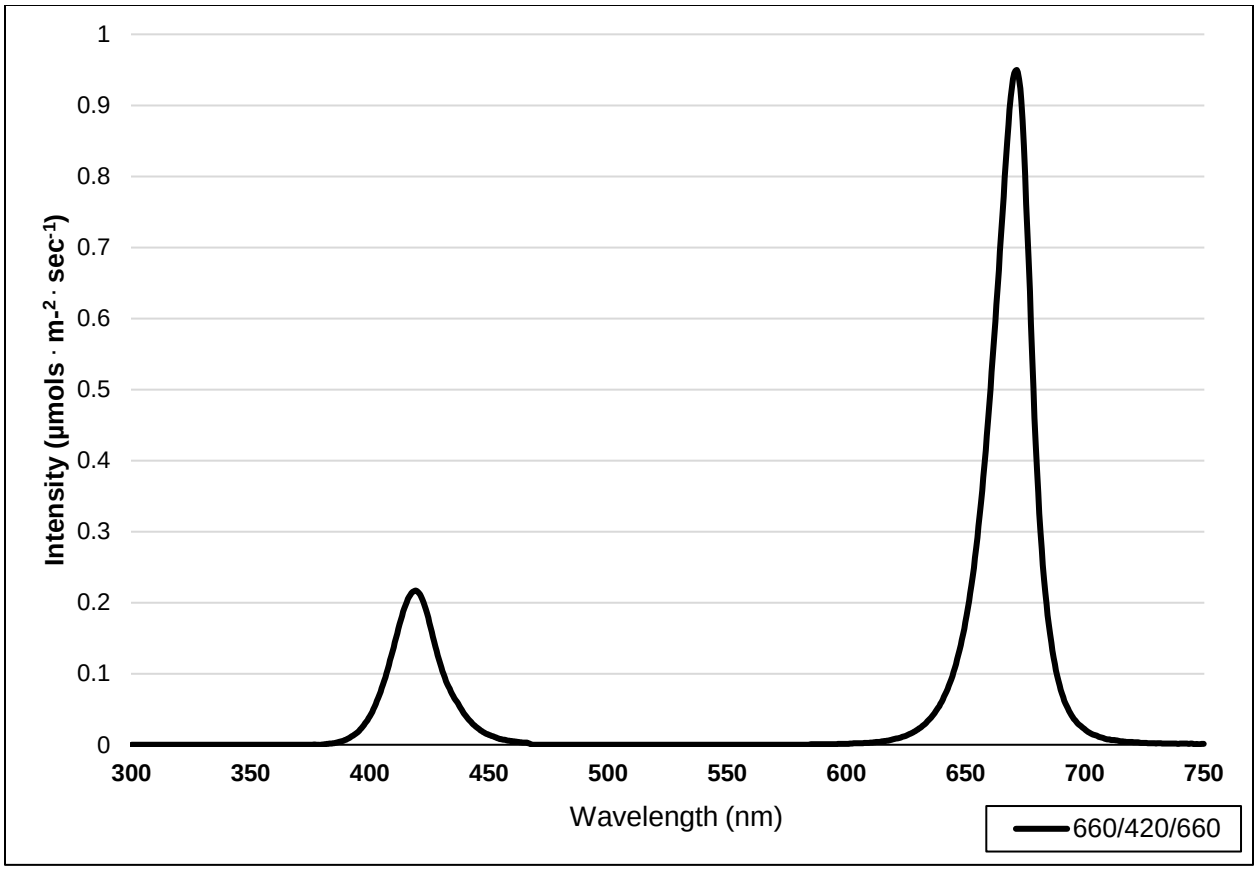

Figure 3.2 (B). Emission spectra of supplemental lighting (SL) treatment 660/420/660 from 300 nm to 750 nm. All SL treatments provided 8.64 mol·m^{-2}·d^{-1} (continuous 100 µmol·m^{-2}·s^{-1}; 24 h·d^{-1}). All lighting treatments were measured with a PS-200 Apogee Spectroradiometer to confirm intensity of specific treatment wavelengths throughout each growing season. Readings were taken at midnight in order to exclude underlying natural solar spectra.

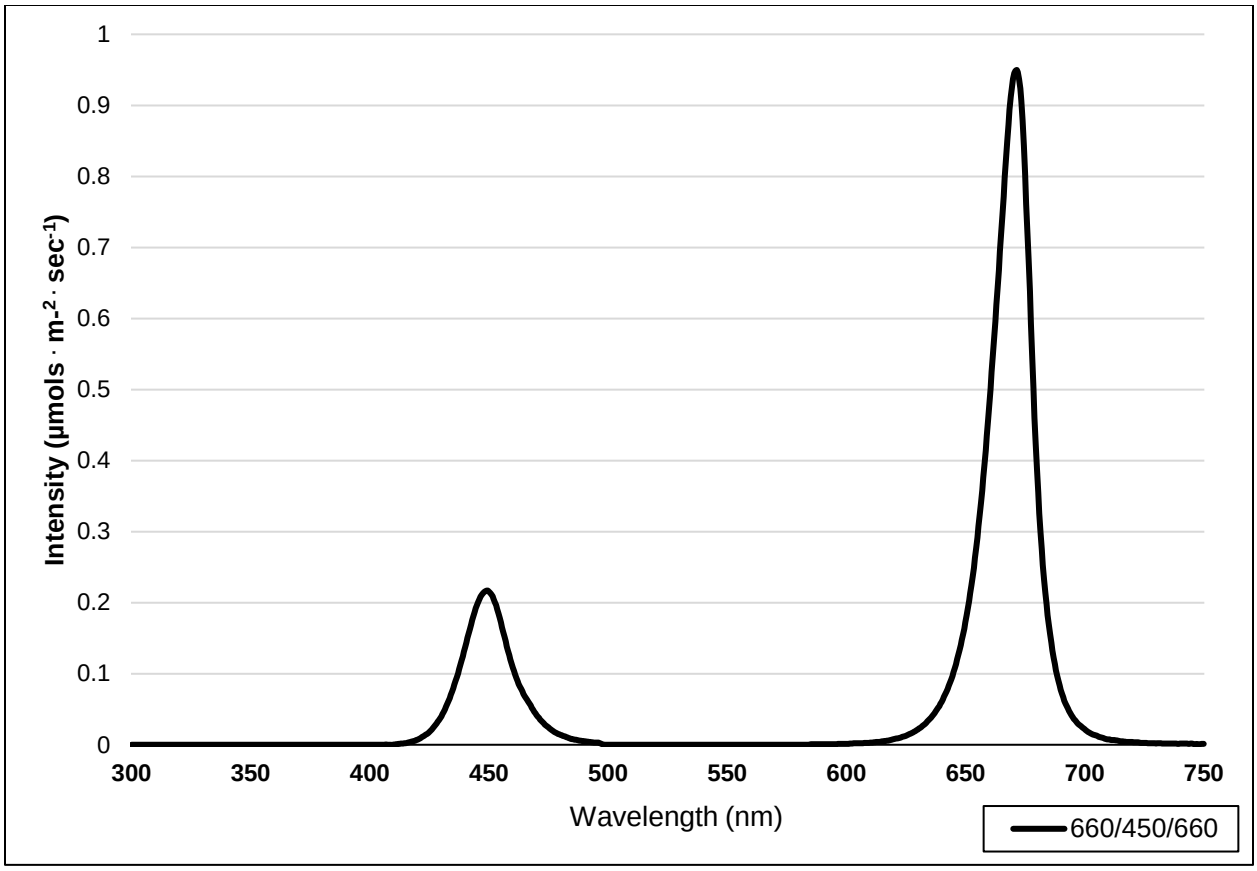

Figure 3.2 (C). Emission spectra of supplemental lighting (SL) treatment 660/450/660 from 300 nm to 750 nm. All SL treatments provided 8.64 mol·m^{-2}·d^{-1} (continuous 100 µmol·m^{-2}·s^{-1}; 24 h·d^{-1}). All lighting treatments were measured with a PS-200 Apogee Spectroradiometer to confirm intensity of specific treatment wavelengths throughout each growing season. Readings were taken at midnight in order to exclude underlying natural solar spectra.

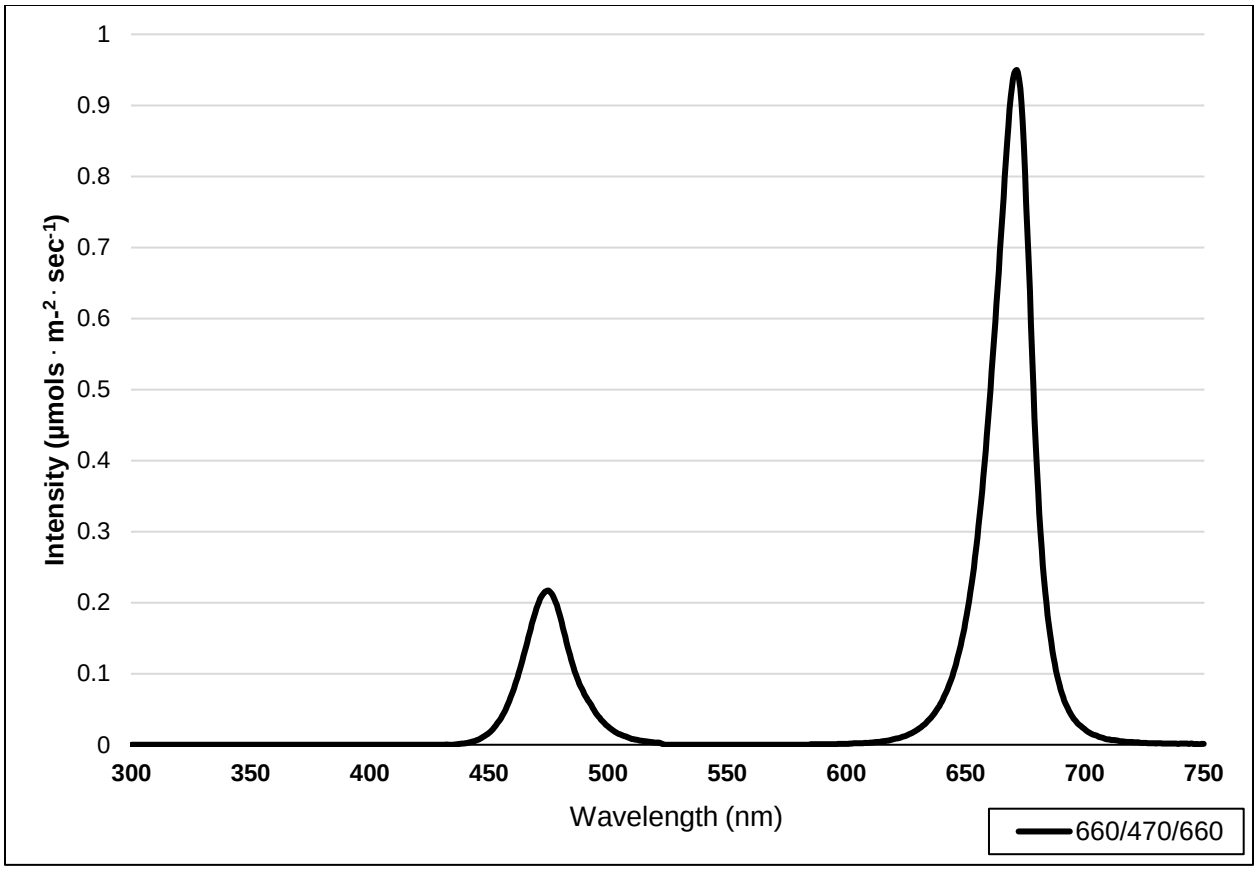

Figure 3.2 (D). Emission spectra of supplemental lighting (SL) treatment 660/470/660 from 300 nm to 750 nm. All SL treatments provided 8.64 mol·m^{-2}·d^{-1} (continuous 100 µmol·m^{-2}·s^{-1}; 24 h·d^{-1}). All lighting treatments were measured with a PS-200 Apogee Spectroradiometer to confirm intensity of specific treatment wavelengths throughout each growing season. Readings were taken at midnight in order to exclude underlying natural solar spectra.

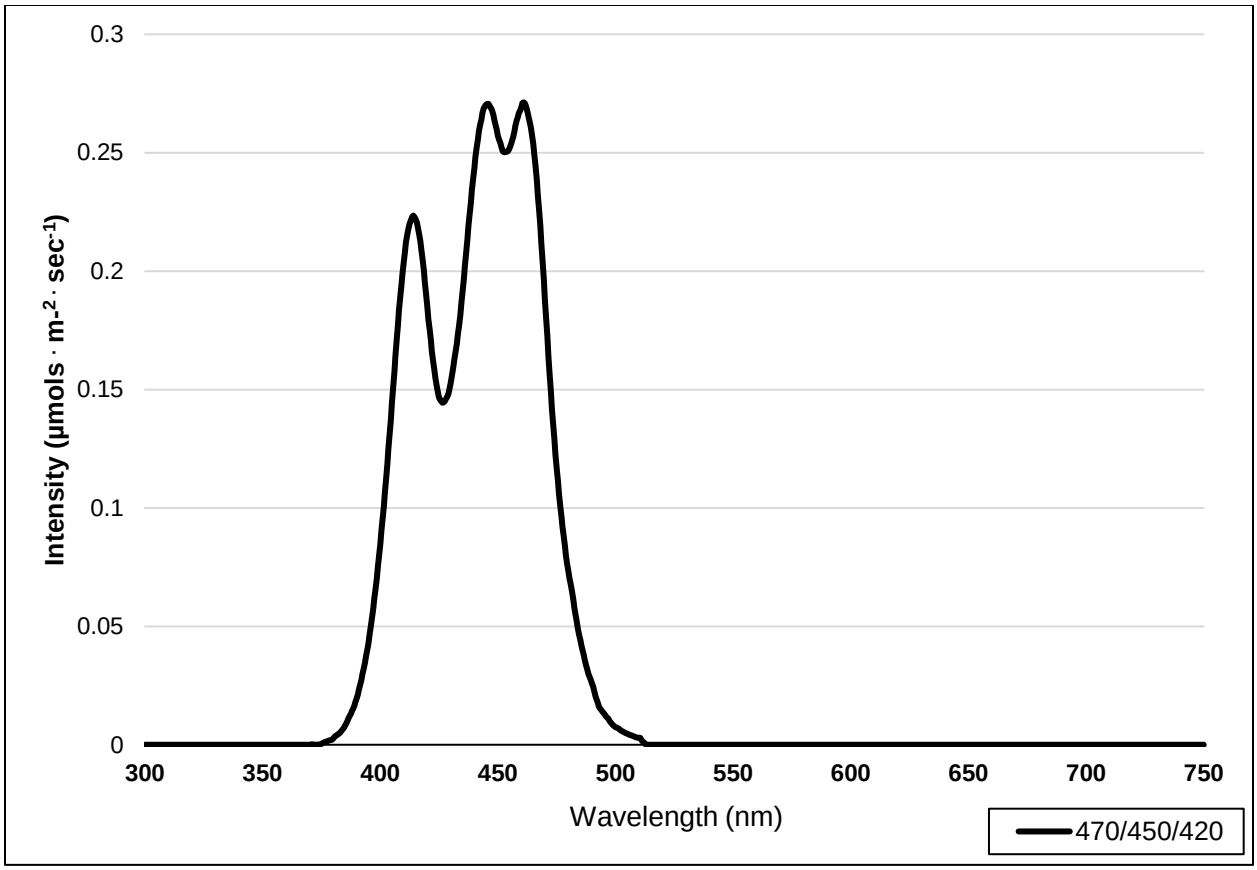

Figure 3.2 (E). Emission spectra of supplemental lighting (SL) treatment 470/450/420 from 300 nm to 750 nm. All SL treatments provided 8.64 mol•m^{-2}•d^{-1} (continuous 100 µmol•m^{-2}•s^{-1}; 24 h•d^{-1}). All lighting treatments were measured with a PS-200 Apogee Spectroradiometer to confirm intensity of specific treatment wavelengths throughout each growing season. Readings were taken at midnight in order to exclude underlying natural solar spectra.

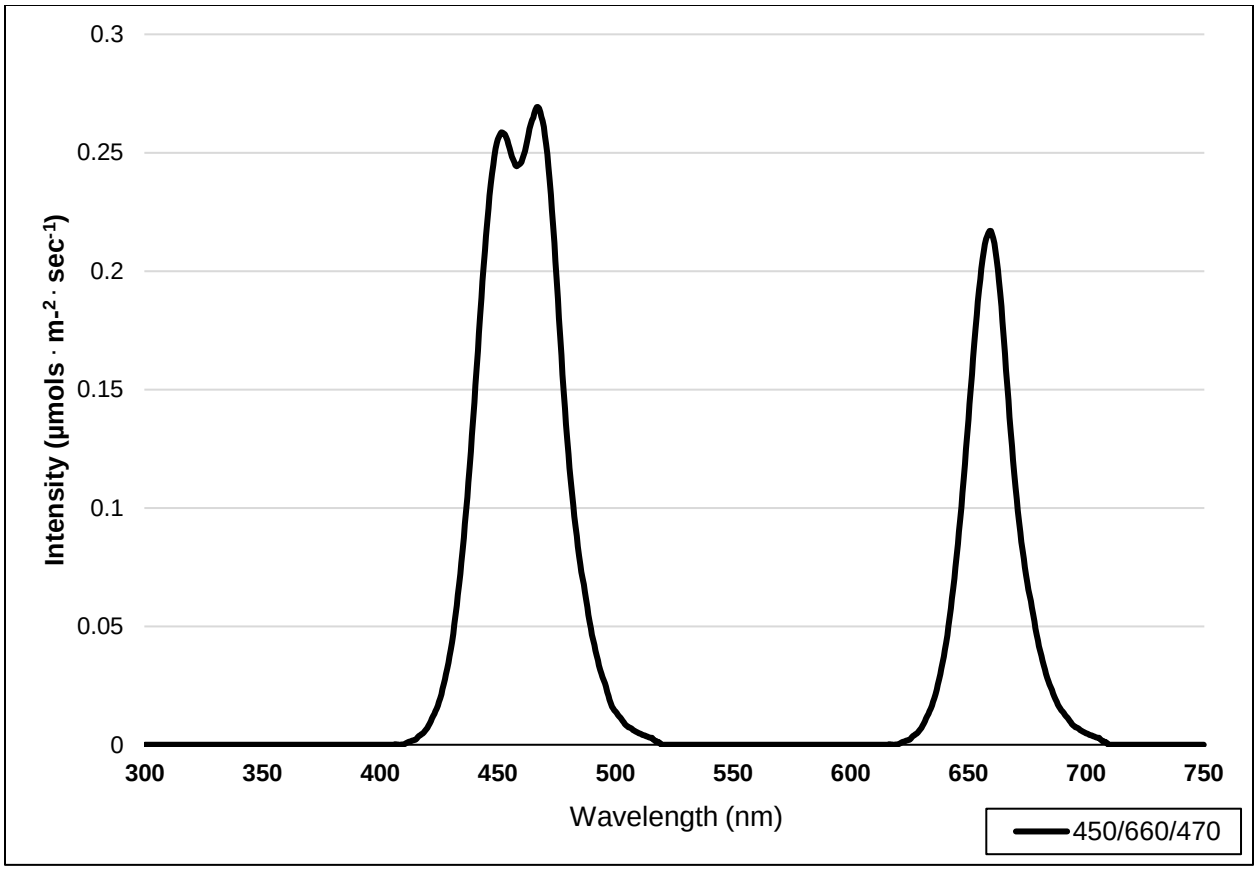

Figure 3.2 (F). Emission spectra of supplemental lighting (SL) treatment 450/660/470 from 300 nm to 750 nm. All SL treatments provided 8.64 mol·m^{-2}·d^{-1} (continuous 100 µmol·m^{-2}·s^{-1}; 24 h·d^{-1}). All lighting treatments were measured with a PS-200 Apogee Spectroradiometer to confirm intensity of specific treatment wavelengths throughout each growing season. Readings were taken at midnight in order to exclude underlying natural solar spectra.

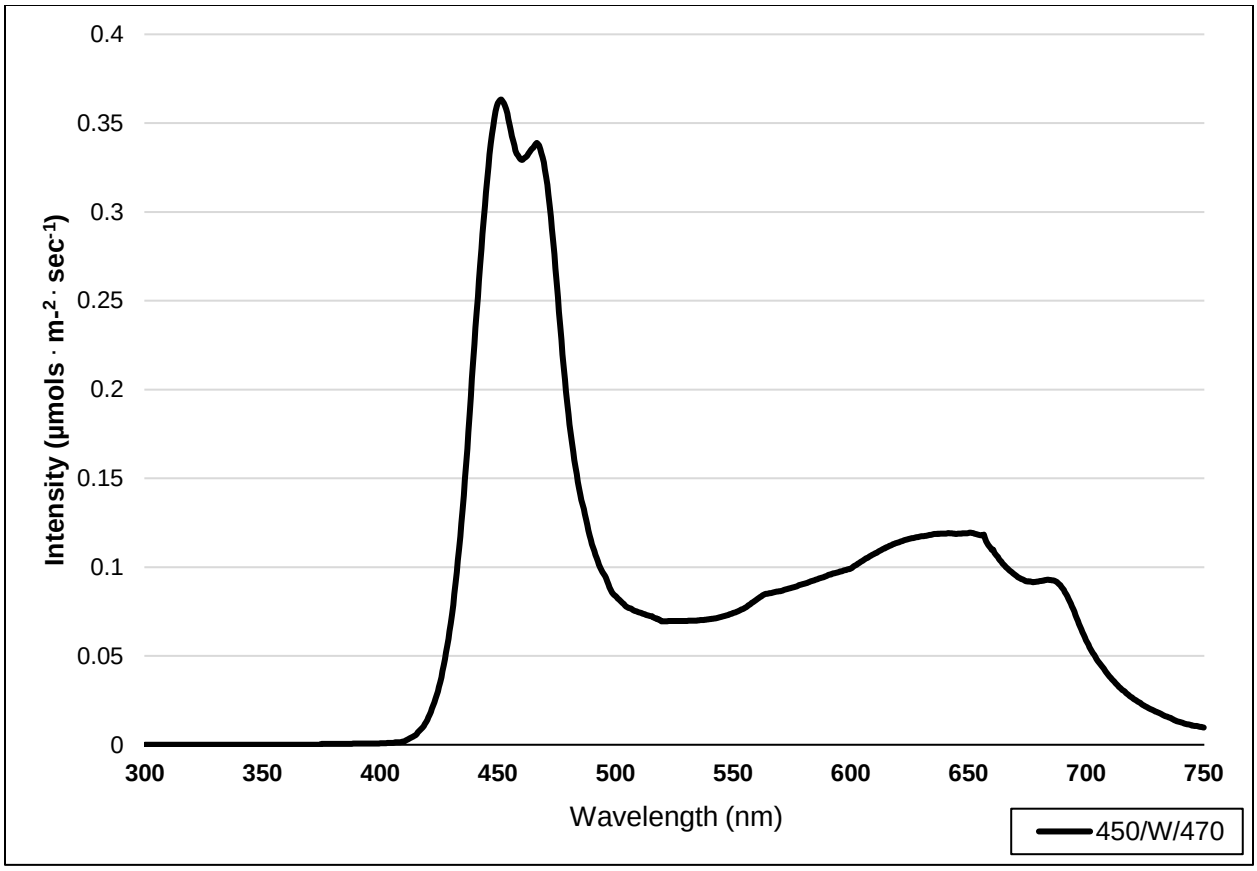

Figure 3.2 (G). Emission spectra of supplemental lighting (SL) treatment 450/W/470 from 300 nm to 750 nm. All SL treatments provided 8.64 mol·m^{-2}·d^{-1} (continuous 100 µmol·m^{-2}·s^{-1}; 24 h·d^{-1}). All lighting treatments were measured with a PS-200 Apogee Spectroradiometer to confirm intensity of specific treatment wavelengths throughout each growing season. Readings were taken at midnight in order to exclude underlying natural solar spectra.

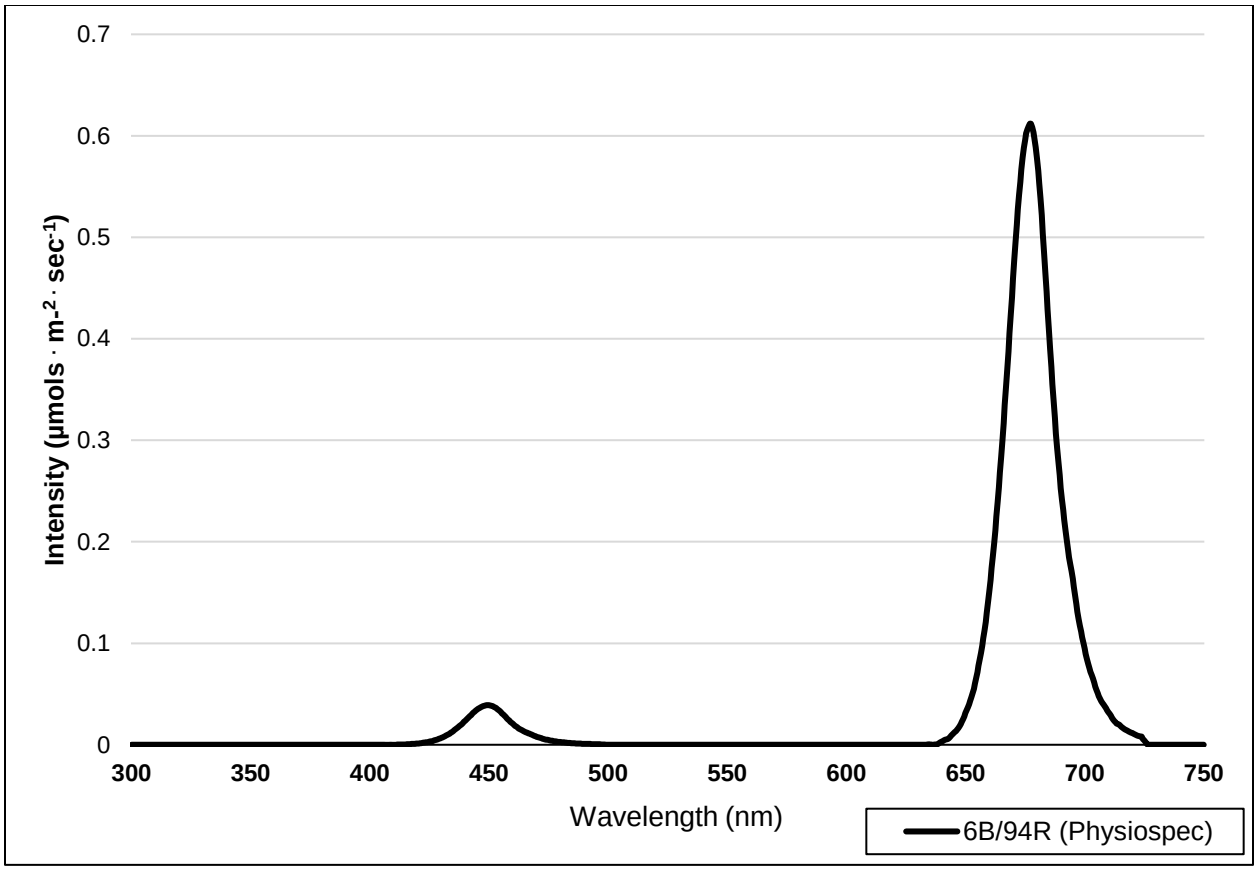

Figure 3.2 (H). Emission spectra of supplemental lighting (SL) treatment 6B/94R (Fluence PhysioSpec™) from 300 nm to 750 nm. All SL treatments provided 8.64 mol•m^{-2}•d^{-1} (continuous 100 µmol•m^{-2}•s^{-1}; 24 h•d^{-1}). All lighting treatments were measured with a PS-200 Apogee Spectroradiometer to confirm intensity of specific treatment wavelengths throughout each growing season. Readings were taken at midnight in order to exclude underlying natural solar spectra.

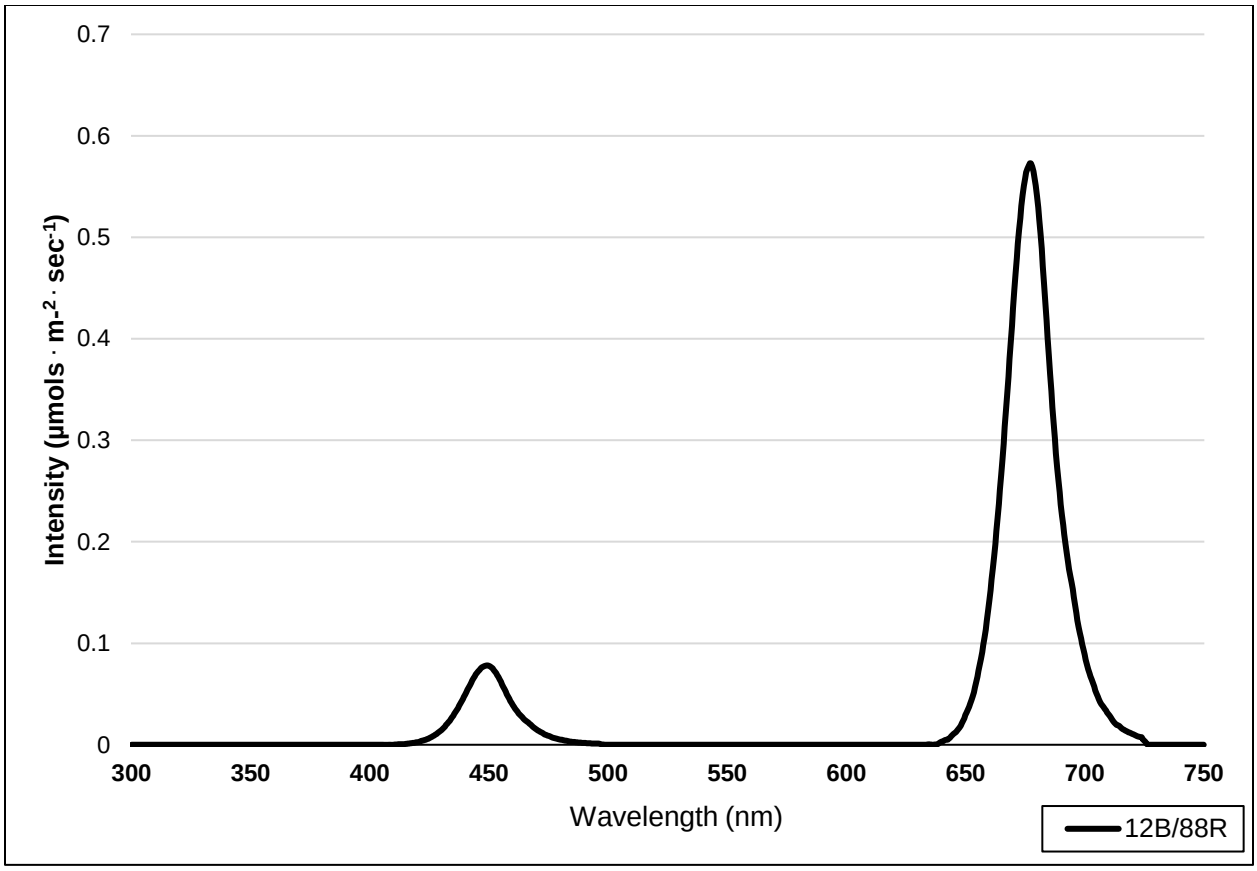

Figure 3.2 (I). Emission spectra of supplemental lighting (SL) treatment 12B/88R (Fluence PhysioSpec™) from 300 nm to 750 nm. All SL treatments provided 8.64 mol·m^{-2}·d^{-1} (continuous 100 µmol·m^{-2}·s^{-1}; 24 h·d^{-1}). All lighting treatments were measured with a PS-200 Apogee Spectroradiometer to confirm intensity of specific treatment wavelengths throughout each growing season. Readings were taken at midnight in order to exclude underlying natural solar spectra.

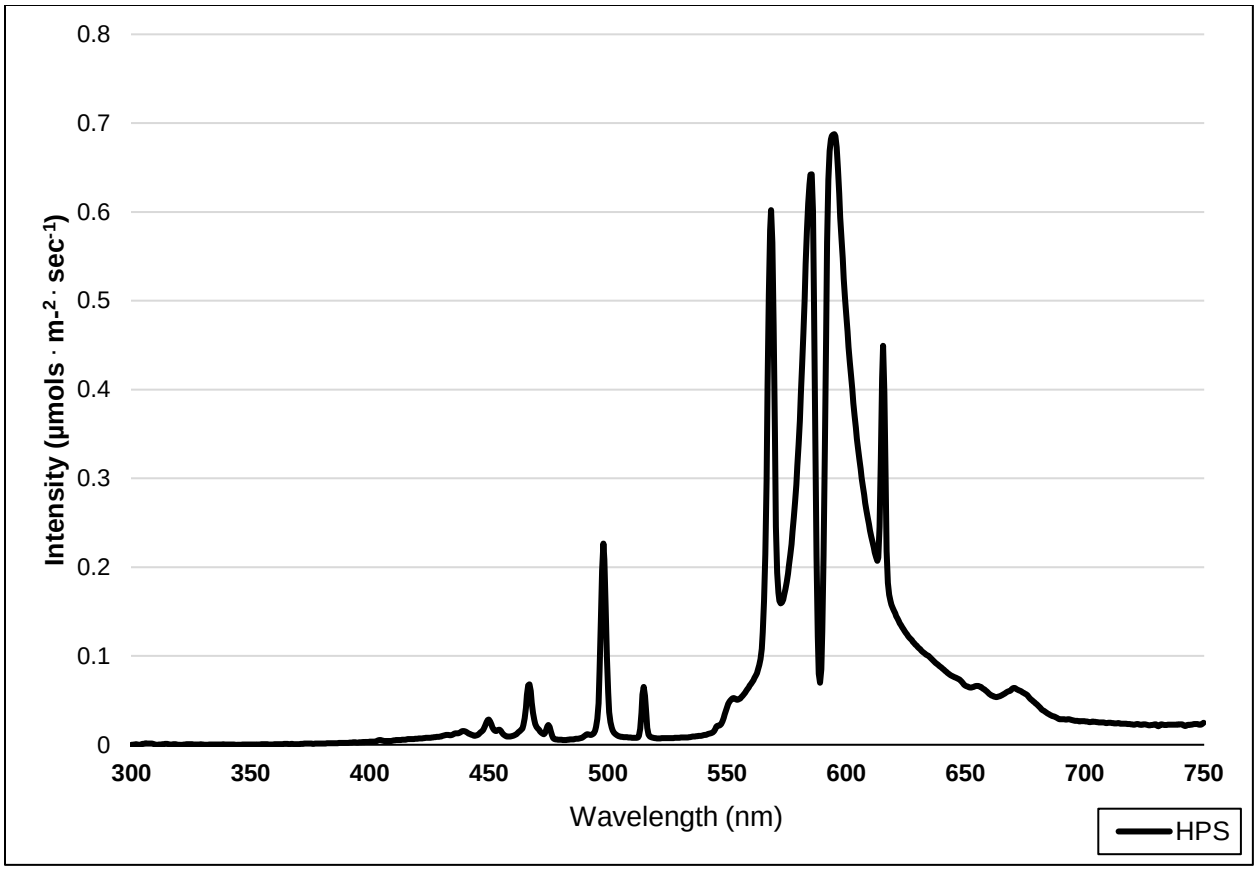

Figure 3.2 (J). Emission spectra of supplemental lighting (SL) treatment High Pressure Sodium (HPS) from 300 nm to 750 nm. All SL treatments provided 8.64 mol·m^{-2}·d^{-1} (continuous 100 µmol·m^{-2}·s^{-1}; 24 h·d^{-1}). All lighting treatments were measured with a PS-200 Apogee Spectroradiometer to confirm intensity of specific treatment wavelengths throughout each growing season. Readings were taken at midnight in order to exclude underlying natural solar spectra.

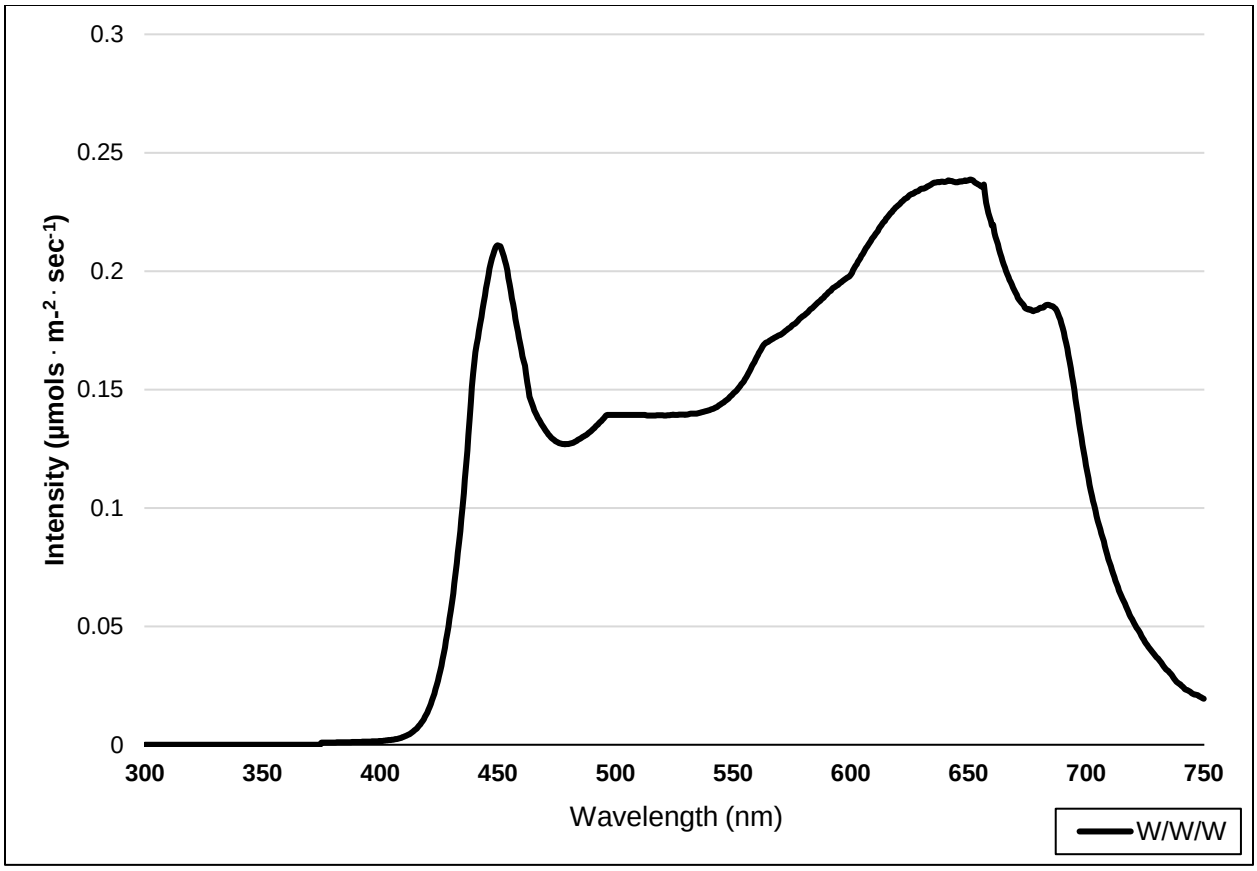

Figure 3.2 (K). Emission spectra of supplemental lighting (SL) treatment W/W/W (full spectrum neutral white) from 300 nm to 750 nm. All SL treatments provided 8.64 mol·m^{-2}·d^{-1} (continuous 100 µmol·m^{-2}·s^{-1}; 24 h·d^{-1}). All lighting treatments were measured with a PS-200 Apogee Spectroradiometer to confirm intensity of specific treatment wavelengths throughout each growing season. Readings were taken at midnight in order to exclude underlying natural solar spectra.

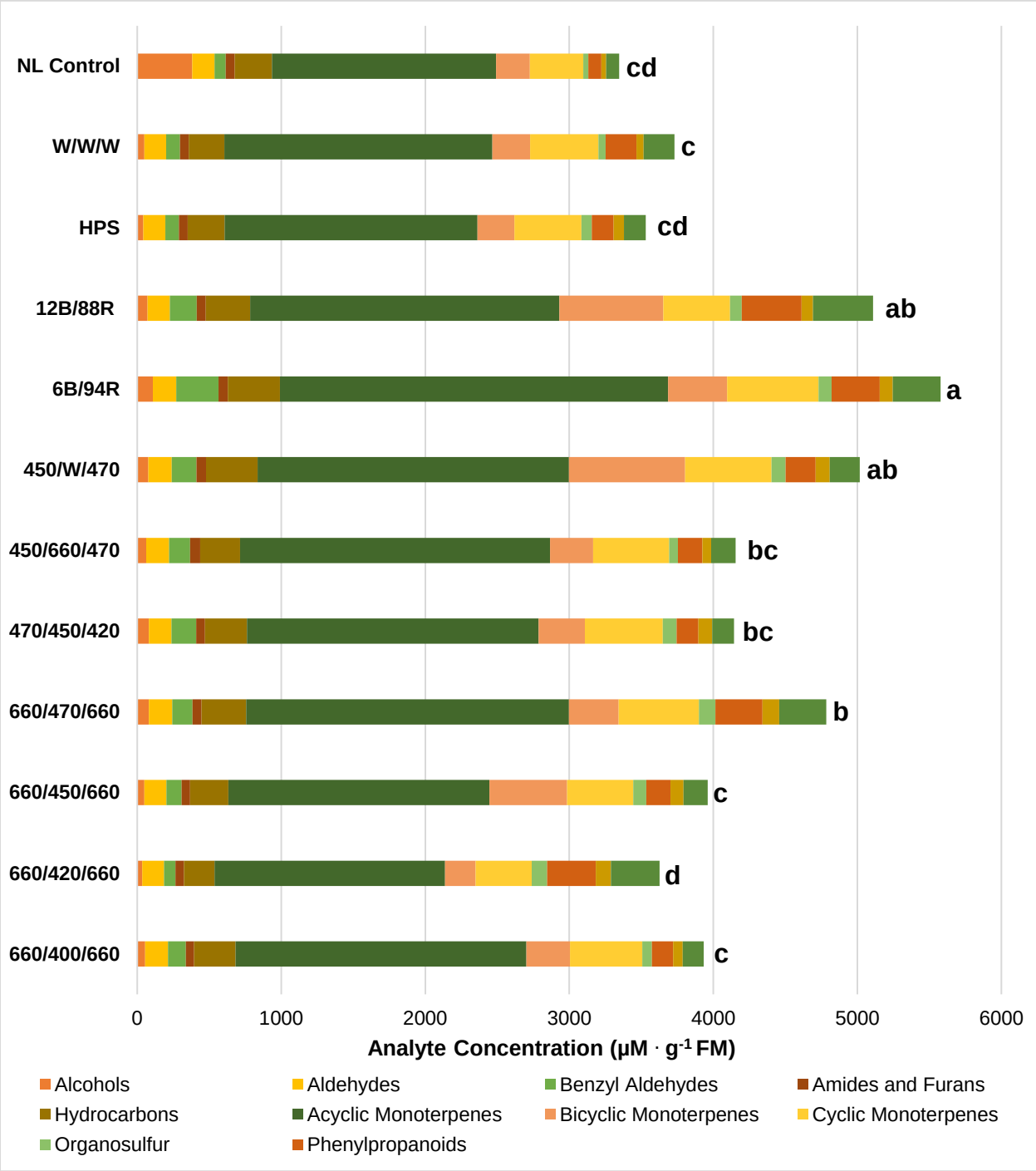

Figure 3.3. Impact of lighting treatment on tissue accumulation of each compound class. All concentrations are presented in micro molarity of analyte per gram of fresh mass ($\mu M \cdot g^{-1}$ FM). Mean values represent two plants per replication and ten replications per treatment. Values for each treatment are averaged across all seasons within that treatment. Total volatile organic compound concentration was analyzed using Tukey's protected least significant difference. Data followed by the same letter are not significantly different ($\alpha = 0.05$).

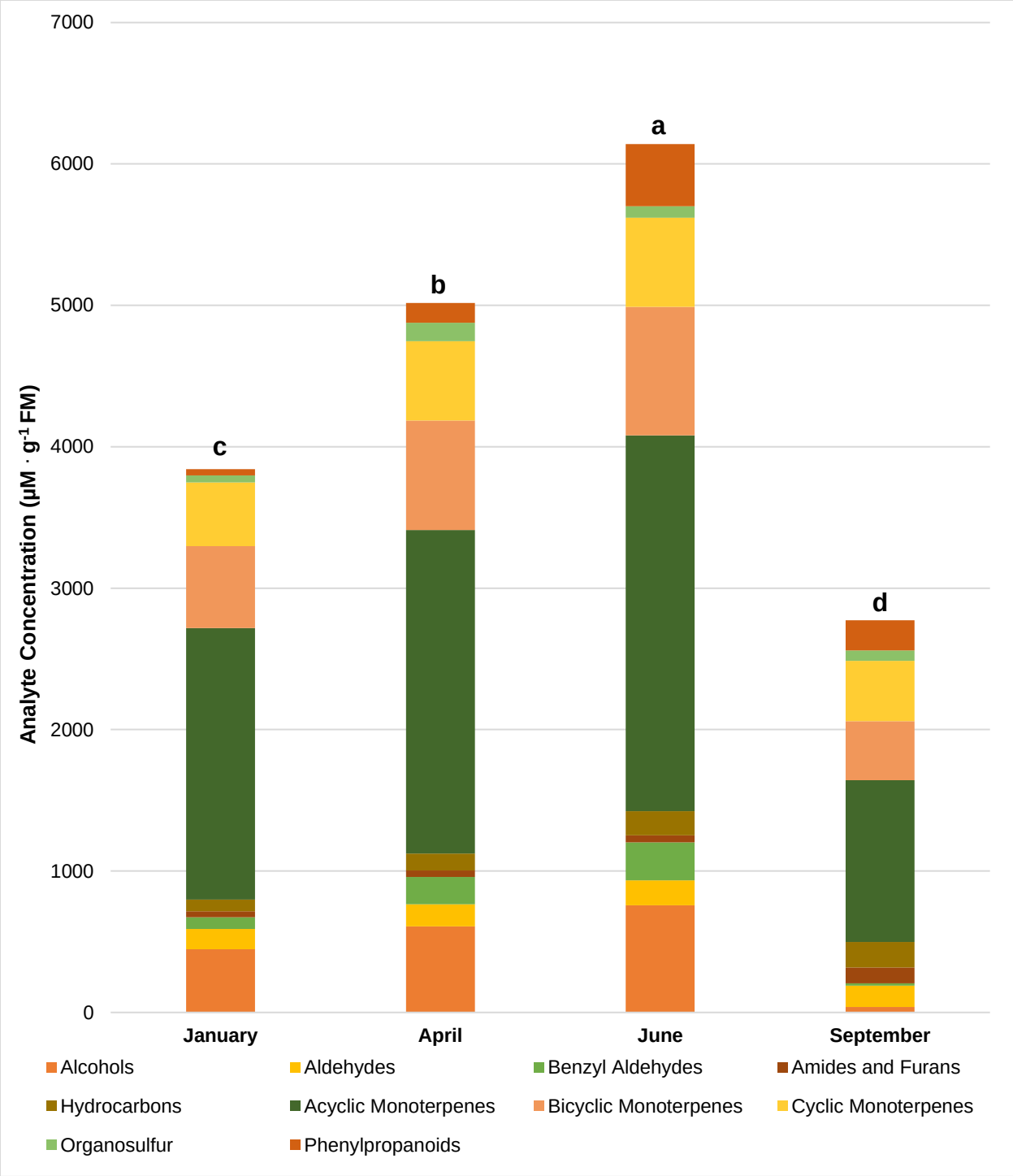

Figure 3.4. Influence of season on compound classes pertinent for aroma perception. All concentrations are presented in micro molarity of analyte per gram of fresh mass (µM·g^{-1} FM). Mean values represent two plants per replication and ten replications per treatment. Values for each season are averaged across all treatments within that season. Total volatile organic compound concentration was analyzed using Tukey's protected least significant difference. Data followed by the same letter are not significantly different ($\alpha = 0.05$).

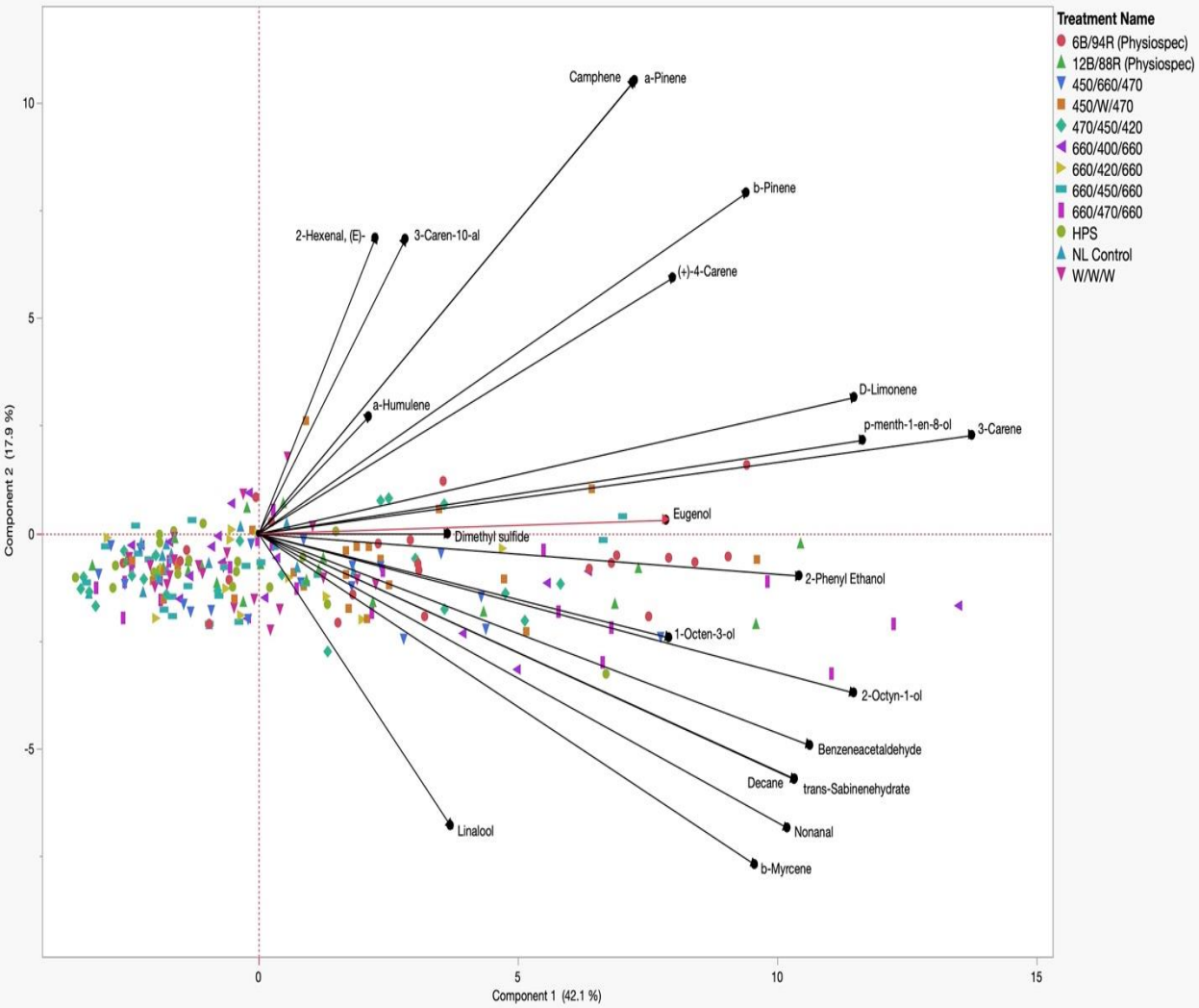

Figure 3.5. Principal Component Analysis (PCA) showing the biplot differentiation between sweet basil 'Italian Large Leaf' (*Ocimum basilicum* L.*)* aroma compound concentrations (black) grown under various supplemental lighting treatments.

CHAPTER 4: TRANSCRIPTOME SEQUENCING SUBSTANTIATES ROLE OF SPECTRAL QUALITY IN YIELD AND NUTRIENT BIOACCUMULATION OF HYDROPONICALLY GROWN SWEET BASIL

Hunter A. Hammock and Carl E. Sams
Department of Plant Sciences, The University of Tennessee, Knoxville, TN 37996

Correspondence: Carl E. Sams, carlsams@utk.edu

Keywords: Controlled Environment Agriculture (CEA), Light Emitting Diodes (LEDs), *Ocimum basilicum*, Supplemental Lighting (SL), Primary Metabolism, Spectral Quality, Differentially Expressed Genes (DEGs), Transcriptome

Author Contributions:
Conceptualization – HAH, CES
Methodology – HAH, CES
Software – HAH, CES
Validation – HAH
Formal analysis – HAH
Investigation – HAH
Resources – CES
Data curation – HAH
Writing (original draft preparation) - HAH
Writing (review and editing) – HAH, CES
Visualization – HAH
Supervision and project administration – CES
Funding acquisition – CES

Author Statement:
All authors have reviewed the manuscript and agree with the reported findings. There are no reported conflicts between the authors and the present study.

Funding:
This research was supported by The AgResearch Dean's Office within the University of Tennessee Institute of Agriculture. No external funds were used for the present study.

Disclosure:
This manuscript and its contents will be submitted to JASHS July 7, 2023.

Abstract

The spectral quality of light received by plants directly influences primary metabolism. Photoreceptors control light-mediated physiological responses vital for sustained life and biomass accumulation. Supplemental lighting (SL) in greenhouse production can be used to modify natural solar spectra for unfavorable locations or seasonal conditions. Narrowband and broadband supplements both have merit for mitigating poor light quality and quantity. Still, species-dependent expression of light-mediated metabolic pathways challenges the establishment of generalized controlled environment agriculture (CEA) lighting protocols. Additional research is needed to ascertain the efficacy of SL spectral distribution in terms of yield and nutritional quality of high-value specialty crops. The objective of this study was to determine the influence of SL spectral quality on various aspects of primary metabolism in greenhouse hydroponically grown basil (*Ocimum basilicum* 'Genovese'). Four light treatments were utilized: non-supplemented natural light (NL) control, 20B/80R narrowband LEDs, Broadband White LEDs (5600 K), and a high-pressure sodium (HPS) lamp. During the growth period, daily light integral (DLI) of NL control averaged 11.58 $mol \cdot m^{-2} \cdot d^{-1}$. Each SL treatment had equal intensity and provided an additional 8.64 $mol \cdot m^{-2} \cdot d^{-1}$ (100 $\mu mol \cdot m^{-2} \cdot s^{-1}$ for 24 $h \cdot d^{-1}$). Fresh mass (FM) and dry mass (DM) were significantly increased by SL treatments over NL control. Broadband White had higher yields than Narrowband B/R, but both had higher FM/DM than NL control. Elemental nutrient tissue analysis was performed using an ICP-MS, showing that treatment significantly influenced many macro and micronutrient tissue concentrations. Principal component analysis (PCA) revealed the B/R treatment was correlated with increased tissue concentrations of Ca, while the white treatment was correlated with increased N, K, B, and Cu. RNA-seq identified a total of 4207 differentially expressed genes (DEGs) across treatments through pairwise comparisons. The B/R narrowband

treatment had 3801 DEGs compared to NL control, while the white and HPS broadband treatments had 278 and 128 DEGs, respectively, compared to NL control. Functional annotations revealed several DEGs involved with primary metabolic functions were significantly up-regulated in the B/R and white treatments. Increased expression of certain genes responsible for metabolic regulation can directly influence yield and nutrient uptake/assimilation. This experiment demonstrates SL spectral quality influences yield and tissue nutrient concentrations through numerous DEGs involved with primary metabolism. Further studies integrating analytic and transcriptomic analyses of specialty crops will improve our understanding of plant/light interaction, which can be leveraged to design lighting strategies with the goal of maximizing yield and nutritional value.

Introduction

Light is a fundamental component of plant growth, underpinning numerous physiological processes (Fraikin et al., 2013; Darko et al., 2014; Thoma et al., 2020). The primary role of light in plant metabolism is its function in photosynthesis, where it serves as the energy source for the conversion of carbon dioxide and water into glucose, a process that fuels plant growth and development (McCree, 1972; Bilger et al., 1989; Ashraf and Harris, 2013). Moreover, plants are equipped with photoreceptors that enable them to perceive variations in light quality, duration, and intensity (Fraikin et al., 2013; Folta and Carvalho, 2015). These photoreceptors control light-mediated physiological responses, such as phototropism, photomorphogenesis, and circadian rhythms, which orchestrate a myriad of developmental and metabolic processes in plants (Rockwell et al., 2006; Chaves et al., 2011; Galvao and Fankhauser, 2015).

In greenhouse production, supplemental lighting (SL) is sometimes employed to augment natural sunlight, particularly in regions or seasons where the solar spectrum may not be ideal for plant growth (Massa et al., 2008; Morrow, 2008; Gómez and Mitchell, 2015). The purpose of SL is to provide additional light, particularly in the photosynthetically active radiation region, to enhance plant productivity and quality (Currey et al., 2017; Weaver et al., 2019; Boldt and Altland, 2022). This is achieved by modifying the natural solar spectra through the use of narrowband and/or broadband supplements, which can mitigate poor light quality and quantity, thereby optimizing plant growth.

However, the formulation of generalized controlled environment agriculture (CEA) lighting protocols presents several challenges. One key challenge is the species-dependent expression of light-mediated metabolic pathways. Different plant species, or even different cultivars within a species, can exhibit diverse responses to light conditions, leading to variations in growth and nutritional quality (Randall and Lopez, 2014; Ouzounis et al., 2015; Singh et al., 2015; Baumbauer et al., 2019; Kyriacou et al., 2019). Therefore, there is a pressing need for more extensive research on impact of SL spectral distribution on plant yield and nutritional quality across a range of plant species.

In addition to recognizing species-dependent differences in light sensitivity, it is also important to consider the cost and energy efficiency when establishing universal lighting protocols for controlled environment agriculture (CEA) systems (Sager et al., 1988; Zhen and Bugbee, 2020; Engler and Krarti, 2021; Jayalath and van Iersel, 2021; Tabbert et al., 2021). As LED systems become increasingly popular due to their higher efficiency and flexibility in providing tailored spectra of light, growers must balance the need for optimized light conditions with economic

considerations such as operational costs. Thus, it is essential to establish protocols that are both economically and energetically viable, while still providing optimal light conditions for the crops.

The objective of this current study is to investigate the influence of SL spectral quality on the primary metabolism of basil (Ocimum basilicum 'Genovese'). We aim to identify which LED spectra provide optimal light conditions for basil growth and nutritional quality. We tested four light treatments: non-supplemented natural light (NL) control, 20B/80R narrowband LEDs, broadband neutral white LEDs (5600 K), and a high-pressure sodium (HPS) lamp. To assess the effects of these treatments, we measured fresh mass (FM), dry mass (DM), performed elemental nutrient tissue analysis, and conducted gene expression profiling using RNA-seq.

Our hypothesis was that different SL spectral qualities elicit varying effects on primary metabolism in basil across growing seasons. We further hypothesized that SL treatments may influence yield and nutrient uptake/assimilation through the differential expression of genes involved in primary metabolic functions. This study aims to fill the knowledge gap in the literature concerning the impact of SL spectral quality on plant primary metabolism, providing insights that can guide the development of more effective CEA lighting strategies.

Materials and Methods

Cultural Techniques and Environmental Growing Conditions

This project was conducted at the University of Tennessee Institute of Agriculture (UTIA) in Knoxville, TN, USA, located at 35°56'44.5"N, 83°56'17.3”W. *Ocimum Basilicum* ‘Genovese’ basil seeds (Johnny’s Select Seeds, Winslow, ME, United States) were germinated in peat moss-based cubes (2 × 2 × 6 cm) (Park’s Bio Dome Sponges, Hodges, SC, United States) at 28.3°C and 95% RH. We chose the 'Genovese' sweet basil due to its intricate flavor, popularity among professional chefs, and high demand in the market.

The seedlings were moved to NFT hydroponic systems with a full-strength general mix nutrient solution after two weeks. The fertility regime remained constant throughout the seasons, and the basil was grown in standard commercial greenhouse conditions. The nutrient solution was kept at a consistent pH of 5.9 and changed weekly. Elemental nutrient concentrations were as follows (ppm): N (207.54), P(50.87), K (298.23), Ca (180.15), Mg (77.10), S (136.45), Fe (3.95), Mn (0.90), Z (0.40), Mo (0.09), Cu (0.90), and B (0.90). To maintain consistent nutrient composition, we used Inductively Coupled Plasma Mass Spectrometry (Agilent Technologies, Santa Clara, CA, United States) to analyze the water samples during each experiment. In both growing seasons, the total growth time was around 45 days.

Day temperatures averaged 28.1 ± 1.5 °C, and night temperatures averaged 21.3 ± 0.4 °C. Relative humidity during the growth period averaged 55%. DLI of the natural light control (i.e., ambient sunlight) averaged 9.9 $mol \cdot m^{-2} \cdot d^{-1}$ across all four growing seasons (daily average ranging from 4 to 20 $mol \cdot m^{-2} \cdot d^{-1}$). Each hydroponic system (treatment) received similar amounts of cumulative ambient sunlight (DLI of ± 0.5 $mol \cdot m^{-2} \cdot d^{-1}$ across treatments) throughout the four growing seasons, in addition to the prescribed SL regime.

Two experimental cycles were performed to determine differences between summer and winter growing seasons under greenhouse conditions and how the interaction between SL and changes in ambient sunlight across growing seasons influences edible biomass, nutrient bioaccumulation, and changes in genetic expression. The tissue samples for all three experimental methods in this study were collected on the same day. Table 4.1 provides detailed growing parameters for each season, gathered through the use of greenhouse control sensors (PRIVA, Ontario, CA), WatchDog 2000 Series sensors (Spectrum Technologies, Aurora, IL, USA), and PS-200 Apogee Spectroradiometer (Apogee Instruments, Logan, UT, USA).

Light Treatments

This experiment evaluated the impact of discrete narrowband and broadband wavelength combinations from SL systems on fresh and dry mass, elemental nutrient composition, and transcriptome of basil. In this experiment, we utilized a Randomized Complete Block Design to establish the lighting treatments. Additionally, we switched the lighting treatments between growing seasons to factor in any potential shading effects caused by the greenhouse. Narrowband blue and red light-emitting diodes of (B/R LED) (Fluence Bioengineering, Austin, TX), Broadband White LEDs (Fluence Bioengineering, Austin, TX), and High-Pressure Sodium lamps (HPS) (Hortilux DE, Mentor OH) provided 8.64 $mol \cdot m^{-2} \cdot d^{-1}$ (equal intensity of 100 $\mu mol \cdot m^{-2} \cdot s^{-1}$ for 24 $h \cdot d^{-1}$) for each SL treatment, in addition to natural sunlight (Fig. 4.1). We created a control group for natural light (NL) control to study how both ambient sunlight and SL impacted plant primary metabolism. The intensity and spectral quality distribution were verified weekly after dark by taking an average of 5 measurements in a Z pattern that covered 1 m x 1 m across the treatment level, aligned with the canopy top. LED treatments were placed 1 m above the hydroponic system, and HPS lamps 1.5 m above hydroponic systems. The Fluence LED systems were made up of three bars (1 m in length) that alternated between blue and red lights. These bars could be adjusted for both spectral quality and intensity, and were designed to provide even lighting for an area of 1.2 m x 1.2 m. Dimmable HPS lamps were placed in targeted reflectors to reduce treatment bleed-over and allow for precise intensity control and uniformity across the 1.2 m x 1.2 m treatment areas. As crops grew, SL intensities were adjusted using dimmers to the target intensity (100 ± 2.5 $\mu mol \cdot m^{-2} \cdot s^{-1}$) four or five times per week (after dark) using a PS-200 Apogee Spectroradiometer (Apogee Instruments, Logan, UT, USA). The average ambient solar spectrum and the supplemental lighting spectra can be found in Figures 4.1 and 4.2, respectively.

To account for seasonal changes in light intensity, spectral quality, and temperature variation in the greenhouse, the lighting treatments were randomized after each experimental cycle. To reduce biological variance and improve statistical power, each measurement unit consisted of two plants. All data is presented on a per-plant basis, and each treatment is considered an experimental unit.

To prevent any interference between treatments, every SL treatment was physically separated. On average, there was a bleed-over of 1.1 ± 0.6 $\mu mol \cdot m^{-2} \cdot s^{-1}$ at the edges of the treatments. 1.2 m x 1.2 m sections of basil were grown, with 1.2 m separation between treatments (i.e., measurement edge-to-edge of hydroponic systems within the greenhouse). Tissue samples were only harvested from within the middle 0.6 m of each treatment to ensure further reduction of SL contamination between treatments (0.3 m around the edge of each treatment was considered the buffer zone and was not used for sampling). SL bleed-over was $<0.1\ \mu mol \cdot m^{-2} \cdot s^{-1}$ within the harvest zone of each treatment (i.e., below the instrumentation detection limit). Given that the bleed-over from SL treatment was not significant, physical barriers such as plastic sheets or boards were not used in the experiment. This was to avoid any negative effects they might have had, such as interacting with the sunlight intensity and DLI, reducing airflow, or creating isolated microclimates that could lead to air temperature variability. To avoid the possibility of DLI and air temperature variations within the greenhouse bay, the SL treatments were randomized between seasons.

Sample Harvest and Biomass Data Collection

The basil plants were harvested when they reached physiological vegetative maturity, which was about 45 days after seeding, and with 9-10 fully developed nodes. The tissue samples

were collected within a four-hour period by replication to ensure consistency across all samples from each growing season. We gathered biomass samples from a 0.6 m x 0.6 m harvest zone, with two plants per measurement unit, and six replicates per treatment. To improve statistical power and reduce the influence of biological variability, two plants were combined for each measurement unit; and all values and calculations presented were normalized (i.e., represented on a per-plant basis). Fresh mass (FM) and dry mass (DM) were determined using an analytical scale (Sartorius L310, Sartorius, Göttingen, Germany). To dry tissue samples, we used a forced air dryer (Heratherm OMH100 Drying Oven, Thermo Scientific, Waltham, MA, USA) at 50 ºC for 128 hours. Once the samples were dry, they were weighed and processed immediately. A summary of statistical results for experimental parameters can be found in Table 4.2, while biomass results are in Figures 4.3-4.6.

Mineral Extraction and Analysis

To determine changes in elemental nutrient tissue concentrations in basil plants across growing seasons and SL treatments, samples were analyzed for macro and micronutrient concentrations according to a method from Barickman et al. (2013). Air-dried samples were ground into a fine powder using a Magic Bullet blender (MBR1101, Homeland Housewares, Los Angeles, CA, USA). We dispensed 0.5 ± 0.01 grams of finely ground and homogenized plant material (<30 mesh) into sterile 15 mL plastic centrifuge test tubes. An Ethos 1112 microwave digestion unit (Milestone, Bergamo, Italy) was used to process the basil samples. Samples were microwaved for 30 min at 150 ºC, then cooled for an additional 30 min. A 9.9 mL of ICP matrix solution (2% nitric acid, 0.5% hydrochloric acid, 97.5% RO water) was placed into 15 mL sterile test tubes. A disposable 1 mL plastic pipette was used to add 0.1 mL of the acid-digested sample

mixture to the 9.9 mL ICP matrix solution. This mixture was then thoroughly shaken to ensure that the acid was uniformly distributed within the matrix. An Agilent 7500 Series Inductively Coupled Plasma Mass Spectrometer (ICP-MS) was used to determine nutrient concentrations of each tissue sample (Barickman et al., 2013). By using this technique, elemental tissue analysis determined the concentration of various elements, including N, P, K, Ca, S, Mg, B, Cu, Mn, Fe, and Zn (Tables 4.3-4.6).

Biomass and Nutrient Bioaccumulation Statistical Analyses

A randomized complete block design was used for this experiment. Lighting treatments were randomized after each experimental cycle to account for seasonal variations in NL intensity, spectral quality, and potential temperature variation within the greenhouse bay. Each measurement unit consisted of two plants to improve statistical power and reduce biological variance. Measurement units are presented on a per-plant basis for FM/DMs (g per plant) and nutrient tissue concentrations (percent fresh weight and ppm). Each treatment is considered an experimental unit. Six replicates (two plants each) were analyzed in each treatment (twelve plants, or six measurement units, per treatment within 0.6 m x 0.6 m harvest zone). Each experimental cycle was repeated across two growing seasons (two experimental cycles). Replicates (6) were nested within treatments (4), which were nested within growing seasons (2). Data sets were analyzed by GLIMMIX and Mixed Model Analysis of Variance procedures using the statistical software SAS (version 9.4, SAS Institute, Cary, NC, USA). Design and Analysis macro (DandA.sas; created by Arnold Saxton) was utilized in addition to Tukey's (protected) adjustment, regression analysis, and univariate/normalization procedures. Treatments and seasons were separated by honestly

significant difference (HSD) at α=0.05. Principal component analysis (PCA) was performed (Fig. 4.7) using JMP PRO 17 (SAS Institute, Cary, NC, USA).

RNA Extraction

Tissue samples were collected for RNA extraction at the same time as samples for other analyses. A leaf from the second and fourth fully expanded leaves from the tops of two basil plants was collected under the harvest zone of each treatment and immediately frozen with liquid nitrogen. Four replicates were analyzed in each treatment. Each experimental cycle was repeated across two growing seasons (two experimental cycles). Replicates (4) were nested within treatments (4), which were nested within growing seasons (2).

Samples were stored in -80 ºC until RNA extractions were conducted. Samples were ground to <30 mesh and homogenized immediately before RNA extraction using liquid nitrogen with a mortar and pestle. Total RNA was extracted from leaf samples using RNeasy Plant Mini RNA isolation kits (Qiagen, Hilden, Germany) according to the provided instructions. Quality and purification of total RNAs were determined before and after the addition of 50 µL Plant RNA Isolation Aid (ThermoFisher Scientific, Waltham, MA). Total RNA extracted from leaf tissue samples was shipped to Azenta Life Sciences (Burlington, MA, USA) for RNA-Seq library construction and sequencing.

Library Preparation with PolyA Selection and Illumina Sequencing

Details regarding library preparation and sequencing workflow can be found in Figure 4.8. RNA samples were quantified using Qubit 2.0 Fluorometer (Life Technologies, Carlsbad, CA,

USA), and RNA integrity was checked using Agilent TapeStation 4200 (Agilent Technologies, Palo Alto, CA, USA).

The RNA sequencing libraries were prepared using the NEBNext Ultra II RNA Library Prep Kit for Illumina using the manufacturer's instructions (New England Biolabs, Ipswich, MA, USA). Briefly, mRNAs were initially enriched with Oligod(T) beads. Enriched mRNAs were fragmented for 15 minutes at 94°C. First-strand and second-strand cDNA were subsequently synthesized. cDNA fragments were end-repaired and adenylated at 3'ends, and universal adapters were ligated to cDNA fragments, followed by index addition and library enrichment by PCR with limited cycles. The sequencing libraries were validated on the Agilent TapeStation (Agilent Technologies, Palo Alto, CA, USA), and quantified by using Qubit 2.0 Fluorometer (ThermoFisher Scientific, Waltham, MA, USA) as well as by quantitative PCR (KAPA Biosystems, Wilmington, MA, USA).

The sequencing libraries were clustered on three flowcell lanes. After clustering, the flowcell was loaded on the Illumina HiSeq instrument (4000 or equivalent) according to the manufacturer's instructions. The samples were sequenced using a 2x150bp Paired End (PE) configuration. Image analysis and base calling were conducted by the Control software. Raw sequence data (.bcl files) generated from the sequencer were converted into fastq files and de-multiplexed using Illumina's bcl2fastq 2.17 software. One mismatch was allowed for index sequence identification.

Transcriptome Analysis

Sequence reads were trimmed to remove possible adapter sequences and nucleotides with poor quality using Trimmomatic v.0.36. The trimmed reads were mapped to the *Ocimum basilicum*

reference genome (Gonda et al., 2020) available on ENSEMBL using the STAR aligner v.2.5.2b. The STAR aligner is a splice aligner that detects splice junctions and incorporates them to help align the entire read sequences. BAM files were generated because of this step. Unique gene hit counts were calculated from the Subread package v.1.5.2. The hit counts were summarized and reported using the gene_id feature in the annotation file. Only unique reads that fell within exon regions were counted.

After the extraction of gene hit counts, the gene hit counts table was used for downstream differential expression analysis. Using DESeq2, a comparison of gene expression between the customer-defined groups of samples was performed. The Wald test was used to generate *P*-values and log2 fold changes. Genes with an adjusted *P*-value < 0.05 and absolute log2 fold change > 1 were labeled significant for each comparison. Results of the differential gene expression analyses for all comparisons are shown in Table 4.6. To account for differences in sequencing amounts, the original values were normalized. The resulting normalized values were used to accurately identify differentially expressed genes. A gene ontology (GO) analysis was performed on the statistically significant set of genes by implementing the software GeneSCF. The analysis of GO and Kyoto Encyclopedia of Genes and Genomes (KEGG) pathways enrichment of differential expression genes (DEGs) were performed. GO and KEGG terms with corrected $P < 0.5$ and deemed significant were used in the comparative analyses between treatments.

Principle component analysis biplots were developed to reveal similarities within and between treatments, using the "plotPCA" function within the DESeq2 R package. The plot shows the samples in a 2D plane spanned by their first two principal components. The top 500 genes, selected by highest row variance, were used to generate the plots in figures 4.9-4.11. DEG biclustering heatmaps for each treatment SL comparison to the NL control were created to

visualize the expression profile of the top 30 genes sorted by their adjusted *P*-values (Figs. 4.12-4.14). Volcano plots for each SL comparison to NL control were created to show the global transcriptional change across seasons and replicates (Figs. 4.15-4.17).

Results

Fresh and Dry Mass

Our investigation into the effects of season and lighting treatment on total fresh and dry masses revealed significant influences from both factors. A one sentence paragraph. Suggest incorporating it into next paragraph. Seasonal changes, characterized by variations in ambient sunlight, had a pronounced impact on the fresh and dry masses samples. During the summer months, we recorded a fresh mass average of 57.8 g per plant, however, this value was only 30.8 g per plant during the winter months. (Fig. 4.3). The dry mass followed a similar pattern, with summer yield of 6.94 g per p ant and winter yield of 3.37 g per plant (Fig. 4.4).

Lighting treatment also significantly affected the fresh and dry masses of basil. The Broadband White treatment resulted in the highest fresh mass of 68.39 g per plant, while the lowest was 32.96 g per plant under the Natural Light (NL) control. Each lighting treatment resulted in statistically different fresh masses. Notably, the Narrowband (NB) Blue/Red treatment yielded about 10 g per plant FM less than the Broadband White (BW), and the HPS treatment yielded 42.64 g per plant, the lowest yield average among supplemental light (SL) treatments (Fig. 4.5).

The different lighting treatments had a similar pattern of dry mass production. All treatments were statistically distinct from each other. The Broadband White treatment yielded the highest dry mass at 7.54 g per plant, whereas the NL control produced the lowest at 4.25 g per plant. The Narrowband B/R treatment yielded about 1 g per plant on less on average than the

Broadband White treatment, and the HPS treatment's yield was more than the NL control but less than that of the B/R treatment (Fig. 4.6).

Elemental Nutrient Tissue Analysis

The influence of season on macronutrient mineral concentrations in hydroponically grown 'Genovese' basil was examined. Nitrogen (N) concentrations of plants were significantly greater in the summer months (5.37%) than in winter (4.98%) (Table 4.3). Phosphorus concentrations remained relatively stable across seasons with 0.92% in the summer and 0.89% in the winter. Potassium concentrations mirrored the trend of N, with a significant decrease from summer (5.69% of dry weight) to winter (4.68% of dry weight). Magnesium concentrations demonstrated an inverse trend compared to N and K. However, Mg concentrations were significantly higher in summer (0.70% of dry weight) than winter (0.73% of dry weight). Calcium dry weight concentrations also increased significantly from summer (3.06%) to winter (3.30%), Sulfur concentrations were relatively consistent from summer (0.46% of dry weight) to winter (0.44% of dry weight).

The influence of season on micronutrient mineral concentrations in 'Genovese' basil was also examined (Table 4.4). Boron concentrations were not significantly different between summer (79.40 ppm) and winter seasons (79.67 ppm). Zinc concentrations, however, were significantly lower in summer (88.24 ppm) than winter (84.54 ppm). Manganese concentrations had a similar trend to Zn, with a significant decrease from summer (183.38 ppm) to winter (168.00 ppm). Iron concentrations were also significantly lower in summer (150.86 ppm) than winter (131.07 ppm). Lastly, copper concentrations had similar trends to Zn, Mn, and Fe with 22.61 ppm in summer and 20.67 ppm in winter.

In addition to season, our study examined the influence of supplemental lighting treatments on macronutrient mineral concentrations of 'Genovese' basil (Table 4.5). Dry weight concentrations of N, P, K, and Ca varied significantly among SL treatments. Concentrations of N were the highest under the NL control (5.61%) and the lowest under Narrowband B/R LED (4.53%). The K concentrations had a were similar trend, with the highest concentration under NL control (5.57%) and the lowest under Narrowband B/R LED (4.44%). In contrast, the highest P dry weight concentration was under Narrowband B/R LED (1.00%) treatment and the lowest was under the NL control (0.79%). Dry weight Mg concentration was the highest under Narrowband B/R LED (0.71%) and lowest was under Broadband White LED (0.67%). Concentrations of Ca varied significantly, with the highest concentration under Narrowband B/R LED (3.48%) and the lowest under HPS (3.03%). Lastly, S dry weight concentrations were highest under Narrowband B/R LED (0.47%) and the lowest under NL control (0.38%).

The influence of supplemental lighting treatments on micronutrient mineral concentrations was also evaluated. B concentrations significantly varied among light treatments (Table 4.6). The highest B dry weight concentration occurred under the HPS treatment (91.08 ppm), while the lowest was under Narrowband B/R LED (63.17 ppm). Dry weight concentration of Cu was also highest under NL control (23.33 ppm), and the lowest under Narrowband B/R LED (19.33 ppm). Concentration of Fe also was highest under HPS treatment (151.75 ppm) and the lowest under Narrowband B/R LED (129.67 ppm) treatment. Interestingly, the Fe concentration under NL control was only slightly lower than that under HPS treatment. Concentration of Zn was highest under the NL control treatment (98.42 ppm), whereas Broadband White LED treatment had the lowest (81.83 ppm). Manganese concentrations had a similar trend, with the highest concentration under NL control (204.25 ppm) and the lowest under Broadband White LED (156.75 ppm).

Principal Component Analysis of Biomass and Tissue Nutrient Concentrations

Principal Component Analysis (PCA) of the data revealed distinct patterns and associations between light treatments, fresh/dry biomass (FM/DM), and nutrient concentrations (4.7). Principal components PC1 and PC3 accounted for a substantial portion of the variability in the data, 43.9% and 12.2%, respectively.

The PCA biplot distinctly segregated the four light treatments of Narrowband Blue/Red (B/R), Broadband White, High-Pressure Sodium (HPS), and Natural Light (NL) control into four quadrants, each representing a unique profile of biomass and nutrient bioaccumulation. The HPS treatment, represented by quadrant I showed strong correlations with FM/DMs and the nutrient S. The Broadband White LED treatment, represented by quadrant II exhibited positive linkages with Fe, N, Cu, B, and K. This may indicate that Broadband White lighting enhances the bioaccumulation of these nutrients. In Quadrant III, where the NL control treatment was located, significant associations with Zn, Mg, and Mn were observed. Lastly, Quadrant IV, which represented the Narrowband B/R treatment, had strong associations with P and Ca, indicating that treatment favored the accumulation of those nutrients.

An intriguing pattern was observed in the loading of PC1, which was positively associated with FM/DM and negatively associated with many of the individual nutrients. This inverse relationship may suggest a trade-off between biomass production and nutrient concentration under different light treatments (Fig. 4.7). Further, the nutrients were evenly distributed across PC3, indicating various levels of positive and negative loading for that component. This indicates the complex interactions between lighting and individual elemental nutrients, as well as synergisms/antagonisms among nutrient uptake and assimilation in hydroponically grown basil.

Transcriptome Analysis

We used RNA Seq and statistical analysis to determine which genes were important for controlling the primary metabolism of basil under different seasons and lighting treatments. By performing pairwise comparisons, a substantial number of differentially expressed genes (DEGs) were identified across both summer and winter growing seasons. In the growing season, 4207 DEGs were identified, while the winter growing season had a larger number with 13110 DEGs (Table 4.7).

Upon further analysis, the DEGs displayed distinct patterns of upregulation and downregulation when exposed to different light treatments during both summer and winter growing seasons. Among the summer growing season treatments, the Narrowband 20B/80R (NB) vs. Natural Light (NL) control comparison had the highest number of DEGs, with 3801 identified Table 4.7). This was followed by Broadband White (BW) vs. NL control with 278 DEGs, and High-Pressure Sodium (HPS) vs. NL control with the lowest number 128 (DEGs). In the winter growing season, NB vs. NL control had the highest number of 5578 DEGs, and the BW vs. NL control having nearly as many with 5609 DEGs. The HPS vs. NL control had the least number of DEGs (1923).

During the summer growing season, there were 2045, 132, and 34 upregulated DEGs in the comparisons of NB vs. NL control, BW vs. NL control, and HPS vs. NL control, respectively. However, during the winter growing season, there were even more upregulated DEGs in all comparisons (NB vs. NL control had 3505, BW vs. NL control had 3262, and HPS vs. NL control had 1228).

Downregulated DEGs also exhibited distinct patterns across the different light treatment comparisons. In the summer growing season, there were 1756, 146, and 94 downregulated DEGs

in the comparisons of NB vs. NL control, BW vs. NL control, and HPS vs. NL control, respectively. During the winter growing season, the number of downregulated DEGs increased, with 2073 for NB vs. NL control, 2347 for BW vs. NL control, and 695 for HPS vs. NL control (Table 4.7).

The total number of uniquely upregulated and downregulated DEGs varied across all comparisons. During the summer growing season, there were 2211 unique upregulated DEGs and 1996 unique downregulated DEGs (Table 4.7). Meanwhile, the winter growing season had a higher number of unique DEGs, with 7995 upregulated and 5515 downregulated. It's interesting to note that during the summer growing season, the NB vs. NL control comparison had the highest number of upregulated, downregulated, and total DEGs. In contrast, the HPS vs. NL control had the lowest number of upregulated, downregulated, and total DEGs. During the winter growing season, e the NB vs. NL control had the highest number of upregulated DEGs, but the BW vs. NL control had the highest number of downregulated and total DEGs. The HPS vs. NL control comparison consistently had the lowest number of upregulated, downregulated, and total DEGs for both growing seasons.

Principal Component Analysis of DEGs

To better understand the relationships between differentially expressed genes (DEGs), we utilized Principal Component Analysis (PCA) biplots. These biplots compared the effects of supplemental lighting treatments with different spectral qualities to the NL control. By projecting the data onto a reduced-dimensionality space represented by the first two principal components, we were able to interpret the inherent structure of the data.

Principal components analysis, revealed that PC1 accounted for 46% of the total variability and PC2 explained an additional 16%, contributing to a total variance of 62% for the comparison

between the impact of Narrowband 20B/80R supplemental lighting (NB) and natural light (NL) (Figure 4.9).

We noticed distinct clusters when comparing NB vs NL control in the PCA biplot. The NL control samples tended to cluster in quadrant IV (positive PC1 and negative PC2), while NB treatment samples formed a cluster (positive PC2) (Figure 4.9?). This indicated that the two lighting conditions had differing effects on the DEGs being studied, with genes having high loadings on PC1 and PC2 being the primary drivers of the differences. The clustering pattern suggested that the NB treatment may have resulted in higher expression levels for genes with positive loadings on PC2, while the NL control was linked to lower expression levels for these genes. Conversely, genes with negative loadings on PC2 may have shown the opposite trend, with the NL control exhibiting higher expression levels compared to the NB treatment. Along with the clear separation between the two groups along the PC2 axis, there was also some degree of separation along the PC1 axis. The NL control cluster in quadrant IV exhibited higher expression levels for genes with positive loadings on PC1 and lower expression levels for genes with positive loadings on PC2 compared to the rest of the NL group.

The effects of Broadband White supplemental lighting (BW) and natural light (NL) control on plant gene expression were compared (Figure 4.10). The first principal component (PC1) explained 67% of the total variability, while the second principal component (PC2) accounted for an additional 9%, cumulatively accounting for 76% of the total variance.

The results showed that the two lighting conditions had different effects on the genes studied. This can be seen in the separation of the positive PC1 and positive PC2 in quadrant I. The genes with high loadings on PC1 and PC2 drove these differences. The NL control group may have had higher expression levels for genes with positive loadings on PC1, and lower expression

levels for genes with positive loadings on PC2 compared to the BW treatment group. On the other hand, the genes with negative loadings on PC1 may have exhibited the opposite trend, with the BW treatment group having higher expression levels than the NL control group. Additionally, a subset of the NL control group showed higher expression levels for genes with positive loadings on PC1 and lower expression levels for genes with positive loadings on PC2 compared to the rest of the group. In the BW treatment group, there were samples of the negative PC1 space, indicating that some samples had gene expression profiles that differed from the NL control group due to the lack of shared negative PC1 attributes (Fig. 4.10).

The effects of HPS supplemental lighting and natural light (NL) control on plant gene expression were compared (Figure 4.11). The first principal component (PC1) explained 44% of the total variability, while the second principal component (PC2) accounted for an additional 18%, cumulatively accounting for 62% of the total variance.

The NL control samples tended to group together in the positive PC1 space (quadrants I and IV), while the HPS treatment samples were more spread along the PC1 axis. Two HPS treatment samples clustered in the positive PC1 space, and three samples clustered in the negative PC1 space (quadrants II and III). This suggested that the two lighting conditions had distinct effects on the DEGs studied, with the primary differences driven by the genes with high loadings on PC1 and PC2. Four NL control samples and two HPS treatment samples formed clusters in the positive PC1 space, which indicated similarities in their gene expression profiles, with higher expression levels for genes with positive loadings on PC1 and varying expression levels for those with positive.

Biclustering Heatmaps Comparing DEGs

We performed biclustering analysis on three sets of heat maps, each comparing the top 30 significantly differentially expressed genes (DEGs) between natural light (NL) control and various supplemental light treatments using RNA-seq data. Biclustering heat maps are a powerful tool for visualizing gene expression patterns across experimental conditions, as they enable simultaneous clustering of both genes and samples, revealing meaningful relationships between genes and their corresponding treatments.

Based on the heatmap and hierarchical clustering, eight clusters of DEGs that were visually distinct (Figure 4.12) for the NB treatment lighting conditions and the NL control. The NB treatment had opposing regulation than NL based on the heatmap clusters, indicating that they had different effects on gene expression. There was little difference in gene expression between summer and winter samples, which suggested that the observed DEGs were primarily caused by differences in lighting conditions and not seasonal variations. The top 30 individual genes with the highest significance showed low variability in expression across different samples within the same treatment type, which highlighted the consistent impact of the NB treatment on gene expression.

Figure 4.13 presents ten visually distinct clusters of DEGs based on the heatmap and hierarchical clustering. The NL control and BW treatment groups generally exhibited opposing regulation based on heatmap clusters, although not as distinct as the differences observed between NL and NB in Figure 4.12. This suggested that the BW treatment may have had a more moderate effect on gene expression compared to the NB treatment. Many of the clusters in Figure 4.13 had higher expression levels than those observed in the other two figures. Some variability in expression was observed across different samples, but among the top 30 individual genes with the

highest significance, there was still low variability in expression across different samples within the same treatment type.

There are six different groups of DEGs in Figure 4.14 that can be visually distinguished through the use of a heatmap and hierarchical clustering. Among these groups, the NL control and HPS treatment groups tended to have contrasting regulation patterns. However, these differences are not as noticeable as they were in the previous two figures. Compared to the NB vs. NL comparison in Figure 4.12, many of the clusters had moderate expression levels. Additionally, some differences in gene expression were found between summer and winter samples, suggesting that seasonal variations may have had a larger impact on this comparison. The top 30 individual genes with the highest significance showed a lot of variability in expression within the same treatment type, indicating that the HPS treatment may have resulted in more diverse gene expression profiles than other treatments.

Visual examination of Figures 4.12-4.14 revealed distinct patterns and trends in DEG regulation in response to different light treatments. The most notable observation was the opposing regulation of DEGs between the NL control and each of the supplemental light treatments, highlighting the impact of these lighting conditions on gene expression. The degree of distinction between the NL control and each supplemental light treatment varied, with the BW treatment, and finally the HPS treatment exhibiting the least distinct differences. This observation suggests that different light treatments may have varying effects on gene expression regulation, with the NB treatment potentially having the most significant impact.

Volcano Plots Comparing DEGs

We analyzed a set of three volcano plots to investigate the global transcriptional changes in basil plants subjected to different supplemental lighting treatments. Volcano plots provide a

visual representation of the relationship between fold change and statistical significance (adjusted *P*-value) for differentially expressed genes (DEGs), with each data point representing a gene. Upregulated genes are indicated by red dots (adjusted *P*-value < 0.05 and log2 fold change > 1), while downregulated genes are represented by blue dots (adjusted *P*-value < 0.05 and log2 fold change < -1).

The comparison between the NL control and NB treatment had the highest number of significantly upregulated and downregulated genes (Figure 4.15) compared to the other treatments. The plot is asymmetrical, with more upregulated genes than downregulated genes. The right side of the plot (upregulated genes) was wider and taller than left side (downregulated genes), indicating a higher density and wider spread of upregulated genes than downregulated genes. In the upregulated group, several genes showed extremely high statistical significance (adjusted *P*-value over 8), which is noteworthy compared to the other treatments. These results suggested that the NB LED supplemental light treatment had a significant impact on gene expression regulation, with a general trend towards upregulation of DEGs.

The BW treatment effects compared with the NL control showed a moderate number of highly significant upregulated and downregulated genes (Figure 4.16). The plot was somewhat symmetrical, but with a higher number of upregulated genes than downregulated genes. The upregulated genes side of the plot is wider and shorter, while the downregulated genes is narrower and taller. This indicated a higher density and wider spread of upregulated genes compared to downregulated genes. Some highly significant upregulated and downregulated genes (adjusted *P*-value higher than 8) were observed, distinguishing them from the other treatments. These results suggested that the BW supplemental light treatment also had a noticeable effect on gene expression regulation, with both upregulated and downregulated DEGs showing high statistical significance.

A comparison between the HPS treatment and NL control showed a moderate number of genes that were significantly upregulated and downregulated (Figure 4.17). There were more upregulated genes than downregulated genes, shown by upregulated gene sin the plot being slightly wider than the downregulated genes. This suggested that there was a wider spread and higher density of upregulated genes compared to downregulated genes. It is noted that there were no genes with an adjusted *P*-value higher than 8 (which is extremely significant), unlike the other two treatments. Additionally, Figure 4.17 had the lowest number of total DEGs compared to Figures 4.15 and 4.16. These findings suggested that when comparing treatments to the NL control, the NB and BW LED treatments had a higher number of statistically significant DEGs than the HPS treatment.

Distinct patterns and trends in DEG regulation in response to different supplemental light treatments were revealed in comparisons of Figures 4.15-4.17. The most striking observation was the difference in the number of highly significant upregulated and downregulated genes among the three SL light treatments. The NB vs. NL control treatment (Fig. 4.15) exhibited the highest number of DEGs, with a strong trend toward upregulation. In contrast, HPS treatment vs. NL control (Fig. 4.17) had the lowest number of total DEGs and lacked any extremely significant DEGs. The general patterns and trends indicated in Figures 4.15-4.17 suggested that different SL light treatments caused varying levels of gene expression regulation. Based on the volcano plots, the NB treatment appeared to have the most significant impact on gene expression, followed by the BW treatment, and finally, the HPS treatment.

Discussion

Influence of Season and Treatment on Biomass

The results of our study highlight the significant effects of both seasonal changes and lighting treatments on the fresh and dry masses of hydroponically grown basil. Seasonal changes, characterized by variations in ambient sunlight, were observed to significantly impact fresh and dry masses. Higher values were recorded during summer months compared to winter months. This was generally expected as summer months typically have higher DLIs and more favorable spectral qualities. The higher DLI during summer months likely provided more photosynthetically active radiation, leading to enhanced photosynthesis and, consequently, greater biomass accumulation (Rihan et al., 2022; Vastakaite-Kairiene et al., 2022). Conversely, the reduced DLI and less favorable spectral quality during winter would limit photosynthetic activity, resulting in lower biomass.

Lighting treatment also significantly influenced fresh and dry masses. Broadband White LEDs led to the highest fresh and dry masses, while the lowest was under the natural light control. Notably, Narrowband B/R LEDs yielded less biomass than Broadband White LEDs. These results can likely be explained by the differences in spectral quality between broadband and narrowband LEDs (Pinho et al., 2016). Broadband white LEDs provide a broad spectrum of light that closely mimics natural sunlight, potentially promoting higher rates of photosynthesis by stimulating multiple pigments and photoreceptors. On the other hand, B/R LEDs target specific pigments and photoreceptors, which could limit the overall photosynthetic efficiency due to the absence of other beneficial wavelengths within the spectrum, such as orange, yellow, and green.

Interestingly, in 24-hour low-intensity supplements, Broadband White LEDs performed better than other treatments in this study. One possible explanation could be that the continuous

provision of a broad spectrum of light enabled plants to sustain photosynthetic activity over a longer period, leading to greater biomass accumulation (Weaver et al., 2019; Boldt and Altland, 2022).

These findings highlight the importance of considering both the DLI and spectral quality when designing lighting strategies for controlled environment agriculture. However, further research is needed to fully understand the complex and species-dependent interactions between light and other environmental factors in influencing plant growth and development. Future studies could explore the effects of these factors on other aspects of plant physiology, such as nutrient uptake and secondary metabolite production.

Elemental Nutrient Tissue Analysis

Nutrient analysis showed that seasonal changes in sunlight and supplemental lighting treatments influenced macro- and micronutrient mineral concentrations in hydroponically grown 'Genovese' basil. The observed patterns in nutrient accumulation can be attributed to the variations in daily light integral (DLI) and spectral quality associated with each season, as well as the distinct spectral qualities offered by different lighting treatments.

Seasonal changes had a substantial impact on the accumulation of certain macronutrients. N and K concentrations decreased significantly in summer compared to winter, a trend that could be attributed to the lower DLI and altered spectral quality during the winter months. Conversely, Mg and Ca concentrations were higher in summer than in winter, suggesting these nutrients may have been more efficiently absorbed or utilized under conditions of lower light intensity or specific spectral qualities associated with winter (Samuoliene et al., 2019; Vaštakaitė-Kairienė et al., 2022a). The relatively stable P and S concentrations across seasons indicated these nutrients may be less influenced by changes in DLI and spectral quality, or other factors may be at play.

A similar pattern was observed for the micronutrients. Z, Mn, Fe, and Cu concentrations were significantly lower in summer than in winter. This suggests that these nutrients may have been more effectively taken up or incorporated into plant tissues under conditions of higher light intensity or particular light spectra present during summer. Boron concentrations, however, remained relatively stable across seasons, indicating its accumulation may be less dependent on light conditions.

When examining the influence of supplemental lighting treatments, it became evident that spectral quality plays a crucial role in nutrient accumulation. For instance, N and K concentrations were highest under the NL environment, which provided a full spectrum of sunlight, and lowest under the Narrowband B/R LED treatment, which offered a limited light spectrum targeting specific photoreceptors. This suggested that a broad spectrum of light, which stimulates multiple photoreceptors, may enhance the uptake or utilization of these nutrients.

Interestingly, P, Mg, Ca and S concentrations were highest under the Narrowband B/R LED treatment, indicating these wavelengths promoted the accumulation of these nutrients. This underscores the complexity of light-nutrient interactions and the potential for optimizing light spectra to enhance nutrient content in crops.

Micronutrient concentrations also varied significantly across the different lighting treatments. The highest concentrations of Z, Mn, and Cu were observed for plants under the NL control, again suggesting that a full spectrum of light may facilitate the absorption or incorporation of these nutrients. However, B and Fe concentrations were highest under the HPS treatment, indicating that the specific spectral quality provided by this light source may enhance the accumulation of these nutrients.

These findings corroborate previous research demonstrating that light conditions, including DLI and spectral quality, can significantly influence nutrient uptake and assimilation in plants (Pinho et al., 2016; Samuoliene et al., 2019; Hammock et al., 2020; Brazaityte et al., 2021; Vaštakaitė-Kairienė et al., 2022a; Vaštakaitė-Kairienė et al., 2022b). They also highlight the potential of manipulating light conditions to optimize nutrient content in crops, particularly in controlled environment agriculture where light can be precisely controlled. Future research should continue to explore these light-nutrient interactions, including the underlying physiological and molecular mechanisms, to further enhance our ability to produce nutritionally superior crops.

Principal Component Analysis of Biomass and Nutrient Analysis

The Principal Component Analysis (PCA) of our data revealed distinct patterns and associations of light treatments effects on fresh/dry biomass (FM/DM), and nutrient concentrations, underlining the complex interplay between light conditions and plant growth and nutrition. Principal components PC1 and PC3 accounted for a substantial portion of the variability in the data, demonstrating the significant influence of light conditions on these parameters.

The PCA biplot distinctly segregated the four light treatments into separate quadrants, each characterized by a unique profile of biomass and nutrient accumulation. This segregation is reflective of the impact of spectral quality on plant physiology, with different light spectra favoring the accumulation of specific nutrients and influencing biomass production.

The HPS treatment was strongly correlated with FM/DM and the nutrient. The Broadband White treatment showed a positive correlation with nutrients Fe, N, Cu, B, and K. This suggests that the broad spectrum provided by Broadband White LEDs enhances the uptake or utilization of these nutrients, leading to their increased accumulation. The NL control displayed a significant association with Zn, Mg, and Mn. This pattern suggested that natural light, with its full spectrum,

may enhance the absorption or incorporation of these nutrients. In contrast, the PCA biplot showed the Narrowband B/R treatment was correlated with P and Ca.

Interestingly, PC1 was positively associated with FM/DM but negatively associated with many of the individual nutrients. This inverse relationship suggests a trade-off between biomass production and nutrient concentration under different light treatments. It could be speculated that under certain light conditions, plants prioritize biomass production and have reduced concentrations of certain nutrients. Alternatively, it could reflect dilution effects, where increased biomass results in a decreased nutrient concentration relative to the total plant biomass.

These findings highlight the potential of manipulating light conditions to optimize both biomass production and nutrient content in crops, particularly in controlled environment agriculture. However, they also underscore the complexity of these interactions and the need for further research to understand the underlying mechanisms fully and to develop effective lighting strategies that balance the need for high yield and nutritional quality.

Transcriptome Analysis

RNA sequencing and transcriptomic analyses were used to investigate the impact of SL and ambient spectra on the regulation of primary metabolism of basil. Our results revealed a significant number of differentially expressed genes (DEGs) across both summer and winter growing seasons, with distinct patterns of upregulation and downregulation observed with different light treatments.

The substantial difference in the number of DEGs identified between the summer and winter growing seasons (4207 vs. 13110, respectively) suggests that the spectral quality and DLI of ambient sunlight significantly influence gene expression and primary metabolism regulation.

During both summer and winter, the Narrowband 20B/80R (NB) treatment had the highest number of DEGs compared to other supplemental lighting treatments, indicating a more pronounced effect on gene expression. In contrast, the High-Pressure Sodium treatment exhibited the lowest number of DEGs, suggesting a lesser impact on gene expression.

Principal Component Analysis of DEGs

The principal component analysis (PCA) biplots provided a valuable visualization of the inherent structure and relationships among differentially expressed genes (DEGs) in our multidimensional dataset, comparing SL treatments of different spectral qualities with the natural light (NL) control. Figures 4.9, 4.10, and 4.11 illustrate the PCA biplots comparing the effects of Narrowband 20B/80R (NB), Broadband White (BW), and High Pressure Sodium (HPS) supplemental (SL) treatments to the natural light (NL) control group on plant gene expression. The clustering patterns observed in these biplots suggest that the different lighting treatments impact gene expression in distinct ways, leading to variations in primary metabolism and nutrient bioaccumulation. For instance, the separation between the NB treatment and NL control along the PC2 axis in Figure 4.6 suggest that the NB treatment may have led to higher expression levels for genes with positive loadings on PC2, while the NL control was associated with lower expression levels for these genes. This observation indicates that the targeted wavelengths provided by the NB treatment, which primarily consists of blue and red light, may impact specific photoreceptors and primary metabolic pathways.

The BW treatment samples formed clusters in Figure 4.10, suggesting higher expression levels for the genes with positive loadings on both PC1 and PC2 compared to the NL control. Broadband White light has been shown to promote the synthesis of certain primary metabolites

due to its ability to provide a more balanced spectrum of light that closely resembles sunlight (Li & Kubota, 2017). This finding implies that the BW treatment may have a positive impact on primary metabolism and nutrient uptake by stimulating gene expression.

The HPS treatment samples in Figure 4.11 exhibited wide variance along both the PC1 and PC2 axes, indicating that the HPS treatment led to a more diverse range of gene expression profiles compared to the NL control group. High Pressure Sodium lighting has been widely used in horticulture, but its predominantly red and orange wavelengths may have a limited impact on primary metabolism and nutrient uptake due to the lack of blue light. The wide variance observed in the HPS-treated samples may suggest that this treatment group has a broader array of primary metabolite production, potentially leading to varying effects on nutrient bioaccumulation.

One notable pattern observed in the PCA biplots was the tendency for the NL control samples to generally cluster in the positive PC1 and negative PC2 space, while the treatment samples formed clusters in other PCA biplot zones. This separation suggests that the specific wavelengths provided by the SL treatments may differentially impact specific photoreceptors and primary metabolic pathways. The clustering patterns observed in these biplots suggest that the different lighting treatments impact gene expression in distinct ways, leading to variations in primary metabolic gene expression.

Variation across PCA biplots demonstrates that different spectral qualities of supplemental lighting treatments significantly impact gene expression in plants, which in turn influences primary metabolism and nutrient uptake.

Biclustering Heat Maps and Volcano Plots

Our findings revealed distinct patterns and trends in differentially expressed genes (DEGs) regulation in response to various light treatments. The most notable observation is the opposing

regulation of DEGs between the NL control and each of the supplemental light treatments (NB, BW, and HPS), highlighting the impact of these SL lighting conditions on gene expression. The degree of distinction between the NL control and each supplemental light treatment varies, with the NB treatment showing the most pronounced differences (Fig. 4.9), followed by the BW treatment (Fig. 4.10), and finally, the HPS treatment exhibiting the least distinct differences (Fig. 4.11). This observation suggests that different light treatments may have varying effects on gene expression regulation, with the NB treatment potentially having the most significant impact.

NL control vs. NB treatment had the most substantial effect on gene expression compared to the other treatments. The intensity of expression (significance) of the top 30 genes is moderate compared to BW, likely because the NB treatment influenced a wider range of the genome.

Compared to the NB treatment, the NL control vs. BW treatment displayed a more moderate effect on gene expression. This observation could be attributed to the presence of all wavelengths in the white light spectrum, resulting in a more balanced regulation of plant growth and development. Moreover, Broadband White light, as well as targeted wavelengths within Broadband White light, have been reported to promote primary metabolism in some plant species.

The least distinct differences were observed with the NL control vs. HPS treatment comparison. This finding may be attributed to the fact that HPS light contains mostly orange and red wavelengths, which are known to influence photosynthesis and plant biomass production primarily. However, HPS light lacks the blue wavelength, which plays a crucial role in primary metabolism regulation. Our analysis also revealed that seasonal variations played a more significant role in the NL control vs. HPS treatment comparison, indicating that environmental factors may also influence gene expression.

Volcano plots confirm these distinct patterns and trends in differentially expressed genes (DEGs), the most notable observation being the opposing regulation of DEGs between the NL control and each of the supplemental light treatments (NB, BW, and HPS). This highlighted the impact of these SL lighting conditions on gene expression. The degree of distinction between the NL control and each supplemental light treatment varied, with the NB treatment showing the most pronounced differences, followed by the BW treatment, and finally, the HPS treatment exhibiting the least distinct differences.

It is clear that the development of species-specific CEA lighting optimization/lighting regimes holds great promise for enhancing crop production and quality. By tailoring light conditions to suit the specific needs of each crop, it may be possible to optimize not just biomass and nutrient quality, but also other critical parameters like taste, aroma, texture, and postharvest shelf life. Such advancements could have far-reaching implications for the CEA industry, improving crop yields and quality while reducing energy costs and environmental impact.

Conclusions

Our study provides compelling evidence that the spectral quality of supplemental lighting (SL) significantly influences primary metabolism, biomass accumulation, and nutrient uptake in hydroponically grown basil. The use of narrowband blue/red (B/R) and Broadband White LEDs resulted in a noticeable increase in fresh mass (FM) and dry mass (DM) compared to natural light (NL) control, underlining the potential of SL for enhancing crop yield in controlled environment agriculture (CEA). Furthermore, our findings demonstrate that different SL treatments can favor the accumulation of specific nutrients, with B/R treatment associated with increased tissue concentrations of Ca and the Broadband White treatment linked to increased N, K, Bo, and Cu.

These results reflect the profound influence of light spectral quality on plant nutrient uptake and assimilation. Importantly, our RNA-seq analysis revealed many differentially expressed genes (DEGs) across treatments, including several involved in primary metabolic functions, suggesting that changes in gene expression under different light conditions can directly impact yield and nutrient content.

This study sets the stage for more extensive research integrating analytic and transcriptomic analyses of high-value specialty crops to further elucidate the complex interactions between light and plant physiology. By deepening our understanding of how plants respond to different light spectra at the molecular level, we can leverage this knowledge to design more effective lighting strategies for CEA. Such strategies could optimize not only yield but also nutritional value, offering significant benefits for greenhouse production. Future studies should explore the effects of light spectral quality on other aspects of plant physiology, such as secondary metabolite production and postharvest shelf life, to fully harness the potential of light manipulation for enhancing crop quality and sustainability.

References

Ashraf, M., and Harris, P.J.C. (2013). Photosynthesis under stressful environments: An overview. *Photosynthetica* 51(2)**,** 163-190. doi: 10.1007/s11099-013-0021-6.

Barickman, T.C., Kopsell, D.A., and Sams, C.E. (2013). Selenium influences glucosinolate and isothiocyanates and increases sulfur uptake in Arabidopsis thaliana and rapid-cycling Brassica oleracea. *J Agric Food Chem* 61(1)**,** 202-209. doi: 10.1021/jf3037227.

Baumbauer, D.A., Schmidt, C.B., and Burgess, M.H. (2019). Leaf Lettuce Yield Is More Sensitive to Low Daily Light Integral than Kale and Spinach. *HortScience* 54(12)**,** 2159-2162. doi: 10.21273/hortsci14288-19.

Bilger, W., Bjorkman, O., and Thayer, S.S. (1989). Light-induced spectral absorbance changes in relation to photosynthesis and the epoxidation state of xanthophyll cycle components in cotton leaves. *Plant Physiol* 91(2)**,** 542-551. doi: 10.1104/pp.91.2.542.

Boldt, J.K., and Altland, J.E. (2022). Comparison of supplemental lighting from high-pressure sodium lamps or light-emitting diodes on morphology and nutrient uptake of greenhouse crops. *Acta Horticulturae* (1337)**,** 313-322. doi: 10.17660/ActaHortic.2022.1337.42.

Brazaityte, A., Miliauskiene, J., Vastakaite-Kairiene, V., Sutuliene, R., Lauzike, K., Duchovskis, P., et al. (2021). Effect of Different Ratios of Blue and Red LED Light on Brassicaceae Microgreens under a Controlled Environment. *Plants (Basel)* 10(4)**,** 801. doi: 10.3390/plants10040801.

Sager, J., O. Smith, W., L. Edwards, J., and L. Cyr, K. (1988). Photosynthetic Efficiency and Phytochrome Photoequilibria Determination Using Spectral Data. *Transactions of the ASAE* 31(6)**,** 1882-1889. doi: https://doi.org/10.13031/2013.30952.

Chaves, I., Pokorny, R., Byrdin, M., Hoang, N., Ritz, T., Brettel, K., et al. (2011). The cryptochromes: blue light photoreceptors in plants and animals. *Annu Rev Plant Biol* 62**,** 335-364. doi: 10.1146/annurev-arplant-042110-103759.

Currey, C.J., Kopsell, D.A., Mattson, N.S., Craver, J.K., Lopez, R.G., Erwin, J.E., et al. (2017). "Supplemental and sole source lighting of leafy greens, herbs, and microgreens", in: *Light management in controlled environments.* (eds.) R. Lopez & E. Runkle. (Meister Media Worldwide, Willoughby, OH).

Darko, E., Heydarizadeh, P., Schoefs, B., and Sabzalian, M.R. (2014). Photosynthesis under artificial light: the shift in primary and secondary metabolism. *Philos Trans R Soc Lond B Biol Sci* 369(1640)**,** 20130243. doi: 10.1098/rstb.2013.0243.

Engler, N., and Krarti, M. (2021). Review of energy efficiency in controlled environment agriculture. *Renewable and Sustainable Energy Reviews* 141**,** 110786. doi: 10.1016/j.rser.2021.110786.

Folta, K.M., and Carvalho, S.D. (2015). Photoreceptors and Control of Horticultural Plant Traits. *HortScience* 50(9)**,** 1274-1280. doi: 10.21273/hortsci.50.9.1274.

Fraikin, G.Y., Strakhovskaya, M.G., and Rubin, A.B. (2013). Biological photoreceptors of light-dependent regulatory processes. *Biochemistry (Mosc)* 78(11)**,** 1238-1253. doi: 10.1134/S0006297913110047.

Galvao, V.C., and Fankhauser, C. (2015). Sensing the light environment in plants: photoreceptors and early signaling steps. *Curr Opin Neurobiol* 34**,** 46-53. doi: 10.1016/j.conb.2015.01.013.

Gómez, C., and Mitchell, C.A. (2015). Growth responses of tomato seedlings to different spectra of supplemental lighting. *HortScience* 50**,** 112-118.

Gonda, I., Faigenboim, A., Adler, C., Milavski, R., Karp, M.J., Shachter, A., et al. (2020). The genome sequence of tetraploid sweet basil, *Ocimum basilicum* L., provides tools for advanced genome editing and molecular breeding. *DNA Res* 27(5). doi: 10.1093/dnares/dsaa027.

Hammock, H.A., Kopsell, D.A., and Sams, C.E. (2020). Supplementary Blue and Red LED Narrowband Wavelengths Improve Biomass Yield and Nutrient Uptake in Hydroponically Grown Basil. *HortScience* 55(12)**,** 1888-1897. doi: 10.21273/hortsci15267-20.

Jayalath, T.C., and van Iersel, M.W. (2021). Canopy Size and Light Use Efficiency Explain Growth Differences between Lettuce and Mizuna in Vertical Farms. *Plants (Basel)* 10(4). doi: 10.3390/plants10040704.

Kyriacou, M.C., El-Nakhel, C., Pannico, A., Graziani, G., Soteriou, G.A., Giordano, M., et al. (2019). Genotype-Specific Modulatory Effects of Select Spectral Bandwidths on the Nutritive and Phytochemical Composition of Microgreens. *Front Plant Sci* 10**,** 1501. doi: 10.3389/fpls.2019.01501.

Massa, G.D., Kim, H.H., Wheeler, R.M., and Mitchell, C.A. (2008). Plant Productivity in Response to LED Lighting. *Hortscience* 43(7)**,** 1951-1956.

McCree, K.J. (1972). The action spectrum, absorptance and quantum yield of photosynthesis in crop plants. *Agricultural Meteorology* 9**,** 191-216. doi: 10.1016/0002-1571(71)90022-7.

Morrow, R.C. (2008). LED Lighting in Horticulture. *HortScience* 43(7)**,** 1947-1950. doi: 10.21273/hortsci.43.7.1947.

Ouzounis, T., Rosenqvist, E., and Ottosen, C.O. (2015). Spectral Effects of Artificial Light on Plant Physiology and Secondary Metabolism: A Review. *Hortscience* 50(8)**,** 1128-1135.

Pinho, P., Jokinen, K., and Halonen, L. (2016). The influence of the LED light spectrum on the growth and nutrient uptake of hydroponically grown lettuce. *Lighting Research & Technology* 49(7)**,** 866-881. doi: 10.1177/1477153516642269.

Randall, W.C., and Lopez, R.G. (2014). Comparison of Supplemental Lighting from High-pressure Sodium Lamps and Light-emitting Diodes during Bedding Plant Seedling Production. *HortScience* 49(5)**,** 589-595. doi: 10.21273/hortsci.49.5.589.

Rihan, H.Z., Aljafer, N., Jbara, M., McCallum, L., Lengger, S., and Fuller, M.P. (2022). The Impact of LED Lighting Spectra in a Plant Factory on the Growth, Physiological Traits and

Essential Oil Content of Lemon Balm (Melissa officinalis). *Plants (Basel)* 11(3). doi: 10.3390/plants11030342.

Rockwell, N.C., Su, Y.S., and Lagarias, J.C. (2006). Phytochrome structure and signaling mechanisms. *Annu Rev Plant Biol* 57**,** 837-858. doi: 10.1146/annurev.arplant.56.032604.144208.

Samuoliene, G., Brazaityte, A., Virsile, A., Miliauskiene, J., Vastakaite-Kairiene, V., and Duchovskis, P. (2019). Nutrient Levels in Brassicaceae Microgreens Increase Under Tailored Light-Emitting Diode Spectra. *Front Plant Sci* 10**,** 1475. doi: 10.3389/fpls.2019.01475.

Singh, D., Basu, C., Meinhardt-Wollweber, M., and Roth, B. (2015). LEDs for energy efficient greenhouse lighting. *Renewable and Sustainable Energy Reviews* 49**,** 139-147. doi: 10.1016/j.rser.2015.04.117.

Tabbert, J.M., Schulz, H., and Krahmer, A. (2021). Increased Plant Quality, Greenhouse Productivity and Energy Efficiency with Broad-Spectrum LED Systems: A Case Study for Thyme (Thymus vulgaris L.). *Plants (Basel)* 10(5). doi: 10.3390/plants10050960.

Thoma, F., Somborn-Schulz, A., Schlehuber, D., Keuter, V., and Deerberg, G. (2020). Effects of Light on Secondary Metabolites in Selected Leafy Greens: A Review. *Front Plant Sci* 11**,** 497. doi: 10.3389/fpls.2020.00497.

Vaštakaitė-Kairienė, V., Brazaitytė, A., Miliauskienė, J., and Runkle, E.S. (2022a). Red to Blue Light Ratio and Iron Nutrition Influence Growth, Metabolic Response, and Mineral Nutrients of Spinach Grown Indoors. *Sustainability* 14(19). doi: 10.3390/su141912564.

Vaštakaitė-Kairienė, V., Brazaitytė, A., Miliauskienė, J., Sutulienė, R., Laužikė, K., Viršilė, A., et al. (2022b). Photon Distribution of Sole-Source Lighting Affects the Mineral Nutrient Content of Microgreens. *Agriculture* 12(8). doi: 10.3390/agriculture12081086.

Vastakaite-Kairiene, V., Samuoliene, G., Sveikauskas, V., Lauzike, K., and Jurkoniene, S. (2022). The Influence of End-of-Day Blue Light on the Growth, Photosynthetic, and Metabolic Parameters of Lettuce at Different Development Stages. *Plants (Basel)* 11(20). doi: 10.3390/plants11202798.

Weaver, G.M., van Iersel, M.W., and Velni, J.M. (2019). A photochemistry-based method for optimising greenhouse supplemental light intensity. *Biosystems Engineering* 182**,** 123-137. doi: 10.1016/j.biosystemseng.2019.03.008.

Zhen, S., and Bugbee, B. (2020). Far-red photons have equivalent efficiency to traditional photosynthetic photons: Implications for redefining photosynthetically active radiation. *Plant Cell Environ* 43(5)**,** 1259-1272. doi: 10.1111/pce.13730.

Appendix D

Table 4.1. Important environmental parameters across growing cycles. All crops grown under greenhouse conditions at The University of Tennessee Institute of Agriculture (UTIA) in Knoxville, TN, USA (35°56'44.5"N, 83°56'17.3"W).

	Summer	**Winter**
Growing Period	7/7/21-8/23/21	12/21/21-02/08/22
Average Day Temp (°C)	28.9	27.1
Average Night Temp (°C)	21.6	20.7
Average Relative Humidity	55%	50%
Average Daily Light Integral (DLI) ($mol \cdot m^{-2} \cdot d^{-1}$)	13.21	7.11
Average Day Length (hours)	13:41	9:50

Table 4.2. Summary of statistical results for pertinent experimental parameters.

	F Value			Pr > F		
Experimental Parameter	Season	Treatment	Season*Treatment	Season	Treatment	Season*Treatment
Fresh Mass	137.33	62.23	9.62	≤0.0001	≤0.0001	0.1235
Dry Mass	68.21	144.21	7.89	≤0.0001	≤0.0001	0.2621
Nitrogen	36.58	11.79	2.47	≤0.0001	≤0.0001	0.0082
Phosphorous	3.68	9.74	2.34	0.0575	≤0.0001	0.0123
Potassium	143.12	9.92	2.67	≤0.0001	≤0.0001	0.0044
Magnesium	6.60	9.82	2.07	0.0115	≤0.0001	0.0278
Calcium	37.85	5.42	1.57	≤0.0001	≤0.0001	0.1155
Sulfur	2.32	4.66	1.77	0.1301	≤0.0001	0.0677
Boron	0.04	10.11	2.39	0.8482	≤0.0001	0.0104
Zinc	4.01	9.11	1.16	0.0475	≤0.0001	0.3201
Manganese	15.51	9.00	1.74	0.0001	≤0.0001	0.0732
Iron	43.40	8.46	2.57	≤0.0001	≤0.0001	0.0060
Copper	21.32	3.23	1.75	≤0.0001	0.0007	0.0707

Table 4.3. Influence of season on macronutrient mineral dry weight concentrations of hydroponically grown 'Genovese' basil (*Ocimum basilicum* var. 'Genovese').

Season	N (%)	P (%)	K (%)	Mg (%)	Ca (%)	S (%)
Summer	5.37[a]	0.92[a]	5.69[a]	0.70[b]	3.06[b]	0.46[a]
Winter	4.98[b]	0.89[a]	4.68[b]	0.73[a]	3.30[a]	0.44[a]

*All concentrations are presented in percent of dry weight (%). Mean values represent 2 plants per replication and 6 replications per treatment. Values were analyzed using Tukey's (protected) HSD, and those followed by the same letter are not significantly different (α=0.05).

Table 4.4. Influence of season on micronutrient mineral dry weight concentrations of hydroponically grown 'Genovese' basil (*Ocimum basilicum* var. 'Genovese').

Season	B (ppm)	Zn (ppm)	Mn (ppm)	Fe (ppm)	Cu (ppm)
Summer	79.40[a]	88.24[a]	183.38[a]	150.86[a]	22.61[a]
Winter	79.67[a]	84.54[b]	168.00[b]	131.07[b]	20.67[b]

*All concentrations are presented in parts per million (ppm). Mean values represent 2 plants per replication and 6 replications per treatment. Values were analyzed using Tukey's (protected) HSD, and those followed by the same letter are not significantly different (α=0.05).

Table 4.5. Influence of supplemental lighting treatments on macronutrient dry weight concentrations of hydroponically grown 'Genovese' basil (*Ocimum basilicum* var. 'Genovese'). A total of four light treatments were added immediately after seedling transplant: Narrowband B/R LED, Broadband White LED, high pressure sodium, and non-supplemented natural light (NL) control.

Light Treatment	N (%)	P (%)	K (%)	Mg (%)	Ca (%)	S (%)
Narrowband B/R	4.53^{d}	1.00^{a}	4.44^{d}	0.71^{a}	3.48^{a}	0.47^{a}
Broadband White	4.94^{cd}	0.92^{ab}	5.03^{bc}	0.66^{b}	3.10^{bc}	0.45^{a}
HPS	5.40^{ab}	0.92^{bc}	5.45^{ab}	0.67^{ab}	3.03^{cd}	0.44^{ab}
NL Control	5.61^{a}	0.79^{d}	5.57^{a}	0.67^{ab}	3.10^{bc}	0.38^{b}

*All concentrations are presented in percent of dry weight (%). Mean values represent 2 plants per replication and 6 replications per treatment. Values were analyzed using Tukey's (protected) HSD, and those followed by the same letter are not significantly different (α=0.05).

Table 4.6. Influence of supplemental lighting treatments on micronutrient mineral concentrations of hydroponically grown 'Genovese' basil (*Ocimum basilicum* var. 'Genovese'). A total of four light treatments were added immediately after seedling transplant: Narrowband B/R LED, Broadband White LED, high pressure sodium, and non-supplemented natural light (NL) control.

Light Treatment	B (ppm)	Zn (ppm)	Mn (ppm)	Fe (ppm)	Cu (ppm)
Narrowband B/R	63.17^{e}	85.08^{abc}	172.92^{bc}	129.67b	19.33^{c}
Broadband White	71.00^{cd}	81.83^{cd}	156.75^{cd}	142.00^{ab}	21.75^{abc}
HPS	91.08^{a}	91.92^{bc}	183.83^{abc}	151.75^{a}	23.00^{ab}
NL Control	77.75^{bc}	98.42^{ab}	204.25^{ab}	146.25^{ab}	23.33^{a}

*All concentrations are presented in parts per million (ppm). Mean values represent 2 plants per replication and 6 replications per treatment. Values were analyzed using Tukey's (protected) HSD, and those followed by the same letter are not significantly different (α=0.05).

Table 4.7. Differentially expressed genes (DEGs) based on comparisons between supplemental lighting treatment and natural light (NL) control.

	Summer			Winter		
DEG Comparison	**Upregulated**	**Downregulated**	**Total DEGs**	**Upregulated**	**Downregulated**	**Total DEGs**
Narrowband 20B/80R vs. NL Control	2045	1756	3801	3505	2073	5578
Broadband White vs. NL Control	132	146	278	3262	2347	5609
High Pressure Sodium vs. NL Control	34	94	128	1228	695	1923

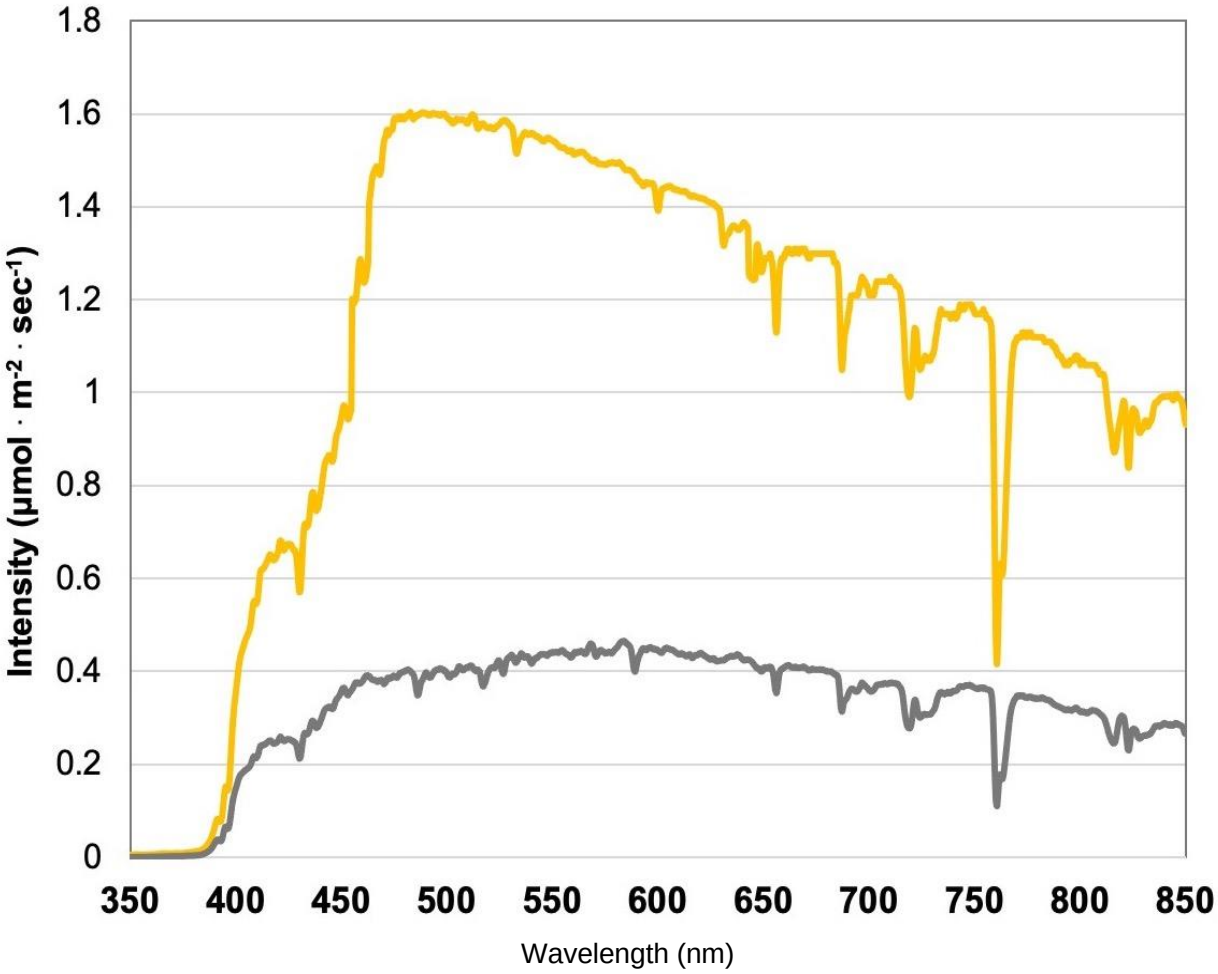

Figure 4.1. Natural light (NL) spectra under greenhouse glass, averaged across all four growing seasons, ranging from 350 nm to 850 nm. Values were taken at solar noon with three replicates for full sun (yellow) and overcast (gray) for each experimental run.

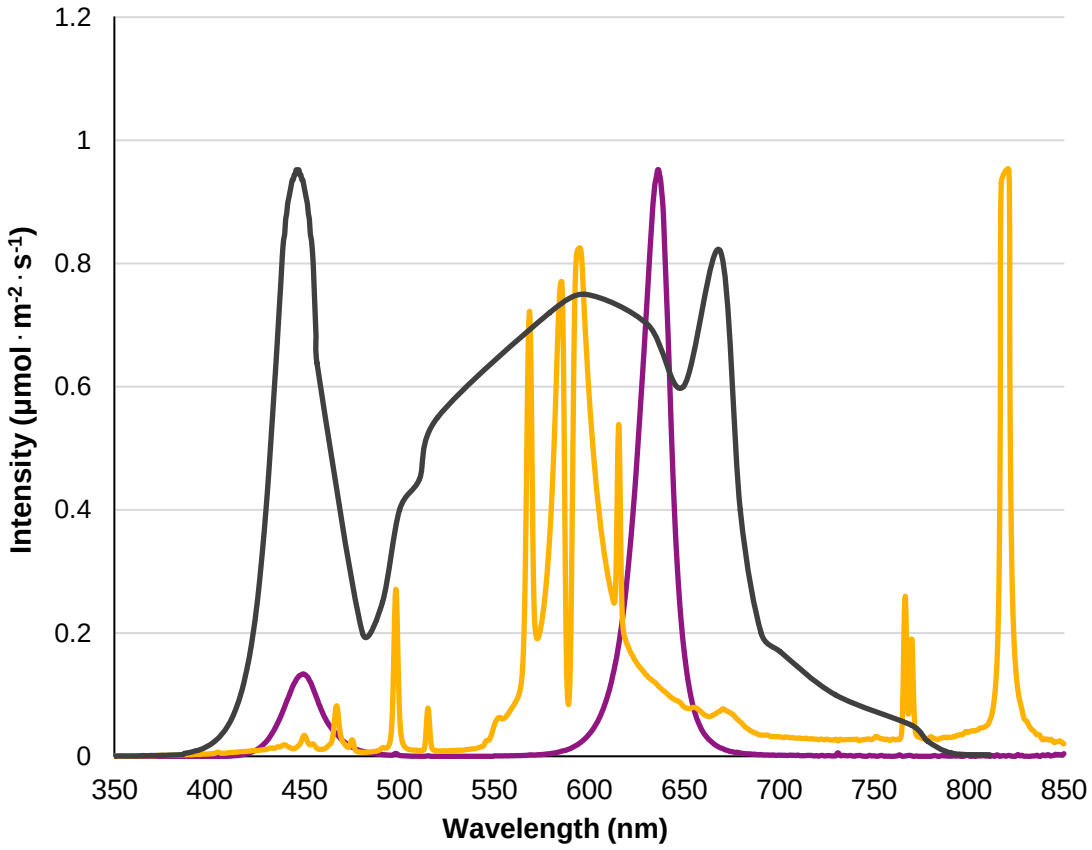

Figure 4.2. Emission spectra of supplemental lighting (SL) treatments from 300 nm to 850 nm: (1) Narrowband 20B/80R LED (purple), (2) Broadband White LEDs (grey), and (3) High Pressure Sodium (yellow). All SL treatments provided 8.64 mol•m^{-2}•d^{-1} (continuous 100 µmol•m^{-2}•s^{-1}; 24 h•d^{-1}). All lighting treatments were measured with a PS-200 Apogee Spectroradiometer to confirm intensity of specific treatment wavelengths throughout each growing season. Readings were taken at midnight in order to exclude underlying natural solar spectra.

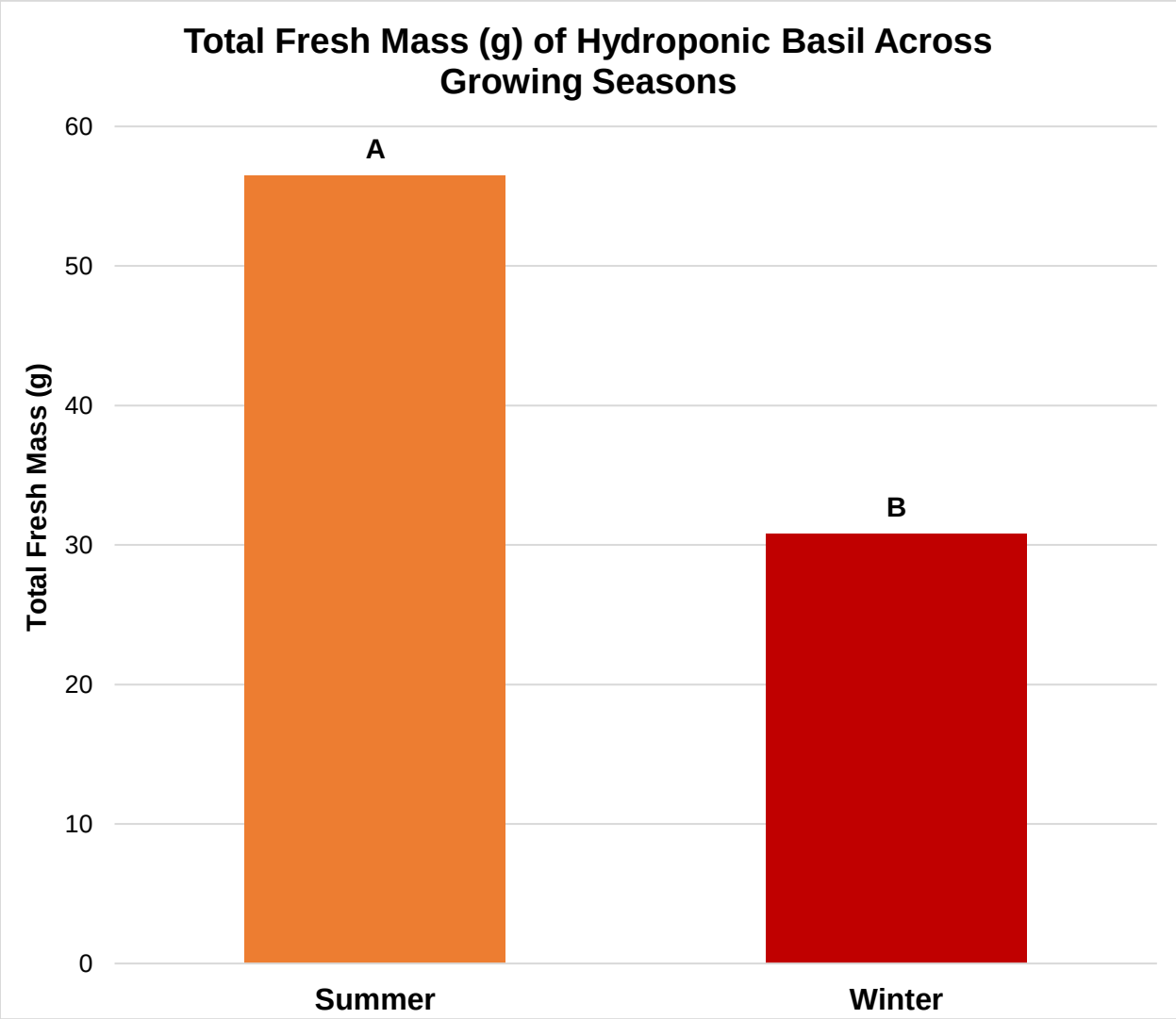

Figure 4.3. Influence of growing season on total fresh mass of hydroponically grown 'Genovese' basil (*Ocimum basilicum* var. 'Genovese'). All weights are presented in grams (g). Mean values represent 2 plants per replication and 6 replications per treatment across each season. Values were analyzed using Tukey's (protected) HSD, and those followed by the same letter are not significantly different (α=0.05).

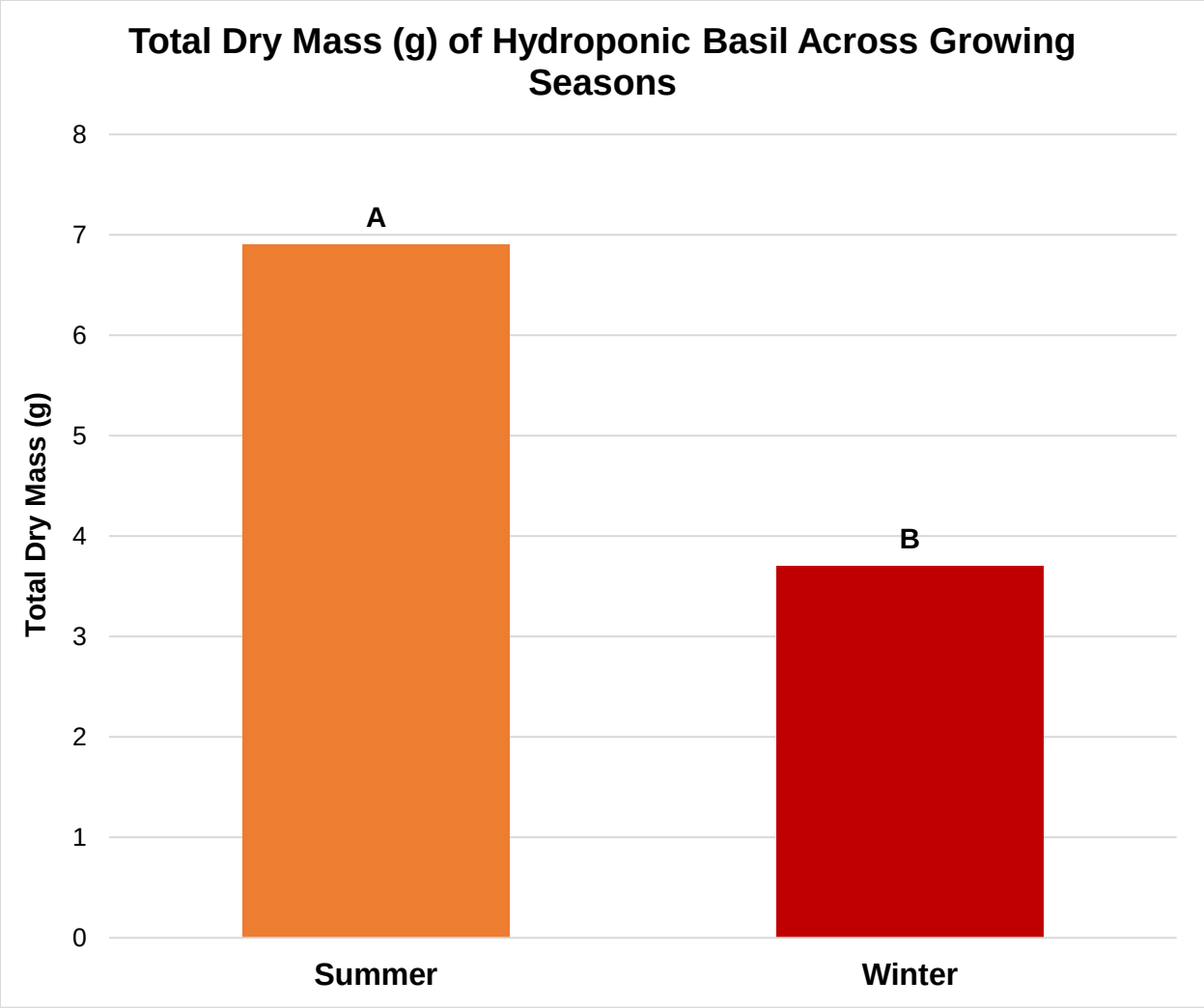

Figure 4.4. Influence of growing season on total dry mass of hydroponically grown 'Genovese' basil (*Ocimum basilicum* var. 'Genovese'). All weights are presented in grams (g). Mean values represent 2 plants per replication and 6 replications per treatment across each season. Values were analyzed using Tukey's (protected) HSD, and those followed by the same letter are not significantly different (α=0.05).

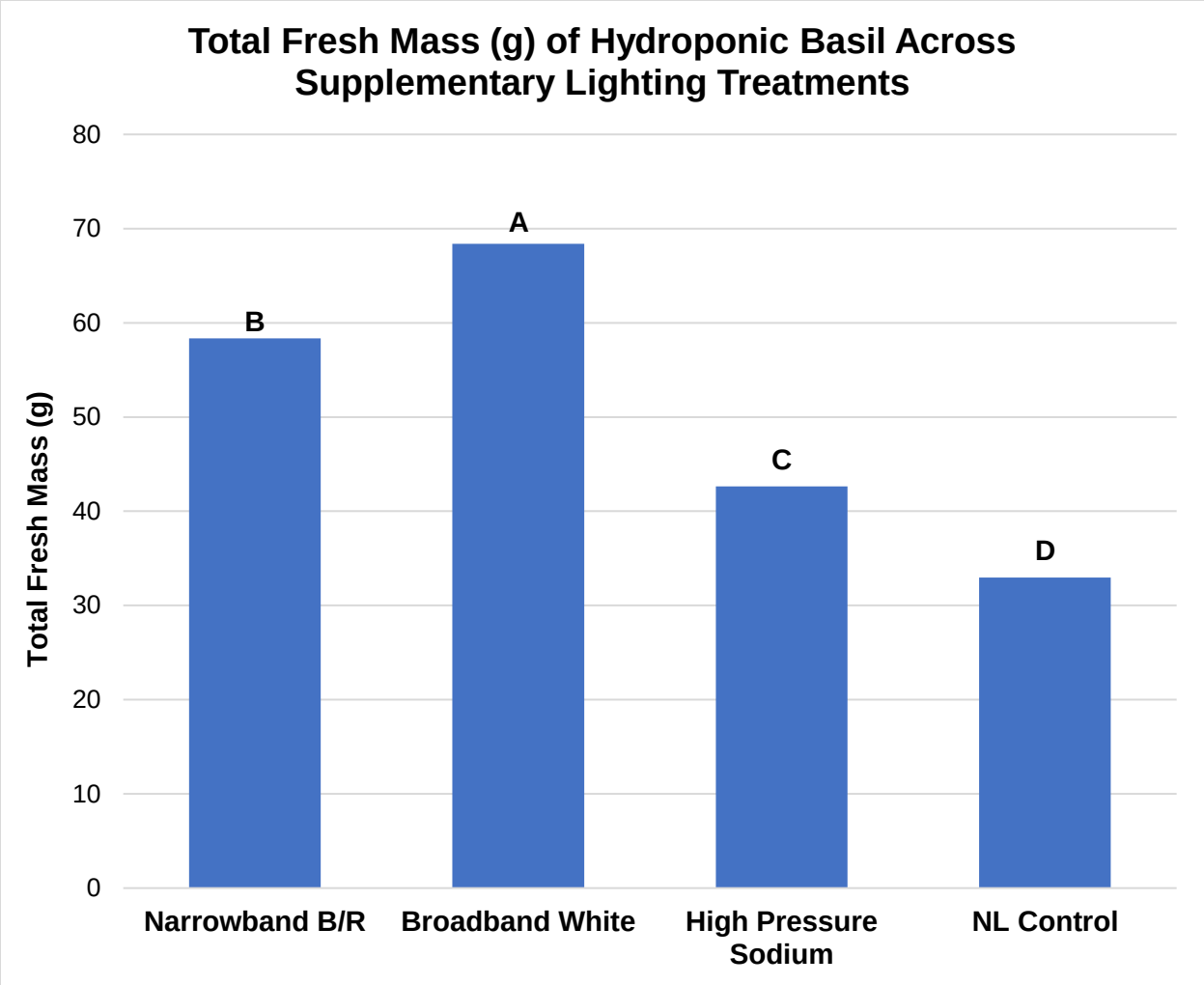

Figure 4.5. Influence of light treatment on total plant fresh mass of hydroponically grown 'Genovese' basil (*Ocimum basilicum* var. 'Genovese'). All weights are presented in grams (g). Mean values represent 2 plants per replication and 6 replications per treatment. Values were analyzed using Tukey's (protected) HSD, and those followed by the same letter are not significantly different (α=0.05).

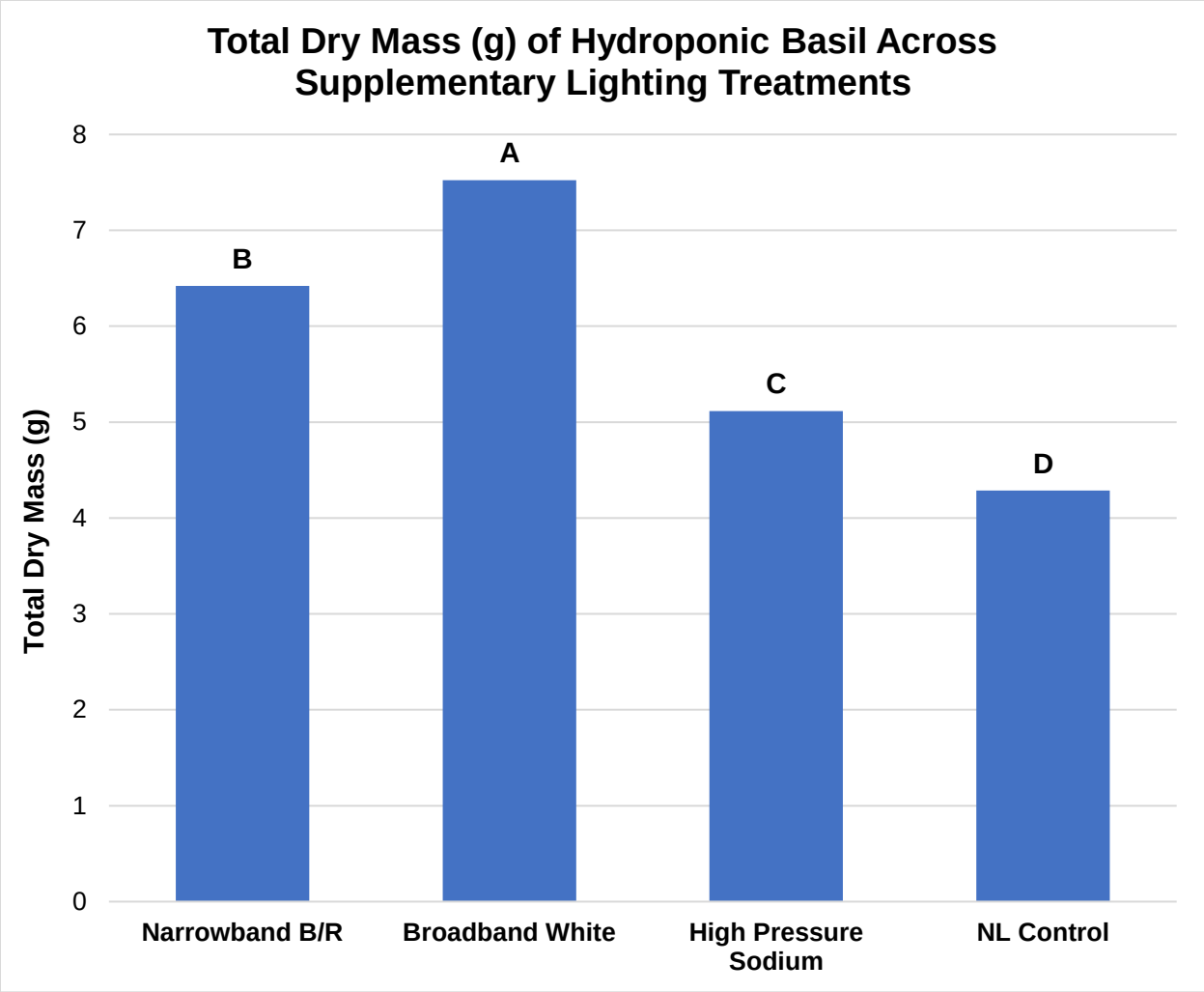

Figure 4.6. Influence of light treatment on total plant dry mass of hydroponically grown 'Genovese' basil (Ocimum basilicum var. 'Genovese'). All weights are presented in grams (g). Mean values represent 2 plants per replication and 6 replications per treatment. Values were analyzed using Tukey's (protected) HSD, and those followed by the same letter are not significantly different (α=0.05).

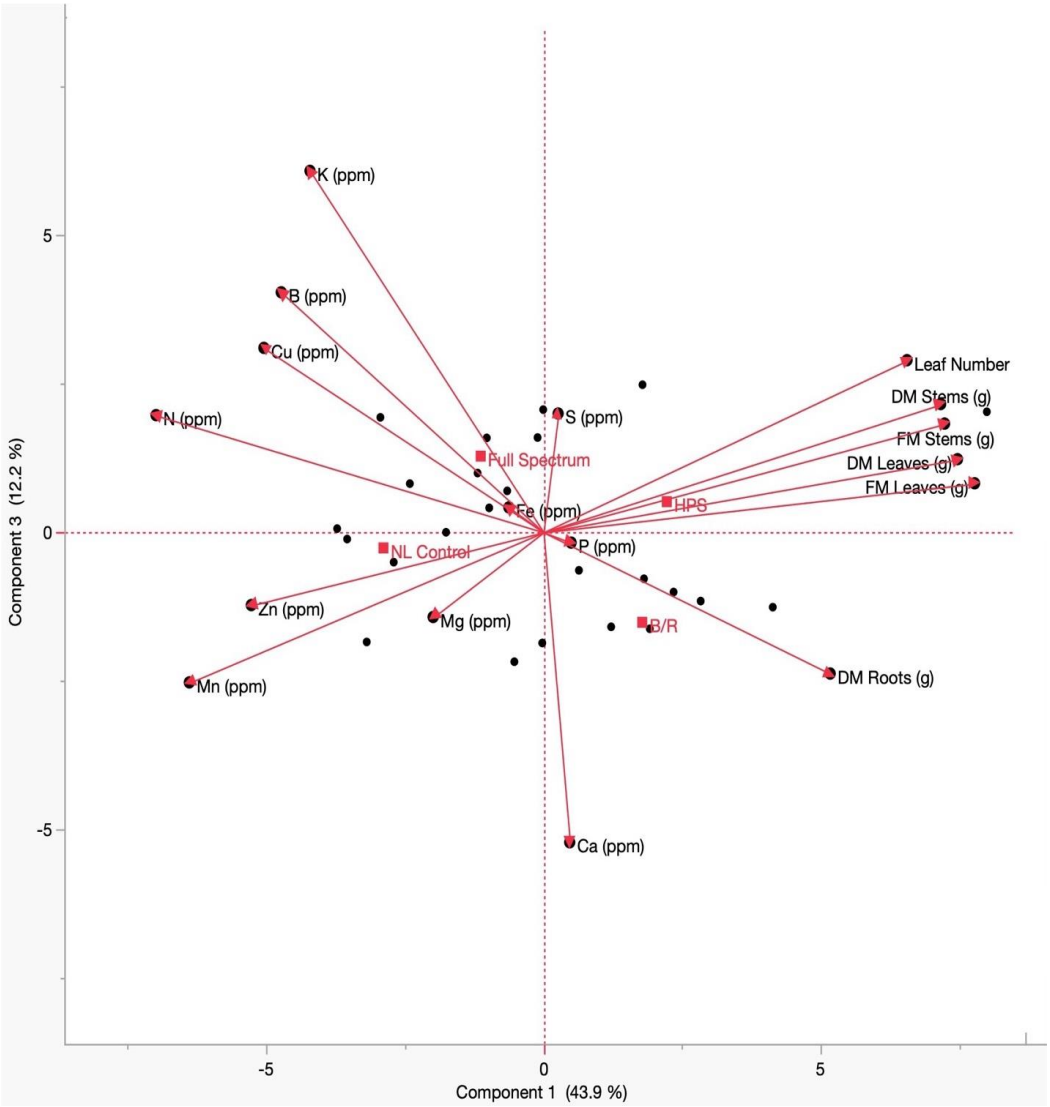

Figure 4.7. Principal component analysis (PCA) comparing all experimental parameters. Helpful to label the treatments larger font than shown. Which represents Full spectrum LED light treatment. If refer to quadrants in body of paper, then label quadrants.

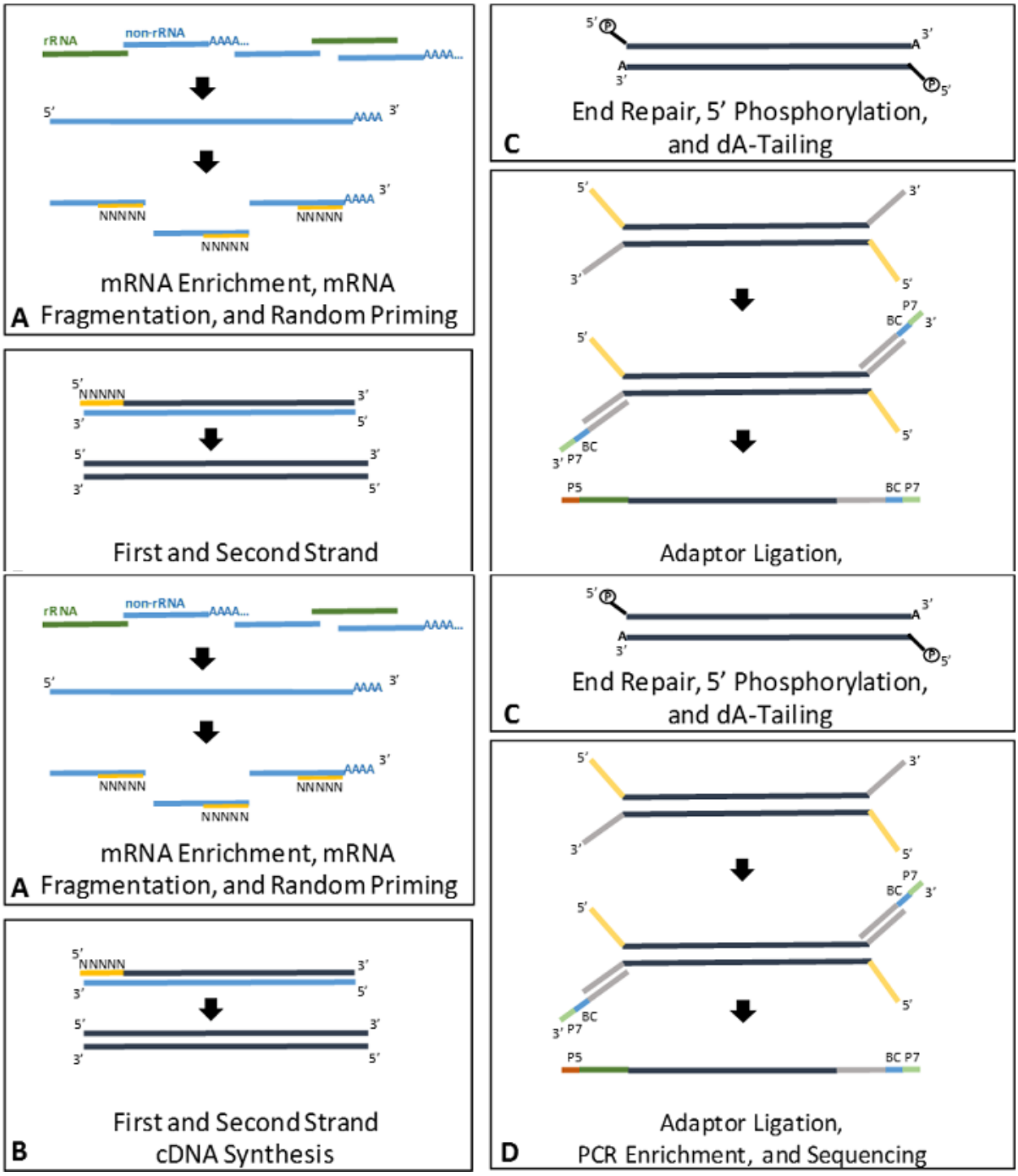

Figure 4.8. mRNA sequencing via polyA selection. Sequencing was performed on the HiSeq 6000 sequencing platform (Illumia, San Diego, USA).

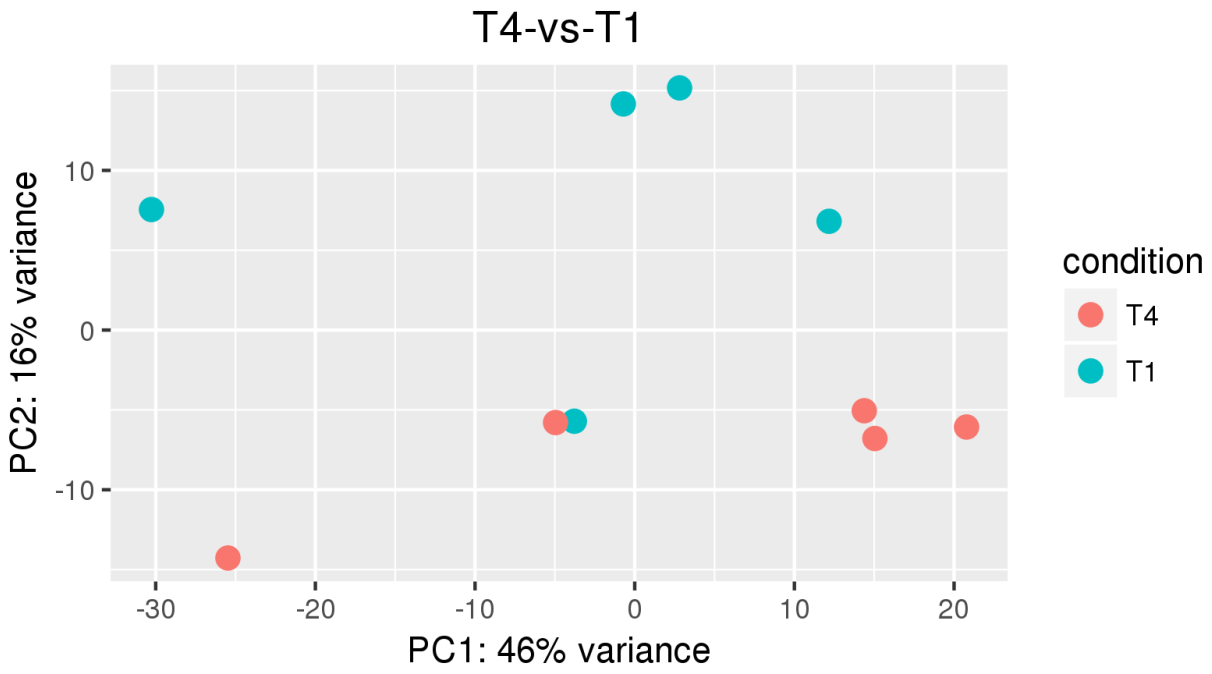

Figure 4.9. Principal component analysis (PCA) comparing DEGs between the Natural Light Control (T4) and Narrowband 20B/80R treatment (T1). If refer to quadrants in body of paper, then label quadrants.

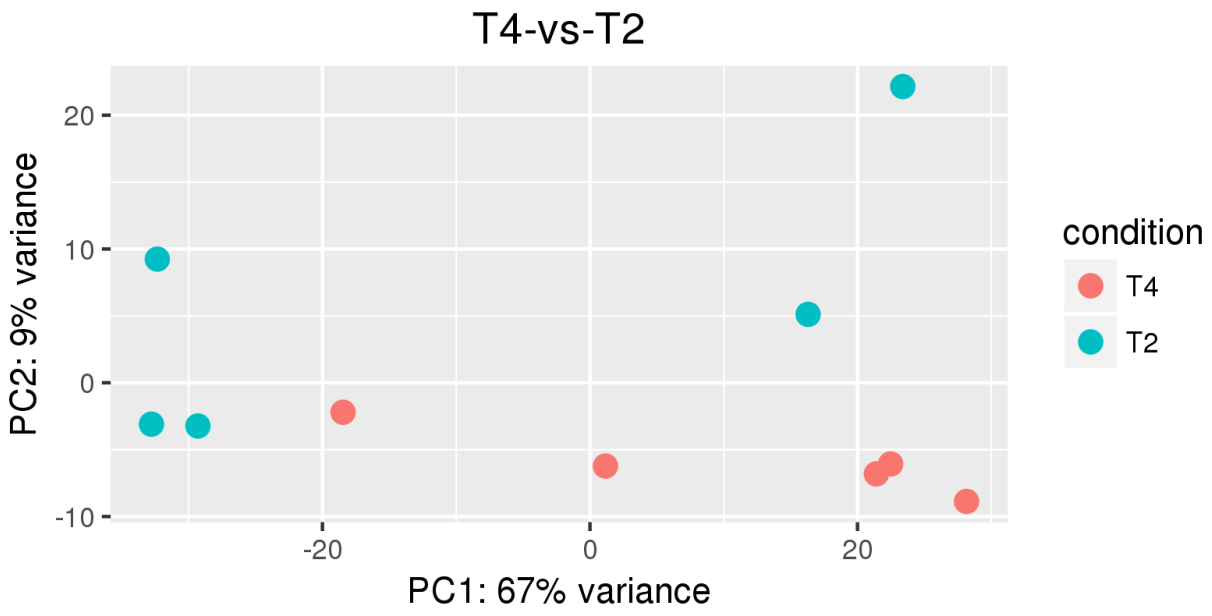

Figure 4.10. Principal component analysis (PCA) comparing DEGs between the Natural Light Control (T4) and Broadband White treatment (T2).

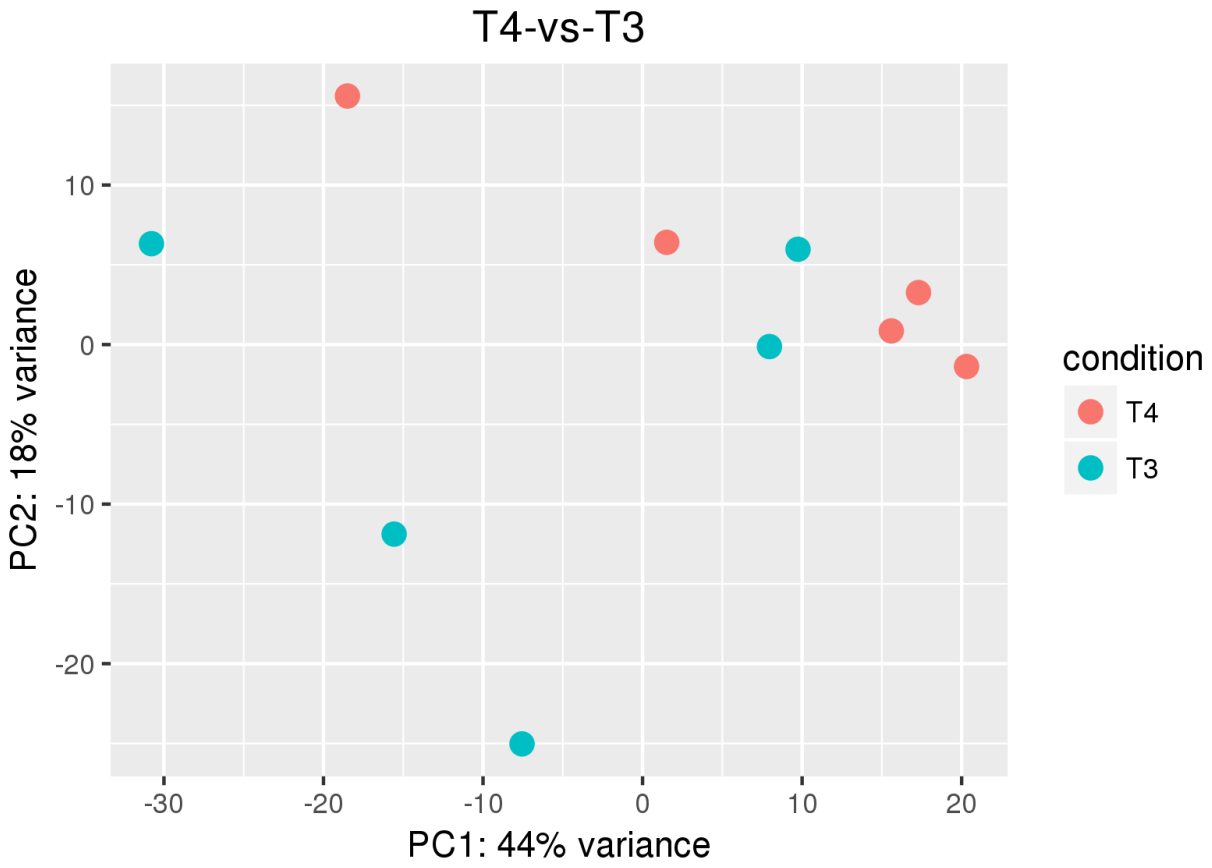

Figure 4.11. Principal component analysis (PCA) comparing DEGs between the Natural Light Control (T4) and High-Pressure Sodium treatment (T3).

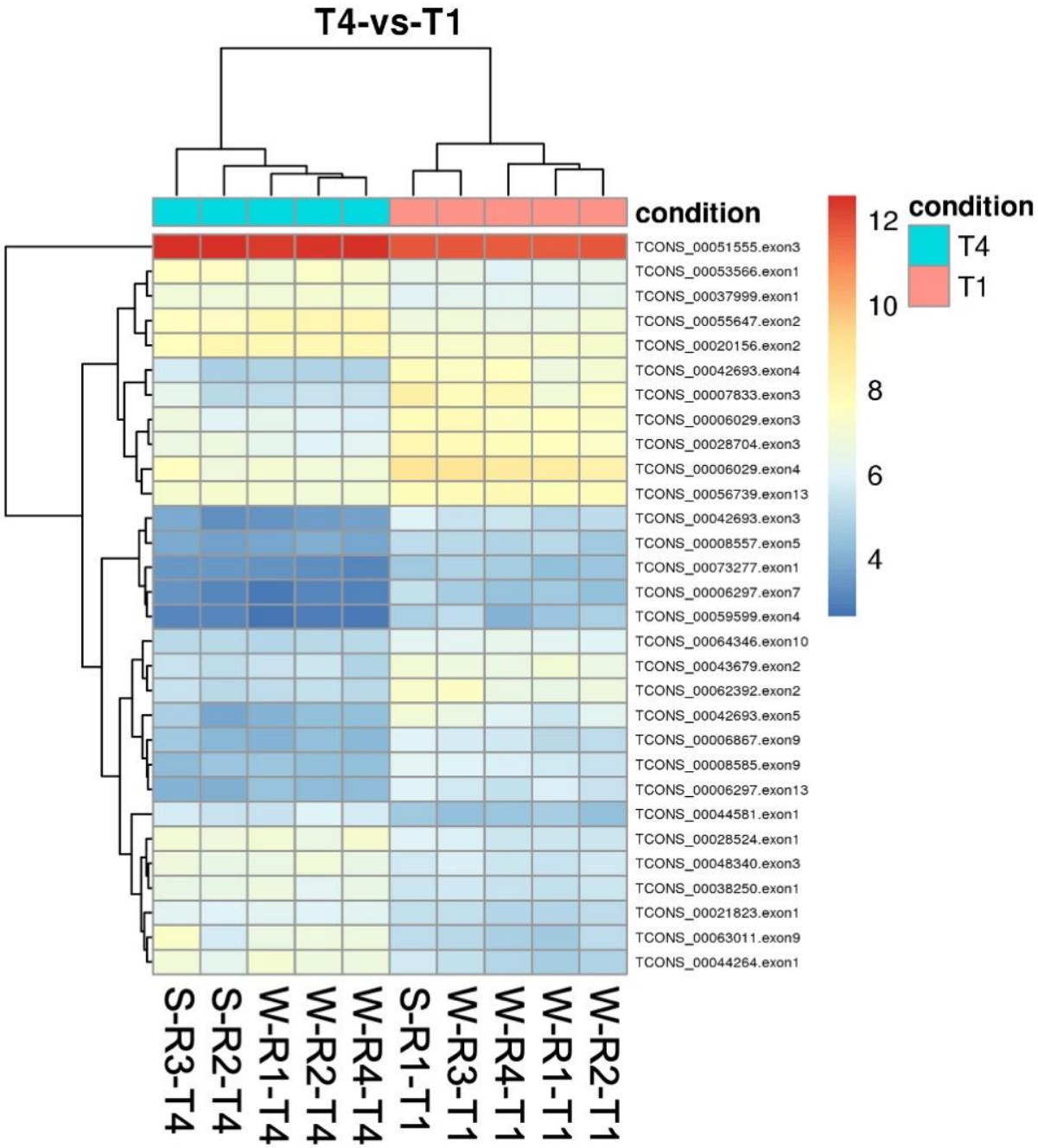

Figure 4.12. Biclustering heat map comparing top 30 significant DEGs between the Natural Light Control (T4) and Narrowband 20B/80R treatment (T1) to identify co-regulated genes. Summer (S) and Winter (W) seasons are compared with four replications (R1-R4).

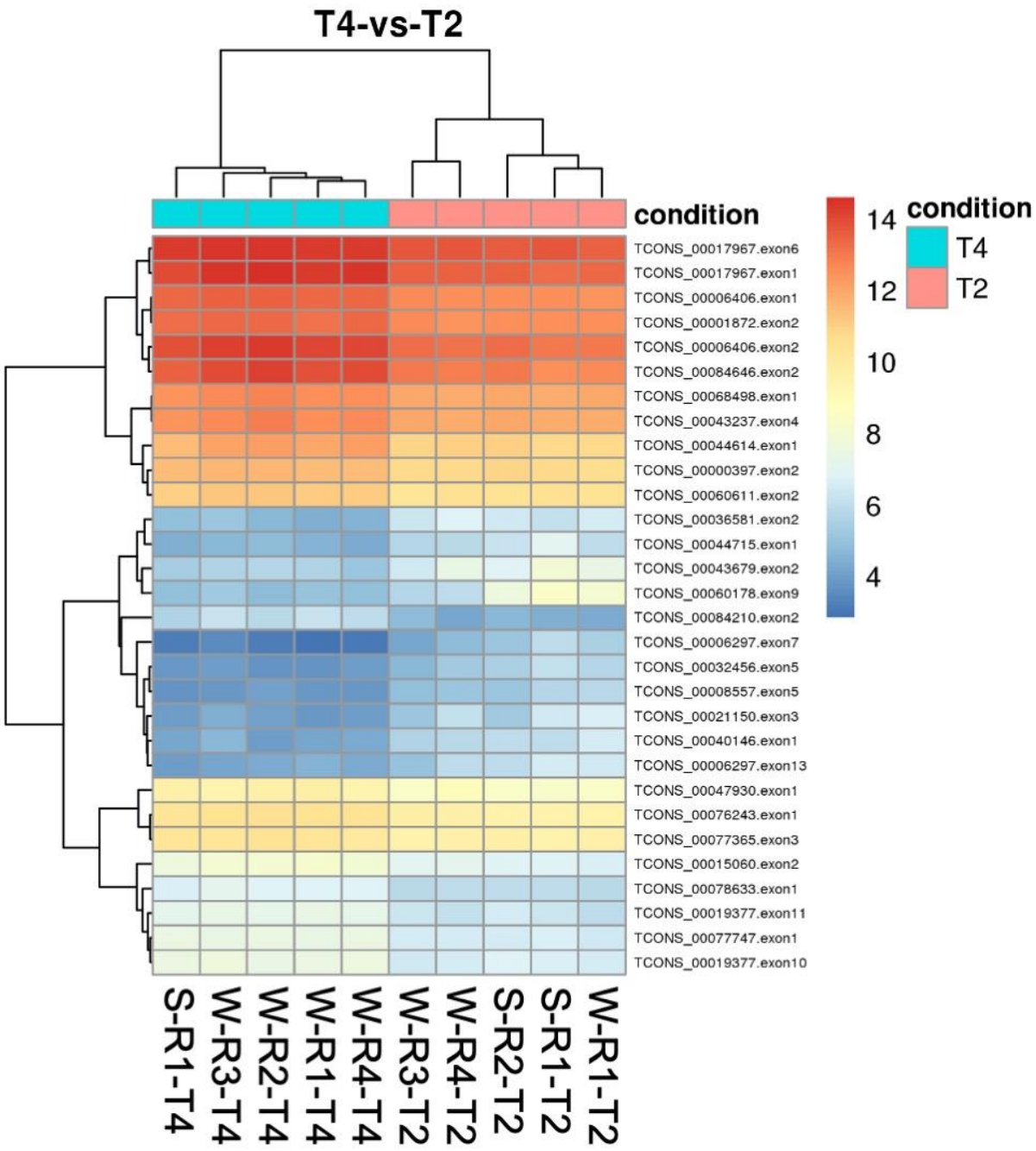

Figure 4.13. Biclustering heat map comparing top 30 significant DEGs between the Natural Light Control (T4) and Broadband White treatment (T2) to identify co-regulated genes. Summer (S) and Winter (W) seasons are compared with four replications (R1-R4).

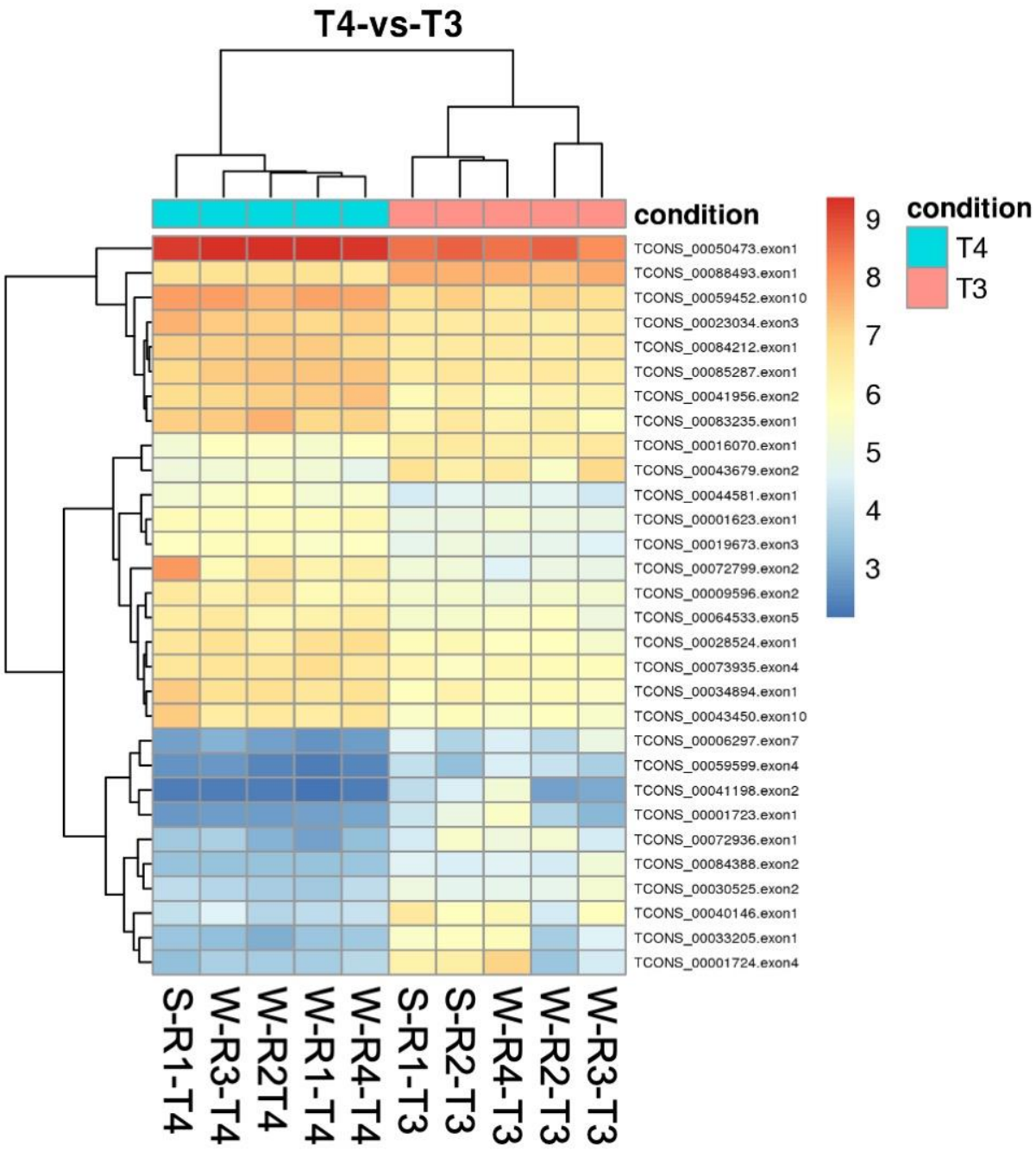

Figure 4.14. Biclustering heat map comparing top 30 significant DEGs between the Natural Light Control (T4) and High-Pressure Sodium treatment (T3) to identify co-regulated genes. Summer (S) and Winter (W) seasons are compared with four replications (R1-R4).

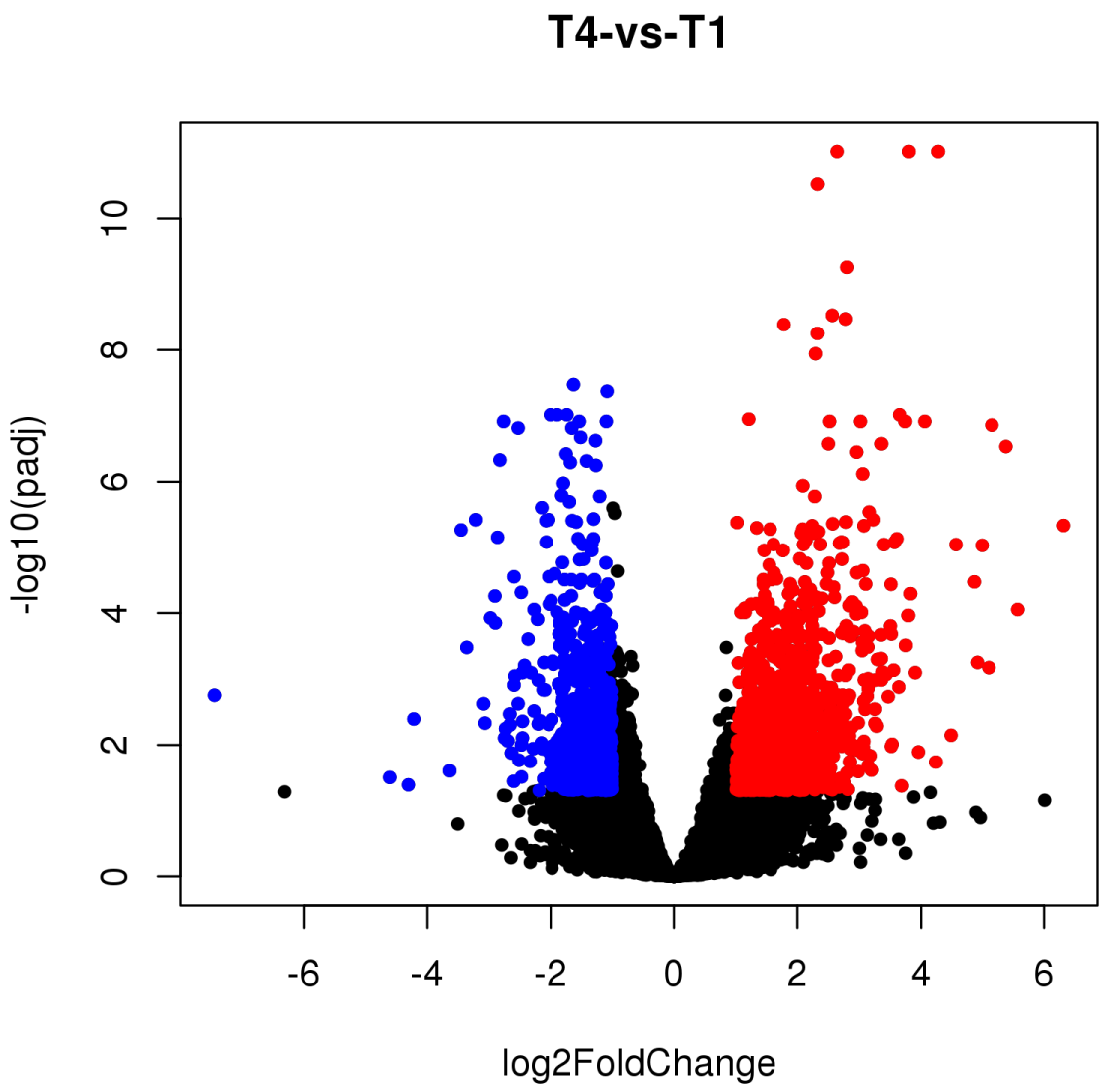

Figure 4.15. Volcano plot showing global transcriptional change between the Natural Light Control (T4) and Narrowband 20B/80R treatment (T1). All the genes are plotted and each data point represents a gene. The log2 fold change of each gene is represented on the x-axis and the log10 of its adjusted p-value is on the y-axis. Genes with an adjusted p-value less than 0.05 and a log2 fold change greater than 1 are indicated by red dots, which represent upregulated genes. Genes with an adjusted p-value less than 0.05 and a log2 fold change less than -1 are indicated by blue dots, which represent downregulated genes.

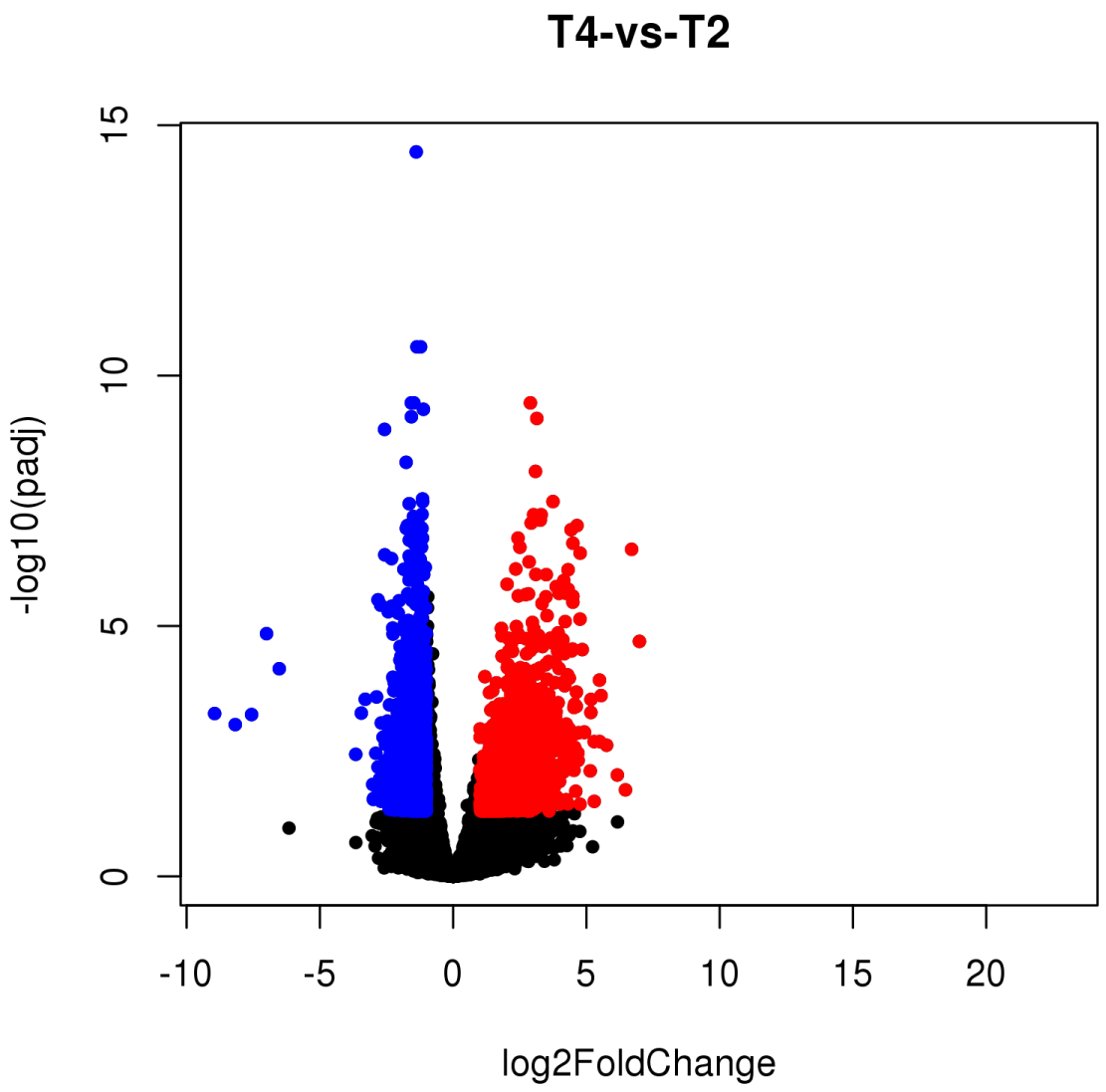

Figure 4.16. Volcano plot showing global transcriptional change between the Natural Light Control (T4) and Broadband White treatment (T2). All the genes are plotted and each data point represents a gene. The log2 fold change of each gene is represented on the x-axis and the log10 of its adjusted p-value is on the y-axis. Genes with an adjusted p-value less than 0.05 and a log2 fold change greater than 1 are indicated by red dots, which represent upregulated genes. Genes with an adjusted p-value less than 0.05 and a log2 fold change less than -1 are indicated by blue dots, which represent downregulated genes.

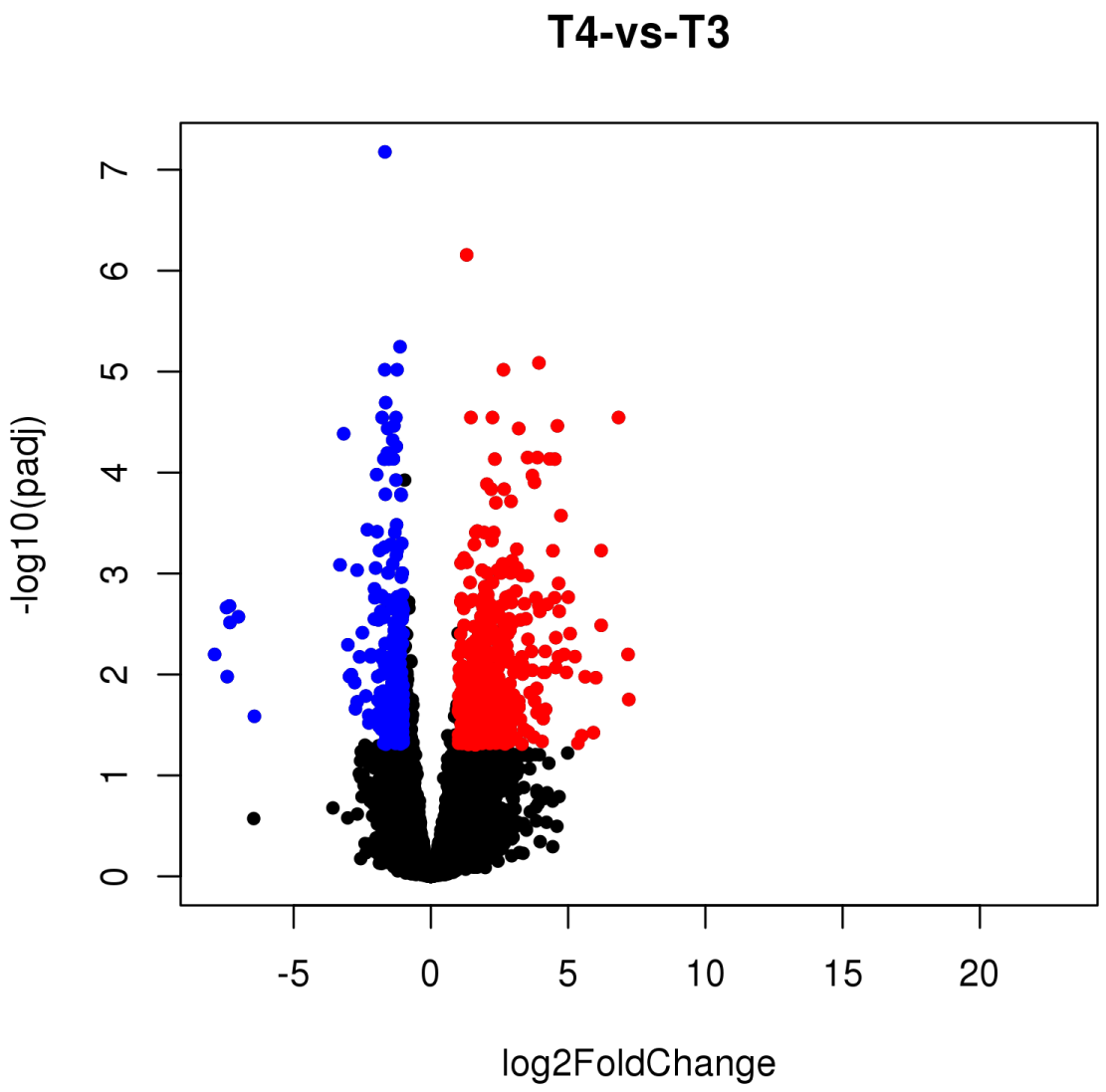

Figure 4.17. Volcano plot showing global transcriptional change between the Natural Light Control (T4) and High-Pressure Sodium treatment (T3). All the genes are plotted and each data point represents a gene. The log2 fold change of each gene is represented on the x-axis and the log10 of its adjusted p-value is on the y-axis. Genes with an adjusted p-value less than 0.05 and a log2 fold change greater than 1 are indicated by red dots, which represent upregulated genes. Genes with an adjusted p-value less than 0.05 and a log2 fold change less than -1 are indicated by blue dots, which represent downregulated genes.

CHAPTER 5: HEADSPACE GAS CHROMATOGRAPHY AND TRANSCRIPTOME ANALYSIS CONFIRMS SENSORY PANEL ASSESSMENT THAT SPECTRAL QUALITY INFLUENCES BIOACCUMULATION OF IMPORTANT AROMA VOLATILES IN SWEET BASIL

Hunter A. Hammock[1], Curtis Luckett[2], and Carl E. Sams[1*]

[1]Department of Plant Sciences, The University of Tennessee, Knoxville, TN, USA, 37996
[2]Department of Food Science, The University of Tennessee, Knoxville, TN, USA, 37996

Correspondence: Carl E. Sams, carlsams@utk.edu

Keywords: Controlled Environment Agriculture, Light Emitting Diodes, *Ocimum basilicum*, Supplemental Lighting, Secondary Metabolism, Sensory Evaluation, Spectral Quality, Terpenes, Transcriptome

Author Contributions:
Conceptualization – HAH, CES
Methodology – HAH, CES
Software – HAH
Validation – HAH, CES
Investigation – HAH
Data curation (GC-MS) – HAH
Data curation (Sensory) – CL, HAH
Data curation (Transcriptome) – HAH
Formal statistical analyses (GC-MS) – HAH
Formal statistical analyses (Sensory) – HAH, CL
Formal statistical analyses (Transcriptome) – HAH
Data Visualization – HAH
Writing (original draft preparation) - HAH
Writing (review and editing) – HAH, CL, CES
Supervision and project administration – CES
Resources – CES
Funding acquisition – CES

Author Statement:
All authors have reviewed the manuscript and agree with the reported findings. There are no reported conflicts between the authors and the present study.

Acknowledgments: The authors of this manuscript would like to thank Tracy Hawk and Terek Hewezi's Plant Molecular Biology Lab for their advice and assistance in reviewing sequencing data.

Funding:
This research was supported by The AgResearch Dean's Office within the University of Tennessee Institute of Agriculture. No external funds were used for the present study.

Disclosure:
This manuscript and its contents were submitted to PLOS ONE on July 2, 2023.

Abstract

The spectral quality of supplemental lighting (SL) used in controlled environment agriculture (CEA) directly influences secondary metabolic resource allocation. Terpenoid metabolism is responsible for the production of volatile organic compounds (VOCs), which influence human sensory perception. Myrcene and Ocimene are two monoterpenes important for the aroma profile of many specialty crops. *Ocimum basilicum* L. var. 'Genovese' is a common culinary herb, popular among professional chefs because of its high yields and unique flavor profile. As horticultural lighting technology continues to advance, it is necessary to explore the spectral quality of SL and its influence on flavor perception and preference. This study aimed to determine the impact of SL spectral quality on basil sensory perception and monoterpene metabolism by corroborating a consumer sensory panel assessment with VOC concentrations and transcriptomic analyses. Four lighting treatments were employed: non-supplemented natural light (NL) control, full-spectrum white LED (5600 K), 20B/80R narrowband LED (447 and 647 nm), and a high-pressure sodium (HPS) light. During the growth period, the daily light integral (DLI) of NL control averaged 9.51 $mol \cdot m^{-2} \cdot d^{-1}$. Each SL treatment provided an additional 8.64 $mol \cdot m^{-2} \cdot d^{-1}$ (100 $\mu mol \cdot m^{-2} \cdot s^{-1}$ for 24 $h \cdot d^{-1}$). A sensory panel was used to discriminate between odor descriptors as well as determine consumer preference and drivers-of-liking. Myrcene and Ocimene were compounds associated with significant drivers of liking, including herbaceous, floral, and fresh descriptors. An Agilent headspace sampler and GC-MS were used to obtain aroma profiles and quantify key VOCs, including Myrcene and Ocimene isomers. Myrcene concentrations were highest in B/R treatment, a 4.9 fold increase over NL control. The ratio of (E/Z)-Ocimene concentrations remained statistically similar under all treatments, except for the B/R supplement. RNA-seq identified a total of 6146 differentially expressed genes (DEGs) across treatments

through pairwise comparisons. Functional annotations revealed several DEGs involved with monoterpene synthesis were significantly up-regulated in the B/R treatment compared to the NL control. A gene that encodes for fenchol synthase (FES), an important enzyme used to synthesize downstream Myrcene and Ocimene isomers, was only up-regulated (2.1 $\log_2$ FC) in the B/R treatment. Increased expression of FES likely explains the increased Myrcene concentrations and unexpected variance in (E/Z)-Ocimene ratio found in the B/R treatment. This experiment demonstrates SL spectral quality influences consumer preference and aroma volatile concentrations in basil. Further studies comparing sensory panels with analytic and transcriptomic approaches will help improve the flavor of culinary herbs and other high-value specialty crops by leveraging environmental controls.

Introduction

Horticultural lighting has gained significant attention in recent years due to its potential to enhance plant growth, development, and secondary metabolite production (Hasan et al., 2017; Garcia-Caparros et al., 2018; Sipos et al., 2020). Spectral quality, which refers to the distribution of wavelengths in light, is a critical factor that influences various physiological and biochemical processes in plants (Ouzounis et al., 2015; Urrestarazu et al., 2016; Pennisi et al., 2019). Advances in lighting technologies, such as light-emitting diodes (LEDs), have enabled researchers and growers to manipulate spectral quality, thereby optimizing plant growth and product quality (Ouzounis et al., 2015; Singh et al., 2015; Pattison et al., 2018).

Sweet basil (Ocimum basilicum L.) is an economically important culinary herb known for its distinctive aroma and flavor, primarily derived from its volatile organic compounds (VOCs) (Hiltunen and Holm, 2003). The influence of spectral quality on the accumulation of these aroma

volatiles in basil has been an area of growing interest (Lee et al., 2005; Carvalho et al., 2016; Litvin et al., 2020; Kivimaenpa et al., 2022). Previous studies have demonstrated that manipulating light conditions can significantly affect the biosynthesis of VOCs, potentially altering the sensory profile of basil and influencing consumer preferences (Kumar et al., 2018; Walters et al., 2020).

Sensory analysis plays a crucial role in evaluating the impact of different light treatments on the overall quality of horticultural products (Lawless, 2010). Sensory panels, consisting of trained individuals or consumers, can provide valuable insights into the perceived aroma, flavor, and overall liking of plant products under varying lighting conditions (Meligaard et al., 2007). This information is essential when determining the effectiveness of novel lighting systems in enhancing product quality and marketability. Consumer acceptance testing is also a crucial method for determining customer preferences and overall liking of food products, including high-value specialty crops. Rapid descriptive methods like check-all-that-apply (CATA) have proven effective at capturing similar data to conventional descriptive analysis (Meligaard et al., 2007; Lawless, 2010).

In addition to sensory analysis, molecular techniques such as mRNA sequencing (mRNA-seq) can be employed to explore the differentially expressed genes (DEGs) in response to varying environmental conditions, including light treatments (Bian et al., 2021; Tang et al., 2021). By identifying DEGs related to the biosynthesis of aroma volatiles, researchers can gain a deeper understanding of how spectral quality modulates the production of these compounds at the genetic level (Lauria et al., 2023; Trivellini et al., 2023).

To obtain a comprehensive understanding of the effects of spectral quality on sweet basil, it is necessary to combine headspace gas chromatography-mass spectrometry (HS GC-MS), sensory panel evaluation, and mRNA-seq analysis. This integrated approach will enable

researchers to link changes in the volatile profile, sensory perception, and transcriptome of sweet basil under different light conditions.

The objective of this study is to determine the influence of supplemental lighting spectral quality on the metabolome, sensory perception, and transcriptome of sweet basil. Specifically, the study aims to identify key aroma compounds and DEGs responsible for consumer preference. The findings from this research will provide valuable insights that can be applied in tailoring horticultural lighting systems to optimize the production of high-quality basil with desirable aroma and flavor attributes.

Materials and Methods

Cultural Techniques and Environmental Growing Conditions

This project was conducted at The University of Tennessee Institute of Agriculture (UTIA) in Knoxville, TN, USA (35°56'44.5"N, 83°56'17.3"W). *Ocimum Basilicum* var. Genovese basil seeds (Johnny's Select Seeds, Winslow, ME, United States) were germinated in peat moss-based cubes (2 × 2 × 6 cm) (Park's Bio Dome Sponges, Hodges, SC, United States) at 28.3°C and 95% RH. The 'Genovese' variety of sweet basil was specifically chosen because of its complex flavor profile, high market demand, and preference among professional chefs.

After two weeks, seedlings were transferred to nutrient film technique (NFT) hydroponic systems with full-strength general mix nutrient solution; the fertility regime was kept constant across the duration of all seasons. Basil was grown under standard commercial greenhouse conditions. The nutrient solution was kept consistent at 5.9 pH and changed weekly. Elemental nutrient concentrations were as follows (ppm): Nitrogen (207.54), Phosphorous (50.87), Potassium (298.23), Calcium (180.15), Magnesium (77.10), Sulfur (136.45), Iron (3.95), Manganese (0.90), Zinc (0.40), Molybdenum (0.09), Copper (0.90), and Boron (0.90). Water samples were analyzed

using Inductively Coupled Plasma Mass Spectrometry (Agilent Technologies, Santa Clara, CA, United States) throughout each experiment to ensure consistent nutrient composition. Total growth time lasted approximately 45 d across all four experimental runs (growing seasons).

Day temperatures averaged 28.1 ± 1.5 °C, and night temperatures averaged 21.3 ± 0.4 °C. DLI of the natural light control (i.e., ambient sunlight) averaged 9.9 $mol \cdot m^{-2} \cdot d^{-1}$ across all four growing seasons (daily average ranging from 4 to 20 $mol \cdot m^{-2} \cdot d^{-1}$). Each hydroponic system (treatment) received similar amounts of cumulative ambient sunlight (DLI of ± 0.5 $mol \cdot m^{-2} \cdot d^{-1}$ across treatments) throughout the four growing seasons, in addition to the prescribed SL regime. Relative humidity during the growth period averaged 55%.

Two experimental cycles were performed to determine differences between summer and winter growing seasons under greenhouse conditions; further, how the interaction between SL and changes in ambient sunlight across growing seasons influences basil VOC profiles, human sensory perception, and changes in genetic expression. Tissue samples for all three experimental methodologies in this study were harvested same day. Specific growing parameters for each of the seasons may be found in Table 5.1, which were collected using greenhouse control sensors (PRIVA, Ontario, CA), WatchDog 2000 Series sensors (Spectrum Technologies, Aurora, IL, USA), and PS-200 Apogee Spectroradiometer (Apogee Instruments, Logan, UT, USA).

Light Treatments

This experiment evaluated the impact of discrete narrowband and broadband wavelength combinations from SL systems on tissue concentrations of plant volatile organic compounds (PVOCs) pertinent to flavor/aroma profile and human sensory perception. A Randomized Complete Block Design was used to set up the lighting treatments in this experiment, and lighting

treatments were moved between growing seasons to account for potential greenhouse shading effects. Narrowband B/R LEDs (447 and 647 nm ± 20 nm) (Fluence Bioengineering, Austin, TX), Broadband White LEDs (5600 K) (Fluence Bioengineering, Austin, TX), and HPS lamps (Hortilux DE, Mentor OH) provided 8.64 $mol \cdot m^{-2} \cdot d^{-1}$ (equal intensity of 100 $\mu mol \cdot m^{-2} \cdot s^{-1}$ for 24 $h \cdot d^{-1}$) for each SL treatment, in addition to natural sunlight (Fig. 5.1). A natural light (NL) control was established to determine how ambient sunlight and SL influenced plant secondary metabolism. Each SL treatment uniformly provided 100 ± 2.5 $\mu mol \cdot m^{-2} \cdot s^{-1}$ across the treatment area throughout the entire duration of the experiment (uniform intensity and spectral quality distribution verified weekly after dark using an average of 5 measurements in a 1 m x 1 m Z pattern across treatment, level with canopy top). LED treatments were 1 m above the hydroponic system, and HPS lamps were 1.5 m above hydroponic systems. The Fluence LED systems consisted of three equally spaced meter-long alternating blue/red bars with adjustable spectral and intensity control, designed to uniformly illuminate 1.2 m x 1.2 m (both spectral quality and intensity). Dimmable HPS lamps were placed in targeted reflectors to reduce SL treatment bleed-over and allow for precise intensity control and uniformity across the 1.2 m x 1.2 m treatment areas. As crops grew, SL intensities were adjusted using dimmers to the target intensity 4-5 times per week (after dark) using a PS-200 Apogee Spectroradiometer (Apogee Instruments, Logan, UT, USA). The intensity and duration of the lighting treatments in this experiment were selected based on current literature with the intention of maximizing the production of key secondary metabolites known to influence flavor perception in basil. Average ambient solar spectrum and supplemental lighting spectra have been provided in Figures 5.1 and 5.2.

Lighting treatments were randomized after each experimental cycle to account for seasonal variations in NL intensity, spectral quality, and potential temperature variation within the

greenhouse bay. Each measurement unit consisted of two plants to improve statistical power and reduce biological variance. Measurement units are presented on a per-plant basis for all data (where applicable). Each treatment is considered an experimental unit.

Each SL treatment was physically separated to ensure no bleed-over effects between treatments (average of 1.1 ± 0.6 $\mu mol \cdot m^{-2} \cdot s^{-1}$ SL bleed-over at the treatment edges). 1.2 m x 1.2 m sections of basil were grown, with 1.2 m separation between treatments (i.e., measurement edge-to-edge of hydroponic systems within the greenhouse). Tissue samples were only harvested from within the middle 0.6 m of each treatment to ensure further reduction of SL contamination between treatments (0.3 m around the edge of each treatment was considered the buffer zone and was not used for sampling). SL bleed-over was <0.1 $\mu mol \cdot m^{-2} \cdot s^{-1}$ within the harvest zone of each treatment (i.e., below the instrumentation detection limit). Harvests for all sample collection types occurred directly after sunrise, and samples were immediately sealed and frozen in liquid nitrogen, then transferred to a -80 °C freezer until the time of analysis to preserve all volatile compounds and inhibit post-harvest changes to metabolism. Under these circumstances, SL treatment bleed-over was deemed non-significant; therefore, physical barriers (i.e., plastic sheets, boards, etc.) were not utilized because of potential deleterious experimental effects (i.e., interaction with ambient sunlight intensity/DLI, reduced airflow, isolated microclimates leading to air temperature variability, etc.). SL treatments were randomized each season to eliminate the potential for DLI and air temperature variability within the greenhouse bay.

Headspace Gas Chromatography and Mass Spectrometry Method

Our research group developed (Barickman et al., 2017) and optimized (Hammock and Sams, 2023) an HS GC-MS protocol, which was used for this experiment. Three g of fresh leaf

tissue (two basil plants per sample rep, 1.5 g of representative material from each plant, nodes four and eight) were placed in 20 mL borosilicate glass vials, then immediately frozen in liquid nitrogen, and stored in a -80 ºC freezer until time of analysis. Samples were run within 72 hours of collection. Frozen samples were placed onto a Network Headspace Sampler (Agilent G1888, Santa Clara, CA, United States). Ten sample replications were used per treatment. Samples were heated to 80 ºC for 10 min and pressurized with Helium (Air Gas, analytical purity) to 95.21 kPa for 1 min. The tube was then vented for 1 min into the headspace transfer line (110 ºC) and injected (port at 250 ºC) into the GC (Agilent Technologies 6890N Network GC System). The volatiles were separated by an HP-5MS capillary column ((5%-Phenyl)-methylpolysiloxane, length: 30 m, ID: 0.250 mm, film thickness: 1 µm, Agilent Technologies) using analytical purity Helium carrier gas at 95.21 kPa with constant column pressure. At the start of data acquisition, the temperature was held at 40 ºC for 5 min, ramped up from 40 ºC to 250 ºC (5 ºC per min), then held constant for the duration of the run. The total run time was 70 min, including post-run and cool-down phases. After sample separation and column elution, the analytes were passed through a mass selective detector (Agilent Technologies 5973 Network Mass Selective Detector) at 250 ºC and collected over the course of the sample run. The transfer line, ion source, and quadrupole temperatures were 250 ºC, 230 ºC, and 170 ºC, respectively. The full scan mass range was set to 40-550 m/z (threshold: 150).

Agilent ChemStation was used for data collection and processing. Over 200 separate compounds were identified throughout this experiment, but emphasis was placed on key aroma compounds (i.e., shown in the literature to be essential for human sensory perception and/or plant metabolic processes) that have been calibrated to our GC-MS and HP-5MS column using pure analytical standards (Sigma-Aldrich, St. Louis, MO) to determine leaf tissue emissions of key

VOCs on a fresh plant weight basis. The MS spectra from pure analytical standards and fresh samples were compared to NIST, ADMIS, and our custom basil reference library created from calibrated analytical standards to confirm peak identity and retention times (i.e., compound identity and concentration confirmed above 99% confidence by comparing known target ions and retention time of each compound). MassHunter Workstation Software Version B.06.00 (Agilent Technologies, Inc., 2012) was used to integrate peaks automatically. Relative peak areas and retention times were automatically adjusted based on authentic analytical standards and multiple library references. Over 200 compounds were identified in this experiment, with approximately 50 of those being quantified using pure analytical standards.

All volatile concentration units are reported in micro molarity of analyte concentration (suspended in a known volume of gaseous headspace matrix) per g of fresh leaf tissue ($\mu M \cdot g^{-1}$ FM) to represent VOC emissions most accurately from the collected headspace sample above fresh plant tissues under specific reproducible analytical conditions. This unit (compared to $\mu mol \cdot g^{-1}$ FM) was utilized because of its commonality in biological headspace GC-MS sampling and incorporates the concentration of each analyte per unit volume of headspace gas above the plant tissue (i.e., samples the dynamic and complex gaseous matrix which contains numerous pertinent VOCs), which is important for sensory-based studies. This provides the foundation for future sensory panel experiments aimed at determining the influence of light on consumer acceptance and preference of basil aroma profiles.

GC-MS data were statistically analyzed using GLIMMIX and Mixed Model Analysis of Variance ($p = 0.05$) procedures using the statistical software SAS (version 9.4, SAS Institute, Cary, NC). Design and Analysis macro (DandA.sas), created by Dr. Arnold Saxton, was utilized in addition to Tukey's adjustment, regression analysis, and univariate/normalization procedures to

provide additional statistical insights on the complete data set. Treatments and seasons were separated by Tukey's honestly significant difference (HSD) at α=0.05. Due to the overwhelming number of compounds analyzed, only statically significant separations of compounds with known plant physiological function and/or human sensory impact were reported in this study (Tables 5.2-5.7). Ten replicates (leaves from two plants each) were analyzed in each treatment (twelve plants, or six measurement units, per treatment within 0.6 m x 0.6 m harvest zone). Each experimental cycle was repeated across two growing seasons (two experimental cycles). Replicates (6) were nested within treatments (4), which were nested within growing seasons (2). Key volatiles were analyzed and presented on a fresh mass (FM) basis as compared to calibration curves created from pure analytical standards.

Consumer Sensory Evaluation

A consumer acceptance test, as well as check-all-that-apply (CATA) section, was used to measure the effects of lighting treatment and season on flavor profile, consumer liking, and drivers of liking. One hundred untrained basil consumers were recruited for each growing season through an online database (n = 600) managed by the Center for Sensory Science at the University of Tennessee Institute of Agriculture. Prescreening was performed to select eligible participants (i.e., indicated regular basil consumption, as well as no vision, smell, or taste impairments), and participant demographics are listed in Table 5.8. Participants only smelled basil aroma (olfaction) and did not consume tissue samples. All participants signed an informed consent form and were compensated for their time. This experiment was conducted according to the Declaration of Helsinki for studies on human subjects and approved by the University of Tennessee IRB review for research involving human subjects (IRB #).

Representative basil samples were collected from each of the four treatments (two leaves from two plants, nodes four and eight, total of four leaves) and delicately placed into 60 mL sealable plastic containers (ULINE, Pleasant Prairie, WI, USA). A small 2 cm x 2 cm piece of damp Kimwipe (Kimberly Clark, Irving, TX, USA) was placed at the bottom of each container to keep the tissue sample hydrated. Basil samples were placed into a chilled cooler (10 ºC) and provided to consumers within 30 min of harvesting. Sensory studies (i.e., tissue sampling and participant olfaction) were conducted from 8 am to 12 pm for both seasons. Participants were given basil from each of the four light treatments in a sequential monadic design dictated by a William's Latin square design. The basil was provided at room temperature with a random 3-digit blinding code. Participants were instructed to open the container to rip the cylinder of basil leaves (into two parts in one swift motion), immediately smell the samples, and rate the aroma in terms of intensity, overall liking, and CATA. Overall aroma intensity was rated on a 15-cm visual analog scale ("Extremely weak" to "Extremely strong") with a midpoint 7.5 anchor. Overall aroma liking questions were on a 9-point hedonic scale ("Like extremely" to "Dislike extremely"). Lastly, CATA questions regarding aroma perceptions for each sample. The time between samples was set to 120 seconds to reduce habituation and adaptation. This procedure was repeated across two experiments "Summer" and "Winter" to evaluate aroma differences in response to ambient sunlight across growing seasons. Consumer data was recorded using RedJade sensory software (RedJade Software Solutions, LLC, Redwood Shores, CA, USA).

A two-way nested mixed model analysis of variance (ANOVA) was used to evaluate consumer overall liking and overall aroma intensity scores, in addition to attribute scores (CATA) with growing season and light treatment (Tables 5.9-5.10). A correspondence analysis was conducted to illustrate the relationship between lighting treatments and basil aroma descriptors.

Differences between conditions with CATA data were estimated using the frequency that each CATA attribute was chosen and was assessed with Cochran's Q Test and Cochran's Armitage Trend Test. Bivariate correlations were analyzed with Pearson's r when appropriate. To assess how overall liking was influenced by attributes from different light treatments, CATA descriptors counts were used to predict overall liking. A partial least squares (PLS) regression model (NIPALS, k=10) was constructed using average overall liking scores and CATA descriptor frequencies to determine drivers of liking (Fig. 5.4). All data for sensory evaluation were analyzed using JMP PRO 17 (SAS Institute, Cary, NC, USA).

RNA Extraction

Tissue samples were collected for RNA extraction at vegetative maturity, approximately 45 d after seeding,. A leaf from the second and fourth fully expanded leaves from the tops of two basil plants was collected under the harvest zone of each treatment and immediately frozen with liquid nitrogen. Four replicates were analyzed in each treatment. Each experimental cycle was repeated across two growing seasons (two experimental cycles). Replicates (4) were nested within treatments (4), which were nested within growing seasons (2).

Samples were stored in -80 ºC until RNA extractions were conducted. Samples were ground to <30 mesh and homogenized immediately before RNA extraction using liquid nitrogen with a mortar and pestle. Total RNA was extracted from leaf samples using RNeasy Plant Mini RNA isolation kits (Qiagen, Hilden, Germany) according to the provided instructions. Quality and purification of total RNAs were determined before and after the addition of 50 µL Plant RNA Isolation Aid (ThermoFisher Scientific, Waltham, MA). Total RNA extracted from leaf tissue

samples was shipped to Azenta Life Sciences (Burlington, MA, USA) for RNA-Seq library construction and sequencing.

Library Preparation with PolyA Selection and Illumina Sequencing

Details regarding library preparation and sequencing workflow can be found in Figure 5.5. RNA samples were quantified using Qubit 2.0 Fluorometer (Life Technologies, Carlsbad, CA, USA), and RNA integrity was checked using Agilent TapeStation 4200 (Agilent Technologies, Palo Alto, CA, USA).

The RNA sequencing libraries were prepared using the NEBNext Ultra II RNA Library Prep Kit for Illumina using the manufacturer's instructions (New England Biolabs, Ipswich, MA, USA). Briefly, mRNAs were initially enriched with Oligod(T) beads. Enriched mRNAs were fragmented for 15 minutes at 94°C. First-strand and second-strand cDNA were subsequently synthesized. cDNA fragments were end-repaired and adenylated at 3'ends, and universal adapters were ligated to cDNA fragments, followed by index addition and library enrichment by PCR with limited cycles. The sequencing libraries were validated on the Agilent TapeStation (Agilent Technologies, Palo Alto, CA, USA), and quantified by using Qubit 2.0 Fluorometer (ThermoFisher Scientific, Waltham, MA, USA) as well as by quantitative PCR (KAPA Biosystems, Wilmington, MA, USA).

The sequencing libraries were clustered on three flowcell lanes. After clustering, the flowcell was loaded on the Illumina HiSeq instrument (4000 or equivalent) according to manufacturer's instructions. The samples were sequenced using a 2x150bp Paired End (PE) configuration. Image analysis and base calling were conducted by the Control software. Raw sequence data (.bcl files) generated from the sequencer were converted into fastq files and de-

multiplexed using Illumina's bcl2fastq 2.17 software. One mismatch was allowed for index sequence identification.

Transcriptome Analysis

Sequence reads were trimmed to remove possible adapter sequences and nucleotides with poor quality using Trimmomatic v.0.36. The trimmed reads were mapped to the *Ocimum basilicum* reference genome (Gonda et al., 2020) available on ENSEMBL using the STAR aligner v.2.5.2b. The STAR aligner is a splice aligner that detects splice junctions and incorporates them to help align the entire read sequences. BAM files were generated because of this step. Unique gene hit counts were calculated from the Subread package v.1.5.2. The hit counts were summarized and reported using the gene_id feature in the annotation file. Only unique reads that fell within exon regions were counted.

After the extraction of gene hit counts, the gene hit counts table was used for downstream differential expression analysis. Using DESeq2, a comparison of gene expression between the customer-defined groups of samples was performed. The Wald test was used to generate p-values and log2 fold changes. Genes with an adjusted p-value < 0.05 and absolute log2 fold change > 1 were called significant for each comparison. The results of the differential gene expression analyses for all comparisons are shown in Table 5.11. To account for differences in sequencing amounts, the original values were normalized. The resulting normalized values were used to accurately identify differentially expressed genes. A gene ontology (GO) analysis was performed on the statistically significant set of genes by implementing the software GeneSCF. The GO list was used to cluster the set of genes based. The analysis of GO and Kyoto Encyclopedia of Genes and Genomes (KEGG) pathways enrichment of differential expression genes (DEGs) were

performed. GO and KEGG terms with corrected $p < 0.5$ and deemed significant were used in the comparative analyses between treatments.

Principle component analysis biplots were developed to reveal similarities within and between treatments, using the "plotPCA" function within the DESeq2 R package. The plot shows the samples in a 2D plane spanned by their first two principal components. The top 500 genes, selected by highest row variance, were used to generate the plot (Figs. 5.6-5.8). DEG biclustering heatmaps were created to visualize the expression profile of the top 30 genes sorted by their adjusted p-values (Figs. 5.9-5.11). Volcano plots were created to show the global transcriptional change across seasons and replicates (Figs. 5.12-5.14).

Results

Volatile Organic Compound Profiles

Plant volatile organic compound (PVOC) leaf tissue concentrations were quantified using HS GC-MS to determine the relationship between basil aroma volatile profiles, metabolome, and human sensory perception as influenced by various spectral qualities of supplemental light. Many of the PVOCs evaluated in the present study were significantly influenced by growing season (i.e., variation in ambient sunlight), lighting treatment (spectral quality), and season*treatment interactions (Tables 5.2 and 5.3).

Table 5.4 shows the influence of growing season on aroma volatile tissue concentrations. A number of compounds had significantly higher tissue concentrations during the summer growing season as compared to the winter season. Propanol, trans-2-Pentenal, and 2-ethyl-2-Butenal had approximately 15-36% higher concentrations during the summer season. p-Menth-1-en-8-ol and 2-methyl-2-Hepten-4-yne were approximately 26% higher during the summer months. (R+/S-)-

Limonene and Eucalyptol were approximately 20% higher during the summer. Methyl Salicylate, Indole, and d-Carvone were approximately 55% higher during the summer, and Methyl Eugenol was 86% higher. Eugenol and Citronellyl acetate concentrations were only detected during the summer months, but were not detected during the winter season. A few compounds had significantly lower tissue concentrations during the summer growing season as compared to the winter season, such as α-Pinene and Camphene. Additionally, 1,3,6-Octatriene, 3,7-dimethyl-, (E) and 1,3,6-Octatriene, 3,7-dimethyl-, (Z) (i.e., (E/Z)-Ocimene) showed opposing changes across seasons. During the summer, (E)-Ocimene tissue concentrations were 20% higher than (Z)-Ocimene concentrations; during the winter, (Z)-Ocimene concentrations were 53% higher than (E)-Ocimene concentrations. Table 5.5 indicates there was no significant difference between VOC total concentrations, despite the ratios of multiple classes of compounds shifting across seasons (Table 5.4). The only ratios influenced by growing season were α/ß-Pinene and γ-Terpinene/Total terpinenes, but only by a few percent (Table 5.5).

Table 5.6 shows the influence of light treatment on aroma volatile tissue concentrations. A number of compounds had significantly higher tissue concentrations under the Narrowband 20B/80R treatment as compared to the NL control, which included 2-cyclo-Pentane, Phenol, ß-Myrcene, 3-Carene, and Propanol (ranging from 1.5-fold to 6-fold increase). Dimethyl Sulfide concentrations were significantly higher in the Narrowband 20B/80R treatment than in any other treatment or the NL control. 2-ethyl-2-Butenal, (E)-2-Hexenal, and trans-2-Pentenal concentrations were significantly higher in the Broadband White treatment than in any other treatment or the NL control. Terpinolene concentrations were increased 3.2-fold under the Broadband White treatment as compared to the NL control, while 3-Menthene was increased 5.1-fold under the Broadband White treatment as compared to the HPS treatment. Linalool and

Cycloheptane showed opposite trends in response to light treatments; linalool was detected under all lighting treatments except for the NL control, while Cycloheptane was only detected under the NL control. Indole and d-Carvone show similar patterns, with approximately a 5-fold concentration increase under the Broadband White as compared to the NL control. Eugenol and Methyl Eugenol followed similar patterns across lighting treatments. Both compounds were detected at similar concentrations (i.e., similar concentration of each compound across treatments as well as the ratio of Eugenol/Methyl Eugenol between treatments). Further, Eugenol and Methyl Eugenol were not detected under the HPS treatment or the NL control. Finally, Table 5.7 shows that the VOC totals were significantly influenced by lighting treatment. The highest tissue concentrations were found under the Narrowband 20B/80R treatments, while the lowest was found under the NL control; all VOC treatment totals statistically separated. The only pertinent VOC ratio to be significantly influenced by lighting treatment was α/ß-Pinene, with the highest ratio under NL control and the lowest under the HPS treatment.

Sensory Evaluation

Two untrained sensory evaluation experiments (summer and winter) were conducted to determine how growing season and supplemental lighting type influenced consumers' overall liking, overall aroma intensity, and identification of key odor descriptors. As shown in Table 5.9, lighting treatment significantly influenced consumers' overall aroma liking scores. The NL control had the highest scores of any treatment during both seasons. During summer experiments, participants indicated they liked the samples under the Broadband White, HPS, and NL Control as opposed to the Narrowband 20B/80R treatment. During the Winter, Broadband White and Narrowband 20B/80R had the lowest scores. Despite there being significant differences among many compound tissue concentrations (Tables 5.2-5.7), there were no statistically significant

differences among consumer aroma intensity scores across lighting treatments and/or growing seasons (Table 5.10).

Using CATA descriptor responses from the sensory evaluation experiments, a correspondence analysis factor map was created (Fig. 5.3), which illustrates the general relationship between basil samples from each lighting treatment and associated CATA responses. Dimension 1 accounts for 57.93% of the variation in CATA response data, while Dimension 2 accounts for 31.48% of the variation in CATA response data. Each of the four lighting treatments was separated into the four quadrants of the CA factor map. As shown in Figure 5.3, the Narrowband 20B/80R treatment was generally associated with the CATA descriptors "anise," "grassy," and "pungent." The Broadband White treatment was generally associated with the descriptors "nutty" and "honey." The HPS treatment was generally associated with the descriptors "herbaceous," "floral," and "fresh." Finally, the NL control was generally associated with the descriptors "medicinal," "spicy," and "fresh."

The CATA descriptor scores were able to predict overall liking relatively well, accounting for over 89.41% of the variance in liking. In total, 11 CATA descriptors were found to be important in predicting liking scores, which surpassed the Variable Importance in Projection threshold set for this Partial Least Squares model (VIP > 0.8). The VIP value indicates the magnitude a descriptor has on predicting overall liking (i.e., higher VIP descriptors are better predictors of overall liking). Regression coefficients were also calculated, which determines the direction of overall liking. Positive coefficients predict an increase in overall liking, while negative coefficients predict a decrease in overall liking (i.e., dislike). Figure 5.4 illustrates CATA descriptors and their respective VIPs (y-axis) and regression coefficients (x-axis). The most influential positive drivers of liking are "fresh" and "flavor intensity." Despite participants not being able to differentiate

overall intensities between lighting treatments or seasons (Table 5.10), the PLS model was able to identify “flavor intensity” as one of the primary drivers of liking. Moderately influential positive drivers of liking include minty, herbaceous, floral, eucalyptus, and green. The most negative drivers of liking include pungent and putrid. Moderately influential negative drivers of liking include bitter and mushroom. Other CATA descriptors fell below the VIP threshold of 0.8 and were not deemed significant drivers of liking. Using this PLS model, the top 11 CATA descriptors, or drivers of liking, can accurately predict overall liking.

Transcriptome Analysis

RNA Seq and statistical analyses were conducted to identify key genes involved in the regulation of secondary metabolism and human sensory perception of basil under various supplemental lighting spectra. By performing pairwise comparisons, a substantial number of differentially expressed genes (DEGs) were identified across both summer and winter growing seasons. In the summer growing season, 4207 DEGs were identified, while the winter growing season yielded a larger number, with 13110 DEGs (Table 5.11).

Further analysis of these DEGs revealed distinct patterns of upregulation and downregulation across different light treatments during both summer and winter growing seasons. In the summer growing season, Narrowband 20B/80R (NB) vs. Natural Light (NL) control comparison had the highest number of DEGs, with 3801 identified, followed by Broadband White (BW) vs. NL control with 278 DEGs, and High-Pressure Sodium (HPS) vs. NL control with the lowest number, at 128 DEGs. A similar pattern was observed during the winter growing season, with NB vs. NL control yielding 5578 DEGs, BW vs. NL control producing 5609 DEGs, and HPS vs. NL control having the least number of DEGs, at 1923 (Table 5.11).

Upon examining upregulated DEGs, the summer growing season showed 2045, 132, and 34 upregulated DEGs in the comparisons of NB vs. NL control, BW vs. NL control, and HPS vs. NL control, respectively. In contrast, the winter growing season exhibited a higher number of upregulated DEGs across all comparisons, with 3505 for NB vs. NL control, 3262 for BW vs. NL control, and 1228 for HPS vs. NL control (Table 5.11).

Downregulated DEGs also exhibited distinct patterns across the different light treatment comparisons. In the summer growing season, there were 1756, 146, and 94 downregulated DEGs in the comparisons of NB vs. NL control, BW vs. NL control, and HPS vs. NL control, respectively. During the winter growing season, the number of downregulated DEGs increased, with 2073 for NB vs. NL control, 2347 for BW vs. NL control, and 695 for HPS vs. NL control (Table 5.11).

The analysis also revealed the total number of uniquely upregulated and downregulated DEGs across all comparisons. For the summer growing season, there were 2211 unique upregulated DEGs and 1996 unique downregulated DEGs. In comparison, the winter growing season exhibited a higher number of unique DEGs, with 7995 upregulated and 5515 downregulated (Table 5.11). Interestingly, during the summer growing season, the NB vs. NL control comparison had the highest number of upregulated, downregulated, and total DEGs by at least 10-fold over the BW vs. NL control or HPS vs. NL control comparisons. In contrast, the HPS vs. NL control had the lowest number of upregulated, downregulated, and total DEGs. A similar trend was observed during the winter growing season, where the NB vs. NL control had the highest number of upregulated DEGs, while the BW vs. NL control had the highest number of downregulated and total DEGs. The HPS vs. NL control comparison consistently had the lowest number of upregulated, downregulated, and total DEGs for both growing seasons (Table 5.11).

Principal Component Analysis of DEGs

Principal component analysis (PCA) biplots were created to visualize and interpret the inherent structure and relationships among differentially expressed genes (DEGs) in our multidimensional dataset, comparing the supplemental lighting treatments of different spectral qualities with the NL control. The PCA biplots facilitated the projection of the original data onto a reduced-dimensionality space represented by the first two principal components for each respective comparison, which together accounted for a substantial proportion of the total variance in the comparison data.

Figure 5.6 compares the effects of Narrowband 20B/80R supplemental lighting (NB) and natural light (NL) control on plant gene expression. The first principal component (PC1) explained 46% of the total variability, while the second principal component (PC2) accounted for an additional 16%, cumulatively accounting for 62% of the total variance. This reduction in dimensionality allowed us to visualize patterns and trends in the data effectively.

When comparing NB vs NL control, we observed multiple distinct clusters within the PCA biplot. The NL control samples showed a tendency to cluster in the positive PC1 and negative PC2 space (quadrant IV), while NB treatment samples formed a cluster in the positive PC2 space (quadrants I and II). This separation suggests that the two lighting conditions have distinct effects on the DEGs under investigation, with the primary differences driven by the genes with high loadings on PC1 and PC2. The observed clustering pattern indicates that the NB treatment may lead to higher expression levels for the genes with positive loadings on PC2, while the NL control is associated with lower expression levels for these genes. Conversely, the genes with negative loadings on PC2 may show an opposite trend, with the NL control exhibiting higher expression levels than the NB treatment. In addition to the clear separation between the two groups along the

PC2 axis, there is also some degree of separation along the PC1 axis. The NL control cluster in quadrant IV, suggests that this specific subset of the NL control group exhibits higher expression levels for the genes with positive loadings on PC1 and lower expression levels for genes with positive loadings on PC2 compared to the rest of the NL group (Fig. 5.6).

Figure 5.7 compares the effects of Broadband White supplemental lighting (BW) and natural light (NL) control on plant gene expression. The first principal component (PC1) explained 67% of the total variability, while the second principal component (PC2) accounted for an additional 9%, cumulatively accounting for 76% of the total variance.

The NL control samples showed a tendency to cluster in the positive PC1 and negative PC2 space (quadrant IV), while BW treatment samples formed a cluster in both the negative PC1 space and the positive PC1 and positive PC2 space (quadrant I). This separation suggests that the two lighting conditions have distinct effects on the DEGs under investigation, with the primary differences driven by the genes with high loadings on PC1 and PC2. The observed clustering pattern indicates that the NL control may lead to higher expression levels for the genes with positive loadings on PC1 and lower expression levels for those with positive loadings on PC2 compared to the BW treatment group. Conversely, the genes with negative loadings on PC1 may show an opposite trend, with the BW treatment exhibiting higher expression levels than the NL control. The NL control again had a cluster in quadrant IV, which suggests that this specific subset of the NL control group exhibits higher expression levels for the genes with positive loadings on PC1 and lower expression levels for genes with positive loadings on PC2 compared to the rest of the NL group. In the case of the BW treatment group, there is a cluster in the negative PC1 space, specifically in quadrants II and III. The presence of these samples in the negative PC1 space

suggests that some BW-treated samples have gene expression profiles that are less like the NL control group due to the lack of shared negative PC1 attributes (Fig. 5.7).

Figure 5.8 compares the effects of High Pressure Sodium supplemental lighting (HPS) and natural light (NL) control on plant gene expression. The first principal component (PC1) explained 44% of the total variability, while the second principal component (PC2) accounted for an additional 18%, cumulatively accounting for 62% of the total variance.

The NL control samples showed a tendency to cluster in the positive PC1 space (quadrants I and IV), while HPS treatment samples were more widely distributed along the PC1 axis, with two samples clustering in the positive PC1 space (quadrants I and IV) and three samples in the negative PC1 space (quadrants II and III). This separation suggests that the two lighting conditions have distinct effects on the DEGs under investigation, with the primary differences driven by the genes with high loadings on PC1 and PC2. In the positive PC1 space, four NL control samples and two HPS treatment samples formed clusters in quadrants I and IV. This observation indicates that these samples share similarities in their gene expression profiles, with higher expression levels for the genes with positive loadings on PC1 and varying expression levels for those with positive loadings on PC2. In the negative PC1 space, the HPS treatment samples exhibited a wide variance along both the PC1 and PC2 axes. This observed wide variance may suggest that the HPS treatment leads to a more diverse range of gene expression profiles compared to the NL control group. The presence of HPS samples in quadrants II and III indicates that these samples exhibit lower expression levels for the genes with positive loadings on PC1 and varying expression levels for those with positive loadings on PC2 (Fig. 5.8).

Biclustering Heatmaps Comparing DEGs

We performed biclustering analysis on three sets of heat maps, each comparing the top 30 significantly differentially expressed genes (DEGs) between natural light (NL) control and various supplemental light treatments using RNA-seq data. Biclustering heat maps are a powerful tool for visualizing gene expression patterns across experimental conditions, as they enable simultaneous clustering of both genes and samples, revealing meaningful relationships between genes and their corresponding treatments.

Eight visually distinct clusters of DEGs based on the heatmap and hierarchical clustering (Figure 5.9). The NL control and NB treatment groups generally show opposing regulation based on heatmap clusters, indicating that these lighting conditions have distinct effects on gene expression. There is very little difference in gene expression across summer and winter samples, suggesting that the observed DEGs are primarily driven by differences in lighting conditions rather than seasonal variations. Among the top 30 individual genes with the highest significance, there was low variability in expression across different samples within the same treatment type, further emphasizing the consistent impact of the NB treatment on gene expression.

Figure 5.10 presents ten visually distinct clusters of DEGs based on the heatmap and hierarchical clustering. The NL control and BW treatment groups generally exhibit opposing regulation based on heatmap clusters, although not as distinct as the differences observed between NL and NB in Figure 5.9. This finding suggests that the BW treatment may have a more moderate effect on gene expression compared to the NB treatment. Many of the clusters in Figure 5.10 show higher expression levels than those observed in the other two figures. Some variability in expression is observed across different samples, but among the top 30 individual genes with the

highest significance, there is still low variability in expression across different samples within the same treatment type.

Figure 5.11 displays six visually distinct clusters of DEGs based on the heatmap and hierarchical clustering. The NL control and HPS treatment groups generally show opposing regulation based on heatmap clusters, but these differences are the least distinct among the three figures. Many of the clusters exhibit moderate expression levels compared to the other two figures and higher than those observed in the NB vs. NL comparison (Fig. 5.9). Some differences in gene expression are noted across summer and winter samples, indicating that seasonal variations may play a more significant role in this comparison. Among the top 30 individual genes with the highest significance, there is high variability in expression across different samples within the same treatment type, suggesting that the HPS treatment may lead to more diverse gene expression profiles compared to the other treatments.

The analysis of Figures 5.9-5.11 reveals distinct patterns and trends in DEG regulation in response to different light treatments. The most notable observation is the opposing regulation of DEGs between the NL control and each of the supplemental light treatments (NB, BW, and HPS), highlighting the impact of these lighting conditions on gene expression. The degree of distinction between the NL control and each supplemental light treatment varies, with the NB treatment showing the most pronounced differences, followed by the BW treatment, and finally the HPS treatment exhibiting the least distinct differences. This observation suggests that different light treatments may have varying effects on gene expression regulation, with the NB treatment potentially having the most significant impact. In terms of general patterns and trends indicated in Figures 5.9-5.11, we observe that the differences in DEG upregulation and downregulation are dependent on the light treatment comparisons, with the most distinct differences observed in the

NL control vs. NB treatment (Fig. 5.9), followed by NL control vs. BW treatment (Fig. 5.10), and the least distinct differences in NL control vs. HPS treatment (Fig. 5.11).

Volcano Plots Comparing DEGs

We analyzed a set of three volcano plots to investigate the global transcriptional changes in basil plants subjected to different supplemental lighting treatments compared to the Natural Light (NL) control. Volcano plots provide a visual representation of the relationship between fold change and statistical significance (adjusted p-value) for differentially expressed genes (DEGs), with each data point representing a gene. Upregulated genes are indicated by red dots (adjusted p-value < 0.05 and log2 fold change > 1), while downregulated genes are represented by blue dots (adjusted p-value < 0.05 and log2 fold change < -1).

The comparison between the NL control and NB treatment is displayed in Figure 5.12. This plot exhibits the highest number of highly significant upregulated and downregulated genes among the three figures. The plot is not symmetrical, with more upregulated genes than downregulated genes. The right side of the plot (upregulated genes) is wider and taller, indicating a higher density and wider spread of upregulated genes compared to downregulated genes. In contrast, the left side of the plot (downregulated genes) is narrower and shorter. A number of genes exhibit extremely high statistical significance (adjusted p-value higher than 8) in the upregulated group, which is notable compared to the other treatments. These findings suggest that the NB supplemental light treatment has a substantial impact on gene expression regulation, with a general trend toward upregulation of DEGs.

Figure 5.13 compares the NL control with the BW supplemental light treatment. This plot shows a moderate number of highly significant upregulated and downregulated genes. The plot is

somewhat symmetrical, but there is still a higher number of upregulated genes than downregulated genes. The right side of the plot (upregulated genes) is wider and shorter, while the left side (downregulated genes) is narrower and taller. This indicates a higher density and wider spread of upregulated genes compared to downregulated genes. In this figure, some highly significant upregulated and downregulated genes (adjusted p-value higher than 8) are observed, distinguishing it from the other treatments. These results suggest that the BW supplemental light treatment also has a noticeable effect on gene expression regulation, with both upregulated and downregulated DEGs showing high statistical significance.

The comparison between the NL control and HPS treatment is displayed in Figure 5.14. This plot shows a moderate number of significant upregulated and downregulated genes. The plot is somewhat symmetrical, with more upregulated genes than downregulated genes. The right side of the plot (upregulated genes) is slightly wider, while the left side (downregulated genes) is narrower and slightly taller. This suggests a higher density and wider spread of upregulated genes compared to downregulated genes. Notably, there are no genes with an adjusted p-value higher than 8 (extremely significant) in this figure, unlike the other two treatments. Additionally, Figure 5.14 has the lowest number of total DEGs compared to Figures 5.12 and 5.13. These observations indicate that when comparing treatments to the NL control, the NB and BW treatments have higher numbers of more statistically significant DEGs than the HPS treatment.

The appearences of Figures 5.12-5.14 reveals distinct patterns and trends in DEG regulation in response to different supplemental light treatments. The most striking observation is the difference in the number of highly significant upregulated and downregulated genes across the three treatments. NL control vs. NB treatment (Fig. 5.12) exhibits the highest number of DEGs, with a strong trend toward upregulation. In contrast, NL control vs. HPS treatment (Fig. 5.14) has

the lowest number of total DEGs and lacks any extremely significant DEGs. The general patterns and trends indicated in Figures 5.12-5.14 suggest that different light treatments cause varying levels of gene expression regulation. Based on the volcano plots, the NB treatment (Fig. 5.12) appears to have the most significant impact on gene expression, followed by the BW treatment (Fig. 5.13), and finally, the HPS treatment (Fig. 5.14), which has the least pronounced effect.

Discussion

This study aimed to investigate the relationship between basil aroma volatile profiles, transcriptome, and human sensory perception as influenced by various spectral qualities of supplemental light across growing season. Plant volatile organic compounds (PVOCs) are crucial in plant defense mechanisms, signaling, and communication. Additionally, they contribute to plants' aroma and flavor profiles, affecting their sensory perception by humans. To determine how ambient sunlight and supplemental lighting treatments influenced aroma, PVOC leaf tissue concentrations were quantified using HS GC-MS. The results showed that many PVOCs were significantly influenced by growing season, lighting treatment, and season*treatment interactions.

Influence of Season on VOC Profiles

The results of this experiment revealed that the growing season had a substantial impact on the aroma volatile tissue concentrations in basil (Table 5.4-5.5). Several compounds exhibited significantly higher tissue concentrations during the summer growing season compared to the winter season, such as Propanol, trans-2-Pentenal, and 2-ethyl-2-Butenal. Additionally, Methyl Eugenol concentrations were 86% higher during the summer months than in the winter. On the other hand, some compounds had significantly lower tissue concentrations during the summer

growing season compared to the winter season, such as α-Pinene and Camphene. A few compounds exhibited opposing changes across seasons, like (E/Z)-Ocimene; during the summer, (E)-Ocimene tissue concentrations were 20% higher than (Z)-Ocimene concentrations while during the winter, (Z)-Ocimene concentrations were 53% higher than (E)-Ocimene concentrations. A few compounds were only detected during the summer season, such as Eugenol and Citronellyl acetate. Patterns among seasonal variation suggest that the chemical class and metabolic origin of each compound are factors in seasonal variation in VOC profiles.

Because greenhouse conditions stabilized environmental parameters across seasons (Table 5.1), the intensity, daily light integral (DLI), and spectral quality, and daylength of ambient sunlight are isolated variables to be explored. It is unlikely that changes in daylength were a major influence, because basil is known to be non-photoperiodic, and our crops were only grown to vegetative maturity. Further, minor seasonal changes in instantaneous intensity (i.e., no extraordinary fluctuations in intensity due to weather, etc.) are unlikely to cause dramatic concentration increases in secondary metabolism. Assuming intensity is within sufficient and saturation ranges, plants are able to integrate changes to intensity across the day and throughout their life (i.e., average DLI is more indicative of plant quality and yield). These findings suggest that ambient sunlight, specifically changes in spectral quality and cumulative DLI from summer to winter, influences VOC concentrations of basil tissue. There are a number of potential reasons multiple VOCs showed significant tissue concentration variation between seasons.

Seasonal variations in ambient sunlight can affect photosynthesis rates in plants, which in turn impacts secondary metabolism and the production of VOCs (Korczynski et al., 2002; Ouzounis et al., 2015; Faust and Logan, 2018). It is generally accepted that ambient sunlight during summer typically has more favorable spectral quality and DLIs (with a few notable exceptions due

to weather patterns and/or location) (Faust and Logan, 2018). During the summer season in our region (Tennessee, USA), increased DLIs and more favorable spectral qualities will likely increase photosynthetic activity, leading to higher production of primary metabolites and energy, which can be diverted into secondary metabolism pathways responsible for VOC biosynthesis of terpenoids and phenylpropanoids. Higher production of primary metabolisms provides the necessary precursors to synthesize VOCs in greater concentrations; however, if this were the only explanation, all concentrations would have shown relative decreases from the summer to winter season. Because of the patterns observed in this experiment (i.e., patterns between compound class and growing season), there are likely other mechanisms involved.

Seasonal changes in ambient sunlight can also influence plant stress response mechanisms. For example, plants are known to increase the production of secondary metabolites and VOCs in response to environmental stresses, such as drought, pathogens, and herbivory. During winter months in our region (Tennessee, USA), it is common for greenhouse crops to experience unsatisfactory DLIs and unfavorable spectral qualities, which can cause plants to perceive increased stress due to lower photosynthesis rates. The resulting increase in stress hormones may lead to changes in gene expression. A lack of primary metabolic products would cause downstream effects, resulting in the production of different compounds at different concentrations, or lack of production to increase the chances of survival. This could explain some of the observations in this experiment, as multiple VOCs showed significantly lower tissue concentrations during winter months compared to summer months; however, the opposite was true for some compounds, indicating this is only one aspect of the complex interactions between seasonal changes in sunlight and secondary metabolism. Because of this mechanism, it is also likely that different PVOCs

exhibit different responses to seasonal stresses due to their own specific metabolic pathways and stress response.

Changes in ambient sunlight spectral quality from summer to winter can affect the absorption of specific wavelengths of light by plant photoreceptors, such as phytochromes, cryptochromes, and phototropins (Yu et al., 2010; Ballare, 2014; Pardi and Nusinow, 2021). These photoreceptors play essential roles in regulating various aspects of plant growth, development, and stress responses, including the biosynthesis of VOCs. Different light treatments with varying spectral qualities may activate or deactivate specific photoreceptors, leading to changes in VOC concentrations in basil tissue. For example, phytochromes respond to red and far-red light by regulating the expression of many genes related to plant growth (Casal, 2007). Similarly, cryptochromes have the potential to modulate VOC biosynthesis through their roles in light stress responses (Lin and Todo, 2005). Thus, changes in ambient sunlight from summer to winter, specifically changes in spectral quality, can lead to different photoreceptor-mediated responses, resulting in alterations in VOC concentrations.

Influence of Light Treatment on VOC Profiles

This study also found that different spectral qualities of supplemental light treatment affected the tissue concentrations of PVOCs in basil (Tables 5.5 and 5.6). Results showed that several compounds had significantly higher tissue concentrations under the Narrowband 20B/80R treatment as compared to the NL control, including 2-cyclo-Pentane, Phenol, ß-Myrcene, 3-Carene, and Propanol. These compounds are known to be produced by plants in response to environmental stress, and their increase in concentration under the Narrowband 20B/80R treatment may indicate that this treatment induces greater stress than the other treatments.

Dimethyl Sulfide concentrations were significantly higher in the Narrowband 20B/80R treatment than in any other treatment or the NL control. This compound is usually produced during the breakdown of sulfur-containing amino acids in plants, which can be influenced by environmental factors such as light quality. It is possible that the Narrowband 20B/80R treatment enhances the breakdown of sulfur-containing amino acids in plants, leading to a higher concentration of Dimethyl Sulfide. Dimethyl Sulfide is characterized by its potent, pungent scent, evoking earthy, fishy, or sulfuric undertones. Frequently associated with the aroma of cooked cabbage, it serves as an odorant for many common food products. With a high level of bioactivity, Dimethyl Sulfide can be detected in remarkably low concentrations – even below 0.1 ppm – which can prompt negative sensory experiences in humans (Sell, 2019). While increasing the concentrations of some compounds can improve the aroma perception of food products, even minuscule increases to certain compounds may completely throw off the flavor profile or cause customer dissatisfactory. For this reason, it is necessary to use sensory panels to determine overall aroma liking and discrimination of key odorants that are vital to consumer acceptance and preference.

In contrast, 2-ethyl-2-Butenal, (E)-2-Hexenal, and trans-2-Pentenal concentrations were significantly higher in the Broadband White treatment than in any other treatment or the NL control. These compounds are known to be involved in synthesizing plant hormones and are also produced in response to herbivore attacks. It is possible that the Broadband White treatment promotes plant growth and enhances defense mechanisms against herbivores. It is also possible that the other wavelengths stimulated certain pathways or photo-mediated responses that triggered downstream effects to secondary metabolism. 2-ethyl-2-Butenal, (E)-2-Hexenal, and trans-2-Pentenal are all aldehydes with distinct odor notes that contribute to the aroma profiles of various

foods and plants. 2-ethyl-2-Butenal possesses a pungent odor and is often found in small concentrations in various fruits, which can contribute to their overall aroma profile. (E)-2-Hexenal is known for its characteristic "green" odor, (E)-2-Hexenal has a fresh, grassy, and leafy aroma that is reminiscent of freshly cut green leaves or unripe fruits. It is commonly found in a wide range of fruits, vegetables, and herbs, such as apples, tomatoes, and mint, and plays a significant role in forming their unique scents. Finally, trans-2-Pentenal has a pungent, green, and fruity odor with bitter almond and red apple notes (Sell, 2019).

Terpinolene concentrations were increased 3.2-fold under the Broadband White treatment as compared to the NL control, while 3-Menthene was increased 5.1-fold under the Broadband White treatment as compared to the HPS treatment. Terpinolene is a monoterpene that is commonly found in essential oils and is known to have antimicrobial and insecticidal properties. 3-Menthene is also a monoterpene that is known for its antifungal and insecticidal properties (Sell, 2019). This was the only terpinene influenced by light treatment, which likely indicates where in terpinene isomer synthesis pathway in influenced by a combination of spectral quality and DLI.

Linalool and Cycloheptane showed opposite trends in response to light treatments; linalool was detected under all lighting treatments except for the NL control, while Cycloheptane was only detected in plants under the NL control. Linalool is a monoterpene that is commonly found in essential oils and has been reported to have various biological activities, including antimicrobial, anti-inflammatory, and anxiolytic properties. Cycloheptane is a cyclic compound that is not usually found in essential oils. Linalool is described as having floral, sweet, and slightly spicy notes with a hint of citrus. Cycloheptane does not have a notable fragrance, but has a strong petroleum and terpinene odor, and increases the dispersion of other VOCs within a gaseous matrix due to its physical and chemical properties (Sell, 2019). The absence of Cycloheptane under other

lighting treatments may suggest that this compound is not synthesized by higher DLI plants or is influenced by some aspect of spectral quality, while sufficient DLIs and light quality are likely required to produce Linalool at detectable concentrations.

Indole and d-Carvone show similar patterns, with approximately a 5-fold concentration increase under the Broadband White as compared to the NL control. Indole is an aromatic heterocyclic compound that is found in many plant species and has been reported to have various biological activities, including antimicrobial and antitumor properties. d-Carvone is a monoterpene ketone that is mainly found in essential oils and is known for its insecticidal properties. Indole has a floral odor at low concentrations, but at higher concentrations, it smells putrid (Sell, 2019). D-Carvone, on the other hand, has a minty aroma with notes of rye, similar to caraway seeds (Sell, 2019).

Eugenol and Methyl Eugenol followed similar patterns across lighting treatments. Both compounds were detected at similar concentrations between treatments. Further, Eugenol and Methyl Eugenol were not detected under the HPS treatment or the NL control. It is possible that the blue wavelengths provided by the Narrowband and Broadband LEDs promoted the production of these compounds, while the lack of extra blue wavelengths from the HPS and NL control did not promote pathway synthesis to a level that was detectable with our instrumentation. Eugenol is a phenylpropene that is commonly found in essential oils and is known for its antioxidant and analgesic properties. Methyl Eugenol is also a phenylpropene that is mainly found in essential oils and is known for its insecticidal properties (Sell, 2019). These compounds are likely influenced by a combination of spectral quality and DLI; further experimentation is needed to confirm.

Finally, the results showed that the VOC totals were significantly influenced by lighting treatment, with the highest tissue concentrations found under the Narrowband 20B/80R treatment,

and the lowest found under the NL control. This shows that different light qualities can have a significant impact on the overall VOC production in plants. The only pertinent VOC ratio to be significantly influenced by lighting treatment was α/ß-Pinene, with the highest ratio under NL control and the lowest under the HPS treatment. This may indicate that different light qualities can also influence the relative proportion of specific VOC isomers produced by plants.

There are several potential reasons why different compound classes would be differentially influenced under different types of lighting. We speculate that spectral quality is the primary factor for this change in secondary metabolism, as it is a crucial factor in plant physiology. Different wavelengths of light can affect various plant processes, such as photosynthesis, growth, stress responses, and secondary metabolism (Quail et al., 1995; Lin and Shalitin, 2003). Different light treatments with varying spectral qualities may activate specific secondary metabolic pathways, such as isoprenoid and phenylpropanoid metabolism, leading to changes in VOC concentrations in basil tissue. As mentioned earlier, light quality can also influence the activity of plant photoreceptors, which regulate various aspects of plant growth, development, and stress responses, including the biosynthesis of VOCs. Narrowband and broadband lighting treatments may differentially activate or deactivate specific photoreceptors, resulting in changes in VOC production.

The Narrowband 20B/80R treatment uses a specific ratio of blue and red narrowband wavelengths, which has been shown to have an impact on the production of stress-related compounds such as Phenol, ß-Myrcene, and Propanol. This could be due to the fact that red and blue light is critical for plant growth and development as well as many photo-mediated responses. Higher levels of blue light, in particular, have been shown to induce enhanced defense responses in plants against biotic and abiotic stress factors.

In contrast, Broadband White treatment contains a wide range of wavelengths, including blue, green, yellow, and red light. The increase in concentrations of compounds such as 2-ethyl-2-Butenal, (E)-2-Hexenal, and trans-2-Pentenal under this treatment may be due to the broader spectrum of light, which can promote plant growth and enhance defense mechanisms against herbivores.

Different light qualities can also affect the synthesis of specific compounds that have antimicrobial and insecticidal properties, such as Terpinolene, 3-Menthene, Indole, and d-Carvone. The increase in concentrations of Terpinolene and 3-Menthene under the Broadband White treatment may be due to its broad spectrum, which can enhance the synthesis of these compounds. Additionally, Indole and d-Carvone have been reported to have herbicidal and insecticidal properties, respectively, and their synthesis is likely induced by light quality.

Overall, different light qualities can influence the production of different compounds in plants, which can have implications for plant growth, development, and secondary metabolism. Further investigation is needed to understand the underlying mechanisms that govern how different light qualities influence the production of specific compounds in plants. It is pertinent to establish this mechanism to understand further the implications of SL spectral quality in consumer sensory perception of high-value specialty crops, and this can be accomplished by employing molecular techniques such as RNA Seq.

Sensory Panel Analysis

The sensory panel evaluations conducted during summer and winter aimed to assess the influence of season and supplemental lighting type on consumers' overall liking (Table 5.9), overall aroma intensity (Table 5.10), and identification of key odor descriptors (Figs. 5.3 and 5.4).

Results revealed that lighting treatment significantly impacted consumers' overall aroma liking scores, with the NL control receiving the highest scores in both seasons. During the summer, participants favored samples grown under Broadband White, HPS, and NL Control compared to those grown under Narrowband 20B/80R treatment. In contrast, Broadband White and Narrowband 20B/80R treatments received the lowest scores during winter. Interestingly, while significant differences were observed among many compound tissue concentrations, no statistically significant differences were found among consumer aroma intensity scores across lighting treatments and growing seasons (Table 5.10).

Our study investigating the influence of different supplemental lighting on the aroma liking of basil revealed several key findings that warrant further discussion. First, consumers preferred the aroma of the NL control over the NB SL treatment in both seasons. Second, during the summer, this preference was likely caused by the difference in spectral quality. Third, DLI is likely not a significant factor because the two SL treatments had the same DLI supplement and perceived daylength as NB, but did not significantly influence (decrease) overall liking scores. Lastly, during the winter season, NL control was preferred over BW, indicating a clear influence from spectral quality, with HPS not statistically separating from the NL control.

The preference for the NL control's aroma over the NB SL treatment could be attributed to natural sunlight providing a broad spectrum of wavelengths, which may contribute to a more balanced and appealing aroma profile in basil. In contrast, the NB SL treatment delivers specific wavelengths that may alter the aromatic compound production in the plants, leading to a less desirable aroma. Furthermore, spectral quality plays a crucial role in plant development and metabolism, and the observed differences in consumer preferences highlight the importance of considering spectral quality when designing SL strategies for basil production.

Extra light and targeted spectra could have increased the concentration of certain compounds, negatively influencing aroma. B/R wavelengths are known to trigger photoreceptors, which in turn can affect secondary metabolism. Narrowband wavelengths within the visible spectrum, as well as ultraviolet (UV) and far-red (FR), have been shown to influence secondary metabolism in various studies, highlighting the need to better understand how these targeted spectra affect the sensory properties of herbs, including basil.

During the summer season, the preference for the NL control could be explained by the fact that summer sunlight already provides sufficient light for optimal basil growth. The addition of NB treatment during this period might have introduced specific wavelengths that altered the balance of naturally occurring light, leading to changes in the aroma profile that was less appealing to consumers. This finding underscores the need to better understand how different light spectra interact with natural sunlight to optimize supplemental lighting strategies for various crop species and growth stages.

DLI does not appear to significantly influence consumer preferences in our study. The two SL treatments (HPS and BW) had the same DLI supplement and perceived daylength as NB, but they did not negatively influence overall liking scores. This observation suggests that other factors, specifically spectral quality, may be more critical in determining consumer preferences for basil aroma during summer, when DLI and spectral quality are sufficient.

During the winter season, NL control was preferred over BW, indicating a clear influence from spectral quality. Having equal DLIs and perceived daylengths, the primary difference between HPS and BW/NB is the higher ratio of red and far-red wavelengths, which are known to influence secondary metabolism. This finding suggests that the targeted ratio of red and far-red wavelengths in HPS may contribute to its similar preference to the NL control. Winter had better

overall liking score separation, likely because the lighting treatments had a greater influence during the winter than the summer. This can be likely be attributed to reduced DLI and unfavorable spectral quality during the winter season. Despite having sufficient DLI and spectral quality, the effects of supplemental lighting were still observed during the summer, with the NB treatment being the least preferred across both growing seasons. The preference for NL control over NB treatment are likely due to specific aroma volatile compounds being manipulated from NB blue and red wavelengths. The targeted wavelengths in NB treatment are known to influence specific photoreceptors, which can trigger changes in secondary metabolism and directly influence aroma perception, ultimately affecting consumer preferences.

Interesting patterns were uncovered in the concentrations of (E)-Ocimene and (Z)-Ocimene, two important aroma compounds known to contribute to basil's aroma perception. (E)-Ocimene has a warm, herbaceous, citrus, tropical, green, grassy, and woody odor. On the other hand, (Z)-Ocimene has a warm, floral, sweet odor with spicy and earthy undertones (Sell, 2019).

During the summer, (E)-Ocimene tissue concentrations were 20% higher than (Z)-Ocimene concentrations, while during the winter, (Z)-Ocimene concentrations were 53% higher than (E)-Ocimene concentrations. These opposing changes across seasons could be linked to variations in light conditions, with supplemental lighting treatments potentially playing a role in modulating these aroma compound concentrations. Notably, (E)-Ocimene concentration was statistically higher in the NB treatment, whereas (Z)-Ocimene was statistically higher in the NL control (Table 5.6).

The observed differences in (E/Z)-Ocimene concentrations between lighting treatments and seasons suggest that changes in light conditions, such as spectral quality, can influence the production of these aroma compounds and, consequently, overall aroma liking. The targeted

wavelengths in SL treatments, particularly NB, may impact specific photoreceptors and secondary metabolic pathways responsible for the synthesis of (E/Z)-Ocimene.

Notably, the treatments did not impact overall aroma intensity perception, despite the substantial differences in total VOC concentrations across treatments. One potential explanation for this observation could be the sampling variation among panelists, which may have introduced inconsistencies in the perception of aroma intensity. Although present in statistically different concentrations, certain VOCs may not have significantly contributed to the perceived intensity due to their individual odor thresholds or interactions with other aroma compounds.

While various sensory evaluation protocols can be used to determine consumer perception and preference, this experiment focused on orthonasal aroma to reduce participant fatigue, sample carryover, and improve olfactory response comparisons to HS GC-MS data. That being said, it is essential to consider that evaluating basil through consumption, encompassing both retronasal aroma and taste, could reveal additional sensory properties that play a crucial role in consumer preference. It has been shown that humans show a different response to the same odors across routes (Heilmann and Hummel, 2004; Pellegrino et. al, 2021). The complex interplay between aroma and taste, as well as other sensory attributes such as texture and mouthfeel, could provide a more comprehensive understanding of the factors that contribute to the overall appeal of basil in the context of varying light conditions and supplemental lighting treatments. Investigating the role of temporal factors and other environmental factors, such as post-harvest treatment and sampling procedures, could also influence sensory perception.

One important factor to consider is that PVOCs have different bioactivities in humans, and a slight concentration increase of certain compounds can dramatically influence its perception as well as the overall flavor of an herb or high-value specialty crop. In multicomponent aromas, such

as basil, the absence or presence of an odorant is infrequently noticed by humans (Luckett el. al, 2021). While the VOC profile (i.e., relative ratios and quantified concentrations of each VOC produced) can influence human sensory perception, specific odorants influence the perceived aroma profile more than others. The enhancement of some compound concentrations outside of the conventionally occurring relative ratios and quantified concentrations can influence flavor perception or preference, which this study reaffirms. Further, the overall aroma preference of basil can be influenced based on lighting treatment and season, while the overall aroma intensity of basil perception is not.

The correspondence analysis factor map generated using CATA descriptor responses provides insights into the general relationship between basil samples from each lighting treatment and associated CATA responses (Fig. 5.3). Consumers were generally able to discriminate specific odor descriptors that are known to be associated with key basil odorants and important for basil sensory perception. Dimension 1 accounted for 57.93% of the variation in CATA response data, while Dimension 2 accounted for 31.48%. The factor map separated the four lighting treatments into distinct quadrants, associating them with specific odor descriptors. Notably, the Narrowband 20B/80R treatment was associated with descriptors like "anise," "grassy," and "pungent," while the Broadband White treatment was linked to "nutty" and "honey" descriptors.

The observed increase in (E)-Ocimene concentrations under the NB treatment is likely responsible for the "grassy" descriptor associated with this treatment and the subsequent decrease in overall aroma liking. In contrast, the NL control exhibited a stronger association with "fresh" and "spicy" descriptors, which are characteristic aroma notes of (Z)-Ocimene. This can likely be attributed to the higher concentrations of (Z)-Ocimene found in the NL control treatment, resulting in a more appealing aroma profile for consumers.

The CATA descriptor scores successfully predicted overall liking, accounting for over 89.41% of the variance in liking. A total of 11 CATA descriptors surpassed the Variable Importance in Projection threshold set for the Partial Least Squares model (VIP > 0.8), indicating their significance in predicting overall liking (Fig. 5.4). The most influential positive drivers of liking were "fresh" and "flavor intensity." Even though participants could not differentiate overall intensities between lighting treatments or seasons, the PLS model identified "flavor intensity" as a primary driver of liking. Further investigation into the 11 descriptors that were found to be relevant to liking the aroma of basil is necessary. This investigation should focus on optimizing aroma perception through the use of specific SL lighting regimes coordinated with the ambient solar spectrum.

Other moderately influential positive drivers of liking included minty, herbaceous, floral, eucalyptus, and green descriptors. On the other hand, pungent and putrid descriptors were the most negative drivers of liking, with bitter and mushroom descriptors being moderately influential negative drivers. Investigating both positive and negative drivers of liking of aroma perception in high-value specialty crops helps researchers better understand how certain environmental variables, such as lighting regimes, affect overall aroma perception. Commercial growing operations can balance economics and environmental control to meet customer preferences and maximize satisfaction by understanding the factors influencing crop sensory quality. Exploring drivers of liking helps create an accurate model for predicting consumer preferences and provides guidelines for optimizing lighting parameters. This experiment has shown that for future experiments investigating supplemental and sole-source horticultural lighting, it will be imperative to integrate sensory panels to ensure that yields and nutrient content are balanced with aroma, flavor, and sensory perception.

Transcriptome Analysis

RNA sequencing and transcriptomic analyses were used to investigate the impact of SL and ambient spectra on the regulation of secondary metabolism and human sensory perception of basil. Our results revealed a significant number of differentially expressed genes (DEGs) across both summer and winter growing seasons, with distinct patterns of upregulation and downregulation observed across different light treatments (Table 5.11).

The substantial difference in the number of DEGs identified between the summer and winter growing seasons (4207 vs. 13110, respectively) suggests that the spectral quality and DLI of ambient sunlight significantly influence gene expression and secondary metabolism regulation. This finding is supported by previous research showing that environmental conditions can significantly impact plant metabolism and gene expression.

During both summer and winter, he Narrowband 20B/80R (NB) treatment had the highest number of DEGs compared to other supplemental lighting treatments, indicating a more pronounced effect on gene expression. In contrast, the High Pressure Sodium (HPS) treatment exhibited the lowest number of DEGs, suggesting a lesser impact on gene expression.

The least preferred treatment was NB, likely due to a number of transcriptional changes caused by this treatment that led to increases in key odorants, resulting in a decrease in overall liking. This finding highlights the importance of understanding the molecular mechanisms underlying the effect of light quality on secondary metabolism regulation and human sensory perception.

Consumers preferred the Natural Light (NL) control treatment for both growing seasons, despite it having a lower daily light integral compared to SL treatments. This preference could be attributed to the balanced spectrum of natural light, which may lead to a more balanced regulation

of gene expression and secondary metabolite production as opposed to more intense narrowband wavelengths. It is likely that most consumers are accustomed to basil not being grown under narrowband lighting sources, and unusual aroma profiles or perceived off notes directly contribute to overall aroma liking. Based on the observed trends in DEGs, it is evident that different spectral qualities from SL treatments significantly influence gene expression, which in turn influences secondary metabolism and overall aroma liking.

Principal Component Analysis

The principal component analysis (PCA) biplots provided a valuable visualization of the inherent structure and relationships among differentially expressed genes (DEGs) in our multidimensional dataset, comparing SL treatments of different spectral qualities with the natural light (NL) control. Figures 5.6, 5.7, and 5.8 illustrate the PCA biplots comparing the effects of Narrowband 20B/80R (NB), Broadband White (BW), and High Pressure Sodium (HPS) SL treatments to the natural light (NL) control group on plant gene expression. The clustering patterns observed in these biplots suggest that the different lighting treatments impact gene expression in distinct ways, leading to variations in secondary metabolism and aroma liking. For instance, in Figure 5.6, the separation between the NB treatment and NL control along the PC2 axis suggests that the NB treatment may lead to higher expression levels for the genes with positive loadings on PC2, while the NL control is associated with lower expression levels for these genes. This observation indicates that the targeted wavelengths provided by the NB treatment, which primarily consists of blue and red light, may impact specific photoreceptors and secondary metabolic pathways responsible for the synthesis of aroma compounds.

In Figure 5.7, the BW treatment samples formed clusters in quadrants I and III, suggesting that this treatment group exhibits higher expression levels for the genes with positive loadings on both PC1 and PC2 compared to the NL control. Broadband white light has been shown to promote the synthesis of certain secondary metabolites, such as flavonoids and phenolic compounds, due to its ability to provide a more balanced spectrum of light that closely resembles sunlight (Li & Kubota, 2017). This finding implies that the BW treatment may have a positive impact on secondary metabolism and aroma liking by stimulating gene expression and enhancing the production of aroma compounds.

The HPS treatment samples in Figure 5.8 exhibited a wide variance along both the PC1 and PC2 axes, indicating that the HPS treatment leads to a more diverse range of gene expression profiles compared to the NL control group. High Pressure Sodium lighting has been widely used in horticulture for its energy efficiency and effectiveness in promoting photosynthesis; however, its predominantly red and orange wavelengths may have a limited impact on secondary metabolism and aroma liking due to the lack of blue light (Nelson & Bugbee, 2014). The wide variance observed in the HPS-treated samples may suggest that this treatment group has a broader array of secondary metabolite production, potentially leading to varying effects on overall aroma liking.

One notable pattern observed in the PCA biplots was the tendency for the NL control samples to generally cluster in the positive PC1 and negative PC2 locations, while the treatment samples formed clusters in other quadrants. This separation suggests that the specific wavelengths provided by the SL treatments may differentially impact specific photoreceptors and secondary metabolic pathways responsible for the synthesis of aroma compounds. The clustering patterns observed in these biplots suggest that the different lighting treatments impact gene expression in distinct ways, leading to variations in secondary metabolism and aroma liking.

Variation across PCA biplots demonstrates different spectral qualities of supplemental lighting treatments significantly impact gene expression in plants, which in turn influences secondary metabolism and overall aroma liking. The NB treatment was found to be most effective at stimulating gene expression and enhancing secondary metabolite production, leading to the highest concentrations of myrcene and ocimene. The BW treatment also showed a positive impact on secondary metabolism, while the HPS treatment led to a more diverse range of gene expression profiles and secondary metabolite production. These findings contribute to our understanding of the role of the light spectrum in shaping plant growth and quality and have practical implications for optimizing lighting strategies in controlled environment agriculture to improve the sensory attributes of plant-derived products. Further experiments are needed to verify gene functionality in *Ocimum basilicum* and to explore the potential of other SL treatments in modulating secondary metabolism and aroma liking.

Biclustering Heat Maps and Volcano Plots

Our findings revealed distinct patterns and trends in differentially expressed genes (DEGs) regulation in response to various light treatments. The most notable observation is the opposing regulation of DEGs between the NL control and each of the supplemental light treatments (NB, BW, and HPS), highlighting the impact of these lighting conditions on gene expression. The degree of distinction between the NL control and each supplemental light treatment varies, with the NB treatment showing the most pronounced differences (Fig. 5.9), followed by the BW treatment (Fig. 5.10), and finally, the HPS treatment exhibiting the least distinct differences (Fig. 5.11). This observation suggests that different light treatments may have varying effects on gene expression regulation, with the NB treatment potentially having the most significant impact.

NL control vs. NB treatment had the most substantial effect on gene expression compared to the other treatments. The intensity of expression (significance) of the top 30 genes is moderate compared BW, likely because the NB treatment influenced a wider range of the genome, but not significantly, which profoundly aroma. Blue light has been reported to influence secondary metabolism and promote the production of terpenoid and phenylpropanoid compounds.

Compared to the NB treatment, the NL control vs. BW treatment displayed a more moderate effect on gene expression. This observation could be attributed to the presence of all wavelengths in the white light spectrum, resulting in a more balanced regulation of plant growth and development. Moreover, broadband white light, as well as targeted wavelengths within broadband white light, have been reported to promote secondary metabolism in some plant species.

The least distinct differences were observed with the NL control vs. HPS treatment comparison. This finding may be attributed to the fact that HPS light contains mostly orange and red wavelengths, which are known to influence photosynthesis and plant biomass production primarily. However, HPS light lacks the blue wavelength, which plays a crucial role in secondary metabolism regulation. Our analysis also revealed that seasonal variations played a more significant role in the NL control vs. HPS treatment comparison, indicating that environmental factors may also influence gene expression and secondary metabolism.

Volcano plots confirm these distinct patterns and trends in differentially expressed genes (DEGs), the most notable observation being the opposing regulation of DEGs between the NL control and each of the supplemental light treatments (NB, BW, and HPS), highlighting the impact of these lighting conditions on gene expression. The degree of distinction between the NL control and each supplemental light treatment varies, with the NB treatment showing the most pronounced

differences, followed by the BW treatment, and finally, the HPS treatment exhibiting the least distinct differences.

The observed differences in DEG regulation among various light treatments suggest that the spectral qualities of supplemental lighting play a vital role in modulating gene expression, which in turn influences secondary metabolism and overall aroma liking. For example, the NB treatment, which exhibited the most distinct differences in DEG regulation compared to the NL control, could potentially lead to enhanced production of secondary metabolites and improved aroma quality due to the synergistic effects of blue and red light on plant physiology and biochemistry. On the other hand, the HPS treatment, which showed the least distinct differences in DEG regulation, may have a more limited impact on secondary metabolism and aroma liking due to its predominantly red and orange wavelengths.

Supplemental Lighting Influences Key Odorants and Sensory Perception

The concentrations of (E/Z)-Ocimene in plants varied based on lighting treatments and seasons, likely from changes to perceived spectral quality. During the summer, (E)-Ocimene tissue concentrations were 20% higher than (Z)-Ocimene concentrations, while during winter, (Z)-Ocimene concentrations were 53% higher than (E)-Ocimene concentrations. Interestingly, (E)-Ocimene concentration was statistically higher in the NB treatment, whereas (Z)-Ocimene was statistically higher in the NL control. This observation indicates that targeted wavelengths in SL treatments, particularly blue/red (NB), may impact specific photoreceptors and secondary metabolic pathways responsible for the synthesis of (E/Z)-Ocimene.

Further, ß-Myrcene concentrations were found to be highest in the B/R treatment, with a 4.9x increase over the NL control. Functional annotations revealed several DEGs involved in

monoterpene synthesis were significantly up-regulated in the B/R treatment compared to the NL control. Specifically, a gene that encodes for fenchol synthase (FES), an important enzyme used in the synthesis of downstream myrcene and ocimene isomers, was only up-regulated (2.1 log2 FC) in the B/R treatment. Increased expression of FES likely explains the increased ß-Myrcene concentrations and (E/Z)-Ocimene, as well as (E/Z)-Ocimene opposing ratios found across treatments. Based on the results of the sensory evaluation, it is likely that these compounds are responsible for the change in overall aroma perception.

The observed differences in gene expression and secondary metabolite production among lighting treatments suggest that spectral quality plays a crucial role in modulating plant growth, secondary metabolism, and overall aroma liking. For instance, the NB treatment, which exhibited the most distinct differences in DEG regulation compared to the NL control, likely lead to enhanced production of secondary metabolites, such as myrcene and ocimene, due to the synergistic effects of blue and red light on physiology and photoresponses. In contrast, the HPS treatment, which showed the least distinct differences in DEG regulation, may have a more limited impact on secondary metabolism and aroma liking due to its predominantly red and orange wavelengths.

Limitations and Future Outlooks

Several analytical chemistry techniques, procedures, and instruments have been developed to identify and quantify important aroma-active compounds. Each method has specific benefits and limitations. Static headspace sampling is a volatile technique commonly used with GC-MS. This technique is performed by placing a sample in a glass tube, applying standardized heat/vibration in some cases, and sampling the equalized headspace over the sample (commonly

using helium or another inert gas for MS). Dynamic headspace sampling is similar, but the headspace is purged with a sizeable known volume of gas and removes a higher concentration of volatiles from the sample. Compounds volatilize into the headspace in an attempt to reach equilibrium as the gas purges the headspace causing disequilibrium, and volatile compounds are directed from the headspace sampler to the GC injection port (Alam, 2012).

Headspace sampling has a wide range of uses and can be paired with many detector types depending on the analysis goals. This is particularly useful for metabolomics and biochemistry research to determine the manipulation of pathways or resource allocation in response to environmental stimuli. In addition, some separation/extraction methods have shown bias and have varying extraction efficiencies toward certain compounds, which could cause issues with the analysis (Loughrin and Kasperbauer, 2003; Alam, 2012; Ochiai et al., 2014).

One of the critical drawbacks is that headspace sampling may not pick up all aroma active odorants in a particular matrix. For this reason, various techniques should be employed before analyzing compounds because of their physical/chemical properties. Most volatiles are unstable and will transform/degrade when exposed to high temperatures. This includes when headspace samples enter the GC inlet. Some volatile compounds are not stable, even at room temperature. Stabilization of key volatiles with other extraction methods has the potential for more reproducible results in this respect (Loughrin and Kasperbauer, 2003; Pourmortazavi and Hajimirsadeghi, 2007; Alam, 2012; Ochiai et al., 2014).

Headspace sampling is also not indicative of sensory perception unless paired with olfactometry or other sensory evaluation procedures. To get the most accurate understanding of aroma (and flavor), it is best to use multiple analytical and sensory techniques. Compounds with lower volatility will not be released at the same rate as high-volatility compounds, which may

cause bias (Meligaard et al., 2007; Lawless, 2010). If headspace is saturated over a sample, some other volatiles with lower vapor pressures may not have the ability to volatilize. This may cause a bias towards samples with high concentrations and high vapor pressures, even though these compounds may not produce a significant flavor response (one benefit of dynamic headspace over static). Metabolism of plants does not end after harvest, and poor sampling techniques could introduce variation into datasets (Buchanan, 2015). Immediate freezing is recommended to halt metabolism for plants and other biological samples, but extreme temperatures or rapid changes in temperatures may cause chemical degradation or alteration to the key compounds in the sample. Unequal treatment of each sample in terms of time in/out freezer, handling samples, etc., can also introduce unwanted variation (Taylor, 1996; Lawless, 2010). Optimization of sampling methods, extraction techniques, and column chemistries to obtain higher recovery/fewer variable results when analyzing key compounds is commonplace and recommended. It is always best to use multiple extraction protocols, instruments, and sampling methods to compare all aroma active compounds (Taylor, 1996; Bayramoglu et al., 2008; Alam, 2012; Selli et al., 2014)

It would be interesting to investigate the molecular mechanisms underlying the observed changes in VOC concentrations under different lighting treatments and growing seasons. This could involve examining the expression levels of genes involved in isoprenoid and phenylpropanoid metabolism, as well as the activity of rate-limiting enzymes in these pathways. Exploring the impact of other environmental factors, such as temperature, humidity, and CO2 levels, on VOC production in basil and other crops could provide a more comprehensive understanding of the factors influencing aroma and flavor profiles.

In this study, the effects of daylength and light intensity could not be separated due to the inherent nature of greenhouse production and supplemental lighting experiments. Future research

should conduct tandem growth chamber experiments to verify the effects of different intensities and treatments. Additionally, the results obtained in this study are species-specific, and further research on more crops is required to verify the observed trends.

The current experiment utilized continuous low-intensity light supplements, which have the potential to manipulate secondary metabolite bioaccumulation while efficiently increasing crop DLI. However, different crops may experience deleterious effects when using continuous low-intensity light supplements. Increasing the intensity and/or manipulating the duration of SL also has the potential to differentially influence secondary metabolic profiles and should be further evaluated under greenhouse and growth chamber conditions. Narrowband B/R wavelengths have been shown to increase total and specific VOC concentrations, but further exploration into discrete narrowband wavelengths at varying ratios is warranted. This could be used to push certain secondary metabolic pathways that could be used to improve flavor, the concentration of phytonutrients, human health benefits, and marketability.

Conclusions

This study demonstrates that both growing season and lighting treatment have significant effects on PVOC tissue concentrations in basil. Using HS GC-MS, we were able to quantify differences in key basil aroma volatiles across seasons and treatments. Sensory panel evaluations were able to discern overall aroma liking and key odorants, preferring the NL control over the NB treatment. RNA Seq identified significant DEGs in relation to basil secondary metabolism and sensory perception. Understanding the factors that influence VOC production and their underlying mechanisms can help optimize plant growth conditions and improve the sensory perception of basil and other high-value specialty crops. Further research is warranted to validate these findings

and explore the potential implications of specific VOCs identified in each comparison on plant physiology, development, and sensory perception. Sensory panels should be incorporated when investigating the influence of environmental control on crop physiology, specifically supplemental and sole source horticultural lighting. A multidisciplinary approach using a variety of analytical, sensory, and molecular techniques would allow for greater insight into the complex interactions between light, plant physiology, and human sensory perception.

References

Alam, M.A., M; Asif, H. (2012). *Textbook of Practical Analytical Chemistry.* London: Elsevier Health Sciences APAC.

Ballare, C.L. (2014). Light regulation of plant defense. *Annu Rev Plant Biol* 65**,** 335-363. doi: 10.1146/annurev-arplant-050213-040145.

Barickman, T.C., Kopsell, D.A., and Sams, C.E. (2017). Effects of abscisic acid and calcium on tomato fruit aroma volatiles. *Journal of Plant Nutrition* 40(14)**,** 2096-2100. doi: 10.1080/01904167.2017.1318919.

Bayramoglu, B., Sahin, S., and Sumnu, G. (2008). Solvent-free microwave extraction of essential oil from oregano. *Journal of Food Engineering* 88(4)**,** 535-540. doi: 10.1016/j.jfoodeng.2008.03.015.

Bian, Z., Wang, Y., Zhang, X., Grundy, S., Hardy, K., Yang, Q., et al. (2021). A Transcriptome Analysis Revealing the New Insight of Green Light on Tomato Plant Growth and Drought Stress Tolerance. *Front Plant Sci* 12**,** 649283. doi: 10.3389/fpls.2021.649283.

Buchanan, B.G., W.; Jones, R. (2015). *Biochemistry and Molecular Biology of Plants, Second Edition.* Wiley Blackwell.

Carvalho, S.D., Schwieterman, M.L., Abrahan, C.E., Colquhoun, T.A., and Folta, K.M. (2016). Light Quality Dependent Changes in Morphology, Antioxidant Capacity, and Volatile Production in Sweet Basil (*Ocimum basilicum*). *Front Plant Sci* 7**,** 1328. doi: 10.3389/fpls.2016.01328.

Casal, J.J. (2007). Phytochromes, Cryptochromes, Phototropin: Photoreceptor Interactions in Plants. *Photochemistry and Photobiology* 71(1)**,** 1-11. doi: 10.1562/0031-8655(2000)0710001pcppii2.0.Co2.

Faust, J.E., and Logan, J. (2018). Daily light integral: A research review and high-resolution maps of the United States. *HortScience* 53(9)**,** 1250-1257.

Garcia-Caparros, P., Chica, R., Almansa, E., Rull, A., Rivas, L., García-Buendía, A., et al. (2018). Comparisons of Different Lighting Systems for Horticultural Seedling Production Aimed at Energy Saving. *Sustainability* 10(9)**,** 3351. doi: 10.3390/su10093351.

Gonda, I., Faigenboim, A., Adler, C., Milavski, R., Karp, M.J., Shachter, A., et al. (2020). The genome sequence of tetraploid sweet basil, *Ocimum basilicum* L., provides tools for advanced genome editing and molecular breeding. *DNA Res* 27(5). doi: 10.1093/dnares/dsaa027.

Hammock, H.A., and Sams, C.E. (2023). Variation in supplemental lighting quality influences key aroma volatiles in hydroponically grown 'Italian Large Leaf' basil. *Frontiers in Plant Science* 14. doi: 10.3389/fpls.2023.1184664.

Hasan, M.M., Bashir, T., Ghosh, R., Lee, S.K., and Bae, H. (2017). An Overview of LEDs' Effects on the Production of Bioactive Compounds and Crop Quality. *Molecules* 22(9). doi: 10.3390/molecules22091420.

Heilmann S, Hummel T. 2004. A new method for comparing orthonasal and retronasal olfaction. Behav Neurosci. 118(2):412–419.

Hiltunen, R., and Holm, Y. (2003). *Basil: The Genus Ocimum.* Amsterdam: CRC Press.

Kivimaenpa, M., Mofikoya, A., Abd El-Raheem, A.M., Riikonen, J., Julkunen-Tiitto, R., and Holopainen, J.K. (2022). Alteration in Light Spectra Causes Opposite Responses in Volatile Phenylpropanoids and Terpenoids Compared with Phenolic Acids in Sweet Basil (Ocimum basilicum) Leaves. *J Agric Food Chem* 70(39)**,** 12287-12296. doi: 10.1021/acs.jafc.2c03309.

Korczynski, P.C., Logan, J., and Faust, J.E. (2002). Mapping Monthly Distribution of Daily Light Integrals across the Contiguous United States. *HortTechnology* 12(1)**,** 12-16. doi: 10.21273/horttech.12.1.12.

Kumar, Y., Khan, F., Rastogi, S., and Shasany, A.K. (2018). Genome-wide detection of terpene synthase genes in holy basil (Ocimum sanctum L.). *PLoS One* 13(11)**,** e0207097. doi: 10.1371/journal.pone.0207097.

Lauria, G., Lo Piccolo, E., Davini, A., Ruffini Castiglione, M., Pieracci, Y., Flamini, G., et al. (2023). Modulation of VOC fingerprint and alteration of physiological responses after supplemental LED light in green- and red-leafed sweet basil (Ocimum basilicum L.). *Scientia Horticulturae* 315. doi: 10.1016/j.scienta.2023.111970.

Lawless, H.H., H. (2010). *Sensory Evaluation of Food.* SpringerLink.

Lee, S.J., Umano, K., Shibamoto, T., and Lee, K.G. (2005). Identification of volatile components in basil (*Ocimum basilicum* L.) and thyme leaves (*Thymus vulgaris* L.) and their antioxidant properties. *Food Chemistry* 91(1)**,** 131-137. doi: 10.1016/j.foodchem.2004.05.056.

Lin, C., and Shalitin, D. (2003). Cryptochrome structure and signal transduction. *Annu Rev Plant Biol* 54**,** 469-496. doi: 10.1146/annurev.arplant.54.110901.160901.

Lin, C., and Todo, T. (2005). The cryptochromes. *Genome Biol* 6(5)**,** 220. doi: 10.1186/gb-2005-6-5-220.

Litvin, A.G., Currey, C.J., and Wilson, L.A. (2020). Effects of Supplemental Light Source on Basil, Dill, and Parsley Growth, Morphology, Aroma, and Flavor. *J. Am. Society for Hortic. Sci* 145(1)**,** 18-29.

Loughrin, J.H., and Kasperbauer, M.J. (2003). Aroma content of fresh basil (*Ocimum basilicum* L.) leaves is affected by light reflected from colored mulches. *J Agric Food Chem* 51(8)**,** 2272-2276. doi: 10.1021/jf021076c.

Luckett, C. R., Pellegrino, R., Heatherly, M., Alfaro Martinez, K., Dein, M., & Munafo, P. J. (2021). Discrimination of complex odor mixtures: a study using wine aroma models. Chemical Senses, 46.

Meligaard, M., Civile, G.V., and Carr, B.T. (2007). *Sensory Evaluation Techniques, Fourth Edition* CRC Press.

Ochiai, N., Tsunokawa, J., Sasamoto, K., and Hoffmann, A. (2014). Multi-volatile method for aroma analysis using sequential dynamic headspace sampling with an application to brewed coffee. *J Chromatogr A* 1371**,** 65-73. doi: 10.1016/j.chroma.2014.10.074.

Ouzounis, T., Rosenqvist, E., and Ottosen, C.O. (2015). Spectral Effects of Artificial Light on Plant Physiology and Secondary Metabolism: A Review. *Hortscience* 50(8)**,** 1128-1135.

Pardi, S.A., and Nusinow, D.A. (2021). Out of the Dark and Into the Light: A New View of Phytochrome Photobodies. *Front Plant Sci* 12**,** 732947. doi: 10.3389/fpls.2021.732947.

Pattison, P.M., Tsao, J.Y., Brainard, G.C., and Bugbee, B. (2018). LEDs for photons, physiology and food. *Nature* 563(7732)**,** 493-500. doi: 10.1038/s41586-018-0706-x.

Pennisi, G., Blasioli, S., Cellini, A., Maia, L., Crepaldi, A., Braschi, I., et al. (2019). Unraveling the Role of Red:Blue LED Lights on Resource Use Efficiency and Nutritional Properties of Indoor Grown Sweet Basil. *Front Plant Sci* 10**,** 305. doi: 10.3389/fpls.2019.00305.

Pellegrino, R., Hörberg, T., Olofsson, J., & Luckett, C. R. (2021). Duality of smell: route-dependent effects on olfactory perception and language. Chemical Senses, 46, bjab025.

Pourmortazavi, S.M., and Hajimirsadeghi, S.S. (2007). Supercritical fluid extraction in plant essential and volatile oil analysis. *J Chromatogr A* 1163(1-2)**,** 2-24. doi: 10.1016/j.chroma.2007.06.021.

Quail, P.H., Boylan, M.T., Parks, B.M., Short, T.W., Xu, Y., and Wagner, D. (1995). Phytochromes: photosensory perception and signal transduction. *Science* 268(5211)**,** 675-680. doi: 10.1126/science.7732376.

Sell, C.S. (2019). *Fundamentals of Fragrance Chemistry.* Wiley.

Selli, S., Kelebek, H., Ayseli, M.T., and Tokbas, H. (2014). Characterization of the most aroma-active compounds in cherry tomato by application of the aroma extract dilution analysis. *Food Chem* 165**,** 540-546. doi: 10.1016/j.foodchem.2014.05.147.

Singh, D., Basu, C., Meinhardt-Wollweber, M., and Roth, B. (2015). LEDs for energy efficient greenhouse lighting. *Renewable and Sustainable Energy Reviews* 49**,** 139-147. doi: 10.1016/j.rser.2015.04.117.

Sipos, L., Boros, I.F., Csambalik, L., Székely, G., Jung, A., and Balázs, L. (2020). Horticultural lighting system optimalization: A review. *Scientia Horticulturae* 273. doi: 10.1016/j.scienta.2020.109631.

Tang, D., Huang, Q., Wei, K., Yang, X., Wei, F., and Miao, J. (2021). Identification of Differentially Expressed Genes and Pathways Involved in Growth and Development of Mesona chinensis Benth Under Red- and Blue-Light Conditions. *Front Plant Sci* 12**,** 761068. doi: 10.3389/fpls.2021.761068.

Taylor, A.J. (1996). Volatile flavor release from foods during eating. *Crit Rev Food Sci Nutr* 36(8)**,** 765-784. doi: 10.1080/10408399609527749.

Trivellini, A., Toscano, S., Romano, D., and Ferrante, A. (2023). The Role of Blue and Red Light in the Orchestration of Secondary Metabolites, Nutrient Transport and Plant Quality. *Plants* 12(10). doi: 10.3390/plants12102026.

Urrestarazu, M., Nájera, C., and Gea, M.d.M. (2016). Effect of the Spectral Quality and Intensity of Light-emitting Diodes on Several Horticultural Crops. *HortScience* 51(3)**,** 268-271. doi: 10.21273/hortsci.51.3.268.

Walters, K.J., Lopez, R.G., and Behe, B.K. (2020). Leveraging Controlled-Environment Agriculture to Increase Key Basil Terpenoid and Phenylpropanoid Concentrations: The Effects of Radiation Intensity and CO(2) Concentration on Consumer Preference. *Front Plant Sci* 11**,** 598519. doi: 10.3389/fpls.2020.598519.

Yu, X., Liu, H., Klejnot, J., and Lin, C. (2010). The Cryptochrome Blue Light Receptors. *Arabidopsis Book* 8**,** e0135. doi: 10.1199/tab.0135.

Appendix E

Table 5.1. Important environmental parameters across growing cycles. All crops grown under greenhouse conditions at The University of Tennessee Institute of Agriculture (UTIA) in Knoxville, TN, USA (35°56'44.5"N, 83°56'17.3"W).

	Summer	**Winter**
Growing Period	7/7/21-8/23/21	12/21/21-02/08/22
Average Day Temp (°C)	28.9	27.1
Average Night Temp (°C)	21.6	20.7
Average Relative Humidity	55%	50%
Average Daily Light Integral (DLI) ($mol \cdot m^{-2} \cdot d^{-1}$)	13.21	7.11
Average Day Length (hours)	13:41	9:50

Table 5.2. Summary of statistical results for pertinent aroma volatile compounds detected using headspace gas chromatography-mass spectrometry.

			F Value			Pr > F		
Compound Name	**CAS**	**RT (min)**	Experiment	Treatment	Experiment*Treatment	Experiment	Treatment	Experiment*Treatment
Propanal	123-38-6	2.099	6.75	2.41	0.69	0.0100	0.0077	0.7470
Dimethyl Sulfide	75-18-3	2.234	1.70	3.32	1.29	0.1943	0.0003	0.2340
2-methyl Furan	534-22-5	2.834	n.d.	n.d.	n.d.	0.0040	0.2561	0.3844
2-ethyl-Furan	3208-16-0	3.840	8.46	1.25	1.07	0.0040	0.2561	0.3844
(Z)-2-Penten-1-ol	1576–95–0	4.488	n.d.	n.d.	n.d.	n.d.	n.d.	n.d.
Dimethyl Disulfide	624-92-0	4.804	n.d.	n.d.	n.d.	n.d.	n.d.	n.d.
(E)-2-Pentenal	1576-87-0	5.504	n.d.	n.d.	n.d.	n.d.	n.d.	n.d.
1-Pentanol	71-41-0	5.504	n.d.	n.d.	n.d.	n.d.	n.d.	n.d.
trans-2-Pentenal	1576-87-0	6.103	10.75	4.76	2.38	0.0012	0.0001	0.0086
Ethanol, 2-Mercapto-	60-24-2	6.162	n.d.	n.d.	n.d.	n.d.	n.d.	n.d.
Hexanal	66-25-1	7.271	n.d.	n.d.	n.d.	n.d.	n.d.	n.d.
(Z)-3-Heptene	7642-10-6	7.447	n.d.	n.d.	n.d.	n.d.	n.d.	n.d.
2-ethyl-2-Butenal	19780-25-7	7.862	7.00	4.87	1.26	0.0088	0.0001	0.2481
(E)-2-Hexenal	6728-26-3	8.255	2.00	5.07	1.65	0.1587	0.0001	0.0883
(E)-3-Hexen-1-ol	928-96-1	8.877	n.d.	n.d.	n.d.	n.d.	n.d.	n.d.
1-Hexanol	111-27-3	9.951	n.d.	n.d.	n.d.	n.d.	n.d.	n.d.
α-Pinene	80-56-8	11.670	14.34	1.15	1.14	0.0002	0.1287	0.3281
Camphene	79-92-5	11.671	14.34	1.51	1.61	0.0002	0.0686	0.0579
Benzaldehyde	100-52-7	12.101	40.76	1.43	2.27	0.0001	0.1620	0.0125
2-cyclopropyl-Pentane	5458-16-2	12.251	2.14	2.01	2.06	0.1453	0.0289	0.0246
Dimethyl Trisulfide	3658-80-8	12.505	n.d.	n.d.	n.d.	n.d.	n.d.	n.d.
β-Pinene	18172-67-3	13.065	3.51	2.26	2.02	0.0625	0.0130	0.0278
1-Octen-3-ol	3391-86-4	13.080	2.09	1.39	0.51	0.1505	0.1788	0.8937
1,4-Octadiene	5675-25-2	13.106	21.47	1.49	1.25	0.0001	0.1372	0.2555
Phenol	108-95-2	13.150	2.85	2.34	2.00	0.0928	0.0100	0.0296
ß-Myrcene	123-35-3	13.256	n.d.	2.36	0.77	0.9960	0.0090	0.6728
3-Carene	13466-78-9	13.329	0.01	2.47	0.75	0.9282	0.0064	0.6855
2-pentyl-Furan	3777-69-3	13.370	0.44	2.93	2.13	0.5083	0.0013	0.0196
Cyclohexane, isocyanato-	3173-53-3	13.474	1.00	1.00	1.00	0.3185	0.4476	0.4476
(E,E)-2,4-Heptadienal	4313-03-5	14.028	0.05	1.54	1.65	0.8295	0.1208	0.8380
Formamide, N-phenyl-	26944-32-1	14.225	0.45	4.27	0.39	0.5020	<.0001	0.9595
2-Isobutylthiazole	18640-74-9	14.816	0.52	2.49	1.39	0.4711	0.0060	0.1797
(R)+Limonene	5989-27-5	14.918	10.19	1.99	2.73	0.0016	0.0305	0.0026
1,3,6-Octatriene, 3,7-dimethy-, (E)	3779-61-1	14.920	7.77	1.96	2.65	0.0058	0.0336	0.0034
(S)-Limonene	5989-54-8	14.941	6.36	1.95	2.60	0.0124	0.0349	0.0040
Eucalyptol	470-82-6	14.949	7.79	1.97	2.65	0.0057	0.0333	0.0034
2-Octyn-1-ol	20739-58-6	14.987	n.d.	n.d.	n.d.	n.d.	n.d.	n.d.
Benzeneacetaldehyde	122-78-1	15.132	2.95	1.88	2.64	0.0872	0.0429	0.0035
3-ethyl-Benzaldehyde	34246-54-3	15.599	1.43	1.17	0.37	0.2331	0.3103	0.9664
α-Terpinene	99-86-5	15.915	0.01	1.46	1.05	0.9066	0.1494	0.4064
Benzamide	55-21-0	16.070	0.67	1.04	1.91	0.4152	0.4135	0.0394
Decane	124-18-5	16.858	2.62	1.36	0.96	0.1069	0.1955	0.4809
Terpinolene	586-62-9	16.865	1.23	3.60	3.92	0.2677	0.0001	<.0001
Sabinene hydrate	546-79-2	16.868	0.48	1.43	0.86	0.4897	0.1595	0.5805
Nonanal	124-19-6	17.034	0.50	1.43	0.85	0.4792	0.1608	0.5895
Linalool	78-70-6	17.272	0.06	1.18	0.60	0.8123	0.2999	0.8314
Fenchyl acetate	13851-11-1	17.314	17.02	1.92	1.64	<.0001	0.0385	0.0889
Ethanol, 2-phenyl-	60-12-8	17.745	n.d.	2.50	3.00	0.9542	0.0057	0.0010
1,5-Decadiyne	53963-03-4	18.065	1.46	1.12	1.67	0.2283	0.3446	0.0819
trans-Pinocarveol	1674-08-4	18.081	1.83	2.99	1.86	0.1776	0.0010	0.0462
3-Menthene	500-00-5	18.226	1.79	2.59	1.81	0.1818	0.0041	0.0542
Sulfamoxole	729-99-7	18.661	n.d.	n.d.	n.d.	n.d.	n.d.	n.d.
3-Caren-10-al	14595-13-2	18.812	1.35	1.32	1.54	0.2470	0.2139	0.1185
Isoborneol	507-70-0	18.946	3.94	1.75	1.60	0.0485	0.0651	0.1015
Cycloheptene	628-92-2	18.962	1.05	1.16	0.46	0.3064	0.3191	0.9265
p-Menth-1-en-8-ol	98-55-5	19.646	23.79	1.55	2.05	<.0001	0.1150	0.0256
Methyl Salicylate	119-36-8	19.745	65.69	1.21	1.28	<.0001	0.2825	0.2399
2-methyl-2-Hepten-4-yne	58275-91-5	19.765	46.60	1.26	1.53	<.0001	0.2470	0.1223
1,3-cis,5-cis-Octatriene	40087-62-5	19.822	0.70	1.01	0.99	0.4046	0.4351	0.4524
p-allyl-Anisole	140-67-0	19.879	1.00	1.00	1.00	0.3176	0.4475	0.4476
Nonylcyclopropane	74663-85-7	20.247	5.17	2.85	3.25	0.0240	0.0017	0.0004
Ethanol, 2-phenoxy-	122-99-6	20.605	n.d.	n.d.	n.d.	n.d.	n.d.	n.d.
Benzenepropanenitrile	645-59-0	21.072	1.00	1.00	1.00	0.3185	0.4476	0.4476
d-Carvone	2244-16-8	21.161	17.97	1.84	2.23	<.0001	0.0489	0.0140
Indole	120-72-9	22.615	18.77	1.99	1.91	<.0001	0.0304	0.0392
1-Octene	111-66-0	23.274	9.51	0.80	2.33	0.0023	0.6372	0.0102
2,6-dimethyl-2,6-Octadiene	2792-39-4	24.139	n.d.	n.d.	n.d.	n.d.	n.d.	n.d.
Eugenol	97-53-0	24.289	7.03	0.91	0.91	0.0086	0.5353	0.5353
Citronellyl acetate	150-84-5	24.552	75.61	1.88	1.08	<.0001	0.0434	0.3796
Methyl Eugenol	93-15-2	25.901	10.58	1.16	1.20	0.0013	0.3136	0.2857
Humulene	6753-98-6	27.263	1.00	1.00	1.00	0.3185	0.4476	0.4476
1,4-Heptadiene	5675-22-9	29.658	0.13	1.66	0.85	0.7174	0.0855	0.5867

Table 5.3. Summary of statistical results for aroma volatile organic compound (VOC) total concentration and pertinent (VOC) ratios detected using headspace gas chromatography-mass spectrometry.

	F Value			Pr > F		
Compound	Experiment	Treatment	Experiment* Treatment	Experiment	Treatment	Experiment* Treatment
VOC Total	1.23	7.90	1.35	0.9607	0.0031	0.1989
α/β-Pinene Ratio	11.64	7.15	3.02	0.0008	<.0001	0.0009
R+/S-Limonene Ratio	0.28	0.89	0.85	0.5981	0.5483	0.5948
(E/Z)-Ocimene Ratio	1.45	2.33	1.68	0.2301	0.0101	0.0797
α-Terpinene/Total Terpinenes	0.51	1.10	1.33	0.4756	0.3598	0.209
γ-Terpinene/Total Terpinenes	5.16	1.24	1.45	0.0241	0.2606	0.1525
Terpinolene/Total Terpinenes	2.66	1.17	1.42	0.1044	0.3074	0.1674
Terpinene Total (α+β+δ)	5.15	1.08	1.34	0.0421	0.0011	0.0005

Table 5.4. Influence of growing season on aroma volatile tissue concentrations in hydroponically grown greenhouse sweet basil (*Ocimum basilicum* var. Genovese).

	Growing Season	
Compound Name	**Summer**	**Winter**
Propanal	0.185 [a]	0.121 [b]
Dimethyl Sulfide	0.328 [a]	0.328 [a]
2-methyl Furan	n.d. [a]	n.d. [a]
2-ethyl-Furan	n.d. [a]	n.d. [a]
trans-2-Pentenal	8.884 [a]	4.772 [b]
2-ethyl-2-Butenal	3.123 [a]	2.463 [b]
(E)-2-Hexenal	0.167 [a]	0.146 [a]
α-Pinene	7.987 [b]	11.516 [a]
Camphene	1.864 [b]	2.164 [a]
Benzaldehyde	0.069 [a]	0.069 [a]
2-cyclopropyl-Pentane	8.620 [a]	9.898 [a]
β-Pinene	86.703 [a]	102.460 [a]
1-Octen-3-ol	3.978 [a]	2.972 [a]
1,4-Octadiene	8.026 [a]	3.431 [b]
Phenol	89.113 [a]	102.390 [a]
ß-Myrcene	122.340 [a]	122.250 [a]
3-Carene	172.010 [a]	174.530 [a]
2-pentyl-Furan	n.d. [a]	n.d. [a]
(E,E)-2,4-Heptadienal	12.734 [a]	12.911 [a]
Formamide, N-phenyl-	17.813 [a]	14.829 [a]
2-Isobutylthiazole	4.580 [a]	4.809 [a]
(R)+Limonene	52.977 [a]	38.227 [b]
1,3,6-Octatriene, 3,7-dimethy-, (E)	259.780 [a]	188.770 [b]
(S)-Limonene	30.901 [a]	23.181 [b]
Eucalyptol	1.328 [a]	0.964 [b]
Benzeneacetaldehyde	12.928 [a]	10.455 [a]
1,3,6-Octatriene, 3,7-dimethy-, (Z)	9.344 [b]	19.573 [a]
γ-Terpinene	2.839 [a]	1.789 [b]
3-ethyl-Benzaldehyde	1.580 [a]	1.325 [a]
α-Terpinene	1.328 [a]	1.352 [a]
Benzamide	4.644 [a]	5.119 [a]
Decane	6.903 [a]	7.939 [a]
Terpinolene	239.670 [a]	217.830 [a]
Sabinene hydrate	7.603 [a]	8.046 [a]
Nonanal	0.241 [a]	0.255 [a]
Linalool	n.d. [a]	0.010 [a]
Fenchyl acetate	0.178 [a]	0.020 [b]
Ethanol, 2-phenyl-	29.229 [a]	29.008 [a]
1,5-Decadiyne	0.046 [a]	0.024 [a]
trans-Pinocarveol	3.403 [a]	2.819 [a]
3-Menthene	23.051 [a]	19.218 [a]
3-Caren-10-al	0.596 [a]	0.799 [a]
Isoborneol	4.226 [a]	6.092 [a]
Cycloheptene	0.012 [a]	0.029 [a]
p-Menth-1-en-8-ol	3.188 [a]	2.163 [b]
Methyl Salicylate	0.996 [a]	0.349 [b]
2-methyl-2-Hepten-4-yne	9.596 [a]	6.049 [b]
1,3-cis,5-cis-Octatriene	3.668 [a]	4.464 [a]
p-allyl-Anisole	0.082 [a]	0.011 [a]
Nonylcyclopropane	0.040 [a]	n.d. [b]
Benzenepropanenitrile	n.d. [a]	n.d. [a]
d-Carvone	0.074 [a]	0.027 [b]
Indole	0.118 [a]	0.040 [b]
1-Octene	n.d. [a]	n.d. [a]
Eugenol	0.028 [a]	n.d. [b]
Citronellyl acetate	31.728 [a]	n.d. [b]
Methyl Eugenol	0.311 [a]	0.028 [b]
Humulene	0.015 [a]	n.d. [a]
1,4-Heptadiene	0.044 [a]	0.036 [a]

All concentrations are presented in micro molarity of analyte per gram of fresh mass ($\mu M \cdot g^{-1}$ FM). Mean values represent two plants per replication and ten replications per treatment. Values for each season are averaged across all treatments within that season. Compound means that were consistently below the instrument detection limit are denoted as n.d. (i.e., not detected). Values were analyzed using Tukey's (protected) honest significant difference test. Data in the same row followed by the same letter are not significantly different ($\alpha = 0.05$).

Table 5.5. Influence of growing season on aroma volatile organic compound (VOC) total concentration and pertinent (VOC) ratios in hydroponically grown greenhouse sweet basil (*Ocimum basilicum* var. Genovese).

	Growing Season	
Compound Name	**Summer**	**Winter**
VOC Total	1300.050 [a]	1307.350 [a]
α/β-Pinene Ratio	0.103 [b]	0.124 [a]
R+/S-Limonene Ratio	1.862 [a]	1.830 [a]
(E/Z)-Ocimene Ratio	32.047 [a]	37.307 [a]
α-Terpinene/Total Terpinenes	0.012 [a]	0.010 [a]
γ-Terpinene/Total Terpinenes	0.017 [a]	0.008 [b]
Terpinolene/Total Terpinenes	0.971 [a]	0.982 [a]

Total concentration is presented in micro molarity of analyte per gram of fresh mass ($\mu M \cdot g^{-1}$ FM). All ratios represent mean values of two plants per replication and ten replications per treatment. Values for each season are averaged across all treatments within that season. Values were analyzed using Tukey's (protected) honest significant difference test. Data in the same row followed by the same letter are not significantly different ($\alpha = 0.05$).

Table 5.6. Influence of light treatment on aroma volatile tissue concentrations in hydroponically grown greenhouse sweet basil (*Ocimum basilicum* var. Genovese).

Compound Name	Lighting Treatments			
	Narrowband 20B/80R	Broadband White	High Pressure Sodium	Natural Light Control
Propanal	0.305[a]	0.201[ab]	0.136[ab]	0.072[b]
Dimethyl Sulfide	3.511[a]	1.922[b]	1.361[b]	1.016[b]
2-methyl Furan	0.004[a]	0.007[a]	0.003[a]	0.006[a]
2-ethyl-Furan	0.004[a]	0.007[a]	0.003[a]	0.006[a]
trans-2-Pentenal	6.340[bc]	17.577[a]	4.690[c]	6.481[bc]
2-ethyl-2-Butenal	2.960[b]	5.377[a]	2.413[b]	2.579[b]
(E)-2-Hexenal	0.160[bc]	0.311[a]	0.123[bc]	0.159[bc]
α-Pinene	12.108[a]	10.229[a]	6.817[a]	7.978[a]
Camphene	13.720[a]	11.591[a]	7.726[a]	9.039[a]
Benzaldehyde	0.429[a]	0.578[a]	0.314[a]	0.288[a]
2-cyclopropyl-Pentane	12.959[a]	12.767[ab]	8.477[ab]	5.728[b]
β-Pinene	131.860[a]	128.720[ab]	82.234[ab]	66.354[ab]
1-Octen-3-ol	2.748[a]	3.125[a]	3.210[a]	2.364[a]
1,4-Octadiene	4.183[a]	6.421[a]	6.745[a]	4.647[a]
Phenol	130.650[a]	129.300[a]	84.157[a]	69.484[b]
ß-Myrcene	242.220[a]	173.060[ab]	107.080[ab]	51.419[b]
3-Carene	345.810[a]	247.070[ab]	152.880[ab]	73.410[b]
2-pentyl-Furan	0.010[abc]	0.004[bc]	0.006[abc]	0.004[c]
(E,E)-2,4-Heptadienal	15.381[a]	15.857[a]	11.245[a]	10.900[a]
Formamide, N-phenyl-	17.168[b]	6.619[b]	15.472[b]	32.528[a]
2-Isobutylthiazole	6.170[a]	5.444[ab]	2.971[b]	3.681[a]
(R)+Limonene	64.896[a]	51.111[ab]	37.550[ab]	33.225[a]
1,3,6-Octatriene, 3,7-dimethy-, (E)	329.100[a]	253.450[ab]	190.860[ab]	154.660[b]
(S)-Limonene	39.572[a]	30.185[ab]	23.199[ab]	18.690[a]
Eucalyptol	1.682[a]	1.295[ab]	0.974[ab]	0.791[a]
Benzeneacetaldehyde	17.089[a]	13.341[a]	9.681[a]	7.187[a]
1,3,6-Octatriene, 3,7-dimethy-, (Z)	7.541[b]	13.317[a]	11.655[a]	14.009[a]
γ-Terpinene	2.980[a]	2.271[a]	2.093[a]	2.137[a]
3-ethyl-Benzaldehyde	1.516[a]	1.341[a]	1.119[a]	2.500[a]
α-Terpinene	1.035[a]	0.870[a]	0.757[a]	0.930[a]
Benzamide	6.188[a]	4.434[a]	3.955[a]	4.303[a]
Decane	8.912[a]	6.155[a]	7.642[a]	5.909[a]
Terpinolene	237.030[abc]	333.710[ab]	178.430[bc]	104.710[c]
Sabinene hydrate	9.580[a]	6.405[a]	7.862[a]	6.263[a]
Nonanal	0.304[a]	0.203[a]	0.249[a]	0.199[a]
Linalool	0.018[a]	0.010[a]	0.011[a]	n.d.[a]
Fenchyl acetate	0.317[a]	0.144[ab]	0.071[ab]	0.031[ab]
Ethanol, 2-phenyl-	20.037[ab]	37.459[ab]	7.290[b]	32.059[ab]
1,5-Decadiyne	0.089[a]	0.076[a]	n.d.[a]	0.020[a]
trans-Pinocarveol	3.099[abc]	4.936[ab]	0.766[c]	3.148[abc]
3-Menthene	21.881[ab]	32.592[a]	6.348[b]	21.481[ab]
3-Caren-10-al	0.497[a]	0.549[a]	0.807[a]	1.207[a]
Isoborneol	4.025[ab]	4.677[ab]	5.362[ab]	7.903[a]
Cycloheptene	n.d.[a]	n.d.[a]	n.d.[a]	0.061[a]
p-Menth-1-en-8-ol	3.028[a]	3.443[a]	2.272[a]	2.478[a]
Methyl Salicylate	0.646[a]	0.995[a]	0.509[a]	0.652[a]
2-methyl-2-Hepten-4-yne	8.788[a]	9.003[a]	6.990[a]	7.476[a]
1,3-cis,5-cis-Octatriene	2.828[a]	3.929[a]	2.648[a]	2.787[a]
p-allyl-Anisole	0.068[a]	0.095[a]	0.077[a]	0.065[a]
Nonylcyclopropane	0.030[b]	0.152[a]	n.d.[b]	n.d.[b]
Benzenepropanenitrile	n.d.[a]	0.002[a]	n.d.[a]	n.d.[a]
d-Carvone	0.044[ab]	0.119[a]	0.039[ab]	0.024[b]
Indole	0.072[ab]	0.192[a]	0.061[ab]	0.038[b]
1-Octene	0.007[a]	0.004[a]	0.005[a]	0.003[a]
Eugenol	0.021[a]	0.021[a]	n.d.[a]	n.d.[a]
Citronellyl acetate	29.671[a]	17.303[a]	24.723[a]	12.007[a]
Methyl Eugenol	0.304[a]	0.303[a]	n.d.[a]	n.d.[a]
Humulene	n.d.[a]	n.d.[a]	n.d.[a]	n.d.[a]
1,4-Heptadiene	n.d.[a]	0.081[a]	0.045[a]	0.126[a]

All concentrations are presented in micro molarity of analyte per gram of fresh mass ($\mu M \cdot g^{-1}$ FM). Mean values represent two plants per replication and ten replications per treatment. Values for each treatment are averaged across all four growing seasons. Compound means that were consistently below the instrument detection limit are denoted as n.d. (i.e., not detected). Values were analyzed using Tukey's (protected) honest significant difference test. Data in the same row followed by the same letter are not significantly different ($\alpha = 0.05$).

Table 5.7. Influence of light treatment on aroma volatile organic compound (VOC) total concentration and pertinent (VOC) ratios in hydroponically grown greenhouse sweet basil (*Ocimum basilicum* var. Genovese).

Compound	Lighting Treatments			
	Narrowband 20B/80R	**Broadband White**	**High Pressure Sodium**	**Natural Light Control**
VOC Total	1771.590[a]	1610.340[b]	1032.100[c]	795.200[d]
α/β-Pinene Ratio	0.093[c]	0.103[bc]	0.072[c]	0.155[a]
R+/S-Limonene Ratio	1.861[a]	1.903[a]	1.803[a]	1.832[a]
(E/Z)-Ocimene Ratio	44.385[a]	25.657[a]	21.536[a]	26.916[a]
α-Terpinene/Total Terpinenes	0.024[a]	0.004[a]	0.007[a]	0.017[a]
γ-Terpinene/Total Terpinenes	0.034[a]	0.008[a]	0.009[a]	0.021[a]
Terpinolene/Total Terpinenes	0.942[a]	0.988[a]	0.984[a]	0.961[a]

Total concentration is presented in micro molarity of analyte per gram of fresh mass ($\mu M \cdot g^{-1}$ FM). All ratios represent mean values of two plants per replication and ten replications per treatment. Values for each season are averaged across all treatments within that season. Values were analyzed using Tukey's (protected) honest significant difference test. Data in the same row followed by the same letter are not significantly different ($\alpha = 0.05$).

Table 5.8. Demographics of participants in sensory evaluation by growing season.

	Growing Season	
	Summer	**Winter**
Sex (*n*)		
Men	68	77
Women	32	23
How often do you consume basil?		
Every day	2	4
3 times a week	14	10
Once a week	30	34
Every 2-3 weeks	26	24
Once a month	19	21
Once every 2-3 months	7	6
Once every 6 months	2	1
Never	0	0

Table 5.9. Consumer overall liking scores of ‘Genovese’ sweet basil across growing season and lighting type.

	Growing Season	
Light Treatment	Summer	Winter
Narrowband 20B/80R	5.66 ± 1.87 [b]	6.22 ± 1.93 [bc]
Broadband White	6.01 ± 1.91 [a]	5.99 ± 1.97 [c]
High Pressure Sodium	6.22 ± 1.45 [a]	6.68 ± 1.54 [ab]
Natural Light Control	6.31 ± 1.21 [a]	6.98 ± 1.29 [a]

Values for each season are averaged across all treatments within that season. Values were analyzed using Tukey’s (protected) honest significant difference test. Data in the same column followed by the same letter are not significantly different ($\alpha = 0.05$). There was no significant difference in overall liking scores between the Summer and Winter growing seasons. (i.e., means of growing seasons are compared in models without significance).

Table 5.10. Consumer overall aroma intensity scores of ‘Genovese’ sweet basil across growing season and lighting type. Means of growing seasons are compared in models without significant interaction terms and different are represented with ascending letters.

	Growing Season	
Light Treatment	Summer	Winter
Narrowband 20B/80R	8.20 ± 3.01 [a]	8.31 ± 3.17 [a]
Broadband White	8.44 ± 3.29 [a]	8.61 ± 3.49 [a]
High Pressure Sodium	8.32 ± 3.14 [a]	8.51 ± 3.31 [a]
Natural Light Control	7.98 ± 3.54 [a]	8.11 ± 3.35 [a]

Values for each season are averaged across all treatments within that season. Values were analyzed using Tukey’s (protected) honest significant difference test. Data in the same column followed by the same letter are not significantly different ($\alpha = 0.05$). There was no significant difference in overall liking scores between the Summer and Winter growing seasons (i.e., means of growing seasons are compared in models without significance).

Table 5.11. Differentially expressed genes (DEGs) based on comparisons between supplemental lighting treatment and natural light (NL) control.

	Summer			Winter		
DEG Comparison	**Upregulated**	**Downregulated**	**Total DEGs**	**Upregulated**	**Downregulated**	**Total DEGs**
Narrowband 20B/80R vs. NL Control	2045	1756	3801	3505	2073	5578
Broadband White vs. NL Control	132	146	278	3262	2347	5609
High Pressure Sodium vs. NL Control	34	94	128	1228	695	1923

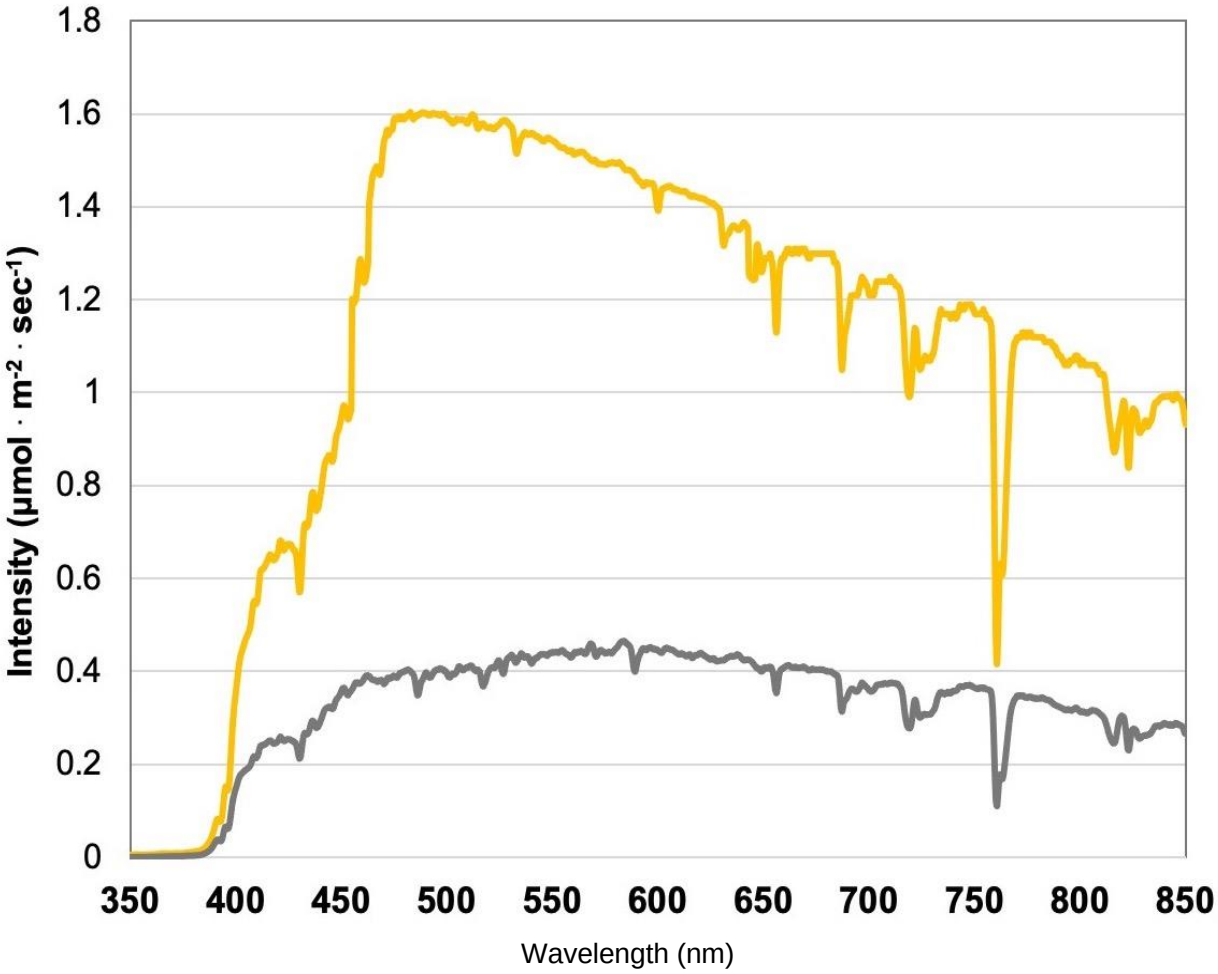

Figure 5.1. Natural light (NL) spectra under greenhouse glass, averaged across all four growing seasons, ranging from 350 nm to 850 nm. Values were taken at solar noon with three replicates for full sun (yellow) and overcast (gray) for each experimental run.

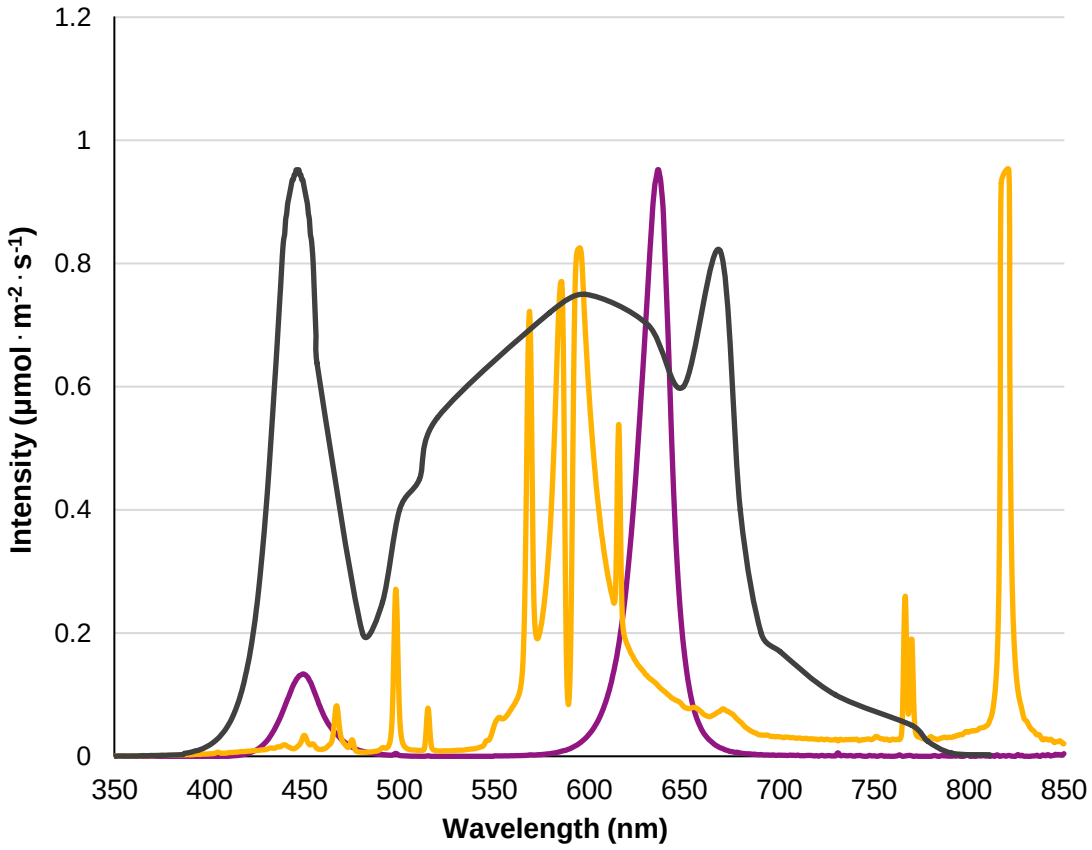

Figure 5.2. Emission spectra of supplemental lighting (SL) treatments from 300 nm to 850 nm: (1) Narrowband 20B/80R LED (purple), (2) Broadband White LEDs (grey), and (3) High Pressure Sodium (yellow). All SL treatments provided 8.64 mol•m^{-2}•d^{-1} (continuous 100 µmol•m^{-2}•s^{-1}; 24 h•d^{-1}). All lighting treatments were measured with a PS-200 Apogee Spectroradiometer to confirm intensity of specific treatment wavelengths throughout each growing season. Readings were taken at midnight in order to exclude underlying natural solar spectra.

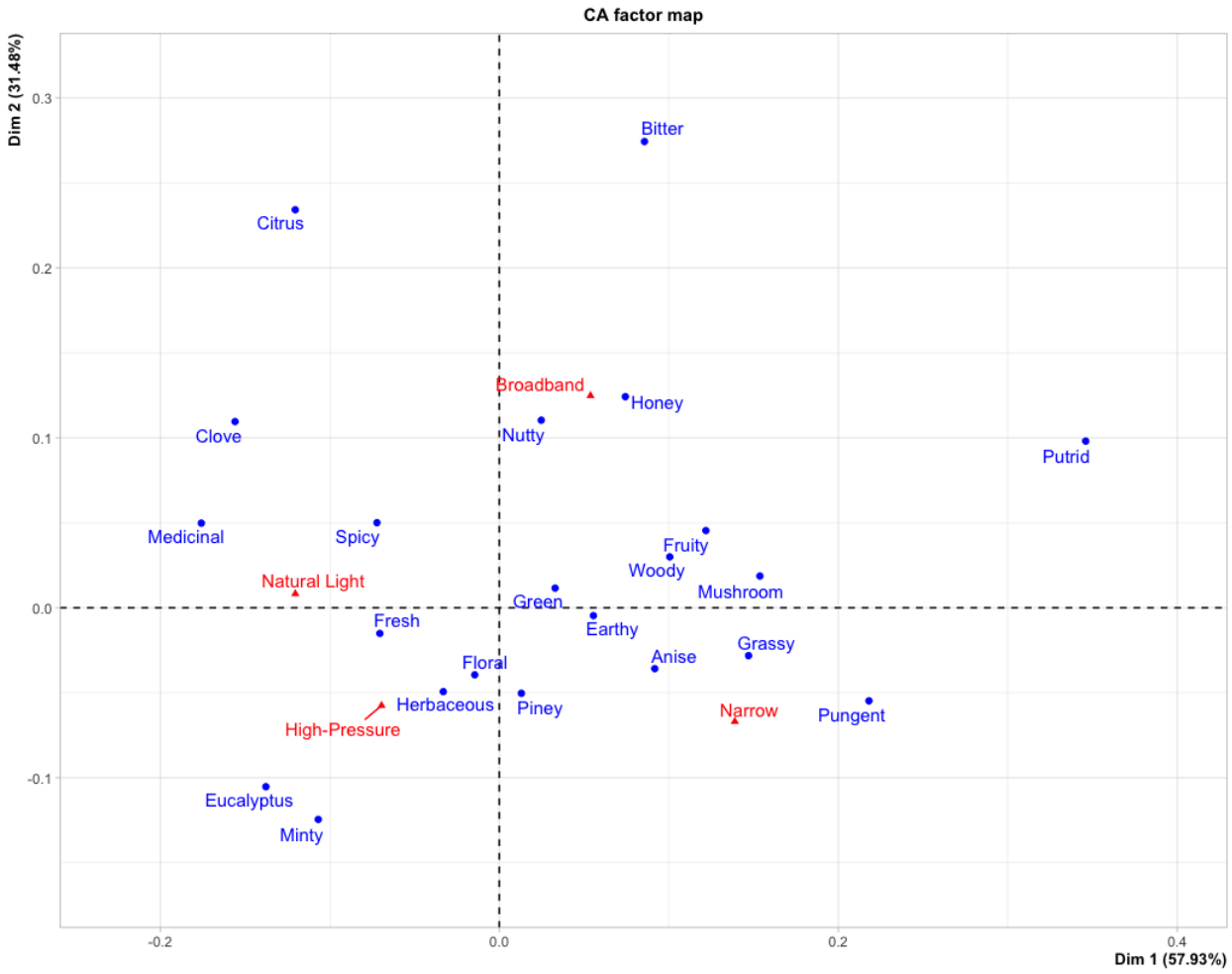

Figure 5.3. Correspondence analysis (CA) factor map illustrating the relationship between lighting treatments (red) and check-all-that-apply (CATA) descriptors (blue) selected by sensory panel participants across both growing seasons.

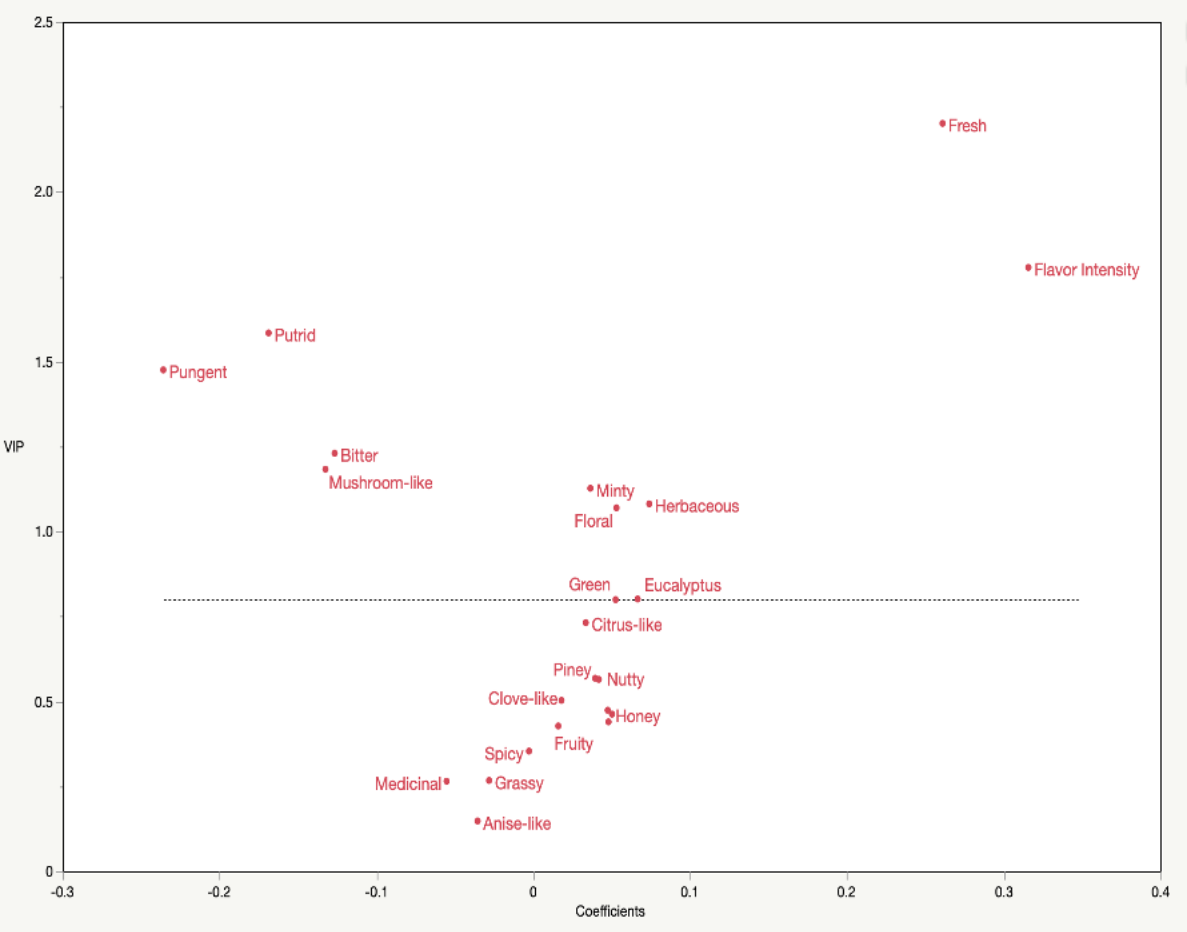

Figure 5.4. Variable Importance in Projection (VIP) and βcoefficients for check-all-that-apply (CATA) frequencies predicting overall liking across both growing seasons. The threshold has been set at VIP > 0.8.

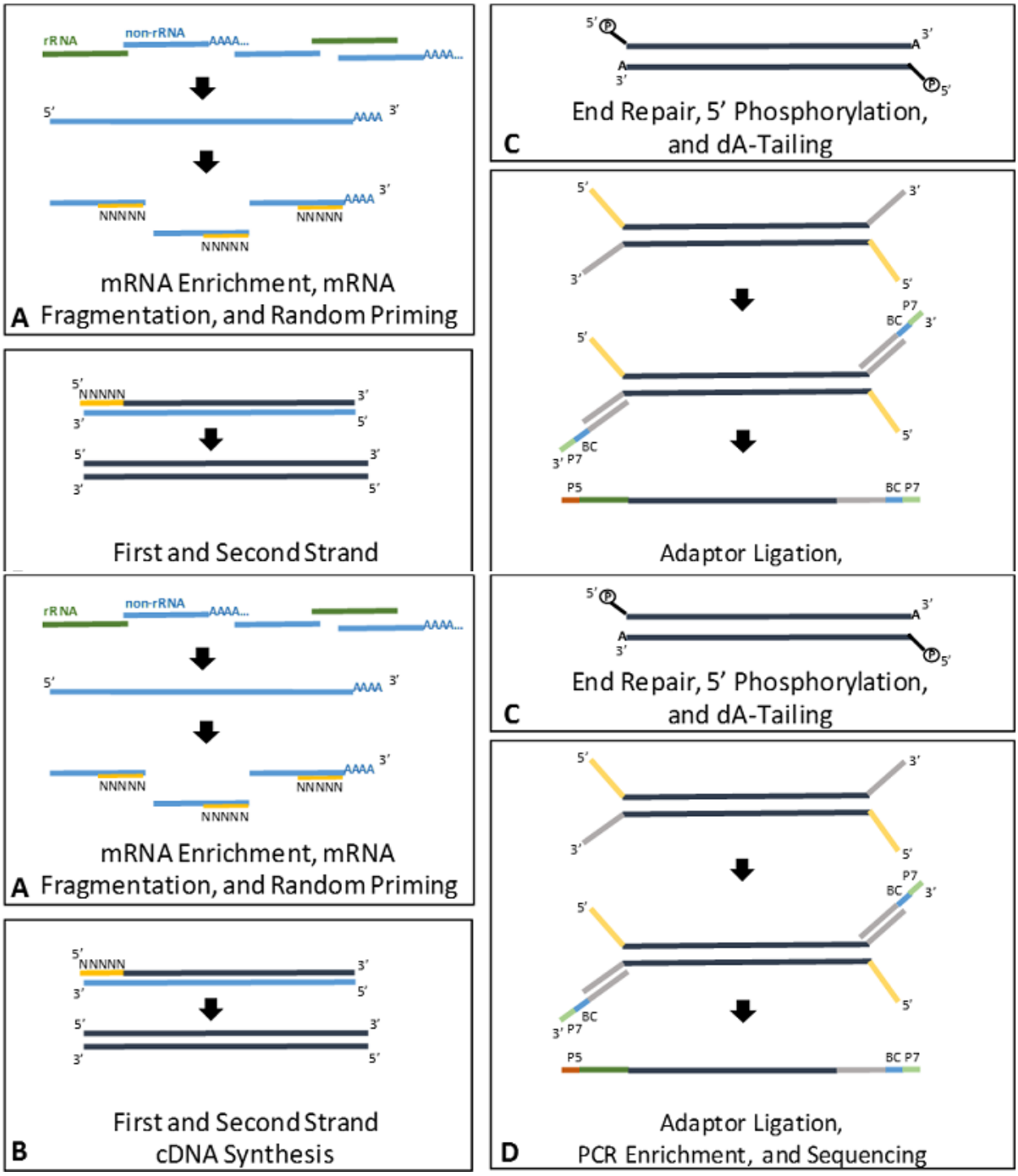

Figure 5.5. mRNA sequencing via polyA selection. Sequencing was performed on the HiSeq 6000 sequencing platform (Illumia, San Diego, USA).

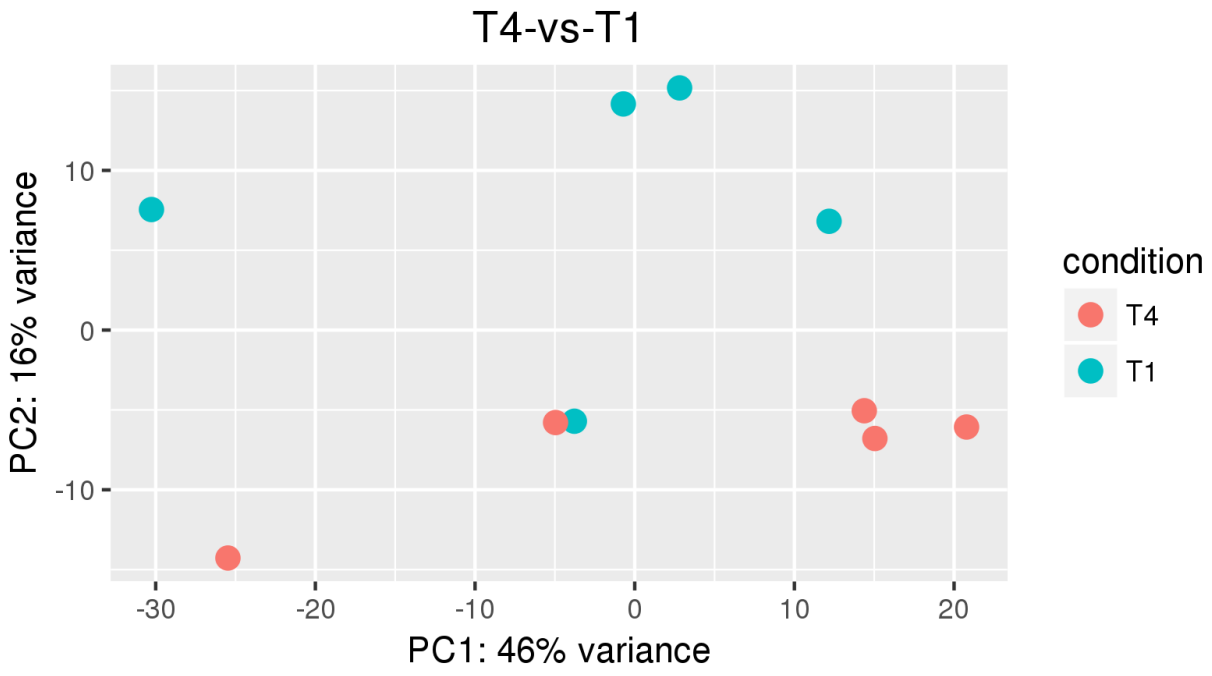

Figure 5.6. Principal component analysis (PCA) comparing DEGs between the Natural Light Control (T4) and Narrowband 20B/80R treatment (T1).

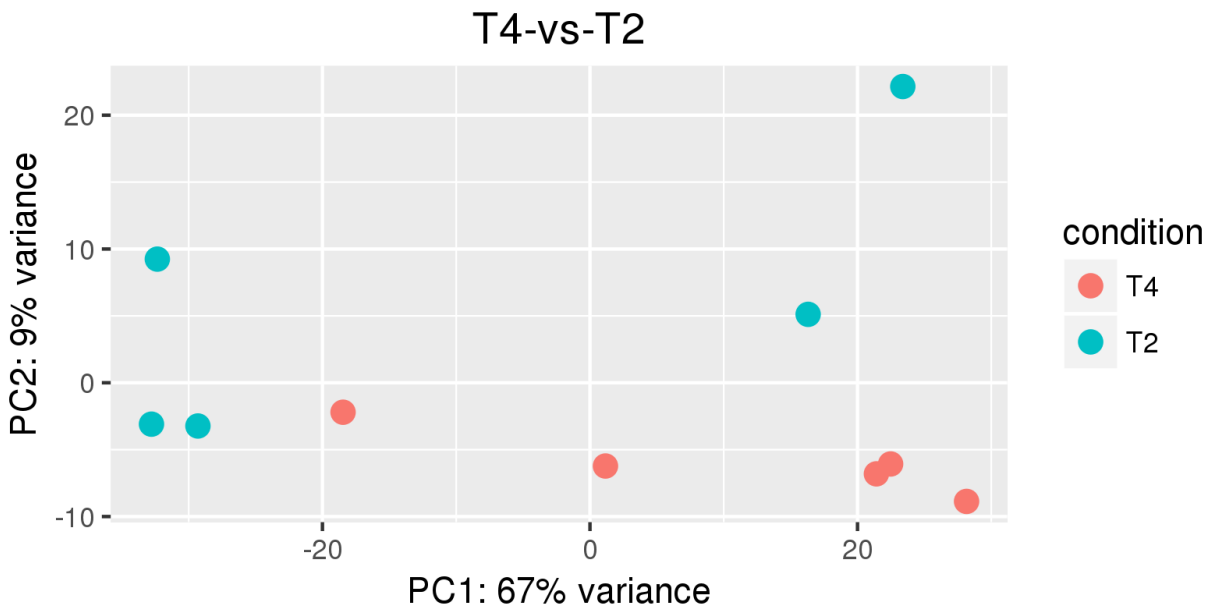

Figure 5.7. Principal component analysis (PCA) comparing DEGs between the Natural Light Control (T4) and Broadband White treatment (T2).

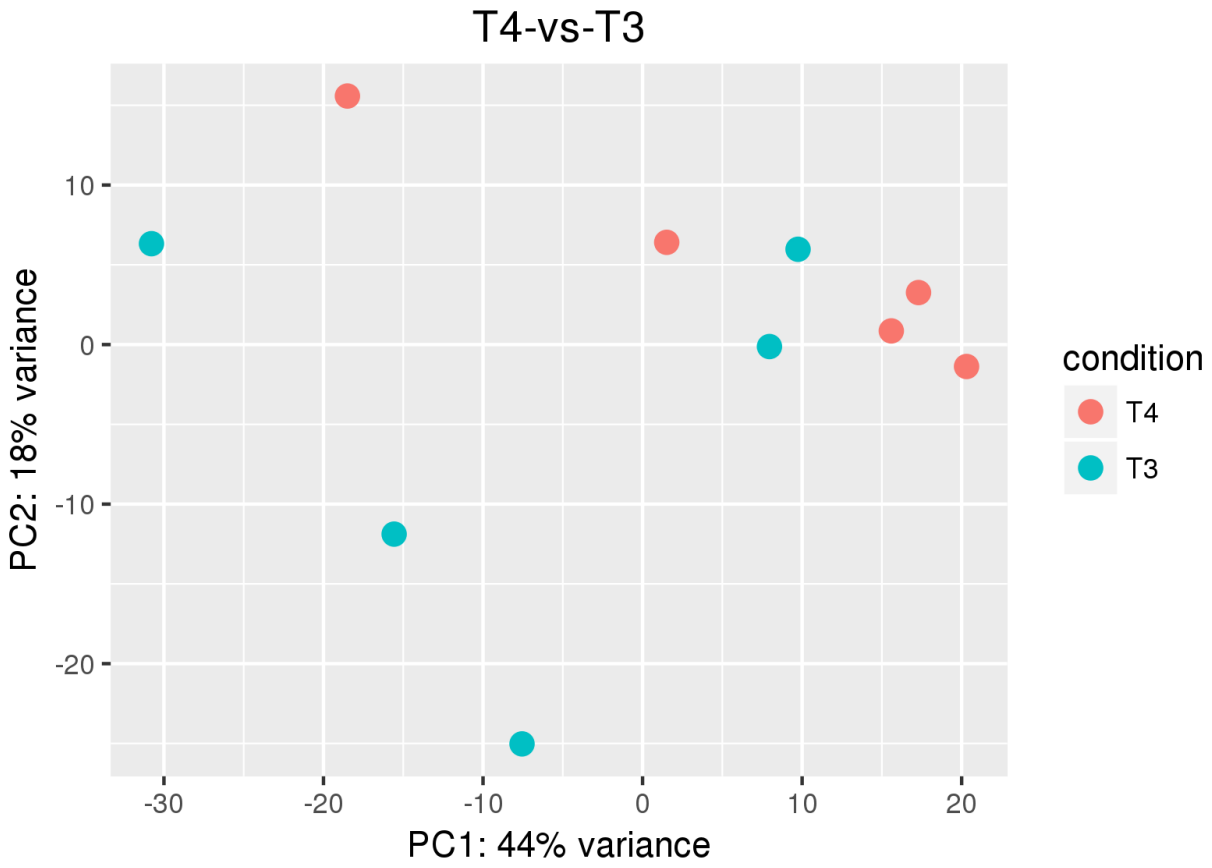

Figure 5.8. Principal component analysis (PCA) comparing DEGs between the Natural Light Control (T4) and High Pressure Sodium treatment (T3).

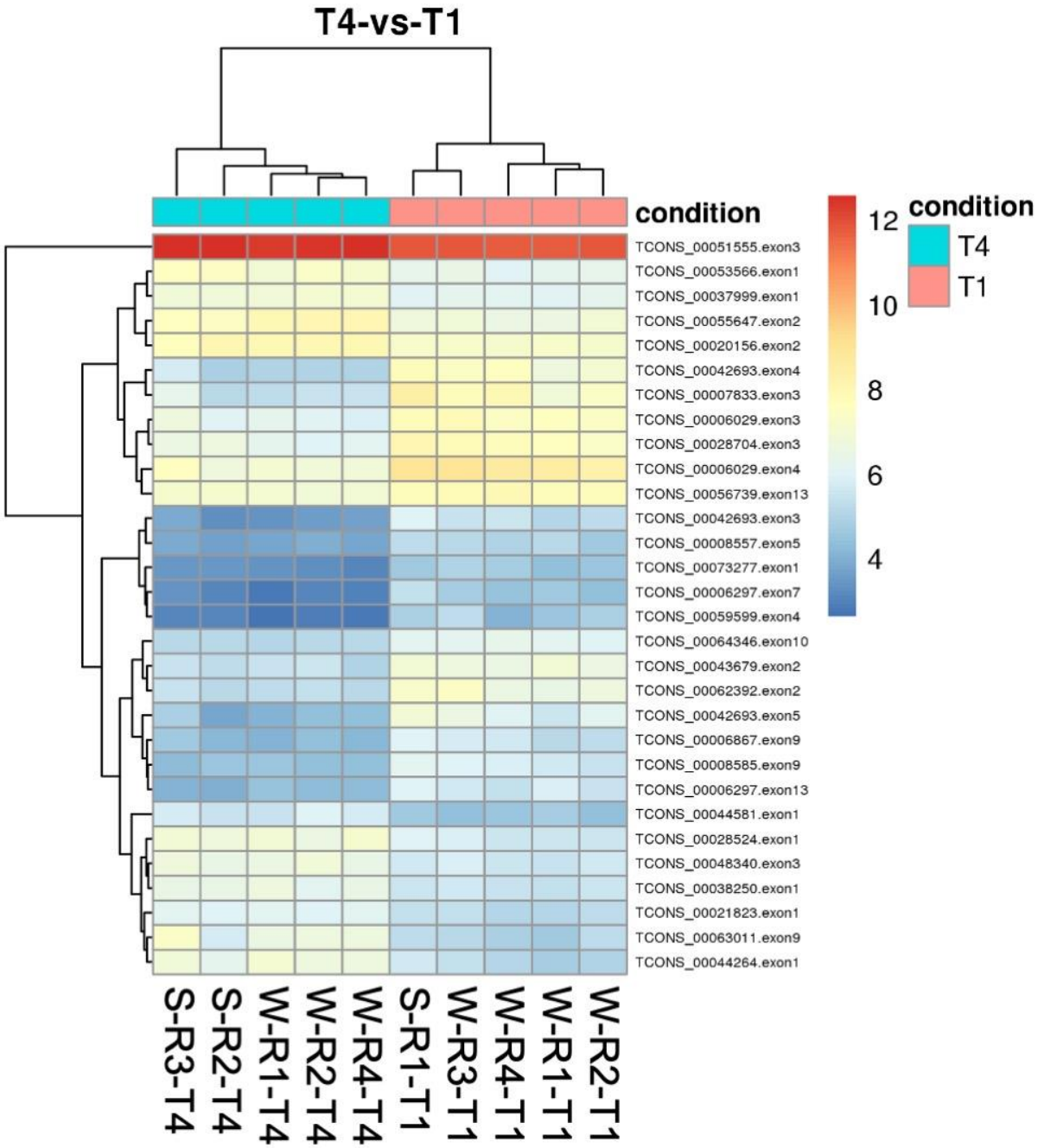

Figure 5.9. Biclustering heat map comparing top 30 significant DEGs between the Natural Light Control (T4) and Narrowband 20B/80R treatment (T1) to identify co-regulated genes. Summer (S) and Winter (W) seasons are compared with four replications (R1-R4).

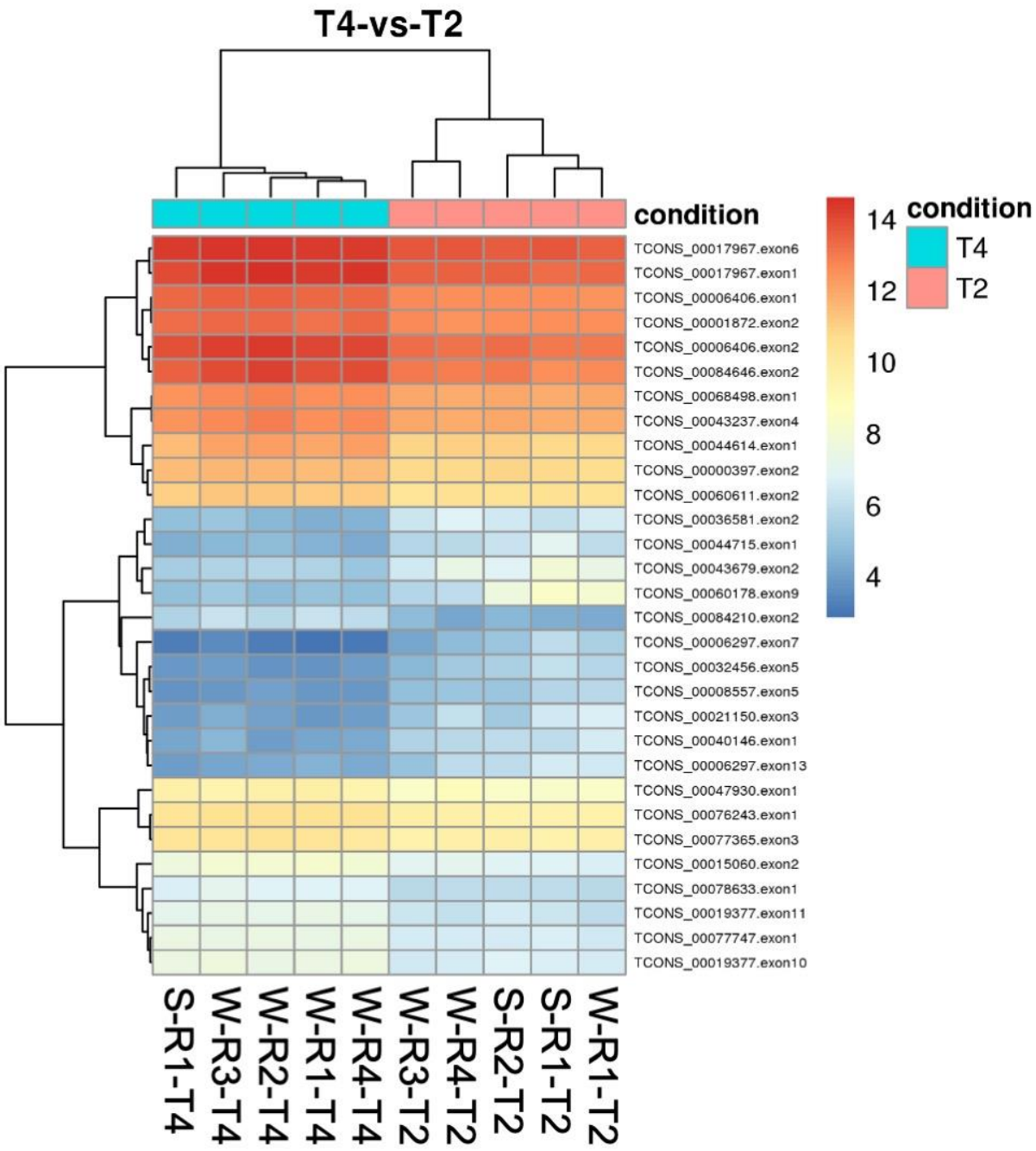

Figure 5.10. Biclustering heat map comparing top 30 significant DEGs between the Natural Light Control (T4) and Broadband White treatment (T2) to identify co-regulated genes. Summer (S) and Winter (W) seasons are compared with four replications (R1-R4).

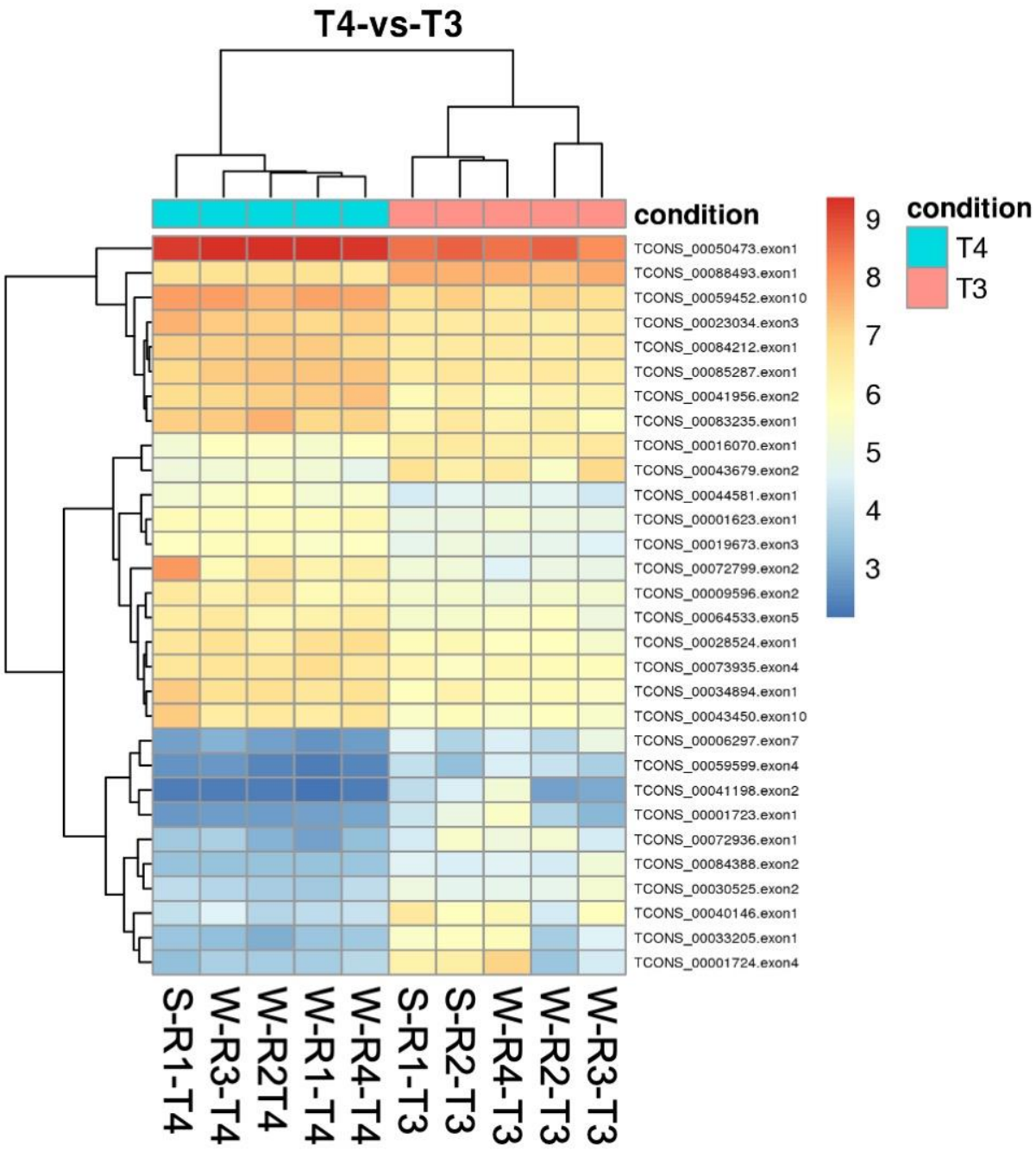

Figure 5.11. Biclustering heat map comparing top 30 significant DEGs between the Natural Light Control (T4) and High Pressure Sodium treatment (T3) to identify co-regulated genes. Summer (S) and Winter (W) seasons are compared with four replications (R1-R4).

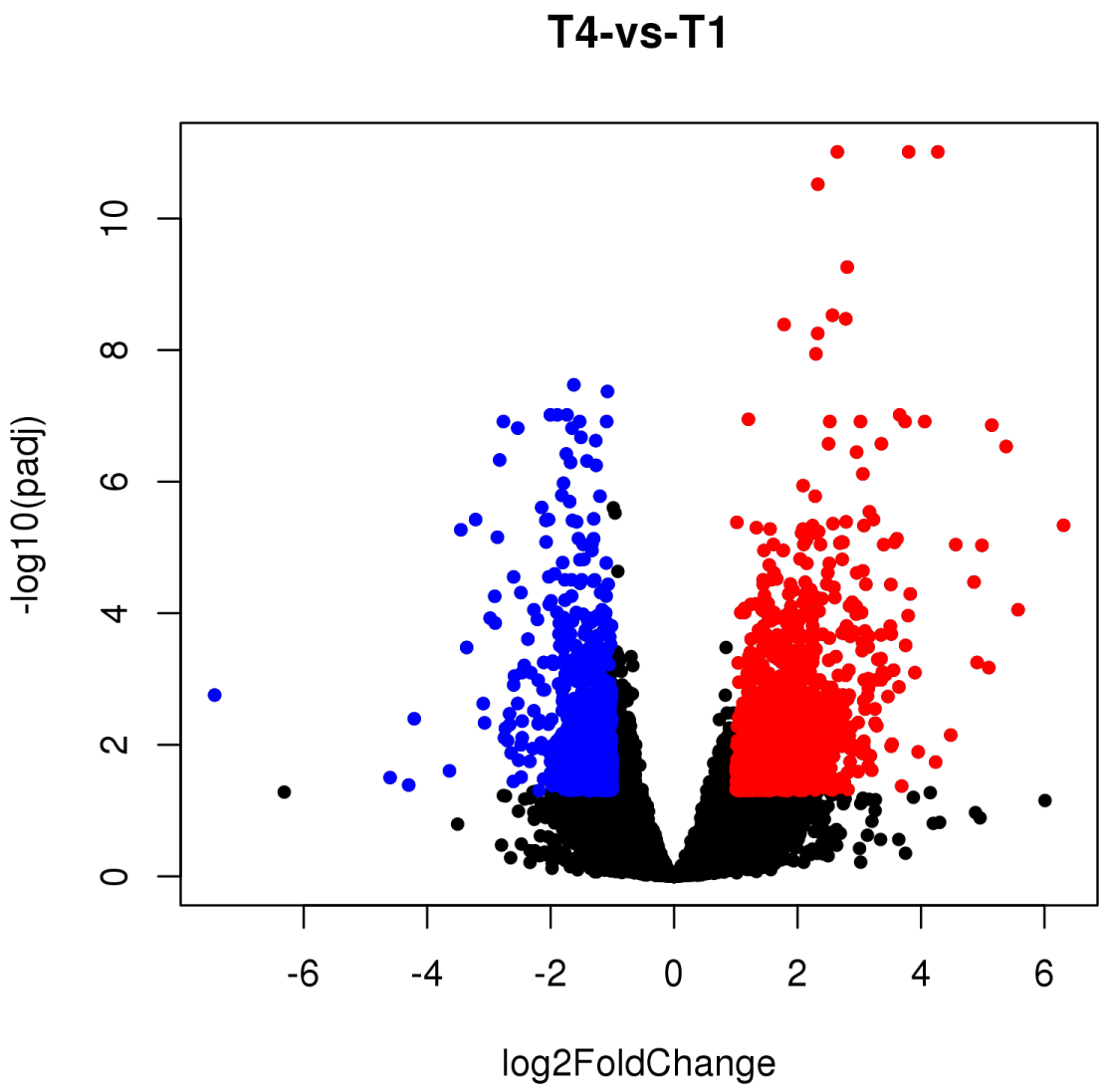

Figure 5.12. Volcano plot showing global transcriptional change between the Natural Light Control (T4) and Narrowband 20B/80R treatment (T1). All the genes are plotted and each data point represents a gene. The log2 fold change of each gene is represented on the x-axis and the log10 of its adjusted p-value is on the y-axis. Genes with an adjusted p-value less than 0.05 and a log2 fold change greater than 1 are indicated by red dots, which represent upregulated genes. Genes with an adjusted p-value less than 0.05 and a log2 fold change less than -1 are indicated by blue dots, which represent downregulated genes.

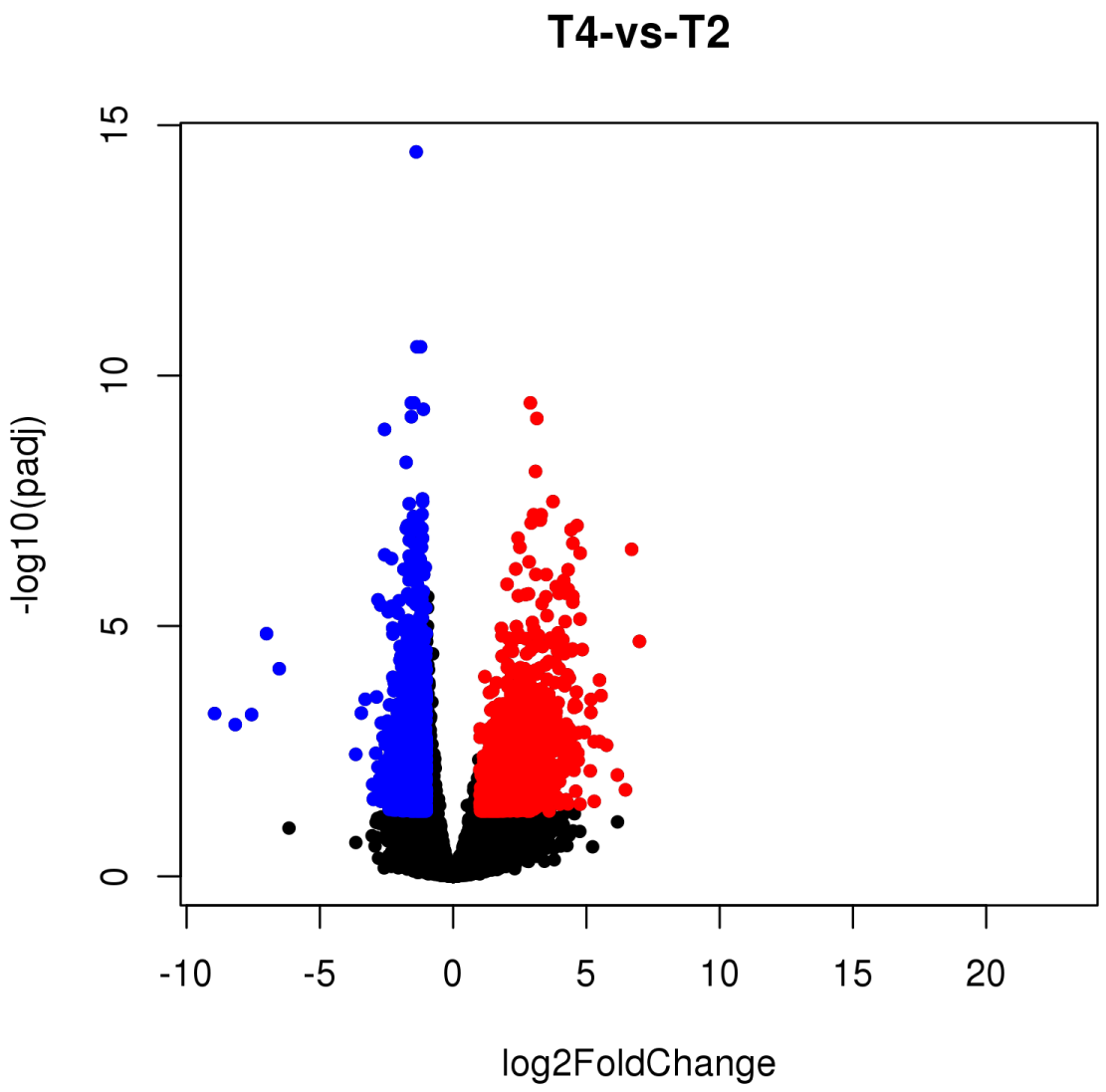

Figure 5.13. Volcano plot showing global transcriptional change between the Natural Light Control (T4) and Broadband White treatment (T2). All the genes are plotted and each data point represents a gene. The log2 fold change of each gene is represented on the x-axis and the log10 of its adjusted p-value is on the y-axis. Genes with an adjusted p-value less than 0.05 and a log2 fold change greater than 1 are indicated by red dots, which represent upregulated genes. Genes with an adjusted p-value less than 0.05 and a log2 fold change less than -1 are indicated by blue dots, which represent downregulated genes.

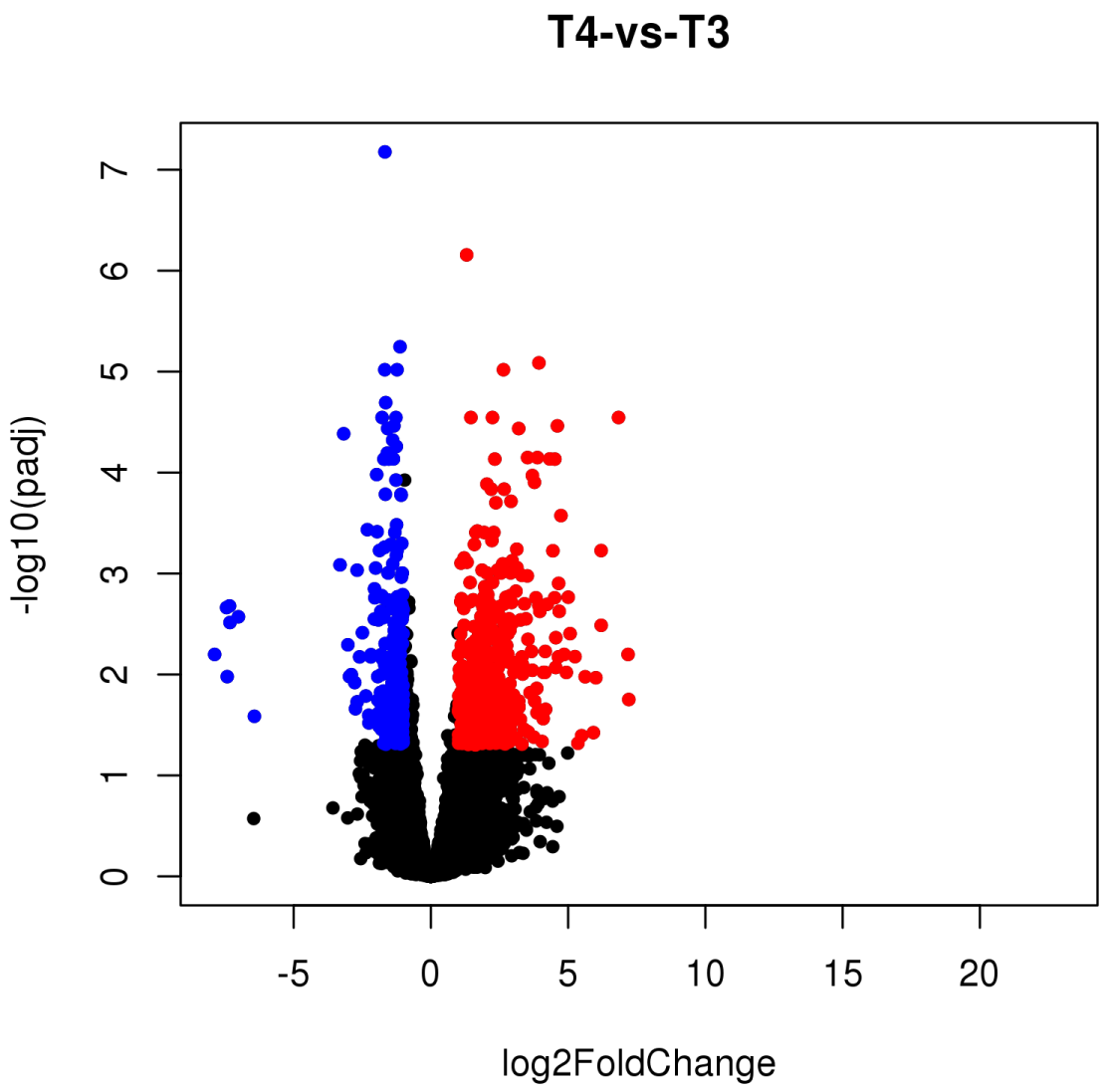

Figure 5.14. Volcano plot showing global transcriptional change between the Natural Light Control (T4) and High Pressure Sodium treatment (T3). All the genes are plotted and each data point represents a gene. The log2 fold change of each gene is represented on the x-axis and the log10 of its adjusted p-value is on the y-axis. Genes with an adjusted p-value less than 0.05 and a log2 fold change greater than 1 are indicated by red dots, which represent upregulated genes. Genes with an adjusted p-value less than 0.05 and a log2 fold change less than -1 are indicated by blue dots, which represent downregulated genes.

CHAPTER 6: CONCLUSION

Conclusion

This dissertation has provided a comprehensive exploration of how spectral quality from supplemental lighting and seasonal changes impact primary and secondary metabolism in hydroponically grown greenhouse basil. The study has made several critical contributions to the field, advancing our understanding of plant/light interactions, and providing practical insights for the horticulture lighting industry.

In Phase 1, we evaluated different basil varieties, establishing a baseline for aroma volatile profiles and concentrations of key secondary metabolites. This phase brought to light the inherent variability among basil varieties and set the stage for subsequent phases.

Phase 2 built on these initial findings, using discrete narrow-band blue/red (B/R) wavelengths to investigate their impact on aroma volatile concentrations and secondary metabolic resource partitioning in basil. The results underscored the influence of both seasonal and supplemental lighting effects on plant metabolism and highlighted the potential of manipulating B/R wavelengths to enhance flavor and phytonutrient content.

In Phase 3, we extended this investigation to full spectrum white LEDs and HPS, comparing their impacts on yield and nutrient accumulation with the optimal narrowband B/R identified in Phase 2. This comparative analysis deepened our understanding of the unique benefits of different lighting regimes.

Finally, in Phase 4, we integrated all previous phases to compare the best narrowband and full spectrum treatments with a traditional HPS treatment and natural light control. Through an interdisciplinary approach that combined photosynthetic and primary metabolic data, sensory panel results, and mRNA sequencing data, we identified a light treatment that optimally balances yield, nutrient content, and flavor preference.

These findings have significant implications for LED manufacturers and commercial growers, providing them with evidence-based guidance on selecting lighting regimes to maximize crop yield and quality.

Looking forward, there are several promising directions for future research. Extending this research to other high-value specialty crops could reveal whether similar lighting strategies can enhance their yield and quality. Additionally, exploring the molecular mechanisms underlying plant responses to different light spectra could deepen our understanding of light-mediated physiological responses. Finally, it would be beneficial to investigate the long-term sustainability of these lighting strategies in terms of energy efficiency and environmental impact. In conclusion, this dissertation significantly broadens our understanding of the complex interplay between light conditions and plant physiology, providing a solid foundation for future research and innovation in controlled environment agriculture.

VITA

Hunter Hammock is a young leader with a growing legacy. He has always been dedicated to his research and serving others. He began his college career at UT in 2010, studying chemistry and psychology. During his time there, he completed over 240 hours of undergraduate community service and was chapter president of NSLS UTK, a leadership organization with over 5,100 members.

During his senior year of college, he started working in Dr. Carl Sams' plant physiology lab. He became passionate about using his organic and analytical chemistry background in combination with controlled environment agriculture to improve current practices and provide high-quality, sustainable food sources. He obtained a BS degree from UTK in May 2015, and accepted a graduate research/teaching assistantship to study the impact of LED lighting on high-value specialty crop production and basil flavor volatile profiles.

Hunter graduated with his MS degree in Plant Sciences in May 2018 and is continuing his research at UTK in pursuit of his doctorate, expecting to graduate in Spring 2023. He served as the Graduate Student Senate President from 2021-2022, and currently serves as chapter advisor of NSLS UTK, in addition to other leadership roles and committees on campus.

After graduation, Hunter wants to continue research in an industry or academic setting. His primary interests include flavor chemistry, LED lighting, spectral quality's interaction with plant secondary metabolism, high-value specialty crops, greenhouse production, hydroponics, and human nutrition. He is driven to continue this research and mentor others in our field because of the fundamental impact it can make on society.

Hunter hopes to leave behind a legacy that reflects his amazing opportunities and experiences at UTK. For all that he has gained on the path to this degree, he wants to give back by

doing what others have done for him -- encourage those around him, inspire those he works among, and not only have, but instill faith in those who look up to him. Hunter is proud to be continuing the legacy of his grandparents, who were highly involved in agriculture. He looks forward to leaving a legacy that will continue to grow and flourish for generations to come.